UNIVERSITÀ DEGLI STUDI DI MILANO

FACOLTÀ DI SCIENZE E TECNOLOGIE

Doctorate School In Chemical Science - XXVI Cycle

Studies on Umami Taste.
Preparation of Hydrolyzed Vegetable Proteins (HVPs) and Glutamate-Ribonucleotide Hybrids

PhD Thesis of
Valeria PAPPALARDO
R09028

Tutor: Prof.ssa Giovanna Speranza

Coordinator: Prof.ssa Emanuela Licandro

Academic Year: 2012/2013

INDEX

1. INTRODUCTION

It is generally accepted that there are five basic tastes: salty, sour, sweet, bitter and umami [Mouritsen, 2012].[1]

While the first four taste modalities have been world-widely accepted for hundreds of years, only recently umami has gained widespread recognition in the West. Umami came to the fore in 2000 when Chaudari and colleagues identified on the tongue and palate the taste receptor for L-glutamate, which is considered to be the prototypical umami substance. The protein they described is a new G-protein-coupled receptor that corresponds to a truncated form of metabotropic glutamate receptor mGluR4 [Mouritsen, 2012].

Though umami is a term that most consumers do not recognise, they are usually familiar with the umami taste sensation. Many foods daily used in both East and West naturally contain components that impart an umami taste, and others form umami substances during curing, aging or fermentation. Just think of food such as tomatoes and parmesan cheese, which can actually be considered the most umami ingredients of the Mediterranean diet [Wyers, 2010]. History shows that from a culinary perspective umami is not new and was around long before Dr. Ikeda discovered this taste in 1908. [referenza]Fermented fish sauces and intense meat and vegetable extracts have been valued in world cuisines for more than 2,000 years. For example, Roman *garum* or *liquamen*, a type of fermented fish stock was regularly added to all dishes of that time (Figure 1.1). Although the Greeks and Romans knew that this stock made food to taste better, they never identified it as a specific taste. They just enjoyed consuming it. In

---

[1] A basic taste is an independent taste which cannot be created even through the combination of other tastes.

1825 the French gastronome Brillat-Savarin, in *The Physiology of Taste*, described a meaty taste as "toothsome" and predicted that the "future of gastronomy" would have belonged "to chemistry". His description of a meaty taste is similar to the Japanese interpretation of umami as "deliciousness" [Marcus, 2009].

Figure 1.1. Ancient Roman fermenting vats, used in the production of *garum* (left). *Garum* jugs from Pompei (right).

One of the impediments to the recognition of umami as a basic taste may have been the lack of traditional words to describe it in Western languages, *i.e.* consumers are very familiar with the umami taste sensation, but not with the term. There is no word in Western languages that is synonymous with umami, which it is most often described as a "savory" or "meaty" taste. Thus, the term "umami" has been imported from Japanese in all our languages [Wyers, 2010].

Science is now realizing what great cooks around the world have instinctively known: that foods and flavor enhancers with umami can be useful in contributing a savory taste and rounding out and heightening the flavor of foods.

1.1. Discovery of Umami

Umami was first discovered by the Japanese Professor Kikunae Ikeda of the Imperial University of Tokyo in 1908 (Figure 1.2). He noticed that a previously unidentified taste quality, quite distinct from the four basic tastes sweet, bitter, sour, and salty was present in highly palatable foods such as fish and meats. He detected it most clearly in soups and broth of flaked *katsuobushi*, made from skipjack fish, and in broth made from *kombu*, dried sea tangle, *Laminaria* sp., both of which have been used traditionally in Japanese cooking (Figure 1.3) [Yamaguchi & Ninomiya, 1998, 2000]. In a short paper "New Seasonings" written in Japanese and published in 1909 in Journal of the Chemical Society of Tokyo, Ikeda noted down "*...physiologists and psychologists recognize*

Figure 1.2. Prof. Kikunae Ikeda, the Umami pioneer.

only the four tastes sour, sweet, salty and bitter. Other tastes are considered to be a mixture of these tastes. However, I believe that there is at least one other additional taste which is quite distinct from the four tastes. It is the peculiar taste which we feel as `UMAI [meaning brothy, meaty, or savory]', arising from fish, meat and so forth. The taste is most characteristic of broth prepared from dried bonito and seaweed [Laminaria japonica] ... I propose to call this taste `UMAMI' for convenience. The next problem is to identify the chemical substance which produces `UMAMI'. It is difficult to prove the existence of a small quantity of unknown taste substance.." [Ikeda, 2002].

Subsequently he investigated the constituents of the dried kombu and found it to contain 2–3 g/100 g dry weight free L-monosodium glutamate (L-MSG, Figure 3) and proposed that MSG is for the umami taste what kitchen salt (sodium chloride) is for the salty taste or what table sugar (sucrose) is for the sweet taste.

In 1913, an Ikeda's disciple, Shintaro Kodama, investigated the constituents of dried skipjack, *katsuobushi*, and reported that inosinate also had umami taste characteristics (Figure 3). Many years later, during a study of 5'-ribonucleotide production through biochemical degradation of yeast RNA, Akira Kuninaka identified guanylate to be another important umami substance. Later, it was shown that guanylate occurs naturally

in dried shiitake mushrooms, which are widely used in Japanese and Chinese cooking (Figure 1.3) [Yamaguchi & Ninomiya, 1998, 2000]. The discovery of inosinic acid can be traced back to Liebig who isolated it from beef broth in 1847. Guanylic acid has been known since 1898, when Bang identified it in pancreatic nucleic acid. Once again the taste of these substances went unnoticed for decades. At present, MSG (monosodium glutamate), IMP (inosine 5'-monophosphate disodium salt) and GMP (guanosine 5'-monophosphate disodium salt) are widely used as food additives in particular as seasonings or condiments to supplement, enhance or round-off the flavor of many savory-based processed foods. They are the best flavor enhancers that are in commercial use worldwide.
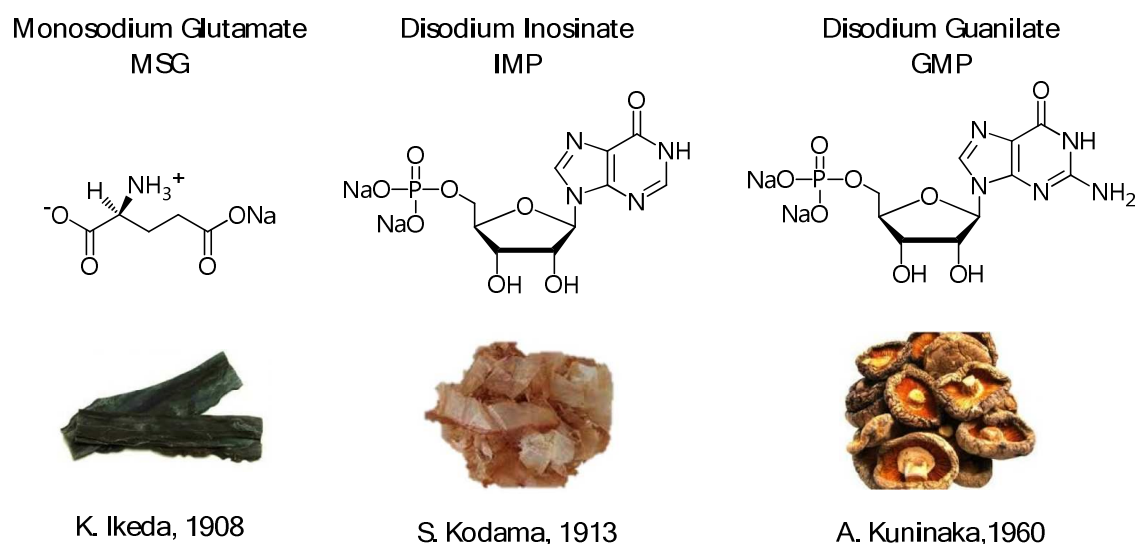
Figure 1.3. Umami substances and their discovery.

1.2. Flavor enhancement

The Japanese word umami means "savory", "delicious" and can denote a really good taste of something, a taste or flavor that is an especially appropriate exemplar of the flavor of thet thing. The taste of MSG by itself does not in any sense represent deliciousness. Instead, it is often described as unpleasant, and as bitter, salty and soapy. Others have described it as a brothy, mouth-watering sensation with a considerable increase in salivation. However, when MSG is added in low concentration to appropriate foods, the flavor, pleasantness and acceptability of the food increases [Halpern, 2000; Löliger, 2000]. As regards 5'-ribonucleotides, IMP is often described as beefy and GMP as oak-mushroom. The use of both compounds was reported to enhance flavor notes described as meaty, brothy, mouthfilling, well-rounded, drying or astringent. It also seems that 1:1 blends of IMP and GMP can suppress some bitter and sour notes, but enhance sweet and salt perceptions [Nagodawithana, 1995; Löliger, 2000].

These compounds not only have their own characteristic taste at a level higher than their threshold levels but also enhance or potentiate the flavor of the food even at a level lower that their threshold levels. In any case, MSG, IMP and GMP can favourably alter the preference for foods. Thus, they are called flavor enhancers, flavor potentiators or sometimes flavor modifiers [Yamaguchi, 1998], that is to have the ability to significantly influence the taste perception of other substances, *e.g.* the components of certain types of food so that these foods become organoleptically attractive to the human palate. According to Kuninaka, "umami" may be defined as a taste of a flavor enhancer at a concentration higher than its threshold level [Kuninaka *et al.*, 1980].

Results of taste panel studies on processed foods indicate that an MSG level of 0.2-0.8% of food by weight optimally enhances the natural food flavor; similarly, the corresponding level of 5'-ribonucleotides required to generate the equivalent taste intensity may be in the 0.02-0.04% range (Nagodawithana, 1995). However, sometimes, the flavor-enhancing activity of a potentiator is noticeable even at concentration which are in the order of its detection threshold. It should be noted that the threshold values reported in the literature for sodium glutamate and

monoribonucleotides show considerable variation, depending on the method of measurement and the sensitivity of the panelists to umami taste [Yamaguchi, 1998].

1.3. Synergistic action between flavor enhancers

What is perhaps the most interesting property about MSG and 5'-ribonucleotides is their capacity to interact synergistically. This remarkable property between the two types of flavor enhancers was first identified by Kuninaka in 1960 [Kuninaka, 1960]. He found that the detection threshold of MSG was markedly lowered in the presence of IMP (or GMP) and vice versa [Sugita, 2002].

For example, the threshold of MSG in water decreased a hundred times when estimated in 0.25% solution of IMP, that is the flavor or MSG is potentiated by the presence of small concentration of nucleotides. In a complementary experiment, the taste threshold of a 1.1 blend of IMP and GMP was found to be about a hundred times lower when the mixture was dissolved into an aqueous solution of 0.8% MSG (see Table 1.1). These data clearly indicate that both GMP and IMP can significantly reduce the glutamate requirement and still maintain the desired flavor enhancing properties in food formulation.

Table 1.1. Taste Threshold of Umami Substances

	Detection Threshold (g/dl)
MSG alone	1.20×10^{-2}
IMP alone	2.50×10^{-2}
GMP alone	1.25×10^{-2}
MSG in 0.25% IMP	1.50×10^{-4}
IMP + GMP (1 : 1 blend)	6.30×10^{-3}
IMP + GMP (1 : 1 blend) in 0.8% MSG	1.30×10^{-5}

It is noteworthy that the synergistic interactions of MSG with IMP and/or GMP also occur in certain savory foods bringing about a flavor effect which is greater than the sum of the individual flavor-enhancing effects.

This phenomenon of synergism is of the utmost importance, because it provides an opportunity for the food processor to use less MSG in the formulation without affecting flavor quality. For instance, it has been found that food processors who use 100 g of MSG can reduce usage levels to 17 g in the presence of 0.9 g of 50:50 blends of IMP and GMP with a substantial (25-30%) cost reduction and without an adverse effect on the organoleptic properties of the processed food [Löliger, 2000].

Several combinations of MSG and GMP and/or IMP are now commercially available for use in the food industry. Most popular blend have MSG:5'-ribonucleotides ratio of about 95:5. Because of the improved efficacy of these blends due to the phenomenon of synergism, these flavor enhancers will be used at relatively low concentration in food formulations thereby providing a cost advantage to the food processor. The lower usage level of blends automatically eliminates the possibility of any flavor contributions by 5'-nucleotides because these compounds are, most likely, introduced to the food formulation at sub-threshold concentrations with respect to taste only to exert the synergistic flavor enhancement. Such low concentrations of 5'-ribonucleotides are capable of providing an impression of a much greater concentration of glutamate than is actually present in the food system [Nagodawithana, 1995].

Umami substances generally improve the intensity and pleasantness of foods only at a certain range of concentrations. Any excess can cause an unpleasant sensation in the palate. Thus the concentration of flavor enhancer intake by humans can be regarded as self-limiting. For example, an optimum amount of MSG appears to be around the concentration found in many natural foods, typically 0.1–0.8% by weight [Mouritsen, 2012].

It must be noted that certain yeast extracts that contain all three of these flavor enhancers (MSG, IMP and GMP) in natural form, are of particular interest to food processors not only because of the effect of synergism but also due to the background flavor these natural extracts elicit in savory food systems.

Yamaguchi investigated the synergistic effect in detail [Yamaguchi, 1998]. The relationship between the proportion of IMP in a mixture of MSG and IMP and the taste intensity of the mixture is shown in Figure 1.4.

MSG + IMP : 0.05g/ml
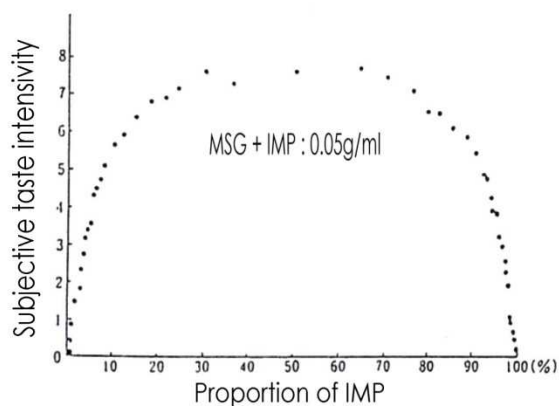
Figure 1.4. Relationship between umami intensity at different ratios of MSG and IMP

In addition Yamaguchi proposed a mathematical model to correlate the taste enhancement of MSG with its concentration and that of the enhancer present in the same aqueous solution. The relationship between the degree of taste enhancement and the two concentrations is expressed by equation 1.1, where u is the concentration of MSG, v is the concentration of the nucleotide, y is the concentration of MSG alone in a solution equivalent in taste intensity to the mixture ($u + v$), and γ is a constant.

$$y = u + \gamma \bullet v \bullet u \qquad\qquad (eq.\ 1.1)$$

Equation 1 is now generally accepted (providing that u is not too far from the subjective threshold value of MSG and v is in the range 2-14% u) and has been validated by studies on the flavor enhancing activity of compounds related to inosine 5'-phosphate. It must be noted that γ ($conc^{-1}$) is specific to the enhancer and is indicative of its synergistic capacity to increase the umami taste of MSG.

The synergistic action between MSG and flavor nucleotides was also demonstrated neurophysiologically. For example, the response of rat chorda tympani to IMP or GMP is greater than that to UMP or CMP, and the response to MSG was synergistically enhanced by addition of GMP (Figure 1.5) [Kuninaka, 1981].

8
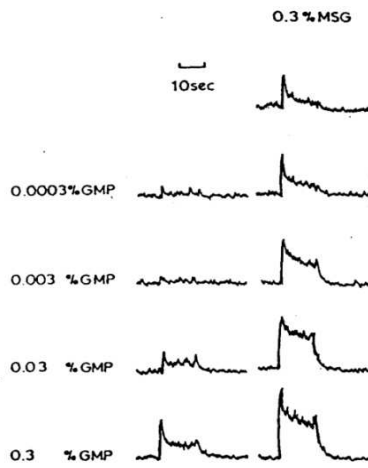
Figure 1.5. Integrated chorda tympani response to stimulation of the rat tongue by 0.3% MSG solution, 0.0003% - 0.3% GMP solutions, and 0.3% MSG solutions containing 0.0003% - 0.3% GMP.

1.4. Natural Occurrence of Umami

Umami compounds make a variety of foods palatable, although umami taste by itself is not particularly palatable. For example, a solution of MSG is not very palatable, but MSG added to soup greatly enhances its palatability. The effect of adding MSG to various foods has been investigated by a number of researchers [Yamaguchi & Ninomiya, 2000]. Think about biting into a cheddar cheeseburger with ketchup, spaghetti with marinara sauce and a dusting of Parmesan cheese or a salt-kissed slice of Jambon de Bayonne – the saliva-inducing, mouth-filling, deep, satiating taste – that is umami. In addition to being a unique standalone taste, umami seems to enhance the taste of foods it is combined with, intensifying other flavors as well.

Since umami flavor is imparted by a combination of substances that interact synergistically, the evaluation of the amount of both MSG and 5' riboucleotides (GMP and IMP) is necessary.

Free glutamic acid is naturally present in most foods, such as meat, poultry, seafood and vegetables [Yamaguchi & Ninomiya, 2000]. In addition, L-glutamic acid is one of the most abundant amino acid of food proteins (plant and animal), where it constitutes about 40% and 10-20% of the protein mass in animal and plant tissues, respectively. Therefore, the "bound glutamic acid" found in many common foods needs to be released to produce umami taste. Similarly, most nucleotides in living organisms are bound in nucleic acids, such as DNA, RNA and ATP. Thus, these nucleic acids have to be degraded and free nucleotides have to be released to produce umami flavor. Consequently, most raw foodstuff materials need to be processed in order to break down the proteins into free amino acids and the nucleic acids into free nucleotides to provide umami [Mouritsen, 2012]. Processes such as cooking, boiling, steaming, simmering, roasting, braising, broiling, smoking, drying, maturing, marinating, salting, ageing and fermenting contributes to the degradation of the cells and the macromolecules of which the foodstuff is made. Among them, fermenting, by microbes such as yeast and bacteria or by enzymes, is by far the most potent method of freeing umami compounds [Mouritsen, 2012].

Table 1.2 and 1.3 provide a selection of foodstuffs, some raw and some processed, along with their concentration of free glutamate and nucleotides as determined in the international literature [Kuninaka, 1981; Sugita, 2002; Behrens *et al.*, 2011].

Table 1.2. Umami compounds occurring naturally in several raw and processed animal foods (mg/100g).

Food		Nucleotides		
	MSG	IMP	GMP	AMP
Beef meat	33	90	4	8
Pork meat	23	200	2.5	9
Chicken meat	44	115	2.2	13.1
Cured ham	340	-	-	-
Clam	150-250	-	-	12
Eel	10	165	-	20.1
Mackerel	40-60	150-190	-	6.4
Oyster	265	-	-	-
Sardine	288	188	-	0.8
Scallop	140	-	-	172
Sea urchin	300-400	2	2	-
Tuna (katsuobushi)	268	630-1310	-	trace
Yellow fin tuna	4-9	286	-	5.9
Cow's milk	1,9	-	-	-
Human breast milk	22	-	-	-
Parmesan cheese	1680	-	-	-
Emmentaler cheese	308	-	-	-
Cheddar cheese	182	-	-	-

Sources: Kuninaka, 1981; Sugita, 2002; Behrens, 2011.

The data in Tables 1.2 and 1.3 show that among ribonucleotides that mostly contribute to the umami taste, GMP and IMP are present in many foods. Inosinate is found primarily in animal foods, whereas guanylate is more abundant in vegetable foods. Another ribonucleotide, 5'-adenylate, is abundant in fish and shellfish [Yamaguchi & Ninomiya, 2000]. However, its umami threshold concentration is lower than those of GMP and IMP. It appears from the Table 1.2 and 1.3 that umami is not a flavor that is found only in the Japanese cuisine, in fact it is associated with well-known and common

foods and food ingredients in western cuisine [Mouritsen, 2011]. For example, meats, ham, sea urchin, mackerel, katsuobushi and clams are the most taste active animal foods (Table 1.2).

Table 1.3. Umami compounds occurring naturally in several raw and processed vegetable foods (mg/100g).

Food	Nucleotides			
	MSG	IMP	GMP	AMP
Asparagus	106	-	trace	4
Beans	39	-	-	-
Broccoli	30	-	-	-
Cabbage	50	-	-	-
Carrots	33	-	1.5	-
Cauliflower	46	-	-	-
Celery	51	-	4-5	-
Eggplant	1-2	-	3	-
Green peas	106	-	-	2
Onion	102	trace	-	1
Potato	180	-	2,3	-
Spinach	48	-	-	-
Sweet corn	100	-	-	-
Tomato	256	-	10	21
Zucchini	16	-	7.5	-
Porcini mushroom	77	-	10	-
Shiitake mushroom	1060	-	216	321
Nori (seaweed)	1608	-	13	-

Sources: Kuninaka, 1981; Sugita, 2002; Behrens, 2011.

During the ripening of cheese, proteins are broken down progressively into smaller polypeptides and individual amino acids. In particular, significant increases in leucine, glutamate, lysine, phenylalanine and valine are noted [Weaver & Kroger, 1978]. Increases in the amount of these amino acids are generally recognized to be a reliable indicator of cheese ripening [Puchades *et al.*, 1989; Weaver & Kroger, 1978], and contribute to the taste and texture of the cheese [Ramos *et al.*, 1987]. For example, Parmesan cheese has the highest level of free glutamate.

Large increases in free amino acid content also occur during the curing of ham; glutamate is the most abundant free amino acid found in the final product [Cordaba *et al.*, 1994].

It is interesting to note that the glutamate content of human breast milk is up to 10 times higher than that in cow milk. Moreover, among the 20 free amino acids in human breast milk glutamate is the most abundant; it accounts for more than 50% of the total free amino acid content [Rassin *et al.*, 1978]. Glutamate presence may influence the taste acceptability to nursing infants (Figure 1.6). A series of studies on facial expressions of infants responding to different tastes showed that they display a happy expression after tasting something sweet, while they screw up their faces after consuming sour and bitter tasting foods. Interestingly, after consuming umami, in the form of vegetable soup with monosodium glutamate added, they display a calm face similar to that when having consumed something sweet [Steiner *et al.*, 1978; Steiner, 1993]. These results suggest that umami is a palatable taste for humans infants; by virtue of its presence in breast milk, it might conceivably contribute to the taste acceptability of this liquid.

| umami | sweet | sour | bitter |

Figure 1.6. The four images show the reactions of infants after tasting umami, sweet, sour and bitter.

Among vegetable foods that provide umami in Western tradition, asparagus, potatoes and peas have the highest levels of free MSG. Furthermore, the tomato is the "most umami" vegetable in the Mediterranean diet (Table 1.3). Its attractive, full, rounded "meaty" flavor comes from its heavy load of glutamates, and this flavor is reinforced by its unique crimson color. For these reasons the tomato is widely used throughout the world to impart the taste of umami in a wide variety of dishes.

The ripening of vegetables generally makes them more flavorful. For example, flavor maturation in ripening tomatoes has been related to the increase in their natural contents

of free amino acids, i.e. glutamate, sugars and organic acids (Figure 1.7) [Yamaguchi & Ninomiya, 2000].
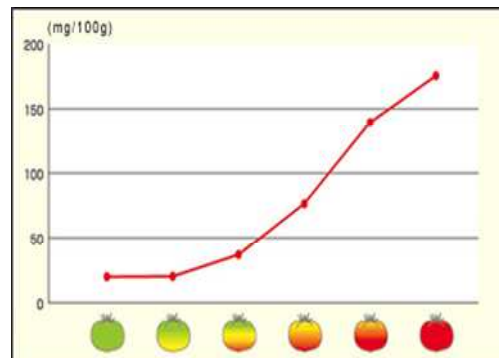
Figure 1.7. Level of free MSG in tomato during ripening

Okumura *et al.* [1968] prepared synthetic extracts of tomato containing citric acid, glucose, potassium hydrogen phosphate, magnesium sulfate, calcium chloride, glutamate and aspartate. The taste of the synthetic extract was greatly affected by the ratio of glutamate to aspartate. The ratio and the coexistence of both amino acids were the most important factors in reproducing tomato taste. When no glutamate was added to the extract, the taste was similar to green tomato or citrus. It is difficult to perceive a clear *umami* taste in tomatoes, but it is one of the most important taste components.

1.5. Manufacture of flavor enhancers

1.5.1. Production of glutamate

When Ikeda discovered MSG as the compound behind umami, he immediately realised the technological importance of his discovery and filed a patent (Figure 1.8) [Ikeda, 1908] for the production of pure MSG to be used as an artificial flavoring agent in foodstuffs [Sano, 2009; Wyers, 2010].
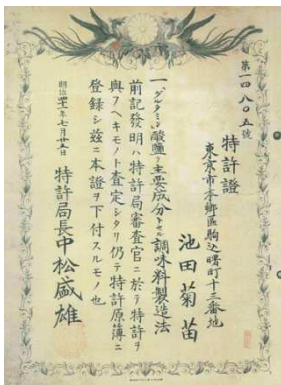
Figure 1.8. Patent on manufacturing seasoning (L-glutamate) filed by K. Ikeda [http://www.ajinomoto.com/features/aji-no-moto/en/basic/history.html].

In 1909 Saburosuke Suzuki, an entrepreneur, and Ikeda began the industrial production of monosodium L-glutamate (MSG).

The first industrial production process was an extraction from hydrolysates of vegetable proteins. The main raw material was wheat gluten, which contained up to 25% glutamic acid by weight. The gluten was subjected to hydrolysis by aqueous HCl. Glutamic acid hydrochloride was then isolated from the hydrolysate and purified by crystallization as MSG. Initial production of MSG was limited because of the technical drawbacks of this method. Better methods did not emerge until the 1950s. One of these was direct chemical synthesis, which was used from 1962 to 1973. In this procedure, acrylonitrile was the starting material, and optical resolution of DL-glutamic acid was achieved by preferential crystallization.

In the 1950s *Corynebacterium glutamicum* was found to be a very efficient producer of L-glutamic acid. Since then fermentation processes with bacteria of the species *Corynebacterium* became among the most important manufacturing methods in terms of tonnage and economical value.

The selected microorganism is cultured with carbohydrates and ammonia and releases the L-form of the amino acid into the culture medium. The cell produces glutamate from 2-oxo-glutarate (2-oxo-pentanedioic acid) by reductive ammonia fixation that uses the enzyme glutamate dehydrogenase, a normal cellular constituent.

The advantages of the fermentation method (*e.g.,* reduction of production costs and environmental load) were large enough to cause all glutamate manufacturers to shift to fermentation [Hermann, 2003].

In 2010, total world production of monosodium glutamate (MSG) was estimated to be 2.1 million MT (metric tonnes) and that of nucleotides 22,000 MT.[2] Ajinomoto, currently an international company, established by Ikeda itself owns about one third of the market for glutamate and 40% of the market for nucleotides.

"To create good, affordable seasonings and turn simple but nutritious fare into delicaciaes" was the motivation of Ikeda for inventing Ajinomoto and this is still the aspiration of Ajiinomoto group (Figure 1.9).

Figure 1.9. [http://www.ajinomoto.com/en/aboutus/principles/#page].
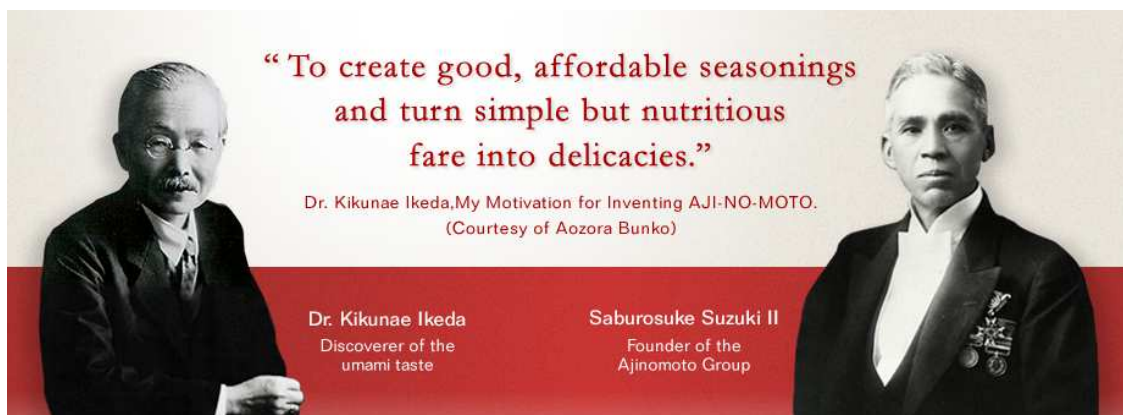
1.5.2. Production of 5'-nucleotides

As in the early days, when MSG was produced from proteins such as gluten, rich in glutamic acids, 5'-nucleotides were also initially from natural sources. In 1950s, production techniques that involve microbial fermentations with a higher level of productivity came into widespread use for both 5'-inosinic and guanylic acids. Today, the most used processes for the production of these flavor enhancers are:

- Fermentation methods
Various microbial sources such as *Candida utilis*, *Penicillium citrinum*, *Saccharomyces cerevisiae*, *Kluyveromyces marxianus*, *Brevibacterium ammoniagenes*, *Streptomyces aureus*, *Bacillus subtilis*, *B. megaterium*, *Micrococcus glutamicus*, *Methylobacter acidophilus*, and *Escherichia coli* have been reported to produce ribonucleotides and their derivatives [Kim *et al.*, 2002]. Mutants of *Brevibacterium ammoniagenes* are currently used because of their ability to overproduce 5'-GMP and 5'-IMP [Nagodawithana, 1995; Sugita, 2002].

- Degradation of microbial RNA using 5'-phosphodiesterase to form 5'-nucleotides. Subsequent conversion of 5'-AMP to 5'-IMP with adenylic deaminase enzyme.
Among the recent advances that were of benefit to food processing industry, production of yeast extracts high in flavor enhancing 5'-nucleotides was clearly a major development. Yeast is especially selected as a potential source of RNA because of its high RNA content (2.5-15%). It is Generally Recognized As Safe (GRAS) and can be grown economically to produce large quantities of biomass, rich in ribonucleic acid. Since nucleotides are the building blocks of RNA, one could expect the release of desired 5'-nucleotides, when RNA is hydrolyzed under controlled conditions in the presence of appropriate enzymes [Sugita, 2002].
MSG, IMP and GMP occur as colorless or white crystals or as white crystalline powders. They are odourless and dissolve in water readily.

1.6. New developments in umami molecules

In recent years, interest for taste (taste-active molecules, taste receptors, taste perception, etc.) is growing rapidly both in academia and in industry. In particular, in industrial field the aim is to find molecules that influence taste properties in a desired direction. Examples are increasing the sweetness of conventional carbohydrate sugars to maintain the positive taste properties of these sugars, while reducing the negative properties like high energy content and caries induction, or increasing the taste perception of salt (NaCl) so that less salt can be added to foods. It is well known that many people consume more salt than their bodies need, since the taste of salt added in foods is undoubtedly appealing. This behavior is especially pronounced in elderly people as we lose some of our sense of taste with age. On the other hand, nutritionists recommend a reduction of sodium chloride in the diet considering its correlation with coronary heart disease and hypertension [Winkel *et al.*, 2008].

In this regard, umami substances can be very useful when added in small amounts to foods with low level of salt by making them more acceptable and appetizing. It has been proven that up to 40% reduction in the NaCl content can be afforded without affecting palatability, provided that 0.6-0.8% MSG is added [Mouritsen, 2012].

Also for umami-tasting molecules there have been raised health concerns. In particular, MSG is accused of causing the so-called *Chinese restaurant syndrome* which was associated with the reporting of certain physiological effects following the intake of Chinese meals in which MSG was used as a flavor enhancer. The syndrome includes an ill-defined set of symptoms, such as numbness and tingling, flushing, muscle tightness, migraine headache and bronchoconstriction in some asthmatics.

Although the scientific evidence for any harmful effects of MSG and for a link between MSG and the symptoms are lacking, there is a slow but steadily growing negative public perception towards this flavor enhancer [Mouritsen, 2012].

It has been reported that the average person consumes between 10 and 20 grams of glutamate from their diet each day, with most coming from the protein-containing foods we eat as part of our normal diet. The body does not distinguish between the glutamate occurring naturally in food and the glutamate added as seasoning, so MSG brings nothing new to the diet. But the negative *aura* around this chemically sounding

ingredient has strongly stimulated research for more natural and clean-label sounding alternatives [Wyers, 2010].

It is not surprising that most of the research to find other umami-tasting molecules was carried out in Japan. Dozens of articles have been published on this topic. In particular, most of investigations have been focused on the constituents of materials commonly used as tasty ingredients in savory dishes because of their umami-like taste attributes and taste-enhancing activity.

Among them, of particular interest are Hydrolyzed Vegetable Proteins (HVPs) and yeast extracts.

1.6.1. Hydrolyzed Vegetable Proteins (HVPs)

Hydrolyzed vegetable proteins (HVPs) have been known for a long time in the food industry but only since the 1930s this product gained prominence as a flavoring agent to improve the flavor of processed foods. It is also used worldwide as a savory ingredient or a seasoning.

HVPs are generally described as either flavor donors, flavor enhancers or flavor donor/enhancer combination products. Flavor donors contribute a taste which becomes a definite feature of the final product. Additionally, the high concentration of glutamates in the product makes it a flavor enhancer enriching the naturally occurring flavor of the savory based foods. HVPs are known to contribute meatiness to foods, enhance and intensify naturally occurring savory flavors and generally round-off and balance the savory characteristics in the food material. It is thus used in soups, gravies, savory snacks, sauces, ready-to-eat meals and other meat-based products. These hydrolysates, like yeast extract, are known for their versatility and ease of application in food systems. Due to the high salt concentration (40-45%), these protein hydrolysates have an excellent shelf-life by normal standards. They contain strong flavor intensities offering low usage levels and thus lower costs in formulating wide range of finished food products. A major advantage of HVPs is its stability under varying process conditions. Hence, it can be used in canning and freezing processes without any

breakdown or change in flavor and also been used successfully in baking flavored snacks and crackers at around 180 °C [Nagodawithana, 1995; Loliger, 2000].

In a typical process for the production of HVPs, the raw materials include proteinaceous materials of plant origin mainly what gluten, corn gluten, defatted soy flour, defatted peanut flour, defatted cottonseed flour, etc. During the early 1950s the major raw material for making HVPs was wheat gluten because of the low cleavage cost, high glutamic acid concentration in this protein and relative abundance of the product. This has been largely replaced lately with 70% soy bean protein concentrates or a blend of these vegetable proteins.

HVPs are mainly prepared by enzymatic and/or acid hydrolysis of proteinaceous materials. The taste of HVPs is rigidly controlled by proper selection and blending of raw materials and appropriate selection of hydrolytic conditions. The large protein molecules are degraded by the acid due to the cleavage of the peptide bonds first into the short chain polypeptides and then to peptides and eventually to amino acids. Parallel to this sequence of reactions are other reactions that break down carbohydrates into flavor or flavors precursors such as 5-hydroxyfurfural, hydroxymethylfurfural and others which further undergo Maillard type reactions to produce other flavor compounds. A high ratio of acid to protein is generally employed to lower the extent of amino acid destruction and to improve the characteristics HVPs flavor. However, excessive usage of acid is generally avoided because of the high salt levels that would result following neutralization with the appropriate base.

Following hydrolysis, the reaction mixture is cooled and neutralized with 13% of pure caustic soda of food grade quality or a mixture of soda ash and caustic soda. The proportion of HCl and NaOH can vary within limits to achieve HVPs of different flavor profiles with definite salt concentrations. Furthermore, the pH after neutralization may vary between 5 and 6 depending on the nature of the original protein that was hydrolyzed or the type of flavor profile that the consumer is looking for in the final product. The salt formed by the acid neutralization contributes to the taste of the product.

To meet individual customer demands for savory flavor and to expand the application capabilities, development and refinement of the hydrolysis techniques have progressed considerably during the past years. The color, taste and salt content have been varied in

the final product by making minor adjustment in process condition and/or by varying the protein blend used in the process. The salt content, typically 40-45%, is directly linked to the level of HCl used in the process.

HVPs serve three important functions when incorporated in savory products such as meat: they contribute taste which becomes a special sensory feature of the food product, they serve as a precursor to develop other desirable flavor during subsequent processing and they also serve as a flavor enhancer thus intensifying the already existing savory notes in the food product.

The overall composition of the HVPs and their possible taste effects have been extensively investigated. Monosodium glutamate and salt (NaCl) are two major water soluble components that are capable of enhancing or "stretching" the flavor effect of other non-volatile taste compounds already existing in the food. HVP blends generally contain 9-12% naturally occurring MSG. Other non-volatile components of HVP with taste properties include amino acids and peptides (particularly dipeptides).

Several glutamyl oligopeptides have been shown to exhibit brothly taste. Other best known short peptides among the products tested with strong savory properties were Glu-Asp, Glu-Gly-Ser, Glu-Glu, Glu-Thr and Glu-Ser with weak brothy character. Analysis of the peptides in an enzymatic hydrolysate of deamidated wheat gluten revealed pyroglutamyl peptides such as pGlu-Pro-Ser, pGlu-Pro, pGlu-Pro-Glu, and pGlu-Pro-Gln as important umami-like-tasting molecules in this liquid seasoning [Schlichtherle-Cerny & Amado, 2002]. Moreover, enzymatic hydrolysis of fish proteins was reported to lead to savory products which are rich in acidic peptides such as Asp-Glu-Ser, Glu-Asp-Glu, Thr-Glu, and Ser-Glu-Glu. Such acidic di- and tripeptides were found to express weak umami activity by themselves but have been demonstrated to be significantly enhanced in the presence of IMP [Behrens *et al.*, 2011].

Brothy tasting compounds were shown to be more acidic, polar and hydrophilic than other flat tasting peptides [Arai *et al.*, 1973].

It must be pointed out that savory peptides are discussed controversially in the literature. For examples, recent work from an Indonesian group stated that the single amino acids L-glutamate and L-aspartate were the main contributors to umami taste in fermented soy sauce [Winkel *et al.*, 2008]. On the other hand, mixtures of amino acids in the proportion found in HVPs do not give the same flavor as the original

hydrolysates. It is thus clear that components of the hydrolysates other than amino acids play an important role in the flavor generation.

For example, chemical analysis of the most intense glutamate-like fraction of the enzymatic hydrolysate of acid-deaminated wheat gluten revealed the presence of different glycoconjugates of glutamate, glutamine and lysine. The most abundant Amadori compound, *N*-(1-deoxy-D-fructos-1-yl)-L-glutamate **1.1** (Figure 1.10) was identified as eliciting an intense umami taste [Schlichtherle-Cerny *et al.*, 2004].
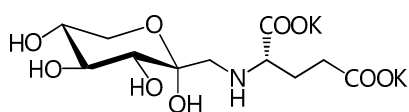
1.1

Figure 1.10.

Moreover, food additives, caramel, salt and MSG are often added to HPVs to generate flavor profiles that meet the specific flavor requirements of food processors. Food flavorists active in the field have been able to formulate several authentic, meat-like savory flavors by the direct controlled reaction between HPVs and reducing sugars such as glucose and xylose in the presence of other ingredients such as fatty acids, salt, spices, certain vitamins, esters of amino acids and sulfides. Such flavorings do play an important role in providing a distinct cooked top notes to savory-based products. Hydrolyzed vegetable proteins provide significant saving other flavorings such as beef extract while maintaining a similar or sometimes even a better flavor profile [Nagodawithana, 1995].

1.6.2. Yeast Extracts

Yeast extract is a concentrate of soluble material derived from yeast following hydrolysis of the cell material, particularly the proteins, soluble carbohydrates and nucleic acids (yeast is generally known for its high RNA content). This is generally carried out by use of its own hydrolytic enzymes (autolysis) or by other methods (plasmolysis or hydrolysis) in order to release the cell content in a highly degraded

form. It is commercially available most commonly as powders of different particle sizes but also as concentrated pastes of varying color, composition and flavor. Yeast extracts have become popular during the last few decades in part due to their usefulness as a natural flavoring agent and also for their ability to promote growth of microorganism in industrial fermentations. A major consideration in their use as a flavoring agent is their cost effectiveness compared to other flavoring agents on the basis of equivalent flavor intensity [Nagodawithana, 1995].

In contrast to MSG, yeast extracts have not shown any adverse reaction in humans and hence have, thus far, received the clean label status by virtue of being natural. They can be used as a natural flavoring or a flavor enhancer in a wide variety of savory food products. In addition, their background flavor characteristics are complementary to beef, pork, poultry and cheese flavor systems. Hence these ingredients provide an added advantage to the food processor.

Although both extracts and autolysates can be produced commercially from both brewers and baker's yeast, they can also be made from other species of yeast such as *Candida utilis* (torula yest) grown on ethanol or other carbohydrates substrates or *Kluyveromyces marxianus* grown on whey. These extracts or autolysates have their unique flavor characteristics different from one another and they are widely used as flavoring agents throughout the food industry.

The choice of the starting material for the production of yeast extracts is directly dictated by the cost and availability of the yeast and the quality expected in the final product. These extracts are commonly used in soups, gravies, broths, sauces etc., as in the case of MSG or 5'-nucleotides. The delivery of similar, if not better, flavor characteristics is primarily due to the background flavor of the yeast extracts, blending well with the flavor notes of the food to which they added. Many types of cheese flavored products such as crackers and fried snacks are commonly improved by the incorporation of yeast extracts. They increase the flavor impact and provide a sharper and more aged cheesy character. Food processors have often been able to reduce their ingredient costs by reducing the level of more expensive ingredients such as natural flavors, cheese and meat extracts. The natural 5'-nucleotides of some of these yeast extracts consistently demonstrate synergistic potentiating effects by interacting with the low levels of natural glutamate present in the extracts as well as in the food substrates to

provide the overall delicious character and enhanced savory attributes of processed foods.

Although a series of studies have been performed on the odor active volatile fraction of yeast extract, knowledge on the taste-active and/or taste-modulating nonvolatiles is rather limited.

Sensory-guided fractionation of a commercial yeast extract led to the discovery of the previously not reported umami-enhancing nucleotide diastereomers (*R*)- and (*S*)-N^2-(1-carboxyethyl)guanosine 5'-monophosphate (**1.2a** and **1.2b** Figure 1.11). Model experiments confirmed the formation of these diastereomers by a Maillard-type glycation of guanosine 5'-monophosphate with dihydroxyacetone and glyceraldehyde, respectively [Festring & Hofmann, 2010]. Sensory studies revealed umami recognition threshold concentrations comparable to that of 5'-GMP, especially for the (*S*)-isomer, and demonstrated the taste-enhancing activity of these nucleotides on MSG solutions.
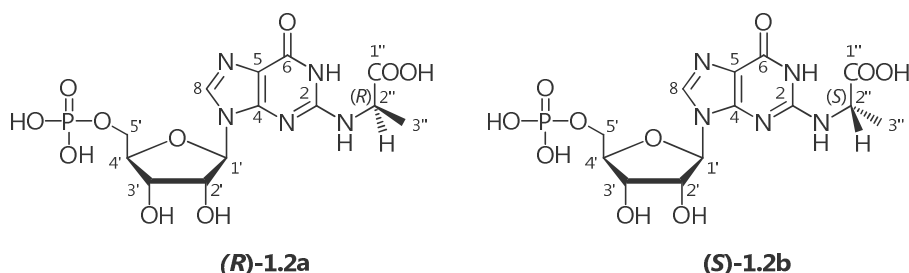
Figure 1.11. Chemical structure of (*R*)-N^2-(1-carboxyethyl)guanosine 5'-monophosphate **1.2a** and (*S*)-N^2-(1-carboxyethyl)guanosine 5'-monophosphate **1.2b**.

1.6.3. Natural Umami Compounds

Besides L-glutamate and ribonucleotides, additional umami-tasting molecules have been identified in various natural sources.

In 1998 Shima *et al.*, working at the *Ajinomoto*, isolated from a beef bouillon a condensation product of L-alanine and creatinine, *N*-(1-methyl-4-hydroxy-3-imidazolin-2,2-ylidene)alanine **1.3** (Figure 1.12), which imparted the favorable "brothy taste". This product was the first of a series of new types of umami molecules [Shima *et al.*, 1998].

1.3
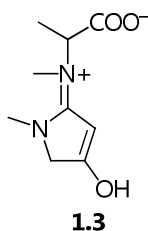
Figure 1.12. Chemical structure of *N*-(1-methyl-4-hydroxy-3-imidazolin-2,2-ylidene)alanine.

More recently, Kaneko *et al.* [2006] investigated the key compounds imparting the umami taste sensation induced by the consumption of so-called "mat-cha", a Japanese green tea, and identified - besides L-glutamate and succinic acid **1.4** - gallic acid **1.5**, (1*R*,2*R*,3*R*,5*S*)-5-carboxy-2,3,5-trihydroxycyclohexyl-3,4,5-trihydroxybenzoate **1.6** (known as theogallin) as well as *N*-ethylglutamine **1.7** (known as L-theanine) as important umami taste enhancing molecules (Figure 1.13).

1.4   **1.5**   **1.6**   **1.7**
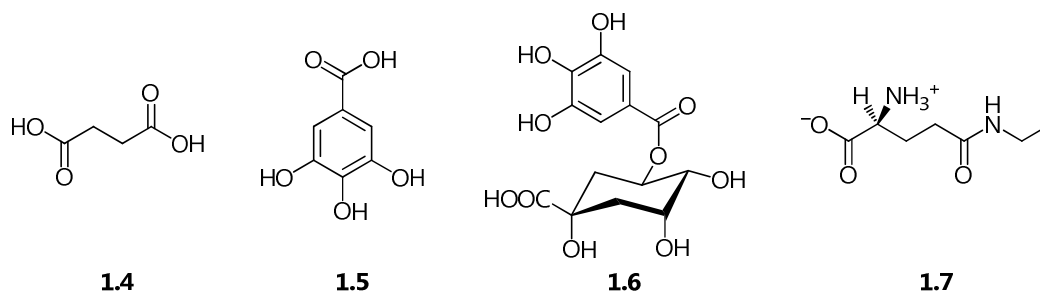
Figure 1.13 Chemical structure of some umami-tasting molecules identified in "mat-cha": succinic acid **1.4**; gallic acid **1.5**; (1*R*,2*R*,3*R*,5*S*)-5-carboxy-2,3,5-trihydroxycyclohexyl-3,4,5-trihydroxybenzoate **1.6** (known as theogallin); *N*-ethylglutamine **1.7**.

Thermal processing including drying has long been known to enhance umami and savory tastes of food products such as, for example, sun-dried tomatoes and mushrooms, respectively.

A so-called "sensomics" approach was developed to enable the targeted discovery of taste compounds and taste enhancing molecules in complex processed foods. This approach combines techniques of advanced natural product analysis and analytical psychophysical tools, and was used to systematically and comprehensively identify, catalog, and quantify the taste-active key metabolites produced upon food processing. Application of this sensomics approach revealed that the attractive savory taste of air-

dried Morel mushrooms is due to the enhancement of the umami taste of L-glutamate by (S)-malic acid 1-O-β-D-glucopyranoside **1.8**. This so-called (S)-morelid **1.8** is generated by the non-enzymatic glucosylation of L-malic acid upon drying the mushrooms [Rotzoll *et al.*, 2005]. A drawback of these condensation products is that they are quite instable and difficult to synthesize. Furthermore, *N*-(1-deoxy- D-fructos-1-yl)-L-glutamic acid **1.9** was identified in sun-dried tomatos in yields of up to 1.5% (on a weight basis), and confirmed to be generated by the Maillard reaction of L-glutamic acid and glucose upon the drying of foods (figure 1.14) [Behrens *et al.*, 2011].
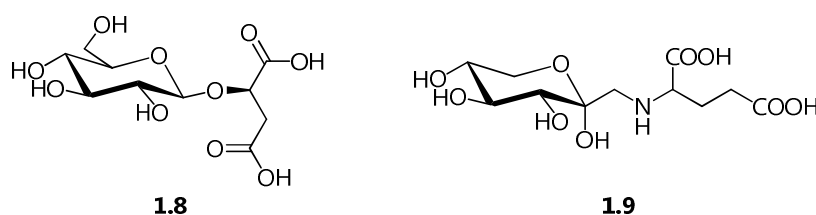
Figure 1.14 Chemical structure of umami-tasting molecules generated by thermal processing: (S)-malic acid 1-O-β-d-glucopyranoside **1.8** (known as (S)-morelid) and *N*-(1-deoxy- d-fructos-1-yl)- L-glutamic acid **1.9**.

Moreover, *N*-(1-carboxymethyl)-6-hydroxymethylpyridinium-3-ol inner salt, named alapyridaine **1.10** (Figure 1.15), was discovered as a taste enhancer in beef bouillon by means of the sensomics approach [Ottinger & Hofmann, 2003].
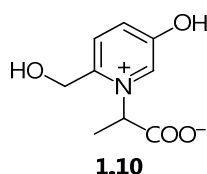
Figure 1.15. Chemical structure of *N*-(1-carboxymethyl)-6-hydroxymethylpyridinium-3-ol inner salt **1.10** (known as alapyridaine).

Model experiments demonstrated that this pyridinium salt is generated as a racemic mixture by the Maillard reaction of L-alanine and glucose from beef broth (Scheme 1.1) [Winkel *et al.*, 2008].
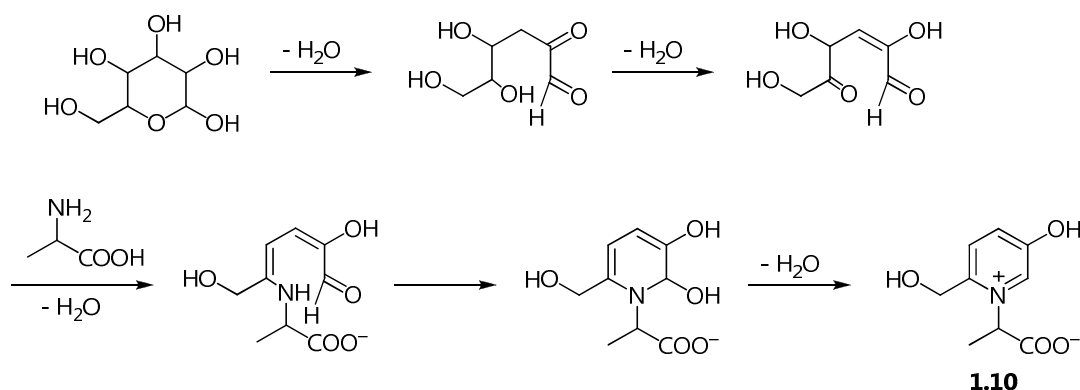
Scheme 1.1. Maillard reaction product of alanine and glucose from beef broth [Winkel *et al.*, 2008].

Although being tasteless on its own, the enantiomer (+)-(*S*)-alapyridaine was confirmed to significantly decrease the human recognition threshold of umami as well as sweet stimuli, whereas (-)-(*R*)-alapyridaine was physiologically not active [Soldo *et al.*, 2003]. A disadvantage of *alapyridaine* was the fact that it was required at equimolar quantities compared with the other umami-taste active compounds . Additional structure-activity relationship studies revealed that substitution of the alanine moiety in **1.10** by a glycine moiety converted the sweetness-enhancing alapyridaine into a bitter taste inhibitor [Soldo *et al.*, 2004].

Frerot and Escher (*Firmenich*) reported in a patent that also succinoyl amides of amino acids had umami-taste properties, such as *N*-succinoyl-*S*-methyl cysteine **1.11** (Figure 1.16) [Frerot & Escher, 2004].

1.11
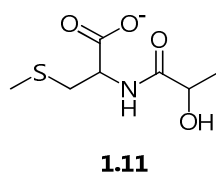
Figure 1.16. Chemical structure of *N*-succinoyl-*S*-methyl cysteine **1.11**.

In 2004 Schlichtherle-Cerny *et al.* (*Nestle*) claimed *Amadori*-rearrangement products, the first condensation step in the *Maillard* reaction, and other *N*-glycosides, pyroglutamyl-peptides and *N*-acetylglycine to have umami taste [Schlichtherle-Cerny *et al.*, 2004].

It is hard to say whether this series of molecules could bind to the glutamate or GMP/IMP binding side of an umami receptor. The structures are not similar but they are also not very different.

A quite different type of umami-tasting molecules came from the screening of a large set of molecules (>10,000) to find a series of very strong umami-tasting molecules [Tachdjian *et al.*, 2006]. As the used libraries had pharmaceutical origin, their molecular structures were very new to foods (Figure 1.17). These molecules have a much lower taste threshold value that is in the low μm to even nm range, and are the strongest umami-tasting molecules found so far. Moreover, since these compounds are very different in structure and hydrophobicity from MSG and IMP/GMP, it is likely that they bind to a different binding site on an umami receptor. The taste profile tests of these molecules are different as well. Probably due to their high affinity for the receptor, the taste is quite long-lasting and reminds a bit of the very strong artificial sweeteners.

1.12   **1.13**
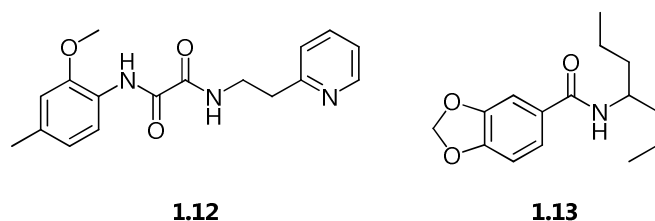
Figure 1.17. Different type of umami-tasting molecules

Among the umami molecules resembling ribonucleotides, the specific taste modulating flavor ingredient *N*-lactoylguanosine 5'-monophosphate **1.14** (*N*-lactoyl GMP, Figure 1.18) was identified in *bonito*, dried and fermentated skipjack, that is used to make *dashi*, a broth that is the basis for many Japanese foods [de Rijke *et al.*, 2007]. The organic synthesis of this compound showed that other amides of GMP had umami taste as well. For example, acetyl GMP **1.15** has a similar taste as lactoyl GMP but it enhances the salty taste as well [Winkel *et al.*, 2008]. These molecules had proved to be ca. 10 to 50 times stronger than GMP itself and therefore their strength is in between the common natural umami molecules and the artificial extremely strong umami molecules.
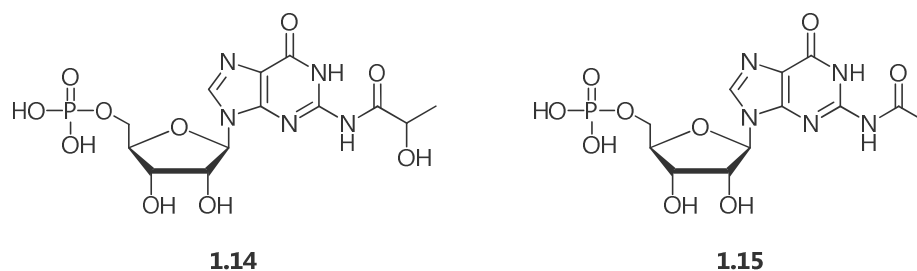
Figure 1.18. Chemical structure of *N*-lactoylguanosine 5'-monophosphate **1.14** and *N*-acetylguanosine **1.15**.

1.7. Ribonucleotides as Flavor Enhancers

As stated already, several 5'-nucleotides, in particular IMP, GMP, XMP (xanthosine 5'-monophosphate) and AMP (adenosine 5'-monophoshate), have particular flavor activity, and IMP and GMP have been used as flavor enhancer since 1961.

It is important to note that 5'-XMP, which has OH groups at C-2 of the purine ring has the weakest taste intensity of the three naturally occurring 6-oxo-purine flavor nucleotides. Hence it is the least important nucleotide of the three, from a commercial standpoint. Of the other two (5'-GMP and 5'-IMP), 5'-GMP in generally perceived as having a higher flavor enhancing intensity than 5'-IMP.

Although the taste intensity is not as strong as IMP or GMP, 5'-adenylic acid (AMP) is another important umami substance which is widely distributed in natural food, especially seafood.

Extensive investigations of the synergistic activity of inosinic acid derivatives were made in the seventies by Japanese researchers and are summarized in Table 1.4 [Imai *et al.*, 1971; Mizuta *et al.*,1972; Yamaguchi *et al.*, 1971; Kuninaka *et al.*, 1980].

Table 1. 4. Relative Flavor-Enhancing Activities of Naturally Occurring Flavor Nucleotides and Their Derivatives
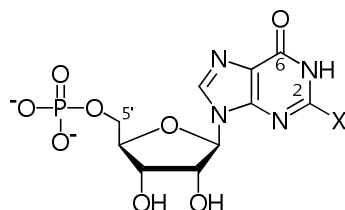
Nucleotide or derivate	Relative flavor activity
5'- IMP · 7.5H$_2$O	1
5'- GMP · 7H$_2$O	2.3 ± 0.07
5'- XMP · 3H$_2$O	0.61 ± 0.04
5'- AMP	0.18 ± 0.03
2-Methyl-5'- IMP · 6H$_2$O	2.3 ± 0.16
2-Ethyl-5'- IMP · 1.5H$_2$O	2.3 ± 0.14
2-Methylthio-5'- IMP · 6H$_2$O	8.0 ± 0.97
2-Ethylthio-5'- IMP · 2H$_2$O	7.5 ± 0.75
2-Methoxy-5'- IMP · H$_2$O	4.2 ± 0.33
2-Chloro-5'- IMP · 1.5H$_2$O	3.1 ± 0.25
2-N-Methyl-5'- GMP · 5.5H$_2$O	2.3 ± 0.15
2-N-Dimethyl-5'- GMP · 2.5H$_2$O	2.4 ± 0.13
2',3'-O-Isopropylidene 5'-IMP	0.21 ± 0.06
2',3'-O-Isopropylidene 5'-GMP	0.35 ± 0.06

Data from such investigations indicated that the structural requirements for MSG-enhancing activity by nucleotide molecules are:

(a) a purine nucleus as the base moiety;

(b) a free phosphate group at 5'-position (2'- or 3'-ribonucleotides have no flavor activity);

(c) an electron withdrawing group at the 6-position of the purine nucleus [Yamaguchi *et al.*, 1971; Kuninaka *et al.*, 1981];

(d) an unaltered ribose moiety (purine/pyrimidine base as well as their nucleosides have no flavor activity. In addition a strongly reduced activity occurs if the 2'-OH is replaced by H or the 2'- and 3'-positions are protected as in isopropylidene derivatives of IMP and GMP) [Yamaguchi *et al.*, 1971].

By contrast, a large variability of the synergistic effect between 5'-nucleotides and MSG was observed in 2-substituted inosinic acids [Kuninaka *et al.*, 1981; Imai *et al.*, 1971]. In particular, 2-alkylthio-IMPs (inosine 5'-monophosphatederivatives) showed pronounced activities when compared with IMP and GMP [Imai *et al.*, 1971] (Table 1.4).

It must be noted that, regardless of the structure/activity relationships (SAR) observed [Mizuta *et al.*,1972] only two N^2-substituted GMPs, i.e., methyl- and dimethyl-guanosine were submitted to sensory analyses indicating an activity comparable to that of GMP [Kuninaka *et al.*, 1981]. For this reason, recently our research group investigated the synthesis and the MSG enhancing activity of N^2-substituted 5'-guanylic acids [Cairoli *et al.*, 2008].

1.7.1. Synthesis of N^2-alkyl and N^2-acyl derivatives of 5'-guanylic acid

The synthesis of guanosine 5'-phosphates alkylated or acylated at the exocyclic amino group is reported in the Schemes 1.2 and 1.3. Proper reaction conditions were developed to optimize the yields of the desired products. In all cases 2',3'-O-isopropylidene protected guanosine was used as starting material.
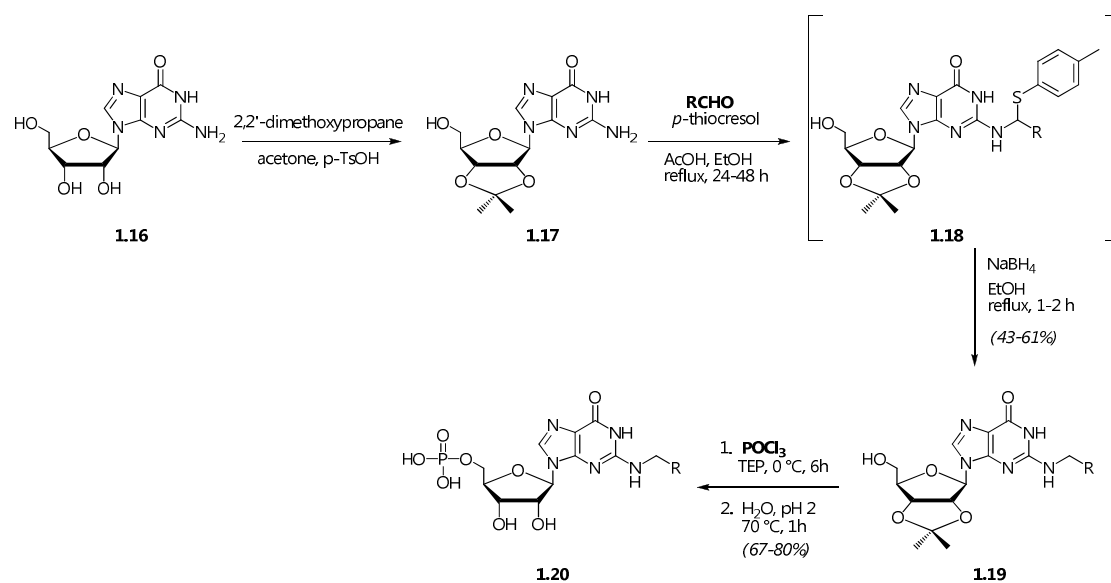
Scheme 1.2. Synthesis of N^2-alkyl derivatives of 5'-guanylic acid

Alkylation was carried out in two steps by reaction of the protected nucleoside **1.17** with an aldehyde and *p*-thiocresol, followed by reduction of the resulting thioadduct [N^2-[1-(*p*-tolylthio)alkyl]-guanosine] **1.18** with NaBH$_4$ in ethanol. The intermediate nucleosides **1.19**, obtained in satisfactory yields, were finally treated with phosphorus oxychloride in triethyl phosphate.

The early introduced protecting group, which was suitable for the next phosphorylation, was then removed in the working up of the last reaction mixture giving rise to nucleotides.

The N^2-alkyl derivatives of 5'-guanylic acid we synthesized and tested for their synergistic effect with MSG are depicted in Figure 1.20. The replacement of the methylene group by a sulfur atom in the aliphatic chain linked to the exocyclic amino group (compounds **1.20b** and **1.20c**) was suggested by the SAR data previously observed for 2-alkylthio inosinic acids [Kuninaka *et al.*, 1981; Imai *et al.*, 1971] as well as taking into account the large variety of sulfur containing compounds which contribute to the flavor of many umami foods (meat, mushroom, onion, garlic and so on) [Kuninaka *et al.*, 1980; Widder *et al.*, 2000].
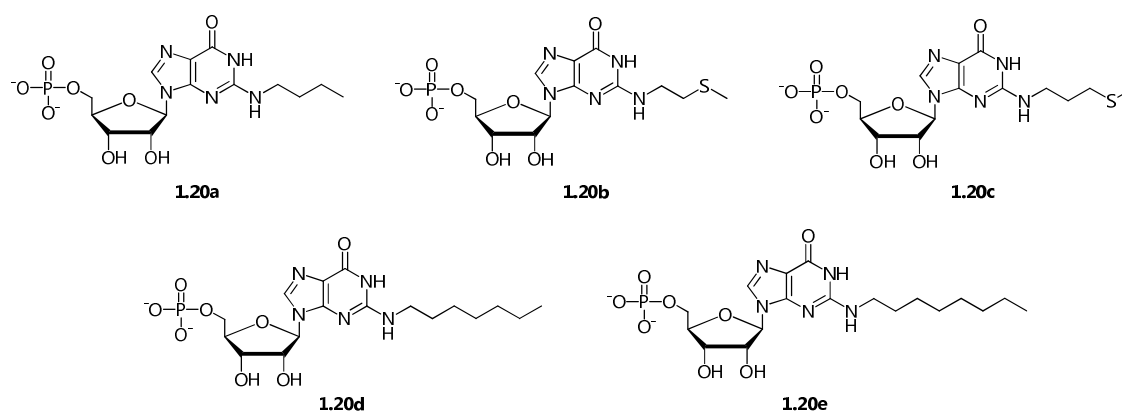
Figure 1.20. N^2-alkyl derivatives of 5'-guanylic acid synthesized.

Acylation of guanosine amino group, performed as reported in Scheme 1.3, was based on a preliminary silylation of 2',3'-*O*-isopropylidene guanosine (**1.17**), followed by treatment of the reaction mixture with the specific acyl chloride at room temperature in one-pot procedure. Such a method is known as transient persilylation and allows to overcome the very low reactivity of the amino group of guanosine and the competition

of the nucleophilic oxygen atom in 6-position in the acylation reaction [Cairoli *et al.*, 2008]. In this way 2',3'-O-isopropylidene-N^2-acylated guanosines (**1.22**) were obtained in good yields and used for the final phosphorylation step which was carried out as previously allowing the simultaneous removal of the protecting group.
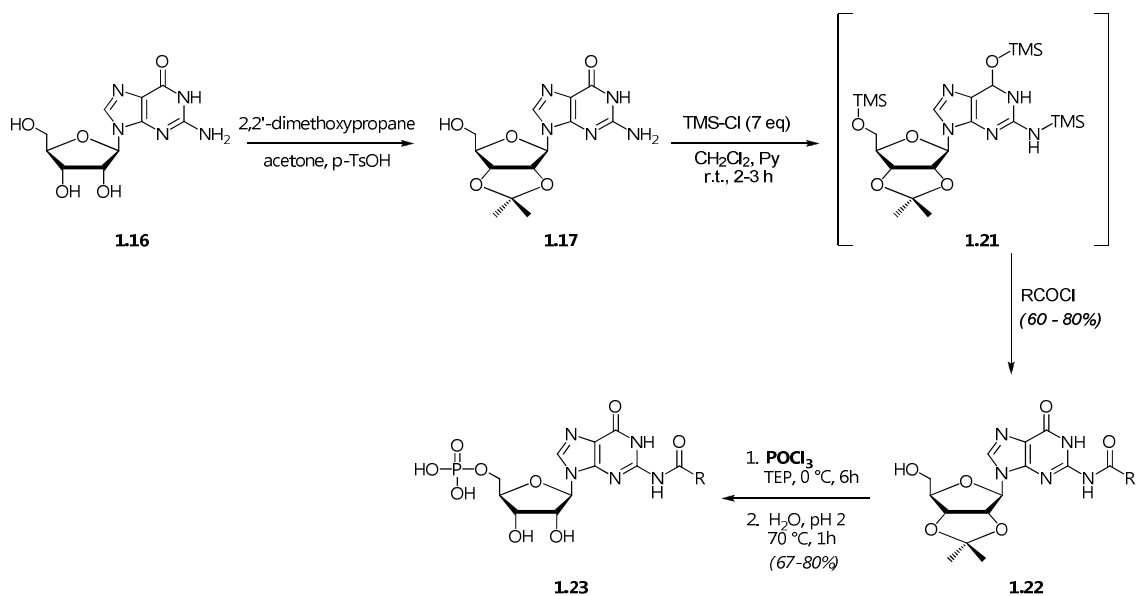
Scheme 1.3. Synthesis of N^2-acyl derivatives of 5'-guanylic acid.

The guanylic acid derivatives we obtained by acylation of the amino group of guanosine are depicted in Figure 1.21.
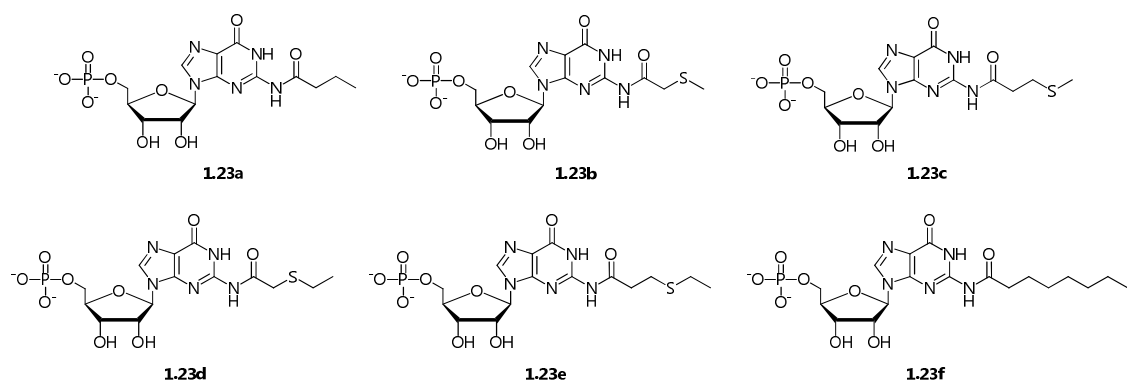
Figure 1.21. N^2-acyl derivatives of 5'-guanylic acid synthesized.

1.7.2. Sensory testing

The umami potential of the synthetic 5'-ribonucleotides **1.20a-e** and **1.23a-f** was estimated for their ability to enhance the taste intensity of MSG [Yamaguchi, 1998; Nagodawithana, 1995; Toyono *et al.*, 2003]. For aqueous solutions containing MSG and a given purine 5'-ribonucleotide disodium salt a general equation (1.2) was proposed by Yamaguchi [1967]:

$$y = u + \gamma uv \qquad\qquad\qquad (eq.\ 1.2)$$

where

u is the concentration of MSG,

v is the concentration of the purine 5'-nucleotide,

y is the concentration of MSG alone in a solution equivalent in taste intensity to the mixture *(u + v)*, and

γ (conc^{-1}) is a constant specific to the 5'-ribonucleotide present in the mixture which can be assumed to be indicative of the synergistic capacity of the nucleotide to increase the umami taste of MSG.

We performed quantitative measurements of such taste enhancement using a panel of trained tasters and the "Probit method" to make the responses of panelists statistically valid.

A solution named "fixed sample" containing MSG (u, 10.0 mM) plus the test compound (v, 0.4 mM) (pH 7.3) was compared, by the "sip and spit" procedure, with single solutions of MSG (five "reference samples" having concentrations determined in logarithmic equal steps at 40% intervals).

Five pairs of the fixed sample and one of the 5 reference samples (40 mL in randomly-coded glasses) were presented to each taster. Panelists were asked to indicate which in each pair had the stronger umami taste. The response for each reference sample was considered as positive when the fixed sample had the stronger taste. Replications were 5 for each panelist,

According to the Probit method, every percentage of positive responses was plotted as ordinate against the logarithm of the MSG concentration of the corresponding reference sample (plotted as abscissa) (Figure 1.22). The best straight line fitting the five points

34

on the coordinate plane was then calculated. For the percentage value of 50 read as ordinate, the abscissa of the line afforded the logarithm of the MSG concentration of a solution equivalent in taste to the fixed sample. Such concentration (y) allowed the γ value to be estimated from *equation 1.2*.
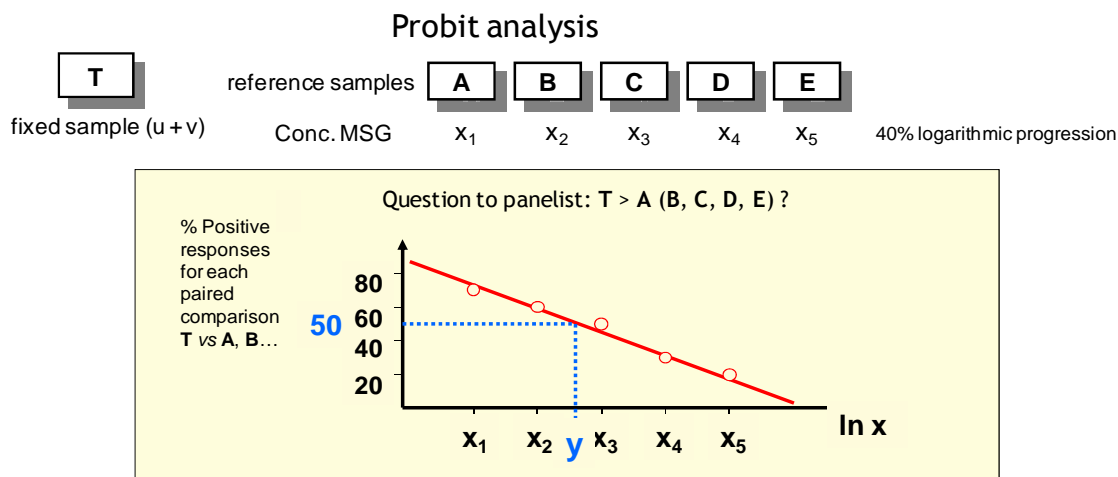
Figure 1.22. Probit analysis carried out.

The γ value of each N^2-alkyl and N^2-acyl derivative of 5'-guanylic acid was then referred to the γ value of IMP (measured with the same procedure), thus expressing the synergistic capacity as β [β being equal to γ (nucleotide) divided b γ (IMP)]. β values of the nucleotides we tested are reported in Figure 1.23.

In the diagram shown in Figure 1.23 the capacities β of N^2-substituted guanylic acids are plotted against the chain length of the substituent. At first glance a dependence of the glutamate taste enhancing activity on the chain length of both the alkyl and acyl substituent appears to be evident. In the range of 1 to 8 terms of the chain, including the sulfur atom, such an activity was found to be higher than that of GMP, reaching a maximum corresponding to about 6 times that of IMP for a number of terms equal to 5.

Two additional features of SAR type may be noticed : the synergistic efficacy decreases slightly when an alkyl chain is replaced by the corresponding acyl substituent; on the contrary, it increases if a sulfur atom is inserted in the methylene chain. Such an increase results to be larger if the replaced methylene group is in δ rather than in γ position.

$$\beta = \gamma \text{ (nucleotide)} / \gamma \text{ (IMP)}$$
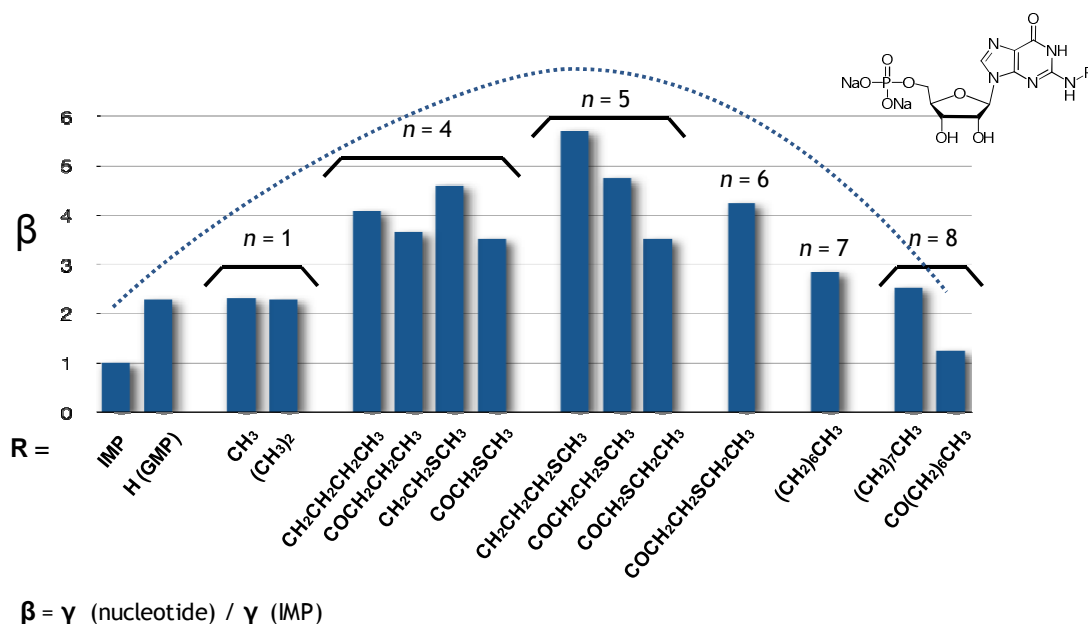
Figure 1.23. MSG-enhancing capacities of N^2-substituted 5'-guanylic acids referred to IMP. n indicates the chain length of the substituent in the 2-position of the purine nucleus.

It is well known that many flavoring and odoriferous natural compunds contain the sulfoxide function [Mithen, 2006]. For instance, some sulfides and the corresponding sulfoxides occur in plants of the genus *Allium*. *S*-alkyl and *S*-alkenyl cysteines, their sulfoxides, and other derivatives from enzymatic degradations are responsible for the characteristic pungent odor of garlic and onion both in intact and crushed bulbs.

R = $H_2C{=}CH{-}CH_2{-}$: alliin (garlic)
R = $H_3C{-}HC{=}CH{-}$: isoalliin (onion)
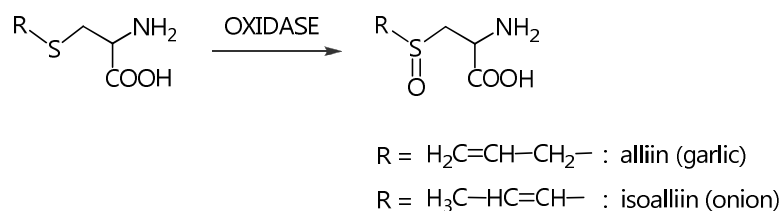
Scheme 1.4. Sulfur compounds occurring in garlic and onion.

Considering this fact, we prepared the sulfoxides of the guanylic acids bearing a sulfur atom inserted into the carbon chain of their N^2-alkyl or N^2-acyl substituents with the aim of comparing them to the corresponding sulfides for the ability to enhance the intensity of MSG taste [Morelli *et al.*, 2010].

These compounds were prepared using the same synthetic strategies of alkylation and acylation of the exocyclic amino group of guanosine described above.

Oxidation of sulfides **1.28** to sulfoxides **1.29** was carried out as the last step, using hydrogen peroxide as reagent under neutral condition to give the desired product in quantitative yield (Scheme 1.5).

If not commercially available, the sulfur-containing aldehydes **1.26** were prepared by reaction of the proper ω-bromo diethylacetal **1.24** with a thiol **1.25** followed by hydrolysis of the acetal function in the presence of the resin Amberlyst-15.
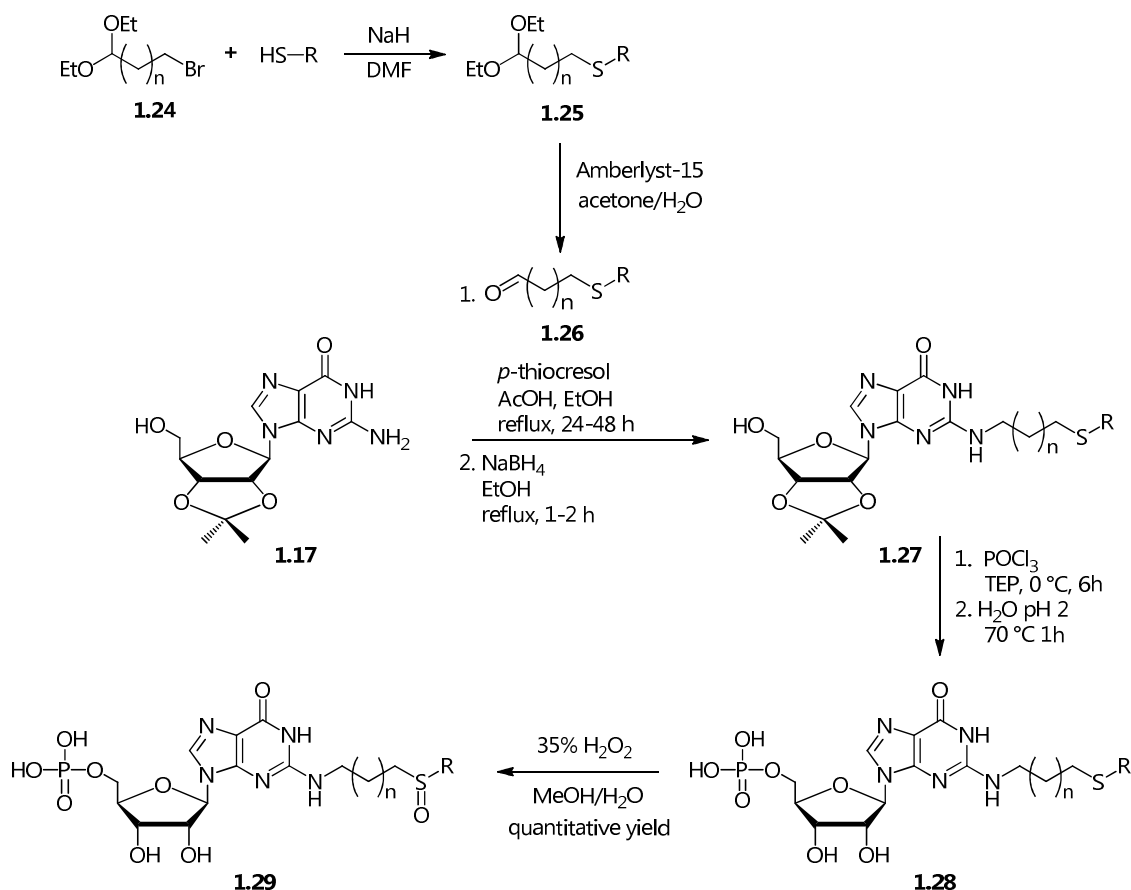
Scheme 1.5. Synthesis of sulfoxides of N^2-alkyl substituted 5'-guanylic acid.

In the case of acyl derivatives, the sequence of reactions was similar to that previously described (Scheme 1.6).

If not commercially available, the sulfur-containing carboxylic acids **1.32** were prepared by reaction of the proper omega-bromo ester **1.30** with a thiol followed by hydrolysis of the ester function as reported here.
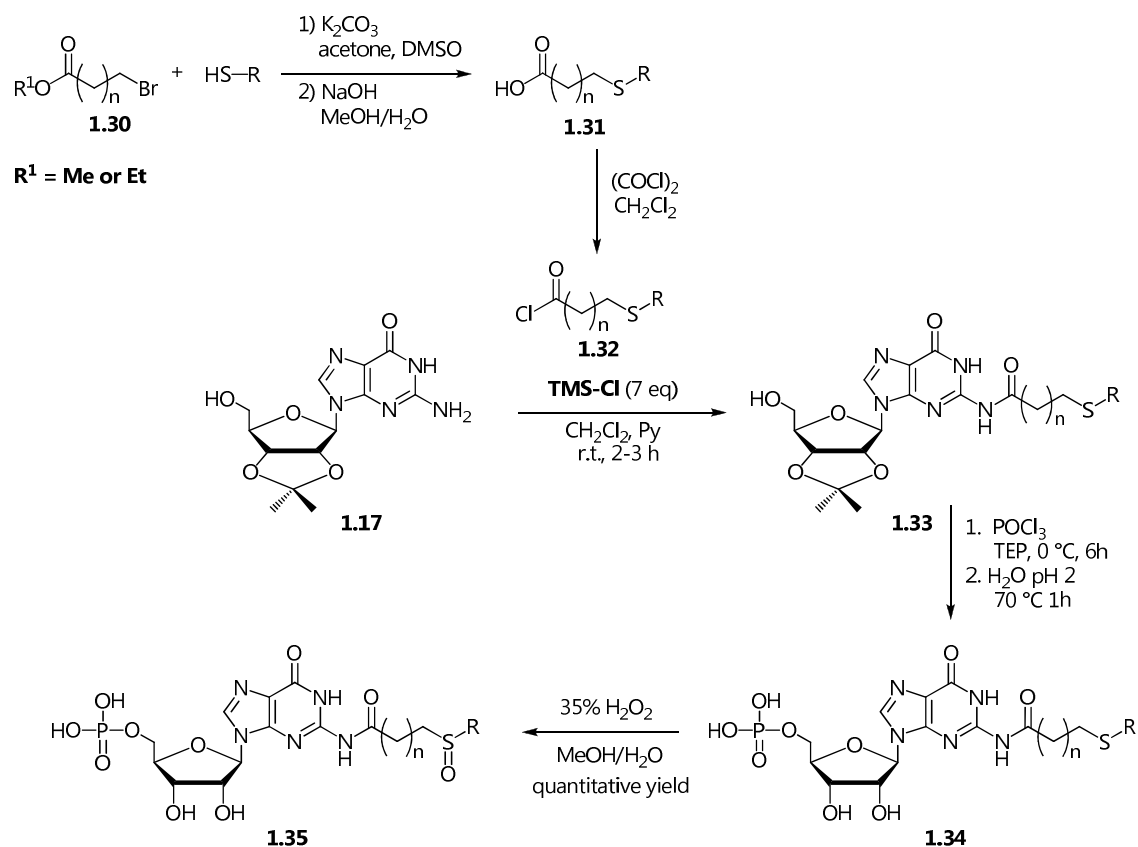
Scheme 1.6. Synthesis sulfoxides of N^2-acyl substituted 5'-guanylic acid.

The sulfides and sulfoxides we prepared by using these strategies are shown in Figure 1.24. At present, only the first three sulfoxides of this list have been tested using the same sensory procedure as described before.

38
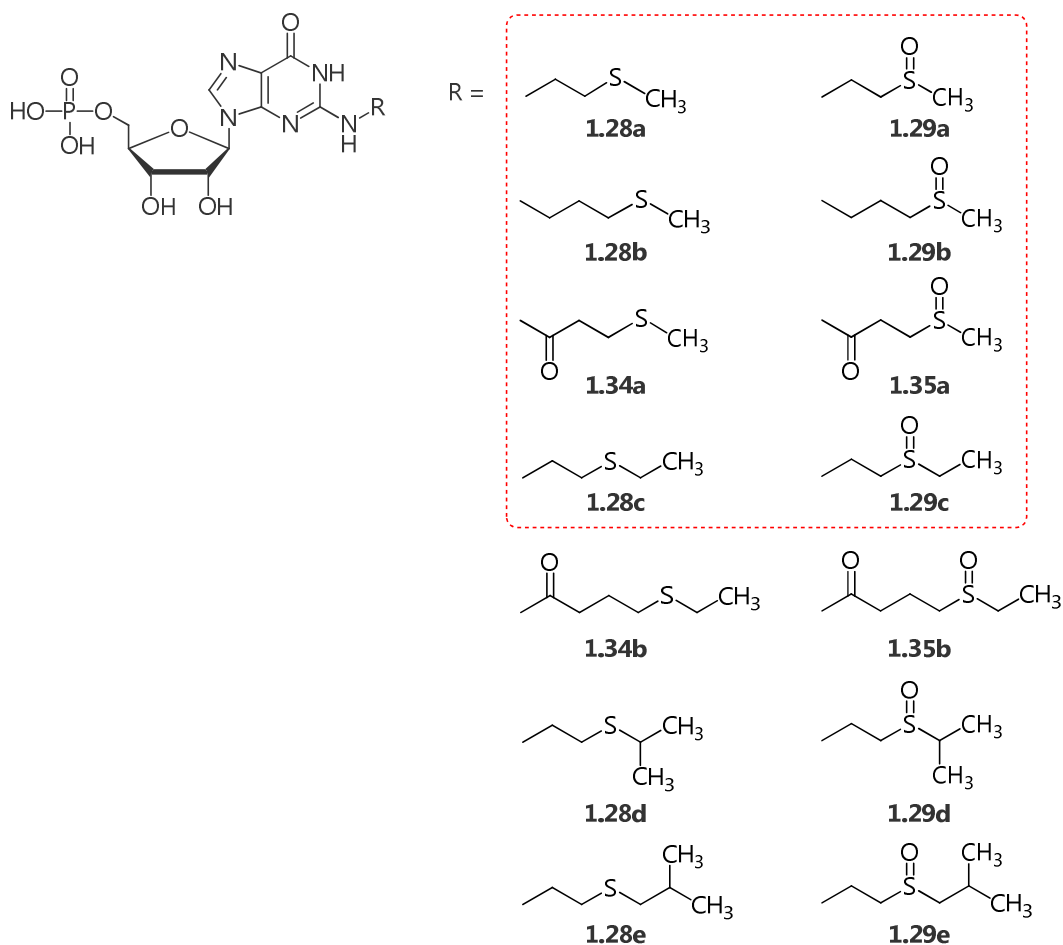
Figure 1.24. Sulfides and sulfoxides derivatives of 5'-guanylic acid synthesized.

As shown in Figure 25, the synergistic activity of each sulfoxide toward MSG when expressed by its β value, resulted to be lower than that of the corresponding sulfide. However, we noticed that in all cases, the perception of the glutamate taste appeared to be affected by some additional, but pleasant, sensory effect.

A possible explanation of the lower β-values observed is that sensory analyses were carried out on the diastereoisomeric mixture of each sulfoxide (**1.29a**, **1.29b**, **1.35a**). In fact, it has been recently reported that the stereochemistry of the N^2-substituent strongly influences the umami enhancing activity of a series of Maillard-modified guanosine 5'-monophosphates [Festring *et al.*, 2011a and 2011b].
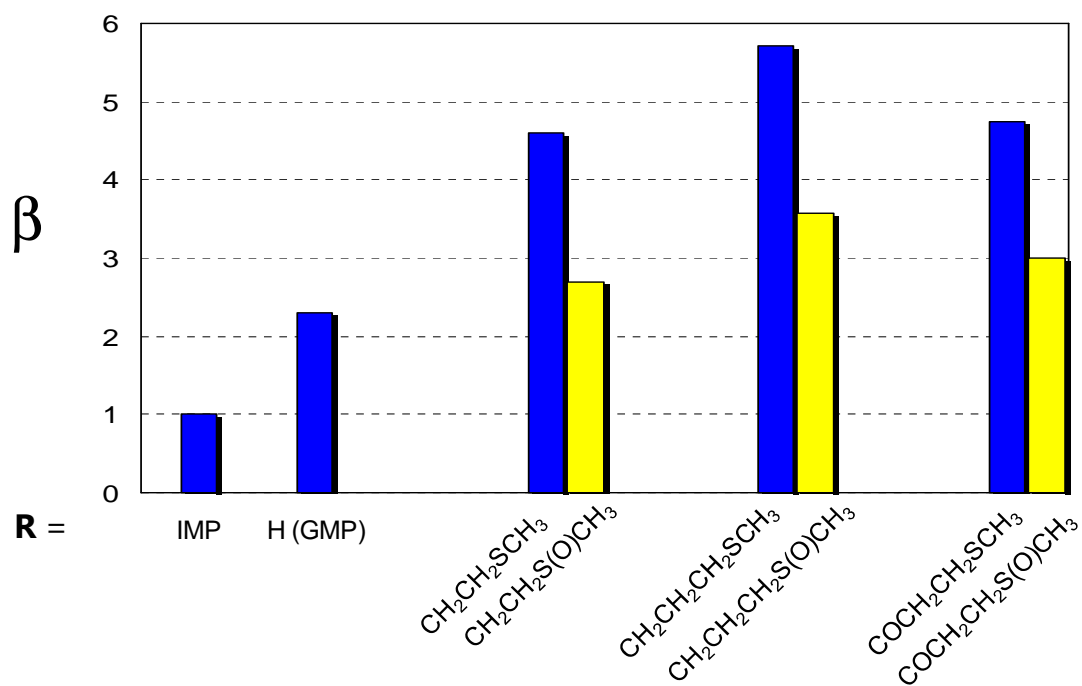
Figure 1.25. MSG-enhancing capacities of sulfides and sulfoxides synthesized.

1.8. Functional Anatomy of the Taste System

The organ primarily involved in taste perception is the tongue. Similar to stimuli of the other basic tastes, umami molecules interact with the apical membrane of specific sensor cells, namely, the taste receptor cells (TRCs) in the oral cavity. TRCs are not of neuronal origin, but are specialized epithelial cells [Behrens *et al.*, 2011]. They are innervated by afferent nerves (transmitting towards the control nervous system) to transduce gustatory signals to the brain [Witt *et al.*, 2003].

TRCs are found together with other cells in small aggregates called *taste buds* which are the proximate sensory organs of taste. These onion-shaped structures contain about 50–150 cells, including sensory neurons, that are embedded in the non-sensory epithelium.

Fingerlike projections called *microvilli*, which are rich in taste receptors, project from one end of each sensory neuron to the surface of the tongue. Nerve fibers at the opposite end of each neuron carry electrical impulses to the brain in response to stimulation by tastants.

Structures called *papillae* contain numerous taste buds. Taste buds are found in the three types of chemosensory papillae on the tongue: the fungiform papillae of the anterior tongue, the foliate papillae of the posterior tongue edges, and the circumvallate papillae of the posterior tongue (Figure 1.26) [Miller, 1995].

Taste buds also occur numerously in the soft palate and are present in the pharynx, larynx, and epiglottis. Extralingual taste buds, however, are not organized in papillae [Sbarbati *et al.*, 2004].
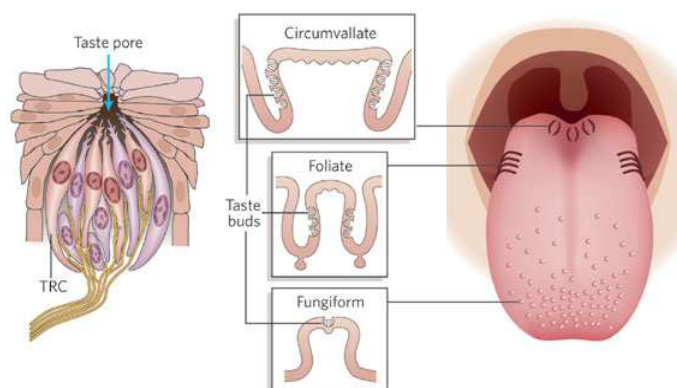
Figure 1.26. Taste buds (left) are composed of 50–150 TRCs, distributed across different papillae [Chandrashekar *et al.*, 2006]

Recent molecular and functional data have revealed that, contrary to popular belief, there is no tongue 'map' (Figure 1.27); indeed, responsiveness to the five basic modalities (bitter, sour, sweet, salty and umami) is present in all areas of the tongue [Chandrashekar *et al.*, 2006] even if with slight differences in the local sensitivity.
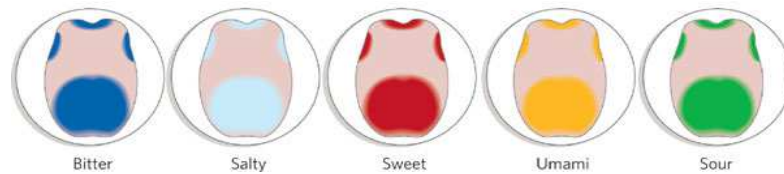
Figure 1.27. Classical tongue 'map' [Chandrashekar et al., 2006]

The perception of taste begins with the interaction of "tasty" molecules with specific receptors present on the membrane of cells (TRCs) constituting the taste buds. This interaction causes electrical changes in taste cells that are transformed into chemical signals and converted to impulses to the brain.

Detection of the gustatory world is mediated by several distinct classes of taste receptors and taste receptor cells (Figure 1.28).
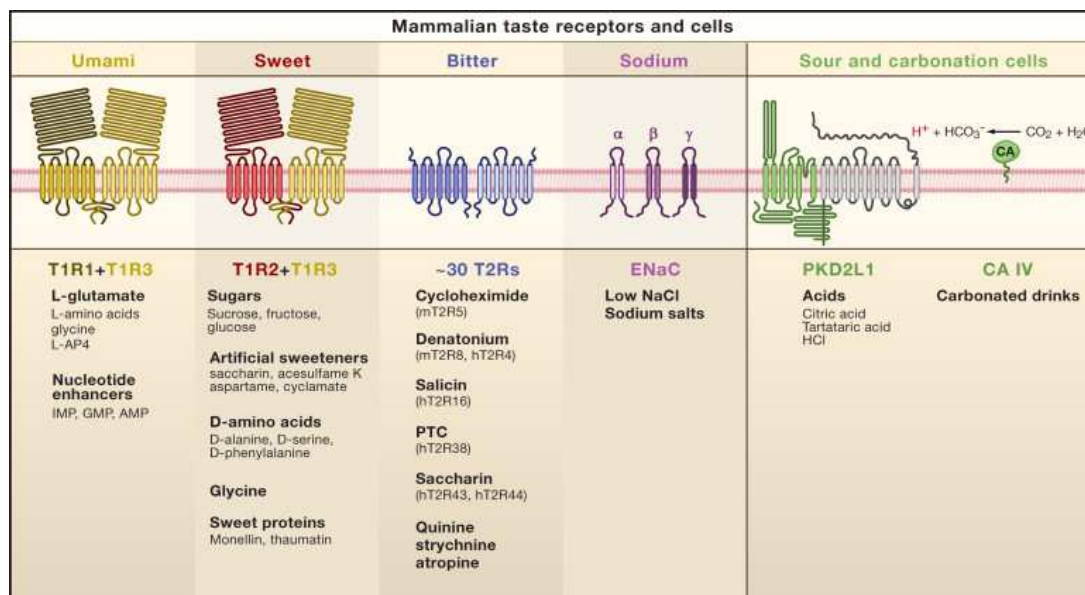
Figure 1.28. Mammalian Taste Receptors, Cells, and Ligands [Yarmolinsky *et al.*, 2009]

Interestingly, both sweet and umami tastes are sensed by heterodimeric G protein-coupled receptors (GPCRs) assembled by the combinatorial arrangement of T1R1, T1R2, and T1R3 subunits [Nelson *et al.*, 2001, 2002; Li *et al.*, 2002].

42

1.9. Umami taste receptors

1.9.1. Taste-mGluR4 and mGluR1tr

The discovery of *umami* receptors using methods of molecular biology is one of the recent highlights of taste research [Lindemann *et al.*, 2002]. In 2000, a metabotropic glutamate receptor, similar to the mGluR4 receptor usually present in the brain, was found on the tongue, specifically in the taste buds. It is a G protein-coupled metabotropic receptor. The taste variety of mGluR4 has a truncated *N*-terminal region to which L-glutamate still binds, even if with reduced affinity (Figures 1.29A-1.29B). Presumably, the truncation adapted the receptor to the high glutamate concentration in food [Chaudari *et al.*, 2000].
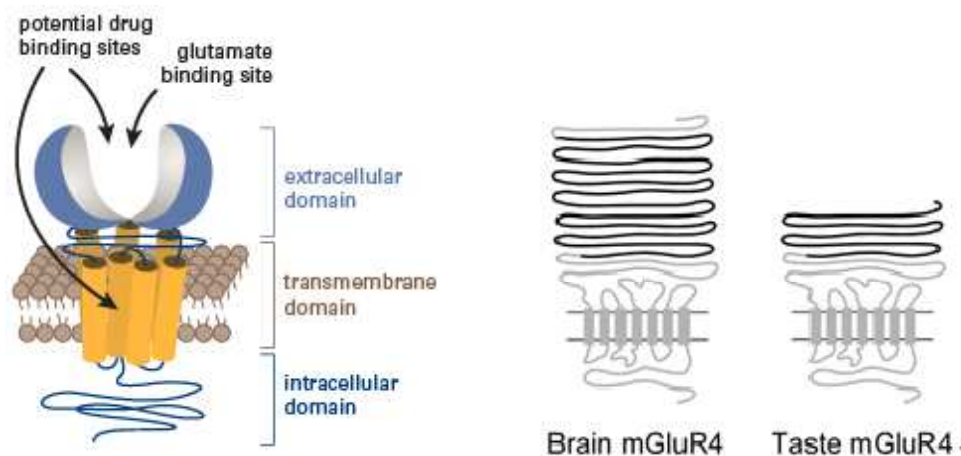
Figure 1.29. A) Structure of the metabotropic receptor of glutamate (GPCR). B) Predicted transmembrane topology of brain- and taste-mGluR4 showing the truncated extracellular N terminal domain followed by seven putative transmembrane helices [Chaudari *et al.*, 2000].

Figure 1.30 shows the 5' end of mGluR4 cDNA from taste papillae (lower lines) aligned with the corresponding region of mGluR4 cDNA from brain (upper lines). Amino acid (bold) and translated nucleotides (regular text) for each sequence are numbered. A stop codon (Δ), in frame with the long open reading frame, is found within the novel region of the cDNA from taste tissue. Sequence identity between the two cDNAs begins abruptly at the codon for R291.

```
264        E  F  D  K  I  I  K  R  L  L  E  T  S  N  A  R  G  I  I  I  F  A  N  E  D
+790    GAGTTCGACAAGATCATCAAACGCCTACTGGAAACATCCAATGCCAGGGGTATCATCATCTTTGCCAACGAGGAT

-128        GCCTGGGGCACCGGCACACAGACTAGGGCAGCTGGGTAGCCTTACATGTCTGGGCTGGGTTGCTGTGT
                                              △


289    D  I  R  R  V  L  E  A  A  R  R  A  N  Q  T  G  H  F  F  W  M  G  S  D  S  W  G
+865  GACATCAGGAGGGTGTTGGAGGCAGCTCGCAGGGCCAACCAGACCGGCCACTTCTTTTGGATGGGTTCTGATAGCTGGGGC
           |||||||||||||||||||||||||||||||||||||||||||||||||||||||||||||||||||||||||
- 60  CCCCACAGGAGGGTGTTGGAGGCAGCTCGCAGGGCCAACCAGACCGGCCACTTCTTTTGGATGGGTTCTGATAGCTGGGGC
   1                                                          M  G  S  D  S  W  G
```

Figure 1.30. Alignment of mGluR4 cDNA 5' ends from taste papillae (lower lines) and brain (upper lines) [Chaudari *et al.*, 2000].

Glutamate activates also a mGlu receptor related to the brain mGluR1 receptor (Figure 1.31). Taste mGluR stimulates maximal inward current at a higher L-glutamate concentration (25 mM) than that required by the brain type (0.1 mM) [San Gabriel, 2007].
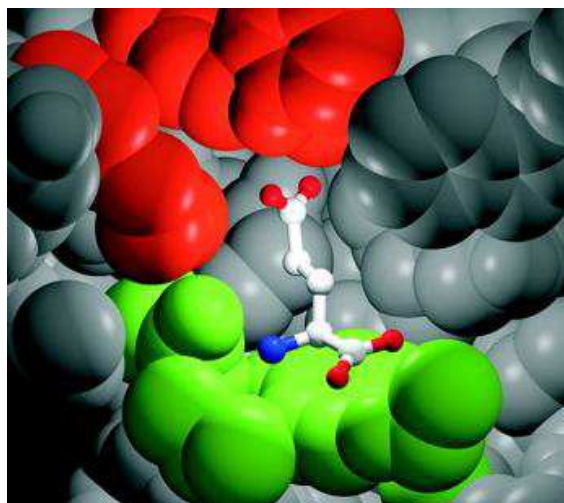
Figure 1.31. Glutamate in the binding site of mGluR1 receptor. Residues in contact with the L-glutamate side chain carboxylate are shown in red, and residues that contact the L-glutamate α-amino acid moiety are shown in green. [Figure from Li *et al.* 2002].

1.9.2. Umami receptor T1R1 - T1R3

More recently, another *umami* receptor was discovered. Interestingly, this is a heterodimer built of the G protein coupled receptors T1R1 and T1R3 [Li *et al.*, 2002; Nelson *et al.*, 2002]. It is related to the sweet taste receptor, which belongs to the same family, being a heterodimer T1R2-T1R3 [Li *et al.*, 2002; Nelson *et al.*, 2001].

44

Therefore, sweet and umami receptors have the subunit T1R3 in common. In mice the heterodimer T1R1-T1R3 responds to many amino acids contained in food, but in humans its response is preferentially to L-glutamate and it is the only known umami receptor sensitive to both glutamate and nucleotides [Nelson *et al.*, 2002]. The T1R1-T1R3 umami receptor is therefore a strong candidate for the synergistic effect between glutamate and guanosine or inosine described previously. As the T1R3 subunit of the dimeric receptor is in common with the umami and the sweet repeceptor, glutamate binding site should be on the T1R1 subunit of the umami receptor. Molecular dynamics calculations strongly support this hypothesis, revealing that glutamate binding to the T1R1 subunit is strongly favored, whereas glutamate binding on the T1R3 subunit occurs only transiently [Lopez Cascales *et al.*, 2010]. Key ligand-binding residues of the mGluR1 metabotropic glutamate receptor (Figure 1.32) are conserved in T1R1 [Li *et al*, 2002].
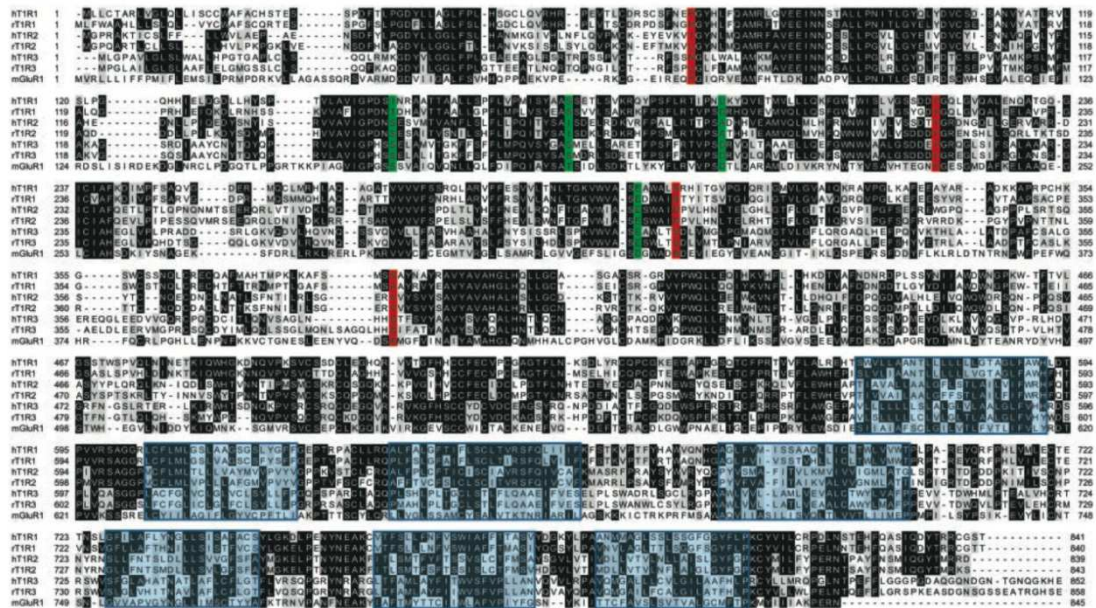
Figure 1.32. Sequence alignment of human and rat TRs with rat mGluR1. Potential transmembrane segments are boxed in blue. Glutamate-binding residues are highlighted following the color scheme of Fig. 3. [Figure from Li *et al.*, 2002].

T1R receptors belong to the class C of GPCRs, along with metabotropic glutamatereceptors (mGluRs). The defining motif in all these receptors is an outer membrane *N*-terminal Venus flytrap (VFT) domain The VFT is connected to the transmembrane helical region through a cysteine-rich domain (Figure 1.33). The VFT

domain of C-GPCRs contains the ligand-binding site and consists of 2 globular subdomains, the *N*-terminal upper lobe and the lower lobe, that are connected by a 3-stranded flexible hinge.
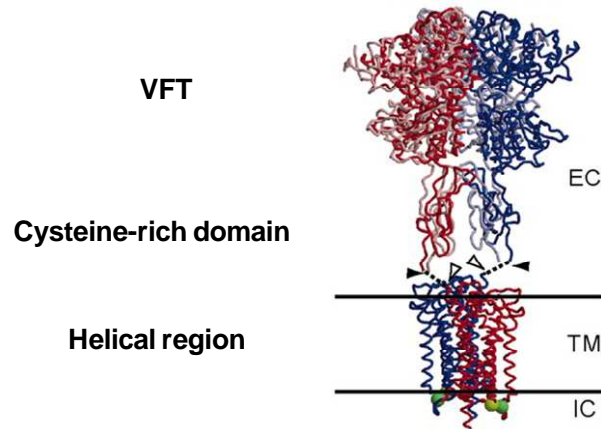
Figure 1.33. General architecture of the mGluRs. EC, extra-cellular; TM, transmembrane; IC, intra-cellular [Modified from Tekanori *et al.*, 2007].

The crystal structures of mGluR1 VFT domains (Figure 1.34) revealed that the bi-lobed architecture can be in an open or in a closed conformation. Glutamate binding stabilizes both the active dimer and the closed conformation [Kunishima *et al.*, 2000].
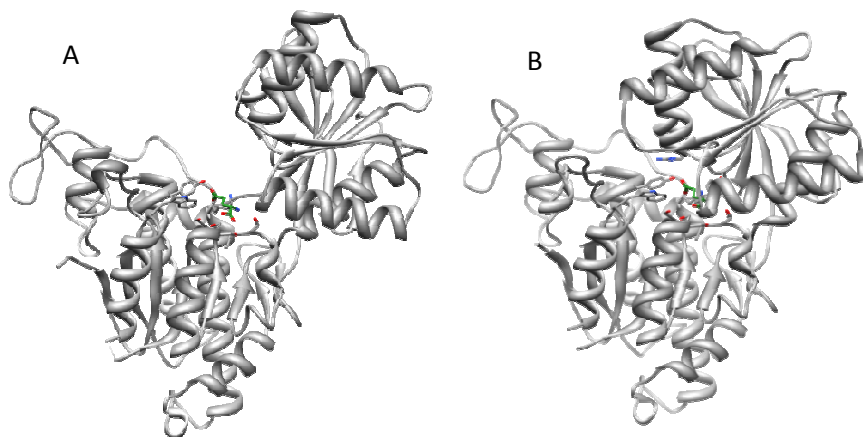
Figure 1.34. Structure of the Venus flytrap domain of mGluR1 receptor (PDB ID 1EWK) in the open (A) and closed (B) form [Kunishima *et al.*, 2000]. The bound glutamate is shown in green. Figure prepared with Chimera [Pettersen *et al.*].

Zhang *et al*. [2008] built homology models of the T1R1 VFT domain in open and closed forms using available structures of mGluR1, mGluR3, mGluR7 from the Protein Databank. Despite low overall sequence identity (≈30%) of T1R1 and T1R3 with

46

respect to mGluR1, residues near the hinge of the VFT domain that connect the 2 lobes and that coordinate the bound glutamate in the mGluR family of proteins are conserved (cfr Figure 1.32). Their assumption is therefore that the glutamate binding mode in T1R1 closely resembles that in the mGluR family of proteins. In their T1R1 model, the α-carboxylate group of glutamate makes hydrogen bonds with a group of residues close to the hinge of the flytrap and conserved in mGluRs, specifically to the backbone nitrogens of S172 and T149 and to the serine side-chain of S172 (Figure 1.35). The α-amino group of L-glutamate is coordinated by upper lobe S172 and lower lobe E301. The ring of Y220 in the lower lobe makes cation-π interactions with the amino group of L-glutamate. Results from mutagenesis analysis confirmed that residues S172, D192, Y220 and E301 are essential for glutamate binding, whereas the mutant T149A showed only a partially reduced activity [Zhang *et al.*, 2008]. Notably, the charged residues that form both direct contacts to the side chain of L-glutamate and stabilizing contacts between the lobes in the closed form of mGluR1 are largely absent in T1R1, which could help to explain T1R1's lower affinity for L-glutamate than mGluRs [Zhang *et al.*, 2008].
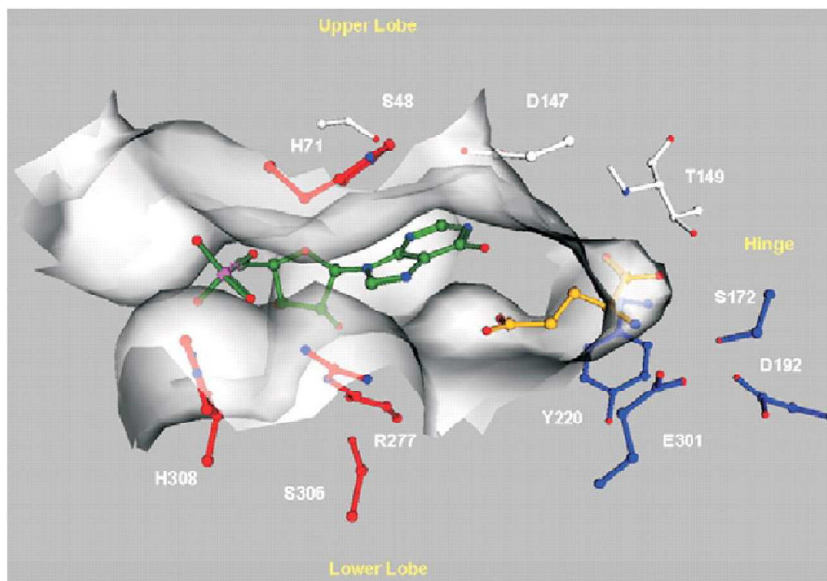
Figure 1.35. Molecular model of T1R1 VFT domain. Key residues for L-glutamate (blue) and for IMP (red) binding. The VFT domain is oriented so that the opening to solvent is horizontal, with the upper lobe on the top and the lower lobe on the bottom. The flytrap hinge region is to the right, and the flytrap opening is to the left. L-glutamate (golden) is located deep inside the VFT domain near the hinge region, while IMP (green) is located close to the opening of the VFT domain [Zhang *et al.*, 2008].

The same authors mapped also the IMP binding site into the VFT domain of T1R1 (Figure 1.35). In the proposed model, the phosphate group of IMP coordinate the positively charged residues that are on the two lobes of the VFT and are brought in proximity to each other when the VFT assumes the closed form. The identity of the involved residues was confirmed by site-directed mutagenesis analysis.

The position and orientation of IMP relative to L-glutamate are further constrained by the shape of the active-site cleft of the flytrap domain and by the nature of residues lining the active-site cleft. In this model, L-glutamate is positioned deeper in the active-site cleft, whereas IMP binds near the opening of the VFT vestibule between the two lobes (Figure 1.35), providing additional stabilizing interactions between the upper and lower lobes. The enhancement activity of IMP may be sufficiently explained by the binding of IMP adjacent to glutamate, stabilizing the closed form of the T1R1 VFT domain through electrostatic interactions [Zhang *et al.*, 2008].

Insights into the energetics of VFT movements are available for an ionotropic glutamate receptor. Indeed, crystal structures exist for the mGluR1 VFT domain in the open conformation, showing glutamate bound to one lobe only (Figure 1.34A). The thermodynamic contributions of flytrap closure have been measured for the VFT domain of ionotropic glutamate receptor iGluR2, revealing fast (≈μs) binding of glutamate (docking) followed by slow (≈ms) stabilization of the closed form (locking) [Lau & Roux, 2011]. A two-step mechanism for flytrap closure was therefore proposed. In the first step, glutamate binds to one lobe and lowers the entropic barrier to form the closed conformation. In a second step, the lobes close up and facilitate interactions between glutamate and the lower lobe, as well as interactions between the upper lobe and the lower lobe. A dynamic picture of the synergic action of glutamate and purine ribonucleotides towards the T1R1 receptor is due to Mouritsen *et al.* [2012]. Analysis of the trajectories of molecular dynamic simulations up to 150 ns showed that the receptor assumes the closed conformations upon binding with glutamate, and the aperture of the VFT is further closed when GMP is present, confirming the stabilization of the closed (active) conformation due to the binding of GMP (Figure 1.36).
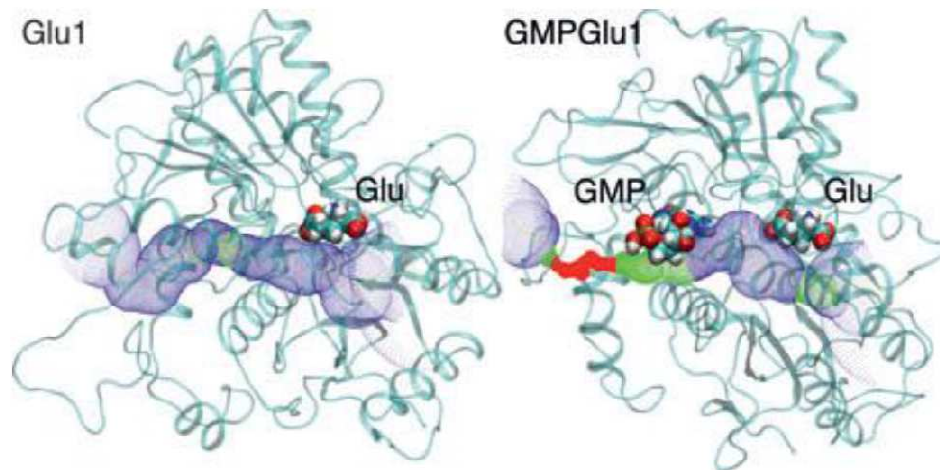
Figure 1.36. The vestibule leading to the GMP-binding site and thereafter the ʟ-glutamate-binding site is color-coded based on to the radius of the largest fitting spherical probe (blue, wide; green, medium; red narrow), calculated using the program HOLE. The simulation snapshots are taken from the final conformations of the Glu and GMPGlu simulations. The radius of the vestibule is significantly reduced (red) in GMPGlu close to the GMP-binding site [Mouritsen *et al.*, 2012].

It is further interesting to note that, in some simulations with GMP, the first principal mode of protein motion is not closure and opening of the VFTD, but a twisting motion around an axis different from the VFTD hinge axis, suggesting that the movement of the VFTD that switches the protein between active and inactive conformations is significantly dampened by addition of GMP. In simulations without any bound ligand, the protein accesses conformations where the two lobes of the VFTD are separated even further than observed in crystal structures of mGluR1s, although it cannot be exclude the possibility that the excess conformational freedom may be a consequence of the simulation. On the other hand, it is possible that the VFTD of the full *umami* receptor is very flexible, perhaps more so than the mGluR1 family of proteins. The single most important phenomenon explained by the simulations is that the presence of nucleotides enhances the sensation of the *umami* taste. The simulations show that the presence of GMP further stabilizes the closed (active) state of the protein once glutamate is bound. An inherent assumption in this analysis is that GMP binds after glutamate. As GMP binds at the entrance of the binding cleft, it is very likely that binding of GMP will be enhanced if glutamate is already bound, because the upper and lower lobes of the VFTD will be closer, and will be optimally positioned for GMP to bind. Furthermore, if GMP bound first, it would sterically block the entrance to the VFTD vestibule, and prevent

access of glutamate to the glutamate-binding site. Thus, it may be that, when both ligands are available, GMP binding after L-glutamate is more likely than the other way around.

2. AIMS

Aims of this PhD thesis are:

1. Valorization of agri-food industry waste rich in proteins as starting material to produce HVPs

Proteins are key ingredients in many foods as they contribute to the nutritional value, flavor and other important functional properties of food systems [Giese, 1994]. Protein hydrolysates constitute an alternative to intact proteins in the development of special formulations designed to provide nutritional support to individuals with different needs, such as patients with particular physiological and nutritional needs or unable to ingest adequate amounts of food in a conventional form. Protein hydrolysates are also utilized extensively as a source of nutrition to the elderly, young children and immunocompromised people. These products have an added advantage in having peptides that are small enough to circumvent possible allergenic reactions occurring with the consumption of larger size peptides or proteins [Nagodawithana, 2010].

For these reasons, there is a growing interest for Hydrolyzed Vegetable Proteins (HVPs) containing bioactive peptides because of their nutritional and therapeutic properties.

HVPs are produced by chemical and/or enzymatic hydrolysis of vegetable raw materials rich in proteins, such as wheat, corn, soybean, peanut, sunflower. The most effective way to obtain protein hydrolysates with defined characteristics is the use of different proteases (endopeptidases and exopeptidases) coupled with the development of post-hydrolysis procedures [Clemente, 2000]. The origin of the starting material and conditions of hydrolysis determine the biological as well as organoleptic properties of

the end product. In fact, these products have been widely used for centuries as flavor enhancers for their glutamate-like "umami" taste, particularly in typical Eastern vegetarian cuisine, as an alternative to glutamate. Other peculiarities of HVPs, such as antioxidant and antiinflammatory properties [De Carvalho-Silva *et al.*, 2012], antihypertensive effect [Li *et al.*, 2007], and antifungal activity [Joo *et al.*, 2004], are rigidly controlled by proper selection and blending of the protein source and appropriate selection of hydrolytic conditions.

Substantial amounts of protein-containing waste are generated in the production of foods and beverages. Examples include vinasse (from sugar beet or cane), distiller's grains with solubles (from wheat or maize), press cakes (from oil seeds), fish silage, proteins from coffee and tea production, and agricultural residues from various crops. Much of this protein material is currently processed as animal feed although it could be valorised as a feedstock for production of high value added chemicals.

Since the early 1990s, attention has been diverted from waste remediation to waste prevention, with the emphasis on applying the principles of "green chemistry" ("prevention is better than cure") [Tuck *et al.*, 2012].

In recent years great attention has been focused on the exploitation of those wastes that are largely unavoidable *i.e.* on ways of getting higher value from the waste using proper "waste valorization" strategies. Because the sources of waste are so diverse, it is convenient to consider the chemistry in terms of four source-independent categories: polysaccharides, lignin, triglycerides (from fats and oils), and proteins. Lignin is challenging to break down into chemically useful fragments. By contrast, pretreatment of polysaccharides, triglycerides, and proteins can lead to their constituent building blocks: monosaccharides, fatty acids plus glycerol, and amino acids, respectively.

Among wastes from agri-food industry rich in proteins, rice middlings (a by-product of the conversion of raw rice into white rice) as well as the seeds of hemp and flax (after the extraction of the oil) have not yet been exploited and deserve further valorization according to the concept of biorefinery.

IEA Bioenergy Task 42 [IEA, 2008] defines biorefineries as the sustainable processing of biomass into a spectrum of marketable products and energy. The biorefinery concept embodies the concepts of system integration, multiple products, and sustainability. It

54

includes a wide range of technologies able to separate biomass[3] resources (wood, grasses, corn, …) into their building blocks (carbohydrates, proteins, triglycerides, …) which can be converted to value added products, biofuels and chemicals. A biorefinery is a facility (or a network of facilities) that integrates biomass conversion processes and equipment to produce transportation biofuels, power, and chemicals from biomass. This concept is analogous to today's petroleum refinery, which produces multiple fuels and products from petroleum [Cherubini, 2010; Wellish *et al.*, 2010].

Biorefineries are emerging around the world in a variety of different forms and sizes. Their development depends on the demand for given products, the availability of biomass feedstock, the existing infrastructure and know-how, the level of investment in research and scale-up facilities, public acceptance, and policies that support the transition to a greener, more efficient hybrid economy [Wellish *et al.*, 2010]. In the United States, it is expected by 2020 to provide at least 25% (compared with 1994) of organic carbon-based industrial feedstock chemicals and 10% of liquid fuels from a biobased product industry. This would mean that more than 90% of the consumption of organic chemicals in the United States and up to 50% of liquid fuel needs would be covered by biobased products[4] [Kamm & Kamm, 2004].

It must be pointed out that investigation of hempseed and flaxseed as raw materials for the preparation of HVPs was carried out in the frame of VeLiCa Project ("From ancient crops materials and products for the future"), funded by Regione Lombardia (Italy).
The main goal of the VeLiCa project is to make again gainful the growing of flax and hemp in Regione Lombardia where it used to be widespread at the beginning of the 20th century. This target is being pursued by the exploitation of all the parts of the plant to make different products with different added value (biorefinery) [www.velica.org].

---

[3] Renewable resources also known as biomass are organic materials of biological origin and are, by definition, sustainable natural resources. Sustainable implies that the resource renews itself at such a rate that it will be available for use by future generations.

[4] Fossil carbon sources, such as petroleum and natural gas, should be replaced by a renewable raw material: biomass, particularly plant biomass. The corresponding products will be called "biobased products" and "bioenergy". The fundamental basic technology, which will be introduced in "biorefineries", as new production plants, will replace petroleum-based refineries. In fact, the term "bioeconomy" will be used.

2. Synthesis of glutamate-ribonucleotide hybrids for the study of umami taste

Umami taste is an essential element in our appreciation of food and is imparted by monosodium L-glutamate (MSG) and disodium salts of 5′-ribonucleotides such as inosine 5′-monophosphate (IMP) and guanosine 5′-monophosphate (GMP). These compounds are currently used as flavor enhancers to supplement, increase and round off the flavor of many savory-based processed foods. They are the best flavor enhancers that are in commercial use worldwide.

A very important peculiarity of MSG and the above-mentioned 5′-ribonucleotides is their capacity to interact synergistically. Such interactions generate amplified and lingering taste sensations, far greater than any single ingredient can produce. Thus, the phenomenon is of great relevance for the food industry, because it provides an opportunity for the food processor to use a ternary varying mixture of MSG, IMP and GMP to enhance the flavor, mouthfulness and palatability of culinary products [Ninomiya, 2002].

Despite extensive investigations on taste receptors, the mechanisms of perception, flavor enhancement, and synergism connected with umami substances have not been completely elucidated at a molecular level.

Recently, to assess the role played by substituents of the purine nucleus of 5'-ribonucleotides in eliciting a synergism with MSG, a number of N^2-alkyl N^2-acyl derivatives of guanosine 5'-phosphate was synthesized by our research group through alkylation and acylation of exocyclic amino group of guanosine. These compounds were finally evaluated for their capacity to enhance the taste intensity of MSG [Cairoli *et al.*, 2008; Morelli *et al.*, 2011].

As described in section **1.9.2.**, Zhang *et al.* [2008] suggested a possible explanation of the phenomenon of synergism at a molecular level in which both glutamate and IMP (or GMP) would interact with the extracellular domain of umami receptor, the so-called "Venus flytrap" (VFT), but at different sites. The binding of MSG would induce the closure of this domain, whereas the binding of 5'-ribonucleotide would stabilize the closed conformation thus determining the synergistic effect.

56

According to this model, to gain further insight into the phenomenon of synergism, we planned to synthesize hybrid compounds containing the two umami moieties (glutamate and purine 5'-ribonucleotide) covalently connected through flexible linkers of variable length with the aim to reach both umami receptor sites through a single molecule (Figure 2.1).
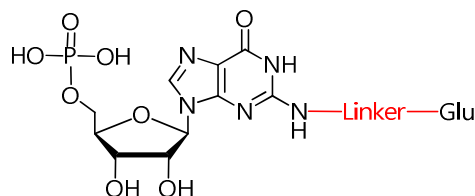
Figure 2.1.

The first hybrids synthesized (Figure 2.2) were obtained by N^2-acylation of the exocyclic amino group of guanosine with several linkers of variable length [Cairoli *et al.*, 2008]. The linker was condensed with the α-amino group of glutamic acid.
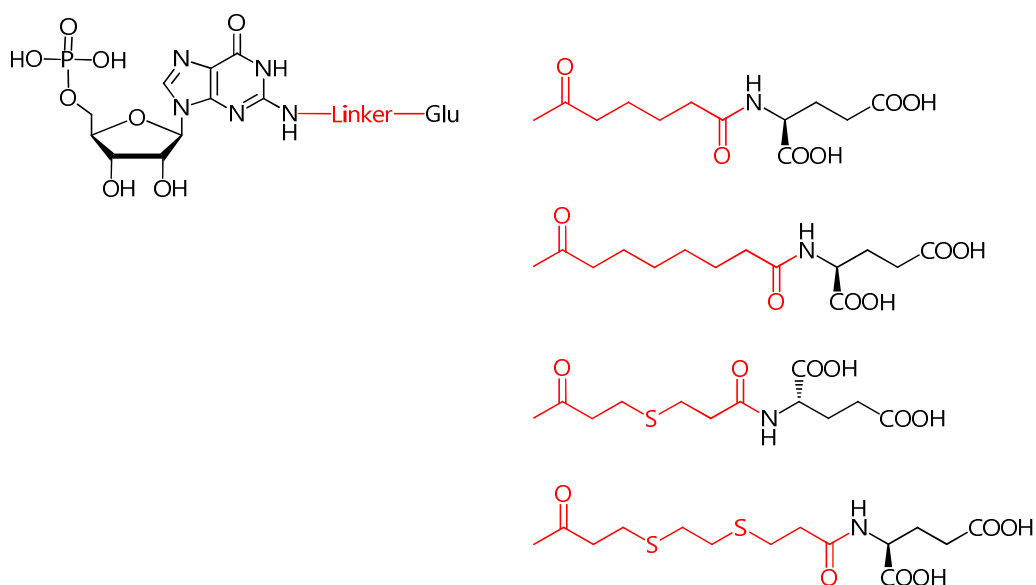
Figure 2.2.

However, in these compounds the α-amino group of glutamic acid, which is involved in the activation of the umami receptor, according to Zhang model, was locked into the binding with the linker. Furthermore, the poor yields obtained prompted us to pursue an alternative strategy in which the linker is condensed with the γ-carboxylic group of glutamic acid (Figure 2.3).
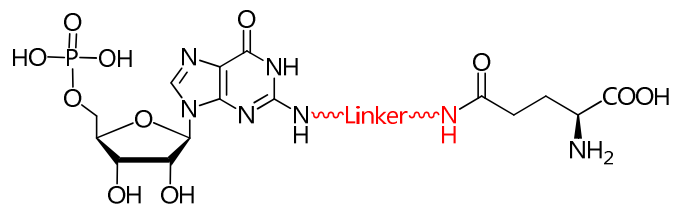
Figure 2.3.

3. RESULTS AND DISCUSSION
PART 1

3.1. Preparation of HVPs from Rice Middlings through Enzyme-catalyzed Hydrolysis

Rice is a very important agricultural resource mainly utilized for food [Bagnasco *el al*, 2013]. Rice feeds almost half the world's population and is one of the most attractive feed ingredients in the world [Ferrari *et al.*, 2009]. In addition, a variety of interesting by-products are obtained when converting raw rice into white rice, such as rice hull, bran, middlings, embryo and small brokens. Although an extensive commercial use of these by-products would be of great interest for a series of reasons, today a relatively small amount of this material is utilized. In fact, these by-products contain excellent quality components (proteins, fibers, vitamins and minerals) whose nutritional and pharmaceutical potential has been well recognized [Saunders, 1990]. Meaningfully they are a renewable resource and their use can reduce waste problems. In particular, rice by-products have a high content of amino acids, such as glutamic and aspartic acid, as well as amides, which makes these matrices a potential source of flavor enhancers for food applications [Hamada *et al.*, 2008].

Rice by-product proteins obviously need to be isolated and purified for their utilization as food stuff, but to date an efficient and reliable method has not yet been developed. The procedure traditionally adopted for the extraction of proteins from rice as well as from other complex plant matrices, such as industrial by-products, is alkaline treatment [Gnanasambandam & Hettiararchchy, 1995; Wang *et al.*, 2008]. However, this method could induce side-reactions, such as hydrolysis and extraction of non-protein components, and protein denaturation with obvious effects on their functional properties [Kinsella, 1981].

To overcome those drawbacks, alternative physicochemical [Anderson & Guraya, 2001; Van Der Borght *et al.*, 2006] and/or enzymatic [Hamada *et al.*, 1998; Tang *et al.*, 2002]

61

procedures were developed to improve the recovery of rice and its by-product proteins. Typically, enzymatic procedures are preferable owing to milder process conditions, easier control of reaction parameters and minimum formation of secondary products [Manneheim & Cheryan, 1992]. In most cases, enzymatic hydrolysis was also used in order to improve the functional properties of proteins or customize the functionality of some proteins for specific needs [Arzu *et al.*, 1972; Kim, Park, & Rhee, 1990].

Developing a protocol as quick and easy as possible for producing protein–peptide mixtures with flavor-enhancing properties from rice middlings could be useful to produce new functional ingredients with a significant umami taste for food industry.

3.1.1. Characterization of protein hydrolysates

3.1.1.1. SDS-PAGE analysis

The SDS-PAGE profiles and the corresponding densitograms obtained after hydrolysis performed on rice middlings in presence of Umamizyme and Flavourzyme are detailed in Figures 3.1 and 3.2, respectively.

A spontaneous degradation of proteins, without the addition of an enzyme, could be observed in comparison with the control lanes. This could be dependent on the presence of intrinsic proteases in the matrix not inhibited through preliminary process, such as by heating at high temperature [Hamada, 2000b]. Since the goal of this work was the development of a hydrolytic method as quick and easy as possible, aimed at an industrial application, the decision was made not to stabilize the matrix by heating or by use of antiproteolytic agents, since protein degradation, spontaneous or induced, was the main purpose of this work. An overall comparison between control and treated samples showed that the intrinsic proteolytic action primarily affected the high molecular mass bands (from 200 to 30 kDa), while the added enzymes degraded the bands at medium-low molecular mass (<30 kDa).

Figure 3.1. SDS-PAGE profile of protein fractions obtained at different sampling times during the hydrolysis of rice middlings by Umamizyme (hydrolysis parameter: pH 7, 45 °C). Lanes 1–3–5–7 are rice middlings samples incubated in the presence of Umamizyme for 1, 5, 11, 24 h, respectively; lanes 2–4–6–8 are rice middlings samples incubated in the absence of Umamizyme for 1, 5, 11, 24 h, respectively. M represents the protein molecular mass marker (97, 66, 45, 30, 20.1, 14.4 kDa). Plot on the side of the picture shows changes in optical density of main proteins during enzymatic reaction. Letters of the curves (A to H) identify the main protein fractions studied. Only five profiles out of eight are represented on the plot due to the overlapping of degradation profile of B, C, E and F proteins. Below are represented the single protein trends for a clearer interpretation of each degradation profile.
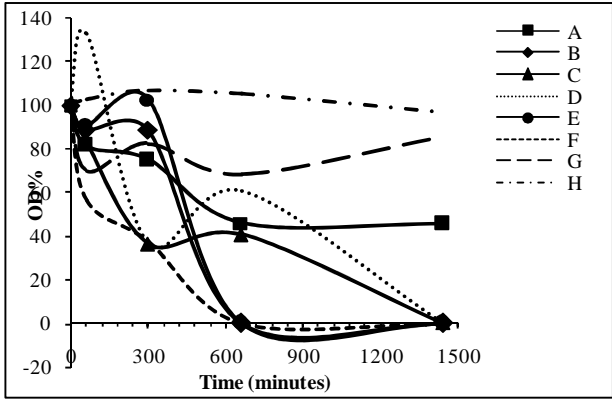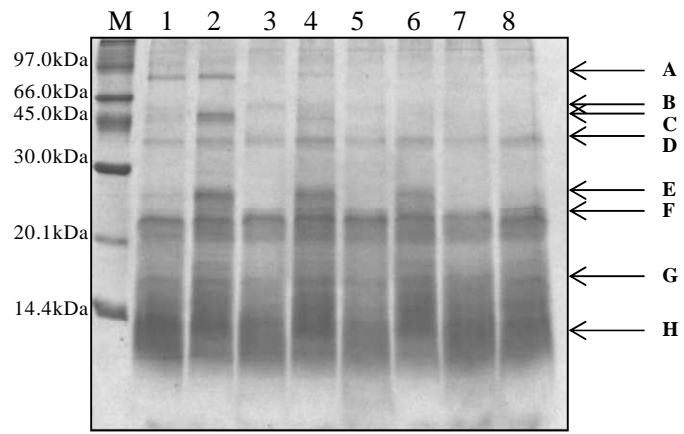
Figure 3.2. SDS-PAGE profile of protein fractions obtained at different sampling times during the hydrolysis of rice middlings by Flavourzyme (hydrolysis parameter: pH 8, 50 °C). Lanes 1–3–5–7 are rice middlings samples incubated in the presence of Flavourzyme for 1, 5, 11, 24, respectively; lanes 2–4–6–8 are rice middlings samples incubated in the absence of Flavourzyme for 1, 5, 11, 24 h, respectively. M represents the protein molecular mass marker (97, 66, 45, 30, 20.1, 14.4 kDa). Plot on the side of the picture shows changes in optical density of main proteins during enzymatic reaction. Letters of the curves (A to H) identify the main protein fractions studied. Below are represented the single protein trends for clearer interpretation.

In order to verify the performance of the two hydrolytic enzymes, a comparison between protein patterns obtained by Umamizyme and Flavourzyme was performed. In the case of Umamizyme, a hydrolysis of the main protein fractions was observed, as evidenced by the quick and general decrease of optical density showed by most bands. In contrast, the catalytic activity of Flavourzyme resulted in a lower and slower decrease of optical density. In particular, after 1 h, the sample treated with Umamizyme was already different from the control sample, since the high molecular mass bands were completely hydrolyzed, whereas in the presence of Flavourzyme, at least 5 h were necessary to have differences between control and treated sample, since all the main bands were not hydrolyzed in the early times of incubation. After 11 h of incubation, the two enzymes showed a comparable behavior: the protein bands with medium-low molecular mass and some high molecular mass subunits (labeled with "D" in Figure 3.1, in the case of Umamizyme and "A", "C" and "D" in Figure 3.2, in the case of Flavourzyme) persisted, while most high molecular bands disappeared. After 24 h of incubation, the greater effectiveness of Umamizyme emerged again, with which only three defined bands ("D", "G" and "H" in Figure 3.1) were not hydrolyzed, while with Flavourzyme the lower part of the gel was still completely marked by protein elements.

The total lane integrated optical density (IOD) reflects the contribution of each protein bands to the lane IOD total and provides a global value of protein degradation [Frazer & Bucci, 1996]. The total lane IOD confirmed that Umamizyme has a greater catalytic activity than Flavourzyme (Figure 3.3). With Flavourzyme the total IOD of protein bands decreases significantly compared to the control sample with increased time of hydrolysis from 1 to 24 h, while with Umamizyme a short time is sufficient to show a significant decrease of total IOD of protein bands.

The higher hydrolytic efficacy of Umamizyme compared to Flavourzyme was illustrated by the measure of the degree of hydrolysis by the Coefficient of Protein Degradation (CPD), calculated for each time on the basis of the optical density of the main protein bands defined in Figures 3.1 and 3.2 (Table 3.1). A significant difference between the two enzymes was shown for each incubation time. After 1 h of incubation, it could be noticed that Umamizyme had a 2-fold higher protein degradation compared to Flavourzyme (15.69±2.52 % and 6.21±3.75 %, respectively), a trend that seemed to be maintained even for the successive times. After 24 h of incubation, it became

apparent that Flavourzyme lead to partial proteolysis, with $24.84\pm1.28\%$ protein degradation. In contrast, with Umamizyme the proteolysis of protein content was almost complete, with a CPD of $67.04\pm0.55\%$.

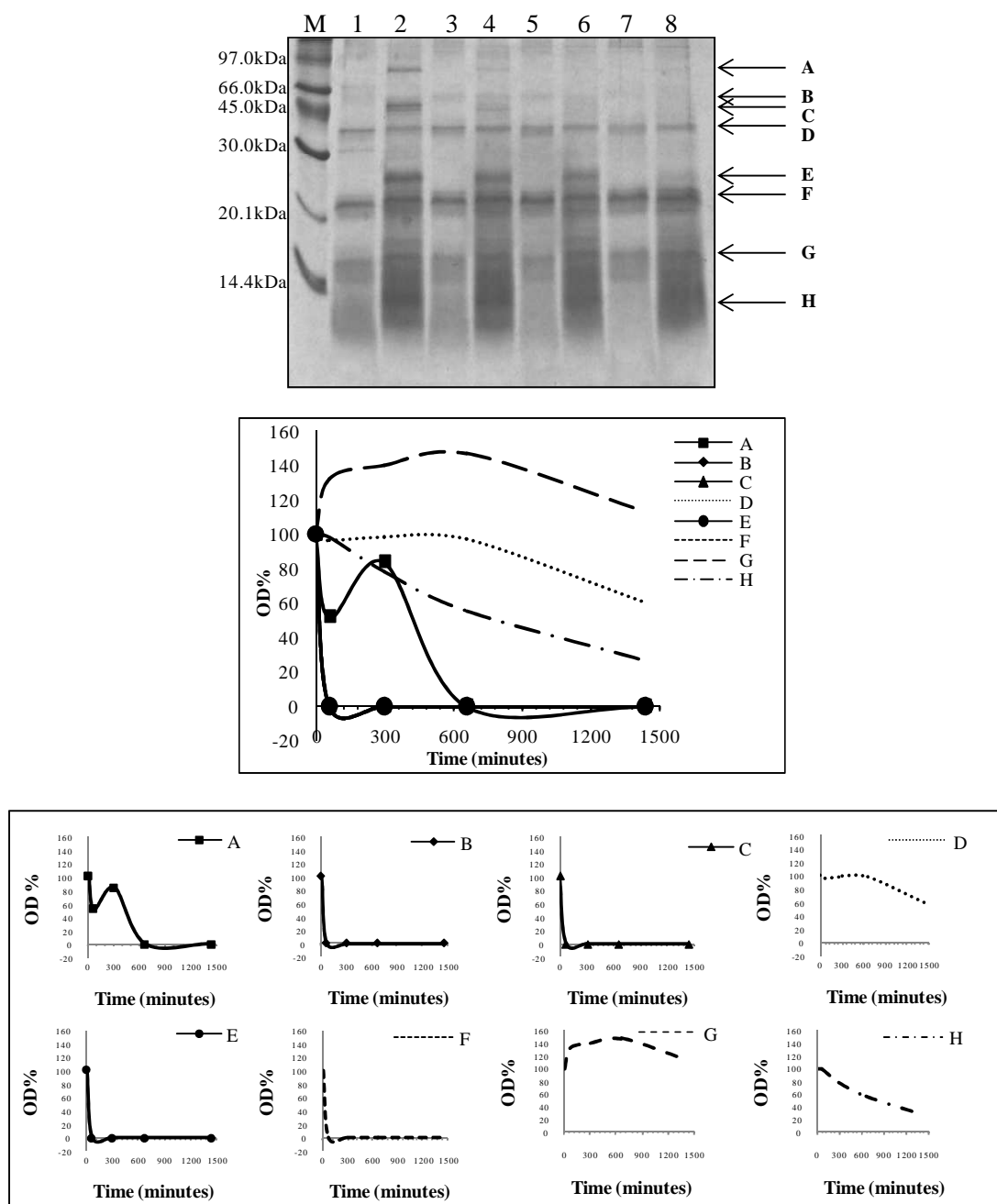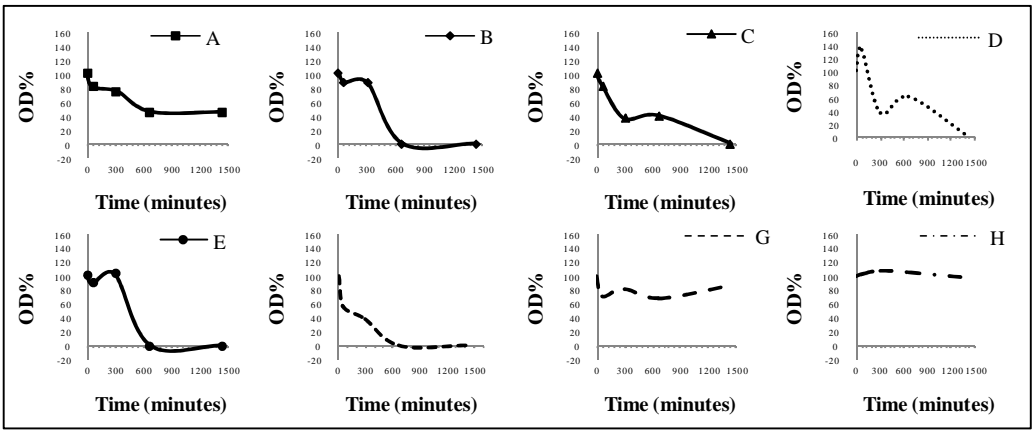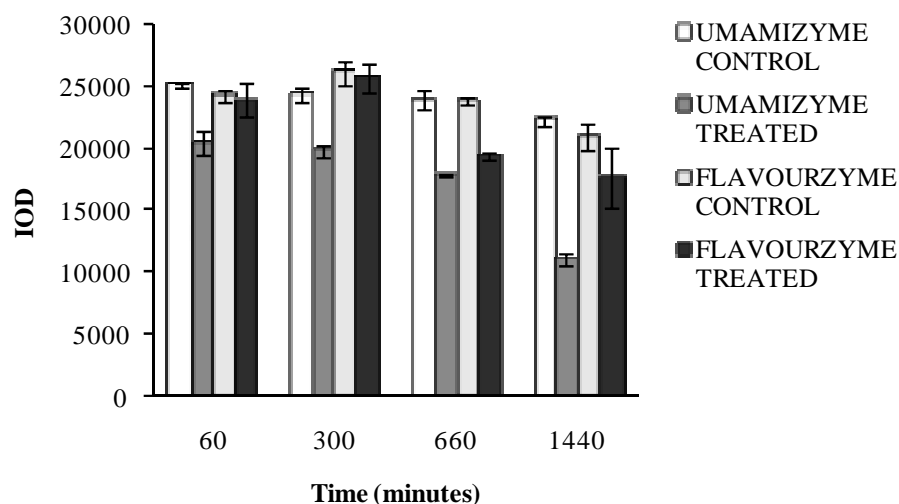*Figure 3.3*. Integrated Optical Density (IOD) of protein fractions obtained at different sampling times during the hydrolysis of rice middlings by Umamizyme (hydrolysis parameter: pH 7, 45 °C) and Flavourzyme (hydrolysis parameter: pH 8, 50 °C). Values represent means$\pm$SE (n=2). The data were evaluated using one-way analysis of variance followed by Tukey's post-hoc test. Different characters (a–c) on the top of the columns indicate a significant different ($p<0.05$) among IOD value of hydrolysates obtained without enzyme, with Umamizyme or with Flavourzyme at a specific sampling time.

Table 3.1. CPD of rice middlings after enzymatic hydrolysis with Umamizyme and Flavourzyme.

Time (minutes)	CPD (%)*	
	Umamizyme Treated	**Flavourzyme Treated**
60	15.69$\pm$2.51 [a]	6.21$\pm$3.75 [a]
300	27.27$\pm$0.76 [a]	8.79$\pm$1.15 [b]
660	42.86$\pm$2.05 [a]	17.37$\pm$2.11 [b]
1440	67.04$\pm$0.55 [a]	24.84$\pm$1.28 [b]

* Values represent means$\pm$SE (n=2). Within the same row, different characters (a-b) indicate significant difference with $p<0.05$ among various samples at a specific hydrolysis time.

The higher hydrolytic capability of Umamizyme compared to Flavourzyme was already reported by Villafuerte Romero [2006] in an enzymatic modification of wheat proteins for flavor generation, but so far a definitive explanation has not been proposed to clarify the different performance of the two enzymes.

66

3.1.2. Functional properties

3.1.2.1. Emulsifying properties

The emulsifying activity index (EAI) and the index of stability of the emulsion (ESI) of selected hydrolysates were analyzed and they are shown in Figures 3.4A-3.4B, respectively.

The samples obtained after 24 h of incubation with Umamizyme and Flavourzyme showed a similar pH-dependent EAI profile. All the samples showed a minimal EAI value at acidic and neutral pH, while a higher value was found at pH 9 (Figure 3.4A). This behavior is in agreement with a previous study on the hydrolysis of vegetable matrices [Yin *et al.*, 2008]. A comparison between emulsifying activity of hydrolysates obtained with Umamizyme and Flavourzyme and the sample control showed that enzymatic hydrolysis using Flavourzyme led to significant declines in EAI at acid and neutral pH. In contrast, the use of Umamizyme did not show a significant difference, regardless of the pH value. These data may imply that Umamizyme produces hydrolysates with an emulsifying index similar to control sample, but with better emulsifying activity compared with hydrolysates obtained using Flavourzyme. The better performance of Umamizyme hydrolysates respect to Flavourzyme peptides could be related to the higher proteolysis induced by the treatment with Umamizyme compared to Flavourzyme. This could account for the lower availability of the free amino acid residues and the subsequent lower surface activity responsible for the emulsifying capacity. As shown by the SDS-PAGE electrophoresis, the production of peptides in Umamizyme was higher than Flavourzyme proteolysis. The emulsifying index no higher than control sample can be due to the formation of the aggregates in the hydrolysates. It might inhibit the formation of a viscoelastic membrane on the oil-in-water surface, thus increasing the oil droplets coalescence [Gbogouri *et al.*, 2004; Yin *et al.*, 2008]. Previous studies about rice protein can confirm the aggregates formation in this matrix [Wang *et al.*, 1999; Kumagai *et al.*, 2006].
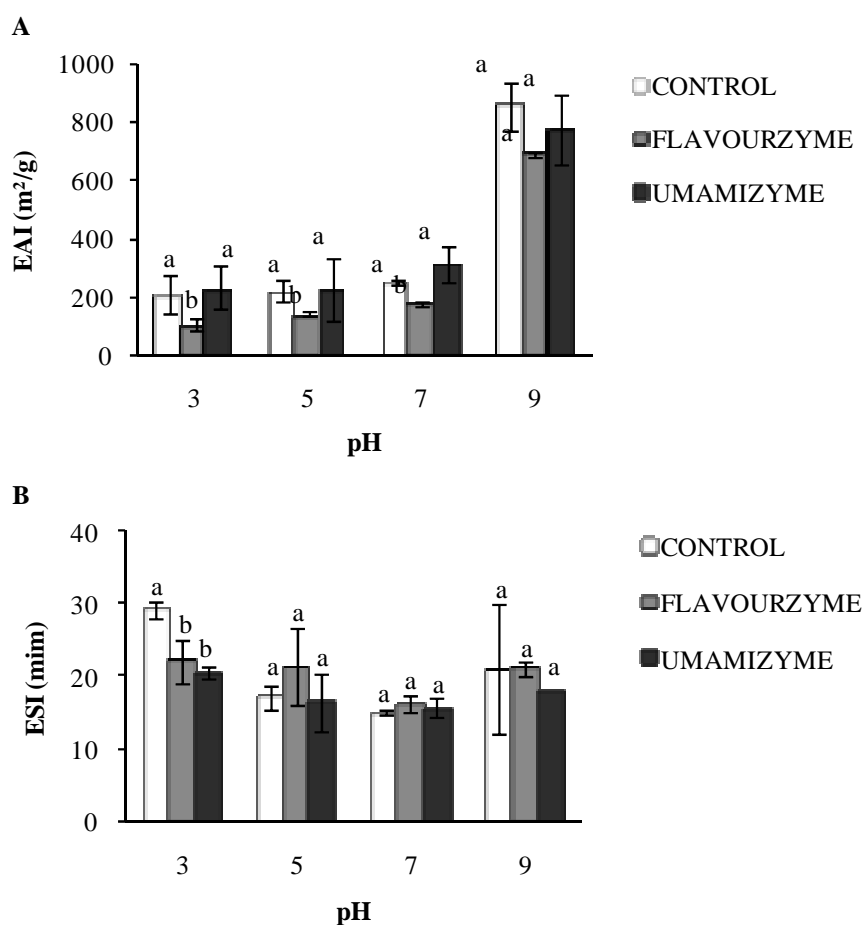
Figure 3.4. Emulsifying activity index (EAI) (A) and emulsion stability index (ESI) (B) of rice middlings hydrolysates after 24 h of incubation with Umamizyme (hydrolysis parameter: pH 7, 45 °C) and Flavourzyme (hydrolysis parameter: pH 8, 50 °C). Values represent means±SE (n=2). Different characters (a–b) on the top of columns indicate a significant difference (p<0.05) among EAI (A) or ESI (B) value of hydrolysates obtained without enzyme, with Umamizyme or with Flavourzyme at a specific pH value.

Enzymatic hydrolysis significantly decreased the ESI values at acidic pH, while no significant effect was observed at alkaline and neutral pH (Figure 3.4B). These effects were already reported by Yin *et al.* [2008], but so far a definitive explanation has not been proposed to clarify the pH dependence of ESI values.

3.1.2.2. Foaming properties

Foaming capacity (FC) and foam stability (FS) were determined at pH 7.0. Table 3.2 shows the effects of enzymatic hydrolysis after 24 h of incubation with Umamizyme

and Flavourzyme on the FC and FS of rice middlings. Enzymatic hydrolysis led to significant decreases in FS, while it seemed to have no significant effect on FC. In particular, hydrolysates obtained with Flavourzyme showed no foam stability: the foam disappeared after less than 30 min. This effect could be due to the lack of formation of a thick, cohesive, and viscoelastic film around gas bubbles that prevented the foams from collapsing [Damodaran, 1990; Halling, 1981].

Table 3.2. Foaming capability (FC) and foam stability (FS) of rice middlings hydrolysates after 1440 minutes of incubation with Umamizyme and Flavourzyme.

Sample	FC (%)*	FS (%)*
Control	75±12.12 [a]	30±8.01 [a]
Flavourzyme Treated	45±7.07 [a]	0±0.00 [b]
Umamizyme Treated	65±6.70 [a]	15±0.57 [a,b]

* Values represent means±SE (n=2). Within the same column, different characters (a-b) indicate significant difference with $p<0.05$ among various samples.

It has been shown that the molecular properties of proteins required for good FC and good FS differ [Cheftel *et al.*, 1985]. The basic requirement for a protein to be a good foaming agent is the ability to rapidly adsorb at the air–water interface during bubbling, undergo rapid conformation change and rearrangement at the interface, and form a cohesive viscoelastic film via intermolecular interaction. Thus, the decreases in chain length of peptides as a result of enzymatic hydrolysis may mainly account for the decreases in FC and FS. The result is consistent with the general viewpoint that the larger the molecular size of a protein, the higher the foaming stability [Damodaran, 1997].

The good foaming ability of the hydrolysates may be explained by an increased interactions between peptides due to their secondary and tertiary structures and resulting in greater flexibility of the chains. It has been reported that foaming capacity is favored when proteins have more flexible random coiled structure [Damodaran, 1990; Halling, 1981]. Moreover, the good foaming activity present in our samples may due to the medium-low molecular mass protein bands identified by electrophoretic analysis of both the hydrolysates.

3.1.3. Sensory analysis

SDS-PAGE analysis showed good proteolytic efficiency through the direct use of food-grade protease Umamizyme and Flavourzyme on rice middlings. By this procedure, the hydrolysates, that are intended for human food, do not derive from a "conventional" chemical process, such as treatments with reducing or denaturant agents, but protein extraction and protein hydrolysate production occur at the same time through the same biotransformation.

In order to evaluate the sensory characteristics of protein–peptide mixtures, the hydrolysates obtained after 24 h of incubation with Umamizyme and Flavourzyme were lyophilized and tested by a team of selected and certified panelists.

Figure 3.5 shows the average taste intensity of the five main flavors for the two hydrolysates analyzed and MSG, as reference substance for umami taste.

Overall, the umami taste was the more intense attribute for both hydrolysates, indicating the good sensory quality of the products. In addition, the ANOVA revealed that there was no significant difference ($p<0.05$) of umami taste between recovered protein hydrolysates and MSG.
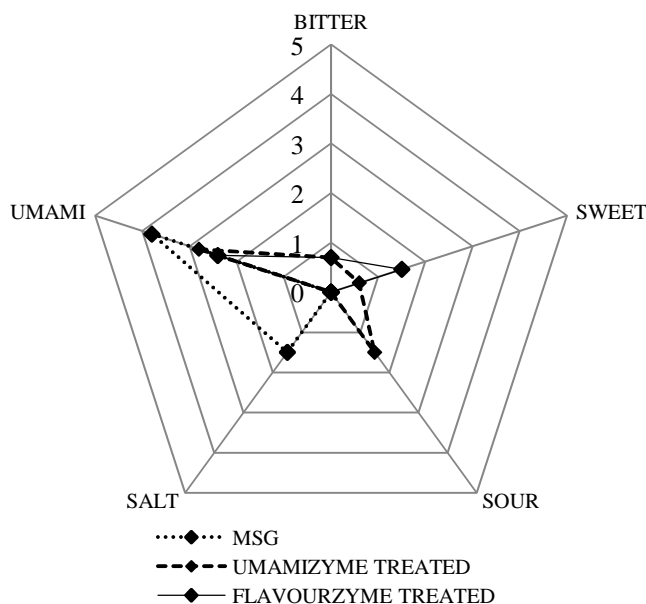
Figure 3.5. Taste profiles of MSG and rice middling hydrolysates after 24 h of incubation with Umamizyme and Flavourzyme. Each value represents the averaged taste intensity scored on a 10-point category scale by five panelists. In the figure the results are represented with a reduced scale for easier interpretation.

70

The bitter taste was slightly present in hydrolysates, as previously suggested by the hydrolysis of vegetable matrices for long times [Hamada, 2000b]. However, this taste did not prevail on the umami taste, since Umamizyme and Flavourzyme cut terminal hydrophobic residues [Pommer, 1995], responsible for the bitter taste. A little sweet taste, meaning pleasantness of taste sensation, was present in both hydrolysates, particularly using Flavourzyme, while a hint of acidity was characteristic of hydrolyzed with Umamizyme. These secondary tastes did not alter taste sensation and they may be at the basis of flavor defined for the hydrolysates. This typical flavor is named "amaretto", that is detected in some typical Italian products, such as almond and apricot based products. This flavor is pleasant, comfortable and soft on the palate. Finally, salty taste, present in MSG reference sample, was completely negligible in the hydrolysates. This seems to confirm that the flavor enhancement observed in our hydrolysate samples can be ascribed to umami taste and not salty compounds.

The described enzyme-assisted aqueous extraction method could be useful to obtain protein–peptide mixtures from rice middlings as raw material with sensory properties. The straightforward approach proposed allows to obtain hydrolysates characterized by high umami and slightly bitter taste, revealing the good performance of our protocol to gain tasty quality products. Thus, the taste profile of our hydrolysates suggests that the proposed approach can be an effective, quick and easy process to produce new umami flavor enhancers from under-utilized industrial products. The potential food industry application can be favored by the functional properties as emulsifying and foaming agents mainly observed in Umamizyme-derived protein–peptide mixtures. This highlights the versatility of the proposed protocol and thus the possibility of using the same process for different applications.

3.2. Preparation of HVPs from Hempseed through Enzyme-catalyzed Hydrolysis

Cannabis sativa, an annual, dioecious herbaceous plant, has been an important source of food, fiber, dietary oil and medicine for thousands of years in Europe, Asia and Africa [Callaway, 2004]. Its cultivation has been prohibited in many countries, due to the presence of the phytochemical drug component delta-9-tetrahydrocannabinol (THC) [Oomah *et al.*, 2002]. However, in the last decades the renewed interest for natural, biological and ecological products brought to the harvest reintroduction of the varieties of *C. sativa* L., containing less THC than common hemp, in the european and american agriculture especially because of hemp seeds properties.

The seeds of *C. sativa* L., commonly referred to 'hempseed', are an excellent source of nutrition [Callaway, 2004]. Hempseed has been documented as a source of food throughout recorded history – raw, cooked or roasted, and its oil has been used as a food/medicine for at least 3000 years [Callaway, 2004]. Hempseed are an important source of essential fatty acids, dietary fiber, vitamins and minerals, and in particular are an excellent dietary source of easily digestible, gluten-free protein. Their overall protein content of about 35% (mainly edestin and albumin) is higher, or comparable to, that of soy. Moreover, hempseed protein content is superior to that found in nuts, other seeds, dairy products, meat, fish, or poultry. Hemp proteins are very nutritional and provide a well-balanced array of all essential amino acids for humans [Wang *et al.*, 2008]. An important aspect of hemp seed proteins is a high content of arginine and histidine, both of which are important for growth during childhood, and of the sulfur-containing amino acids methionine and cysteine, which are needed for proper enzyme formation. Hemp proteins also contain relatively high levels of the branched-chain amino acids that are important for the metabolism of exercising muscle. For these properties, hemp proteins

are of interest in new value-added products. Furthermore, HVPs from hempseed have good potential to be applied as a valuable source of proteins for human nutrition as well as products to be investigated for their potential in several market sectors (food, pharma, cosmesis).

3.2.1. Hempseed meal: defatting and protein extraction

Hempseed protein extraction was carried out according to the protocol described by Tang *et al.* (2006) with a few modifications. Hemp seeds were ground using a home-style grinder, defatted by stirring with *n*-hexane and air-dried. The organic phase was dried *s.v.* at 30 °C and the composition of the resulting dark yellow oil (yield=30±5%) with regard to fatty acid content was assessed at the University of Pavia by GC-FID analysis according to a well-established protocol [FIL-IDF International Dairy Federation, 1999. Milk Fat. Preparation of fatty acid methyl esters. Standard 182:1999. IDF, Brussels, Belgium]. The hempseed meal, about 65-70% of the starting material, was used for protein extraction by alkali solubilization/acid-precipitation methods using two different approaches. According to the former process, as described by Wang *et al.* [2008], NaOH was used for alkali extraction and the resuspended proteins were precipitated with HCl. In the latter method, NH_3 and HCOOH were used instead of NaOH and HCl, respectively, in order to avoid the presence of NaCl in the final product. In both cases proteins were extracted using a base, NaOH in the first case and NH_3 in the second case, and precipitated using an acid, hydrochloric acid and formic acid, respectively. In both cases recovered protein precipitates were resuspended in distilled water. The resulting solutions were dialyzed using a 3500 MWCO membrane, and finally freeze-dried. An aliquot of this product was analyzed by ^{1}H NMR spectroscopy (1D 500 MHz, pH 7, 37 °C).

From the inspection of ^{1}H NMR spectra of the proteins extracted by NH_3/HCOOH or NaOH/HCl treatment it clearly appears that both the protocols allowed the extraction of the same proteins, as depicted by ^{1}H NMR spectra overlapping (Figure 3.6). The presence of signals in the 3-4 ppm range can be ascribed to the presence of sugars. The widened signals suggest the presence of unfolded proteins, probably glicoproteins that

74

might be precipitated upon the extraction process. Figure 3.7 shows that a higher amount of sugars was obtained when NaOH/HCl extraction was performed.
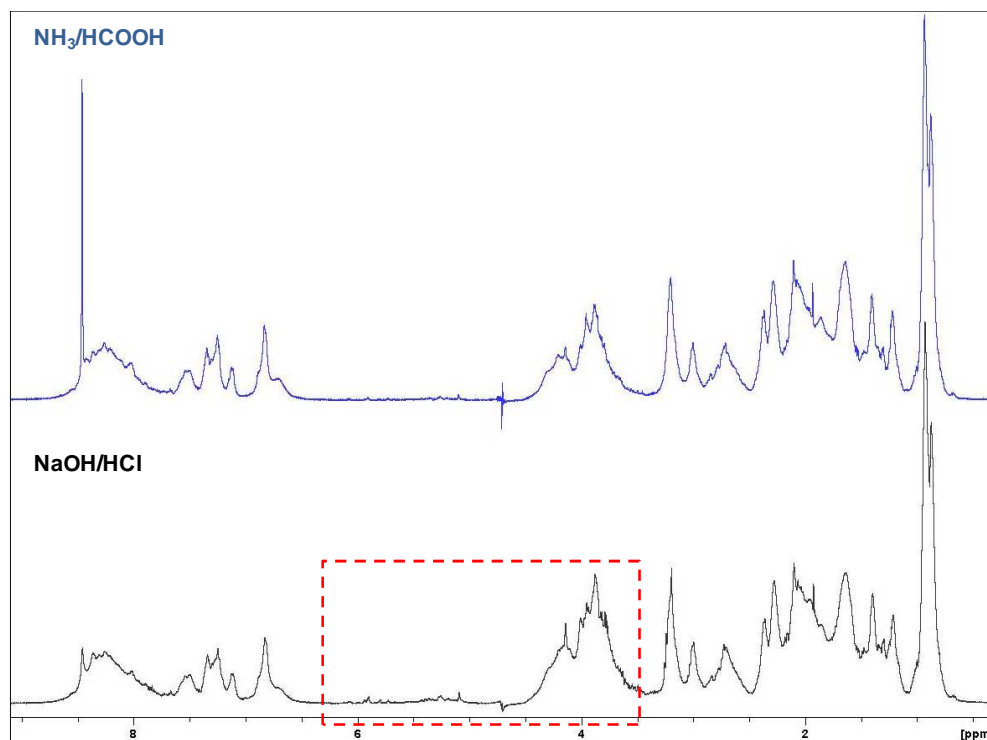
Figure 3.6. 1D ^{1}H NMR performed using a 500-MHz NMR instrument at pH 7 and 37 °C. Comparison of ^{1}H NMR spectra of the proteins extracted by NH$_3$/HCOOH (above) or NaOH/HCl (below) treatment.
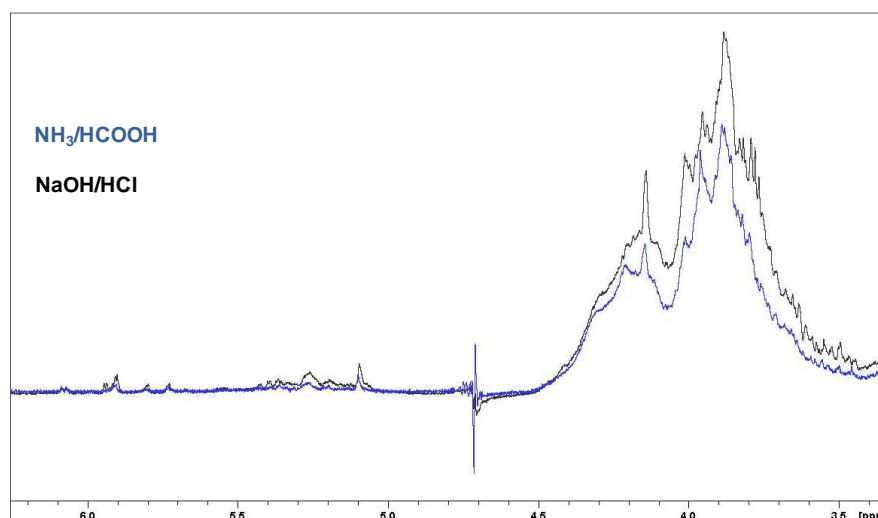
Figure 3.7. Overlapping of ^{1}H NMR spectra of the proteins extracted by NH$_3$/HCOOH (blue) and NaOH/HCl (black) treatment.

3.2.2. Enzymatic Hydrolysis - SDS–PAGE

3.2.2.1. SDS–PAGE of protein extract

The SDS-PAGE (sodium dodecyl sulphate-polyacrylamide gel electrophoresis) profiles of hempseed protein constituents in the presence and absence of 2-mercaptoethanol (2-ME) are depicted in Figure 3.8. The estimated molecular weights and the relative contents of the different subunits are reported in Table 3.3.

Hempseed proteins include a kind of legumin, the so-called "edestin". Edestin is the major storage protein of hemp seed and accounts for about 60-80% of the total protein content; whereas the second most abundant protein is the globular protein albumin. Edestin is easily digested and contains all essential amino acids for humans [Callaway, 2004]. This protein was reported to be similar to serum globulins, and could be metabolized in the human body to biosynthesize immunoglobulins, hormones, haemoglobin, and enzymes [Tombs, 1960]. Using crystallographic techniques Patel *et al.* [1994] showed that, like the hexamer of soy glycinin, the edestin molecule is composed of six identical subunits, and each one consists of an acidic subunit (**AS**) and a basic subunit (**BS**) linked by one disulfide bond [Tang *et al.*, 2006; Kim & Lee, 2011]. BS is more heterogeneous than AS.

In absence of 2-ME (non-reducing conditions) the disulphide bonds between the acidic and the basic subunits are not totally destroyed, and thus the subunits of edestin would be mainly in the form of various AB units. As expected, the subunits marked as AS, BS1 and BS2 were in small amount (relative content <20%) in the SDS-PAGE profiles (unreduced) and, accordingly, there were miscellaneous bands of about 60-65 kDa (marked as AB unit) which were clearly attributed to the AB unit (Table 3.3 and Figure 3.8). Furthermore, under these conditions, all samples contained a relatively high content of aggregates stacking on the top of separating gel, or even not entering the stacking gel.

Table 3.3. Molecular weight (MW) and relative content of the major subunits of hemp proteins from hempseed meal defatted by *n*-hexane.

Extraction solution	MW and content	Non-reducing Sample Buffer				
		AB unit	Other bands	AS	BS1	BS2
NaOH	MW (kDa)	61.88±0.69	/	35.22±0.53	17.78±0.57	15.78±0.03
	Relative content (%)	36.00±1.04	/	44.66±1.90	8.30±1.09	11.03±1.05
HCl	MW (kDa)	61.55±0.23	/	34.44±0.19	17.84±0.07	15.82±0.15
	Relative content (%)	39.46±2.27	/	47.62±1.27	9.39±1.54	8.53±0.93
SDS/UREA	MW (kDa)	62.04±0.46	/	35.88±0.13	20.78±0.12	19.01±0.28
	Relative content (%)	71.72±1.25	/	26.63±1.57	1.06±0.18	0.60±0.14
SDS/UREA/DTT	MW (kDa)	/	55.29±0.10	33.67±0.25	20.18±0.11	18.25±0.17
	Relative content (%)	/	8.92±0.68	72.48±0.77	8.69±2.37	9.91±0.93

Extraction solution	MW and content	Reducing Sample Buffer				
		AB unit	Other bands	AS	BS1	BS2
NaOH	MW (kDa)	63.04±1.89	55.16±0.34	34.95±1.05	18.94±0.46	16.97±0.38
	Relative content (%)	18.27±1.70	3.51±1.43	60.50±2.37	5.77±0.03	11.95±0.27
HCl	MW (kDa)	62.37±0.23	57.72±4.46	34.53±0.32	19.12±0.43	17.54±0.10
	Relative content (%)	17.30±0.51	2.63±0.25	56.01±1.01	6.98±1.83	17.09±1.08
SDS/UREA	MW (kDa)	63.63±2.02	56.71±1.70	33.77±1.01	19.76±0.33	17.47±0.20
	Relative content (%)	11.65±1.23	2.73±0.61	64.20±0.02	9.32±0.33	12.10±1.54
SDS/UREA/DTT	MW (kDa)	/	56.93±0.11	33.85±0.38	19.91±0.04	17.84±0.13
	Relative content (%)	/	8.22±0.23	66.26±1.41	10.77±0.68	14.75±1.50

By adding a reducing agent (such as dithiothreitol, DTT) or using a sample buffer containing 2-ME, there were two major kinds of protein constituents, corresponding to AS and BS subunits of edestin, respectively. In this case, the AS of about 30-40 kDa was relatively homogeneous, while the BS mainly consisted of two subunits of about 20 kDa and 18 kDa respectively. From these MWs and the relative content data, the MW of edestin (hexamer form) can be estimated to be about 300-400 kDa. Besides the bands of acidic and basic subunits of edestin, under reducing conditions, all samples contained minor components at about 45-55 kDa and some peptides with MW lower than 17 kDa.
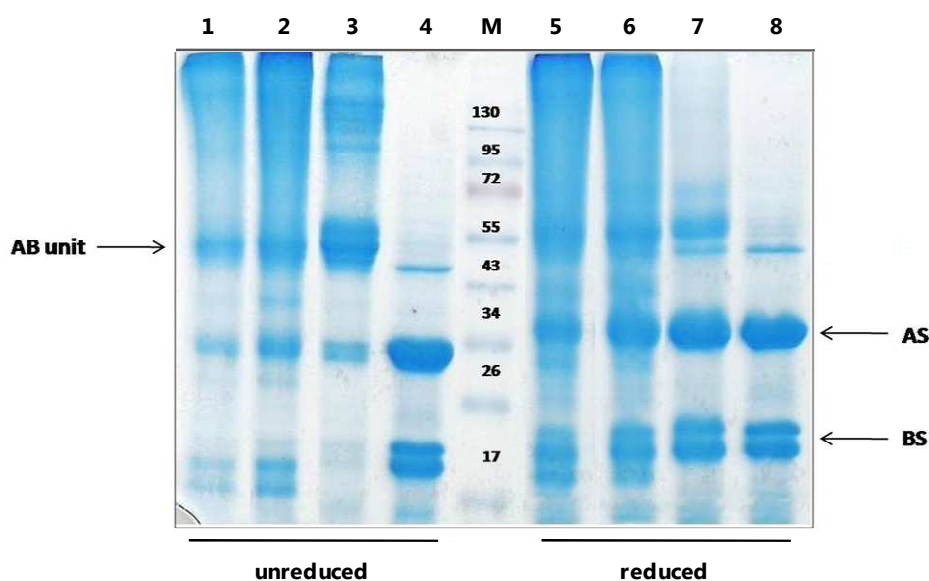
Figure 3.8. SDS-PAGE profiles of hemp proteins from hempseed meal defatted by *n*-hexane, in absence (non-reducing conditions) or in presence (reducing conditions) of 2-ME. AB unit represents the miscellaneous bands of hemp edestin, while AS and BS represent the acidic and basic subunits of hemp edestin. Lanes 1 and 5 are the hempseed protein solution extracted with NaOH (2 h, 37 °C). Lanes 2 and 6 are the hempseed proteins precipitated with HCl and resuspended in 50 mM Tris/0.05% SDS pH 8.0. Lanes 3 and 7 are the hempseed protein solution extracted with 2% SDS/6 M urea (2 h, 37 °C). Lanes 4 and 8 are the hempseed protein solution extracted with 2% SDS/6 M urea/1%DTT (1:20, 2 h, 37 °C). M represents the protein molecular mass marker (130, 95, 72, 55, 43, 34, 26, 17 kDa).

The relative content of edestin and other components was approximately estimated by densiometric scanning technique (Figure 3.9). The results showed that edestin (including AS and BS) is the major protein component in hemp proteins, consisting of about 85% of total proteins. The other subunits were about 15%. These results are consistent with literature data [Patel *et al.*, 1994; Tang *et al*, 2006; Kim & Lee, 2011].

78
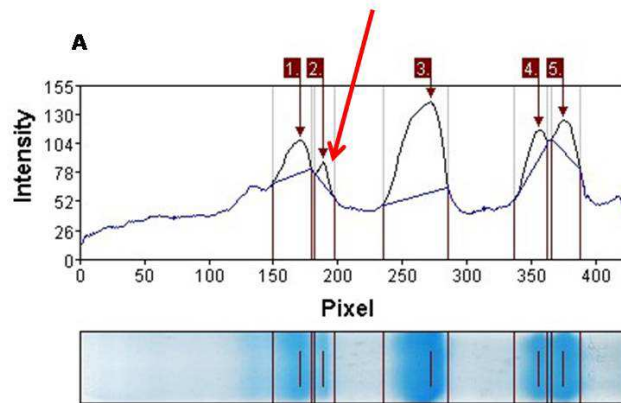
Figure 3.9. Densiometric profile in presence of 2-ME of hempseed meal proteins extracted with 2% SDS/6 M urea solution. Red arrow indicates the difference in the distribution of the minor component.

3.2.2.2. SDS–PAGE of protein hydrolysates

Enzymatic hydrolysis of defatted hempseed meal was performed using two commercial food grade protease cocktails (Flavourzyme® and Umamizyme®), in ammonium bicarbonate as a buffer. Defatted hempseed cake was incubated under the same experimental conditions without the enzyme as a control. The reaction was stopped after 1, 5, 11 and 24 h by addition of formic acid to the mixture, and finally centrifuged.

The characterization of molecular weight profile of enzymatic hydrolysates is important, especially when these compounds are used for clinical nutrition or allergic patients [Tossavainen *et al.*, 1997]. Several authors reported the use of SDS-PAGE to evaluate and quantify the level of protein hydrolysis [Nugent *et al.*, 1983; Savoie, 1994]. Indeed, this approach is useful for the assessment of the role of individual enzymes in protein breakdown. In 2001 Alacorn *et al.* [2001] suggested the possibility of using a calculated numerical index taking into account both the percentage of reduction in optical density for each protein band after a given reaction time, and the relative proportion that such band represents to total protein in the sample. Thus, SDS-PAGE was used to evaluate the degree of hydrolysis (DH), which is defined as the percent ratio of the number of peptides bonds cleaved to the total number of peptides bonds in the substrate. DH is a measure of the extent hydrolytic degradation of proteins

and is also the most used indicator for comparison among different proteolytic process [Alacórn *et al.*, 2001].

The SDS-PAGE profiles and the corresponding densiometric profile obtained after hydrolysis performed on hempseed meal in presence of Umamizyme® and Flavourzyme® are detailed in Figures 3.10, 3.11 and 3.12.
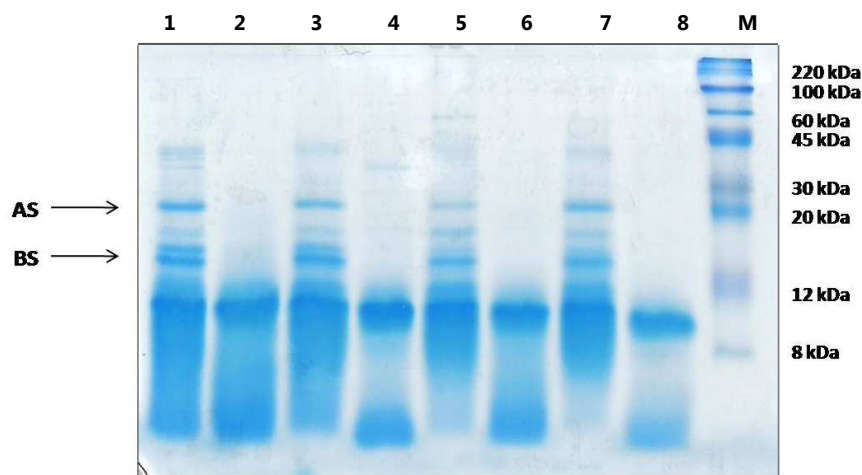
Figure 3.10. SDS-PAGE profile of protein fractions obtained at different sampling times during the hydrolysis of hempseed meal by Umamizyme® (hydrolysis parameter: pH 7, 45 °C). Lanes 1, 3, 5 and 7 are 1, 5, 11, 24 h of control digestion, respectively. Lanes 2, 4, 6, 8 are 1, 5, 11, 24 h of hempseed meal digestion, respectively. M represents the protein molecular mass marker (130, 95, 72, 55, 43, 34, 26, 17 kDa).
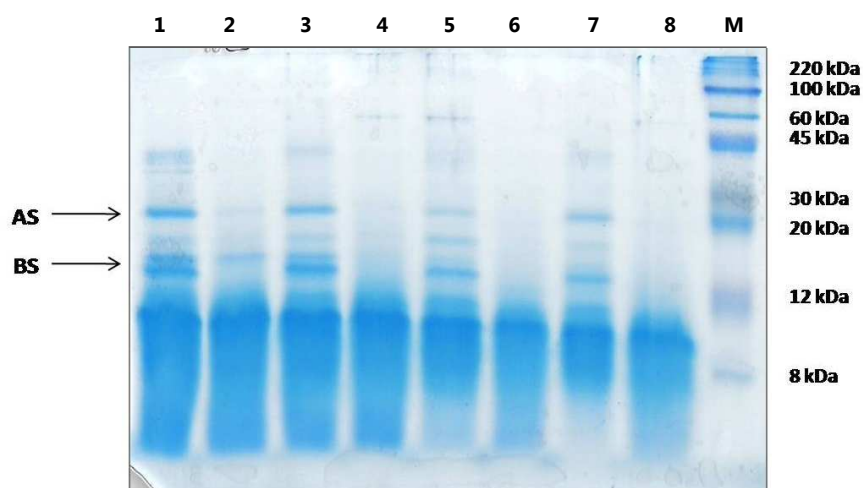
Figure 3.11. SDS-PAGE profile of protein fractions obtained at different sampling times during the hydrolysis of hempseed meal by Flavourzyme® (hydrolysis parameter: pH 8, 50 °C). Lanes 1, 3, 5 and 7 are 1, 5, 11, 24 h of control digestion, respectively. Lanes 2, 4, 6, 8 are 1, 5, 11, 24 h of hempseed meal digestion, respectively. M represents the protein molecular mass marker (130, 95, 72, 55, 43, 34, 26, 17 kDa).

80
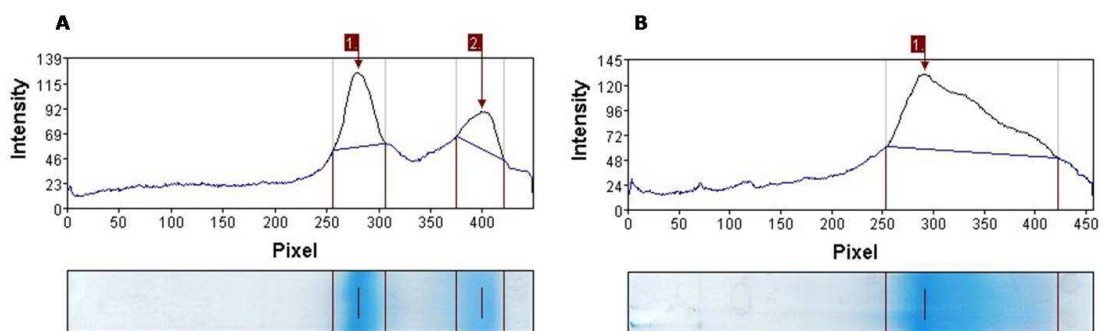
Figure 3.12. Densiometric profile of hydrolyzed hempseed meal after 24 h incubation. **A.** Umamizyme®-catalysed process. **B.** Flavourzyme®- catalysed process.

A limited, spontaneous degradation of proteins, in the absence of the enzyme, could be observed in comparison with the control lanes. A comparison between protein patterns obtained by Umamizyme® and Flavourzyme® revealed a similar performance of the two hydrolytic enzymes. A significant hydrolysis of the main protein fractions (edestin subunits, indicated as AS and BS) was observed for both proteases, as evidenced by the fast and general decrease of optical density showed by these bands (Figure 3.12). In particular, after 1 hour, samples treated with both enzymes were already significantly different from the control samples, since the AS and BS bands were completely hydrolyzed, particularly when Umamizyme® was used as the biocatalyst. After 5 hours of incubation, in the sample treated with Umamizyme® also the protein bands with the molecular weight range from 10 kDa to 2-3 kDa disappeared, whereas with Flavourzyme® the lower part of the gel (<10 kDa) was still completely spotted by protein elements. For both enzymes, no further proteolysis was detected after 11 h and 24 h, as shown by the protein profiles. In conclusion, Umamizyme® hydrolyzed all proteins with high molecular weight after 1 h incubation and only two defined bands (about 10 kDa and about 2-3 kDa) were not hydrolyzed after 5 h. On the other hand, Flavourzyme® hydrolyzed all proteins with a molecular weight >10 kDa after 5 h, whereas protein bands with low molecular weight (>10 kDa) were unaffected after 24 h incubation. For both enzymes, a 5 h incubation process was shown to be suitable to achieve the highest hydrolysis.

3.2.3. Protease activity assay

The activity of the enzymes (Umamizyme[®] and Flavourzyme[®]) used to obtain the hempseed HVPs was evaluated by a non-specific protease activity assay (casein assay). This assay uses casein as the substrate and Folin & Ciocalteu Phenol (F-C), or Folin's reagent, as the indicator [Folin, 1927; Anson, 1938]. When a protease digests casein, the amino acid L-tyrosine is liberated along with other amino acids and peptide fragments. F-C reagent primarily reacts with free L-tyrosine to produce a blue colored chromophore, which is quantifiable by measuring spectrofotometrically the absorbance at 750 nm (Figure 3.13).
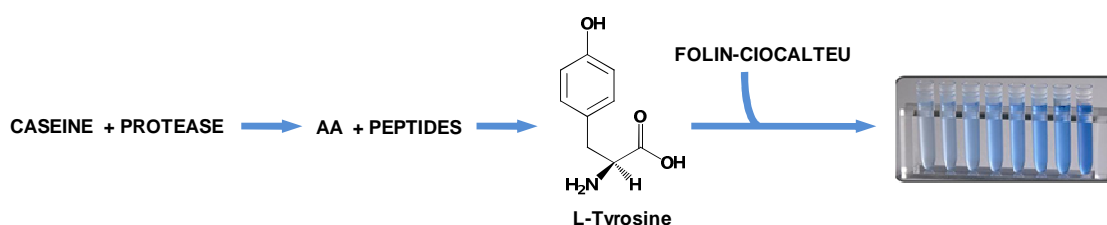
Figure 3.13. Casein assay for protease activity determination

The more L-tyrosine is released from casein, the more chromophores are generated and the stronger the activity of the protease is. The absorbance values generated by the protease are compared to a standard curve which is obtained by reacting known amounts of L-tyrosine with the F-C reagent and by correlating the changes in absorbance with the micromoles of L-tyrosine. From the standard curve the protease activity is determined in terms of units (U), which are the equivalents of L-tyrosine (µmol) released from casein per minute [Cupp-Enyad, 2008].

The assay is performed in two steps. In the first one a sample solution is prepared by adding a known volume of protease to casein, which releases L-tyrosine; after 5 minutes the hydrolysis is stopped by addition of trichloroacetic acid (TCA). In the second step the solution is mixed with the F-C reagent; the reaction between the released L-tyrosine and the F-C reagent produces blue colored chromophores which are quantified by measuring the absorbance at 750 nm. At the same time the absorbances of a blank and a control solution are evaluated. The blank solution contains the reagents of the protease solutions except that TCA is added before the protease in order to inactivate it

immediately. The control solution, instead, contains the reagents of protease solutions except for the enzyme. The μmoles of released L-tyrosine equivalents are determinated by using the calibration curve. The activity of Flavourzyme® was calculated by using equation 3.1.

$$U/ml\ enzyme = \frac{(\mu mol\ of\ tyrosine\ equivalents\ released)x(ml\ used\ in\ step\ 1)}{(ml\ of\ enzyme)x(reaction\ time,\ min)x(ml\ used\ in\ step\ 2)} \quad (3.1)$$

where, the μmoles of released L-tyrosine, the volume of the enzyme assay (ml), the amount of enzyme used (ml), the reaction time (minutes) and the volume of the colorimetric assay (ml) are used.

As Umamizyme® is available as a solid, the enzymatic activity was calculated by dividing the activity in U/ml by the starting concentration of the solid (in mg/ml), as reported in equation 3.2.

$$U/mg\ enzyme = \frac{U/ml\ enzyme}{mg\ protein/ml\ enzyme} \quad (3.2)$$

Figure 3.14 shows the standard curve obtained by the reaction of increasing amounts of 1.1 mM L-tyrosine solutions with the F-C reagent. The calculated protease activities are reported in Table 3.4.

	L-Tyrosine	
Conc. (mM)	μmol	ABS (750 nm)
30	0.033	0.1433
60	0.066	0.2880
80	0.088	0.3891
120	0.132	0.5597
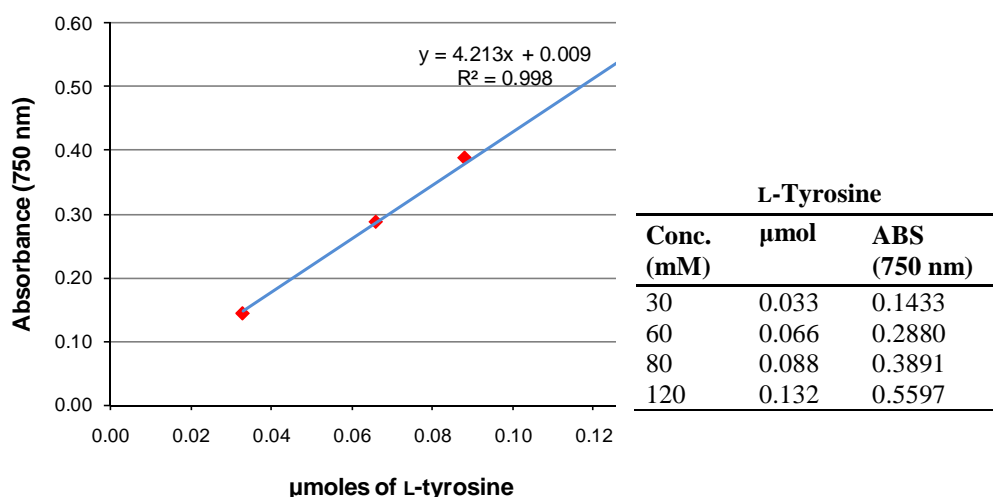
Figure 3.14. a) Standard curve obtained by plotting the change in absorbance (ABS) recorded (λ=750) (Y axis) *versus* the μmoles of L-tyrosine (X axis). b) In the Table the used amounts of L-tyrosine for the standard curve and the recorded absorbance values are reported.

Table 3.4. Calculated protease activities (IU) of Umamizyme® and Flavourzyme®.

Enzyme	IU (as supplier)	Amount add	ABS (750 nm)	Equivalentes of L-tyr (µmol)	IU (calculated)	IU (calculated)
Umamizyme®	74.3 U/g	0.03 mg	0.156	0.035	258.3U/g	261 U/g
		0.06 mg	0.306	0.072	263.7 U/g	
Flavourzyme®	500 U/ml	0.02 µl	0.173	0.039	429 U/ml	432 U/ml
		0.04 µl	0.342	0.079	435 U/ml	

3.2.4. Chemical characterization of hempseed HVPs

Total nitrogen of defatted hempseed meal was assessed by Kjeldahl method performed by Centro di Ricerca per le Produzioni Foraggere e Lattiero-Casearie (CRA) of Lodi (Italy). Crude protein content was estimated by multiplying total nitrogen content by the conversion factor 6.25 (Table 3.5).

The Kjeldahl method is considered *the* standard method for estimating the protein concentration in foods, due to the high precision and reproducibility [AOAC, 1980]. A food is heated in presence of a strong acid (usually sulfuric acid) and releases nitrogen which can be determined by a suitable titration technique. Since the Kjeldahl method does not measure the protein content directly, a conversion factor is needed to calculate the amount of protein present from the measured nitrogen concentration. In most applications the average value 6.25 (equivalent to 0.16 g nitrogen per gram of protein) is used as a conversion factor [McClements, 2009].

Table 3.5. Calculated protein content in defatted hempseed meal by Kjeldal method.

Number of analysis	N total g/100g of meal	% Protein (N total X 6.25)
27	5.73	35.8

3.2.5. 1,1-Diphenyl-2-picrylhydrazyl (DPPH) radical scavenging activity

Free radical reactive oxygen species (ROS) are usually formed from normal essential metabolic processes in the human body, or from external sources such as exposure to X rays, ozone, cigarette smoking, air pollutants, and industrial chemicals [Lobo *et al.*, 2010].

A free radical is a molecular species containing an odd electron in an atomic orbital. Many radicals are unstable, highly reactive, and able to either donate to or accept an electron from other molecules. The most dangerous oxygen-containing free radicals are hydroxyl radical ($OH^•$) superoxide anion radical ($O_2^{•-}$), hydrogen peroxide (H_2O_2), oxygen singlet ($^1O_2$), hypochlorite (ClO^-), nitric oxide radical ($ONOO^-$), and peroxynitrite radical ($ROO^•$). Indeed, these species appear to be responsible for damaging of the nucleus and the membranes of cells in human body, because they are able to attack lipids, nucleic acids, proteins and carbohydrates [Young and Woodside, 2001]. As a result, free radicals may contribute to the development of degenerative or pathological processes such as aging, cancer, coronary heart disease and neurodegenerative diseases [Uttara *et al.*, 2009].

Oxidative stress is a term used to describe a oxidative damage resulting from the imbalance between free radical production and antioxidant defenses in the body [Rock *et al.*, 1996]. For example, this condition could arise from a tissue injure, *i.e.* trauma or infection.

An antioxidant is a stable molecule capable to donate an electron to a free radical and neutralize it.

To detoxify from the free radical usually formed in the human body, both enzymatic and non-enzymatic antioxidants exist in the intracellular and extracellular environment [Frie *et al.*, 1988]. Among non-enzymatic antioxidant systems, glutathione, ubiquinol, and uric acid are produced during normal metabolism in the body [Shi *et al.*, 1999]. Other antioxidants are the vitamins E (α-tocopherol), C (ascorbic acid), and B-carotene. The body cannot produce these latter micronutrients, so they must be supplied in the diet [Levine *et al.*, 1991].

Hence, diet-derived antioxidants may be particularly important in protecting against the diseases arising from oxidative stress. The role of compounds with antioxidant potential in nutrition is an area of increasing interest. For example, several reports about the antioxidant activities of natural compounds in fruit and vegetables (such as anthocyanin, the storage proteins of sweet potato root yam tuber, yam mucilage and potato tuber) were published [Liu *et al.*, 2007].

Antioxidants are used to mitigate the consequences of oxidative damage in the human body and also as food preservatives. Indeed, these compounds can prolong the shelf life and maintain the nutritional quality of lipid-containing foods [Halliwell *et al.*, 1995].

Proteins are key nutrients for humans and also play an important functional role in food processing.

Several peptides derived by partial hydrolysis of proteins show high antioxidant activity in food, for their ability to retard lipid and protein oxidation, associated with deterioration of food quality during the processing and storage [Yang *et al.*, 2013]. Natural antioxidant peptides can be produced from a variety of protein sources, including whey protein [Peña-Ramos *et al.*, 2004], potato protein [Wang & Xiong, 2005], maize zein [Zhu *et al.*, 2008] and buckwheat protein [Ma & Xiong, 2009].

A further advantage to use protein hydrolysates to improve the antioxidant activity in food is that they confer nutritional value. This property depends on amino acid composition of the peptides released, which on its turn depends on the type of proteases used, as well as on pH, temperature, substrate concentration and enzyme-substrate (E/S) ratio used in hydrolysis process [Chen *et al.*, 1995].

Antioxidant activities of hempseed and flaxseed hydrolysates were reported by Tang *et al.* [2008] and Udenigwe *et al.* [2009], respectively.

Several methods are routinely used to evaluate the efficiency of synthetic/natural antioxidants. Among them, the DPPH assay is one of the best-known and frequently employed for measuring the radical scavenging activity. DPPH (1,1-diphenyl-2-picrylhydrazyl) is a stable free radical because of its spare electron delocalization over the whole molecule, so that the molecules do not dimerize such as the most of free radicals. The delocalization causes a deep purple color with a strong absorption maximum around 520 nm in ethanol solution.

When a solution of DPPH is mixed with a substrate acting as a hydrogen atom donor (a free radical scavenger), a stable non-radical form of DPPH reduced (DPPH-H) is obtained. Simultaneously the color of solution turns from purple to pale yellow (due to picryl group still present) and the molar absorbance at 517 nm decreases from 9660 to 1640 [Molyneux, 2004; Szabo *et al.*, 2007]. The resulting decolorization is stoichiometric with respect to the number of electrons captured which depends on the antioxidant activity of the substrate. The reaction is depicted in Figure 3.15.
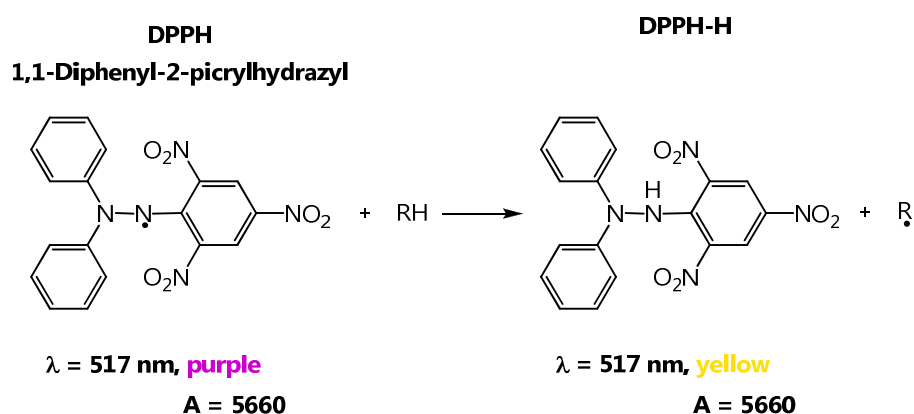
Figure 3.15. Principle of antioxidant (DPPH) assay.

The scavenging effects against DPPH radical was evaluated both for hempseed HVPs obtained by enzyme treatment (ultrafiltered fractions with MW<10 kDa) and by chemical hydrolysis according to previously reported procedures [Li et *al.*, 2007; Udenigwe *et al.*, 2009]. Defatted hempseed meal incubated under the same experimental conditions without the enzymes was used as the negative control; whereas reduced glutathione (GSH) and butylated hydroxytoluene (BHT) were used as the positive control. All assays were performed in triplicate. Concentration-dependence of the scavenging properties against DPPH was also determined using three concentrations of the peptide fractions. The antioxidant activity was evaluated as IC_{50} value, that is the concentration of the hydrolysates at which 50% of antioxidant activity is observed. The IC_{50} value thus describes the scavenging activity: the lower the IC_{50} value, the higher is the free radical scavenging ability.

Table 3.6 and Figure 3.16 report the IC_{50} values obtained for hempseed enzymatic hydrolysates.

Table 3.6. DPPH radical scavenging activity of HVPs obtained at hydrolysis time of 1, 5, 11 and24 h.

Time of hydrolysis	Enzyme		Control
	Flavourzyme[®]	Umamizyme[®]	
1 h	2.8±0.1	2.6±0.5	2.95±0.6
5 h	2.3±0.4	1.8±0.5	2.9±0.2
11 h	1.9±0.1	1.7±0.7	2.8±0.17
24 h	2.5±0.1	1.6±0.6	2.8±0.1

Results are expressed as half maximal effective concentration (IC_{50}, mg protein/mL) ± confidence interval (CI, α=0.05), n=6.
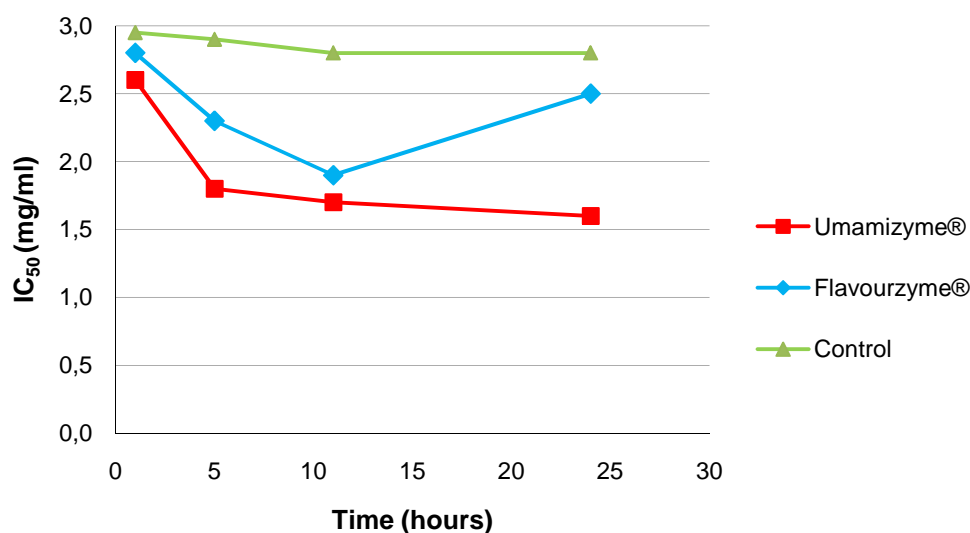
Figure 3.16. DPPH radical scavenging activity of HVPs obtained at hydrolysis time of 1, 5, 11 and 24 h.

The assay showed that the release of DPPH-scavenging peptides from hempseed proteins depends in part on the specificity of the proteases used in hydrolysis. In particular, the antioxidant activity of the samples treated with Umamizyme[®] increases as much as the hydrolysis up to 1.6 mg/ml after 24 hours of hydrolysis. By contrast, the activity of the samples treated with Flavourzyme[®] increases up to 1.9 mg/ml after 11 hours and slightly decreases at 24 hours.

Several studies reported that the DPPH scavenging activities of food protein hydrolysates may depend on both buffer and pH used in the assay, as well as on the size of their constituent peptides [Udenigwe et *al.*, 2009; Lin et *al.*, 2008]. To investigate the

effect of buffer and pH on the DPPH scavenging properties, the assay was also performed by dissolving the hydrolyzed fractions at 24 hours in three different buffers: acetate (pH 4.0), phosphate (pH 7.0) and sodium carbonate (pH 9.0). The hydrolyzed fractions exhibited better radical-scavenging activity in acetate buffer at pH 4.0 (Table 3.7). These preliminary results are in agreement with those previously reported [Udenigwe et *al*., 2009; Lin et *al.*, 2008] and show that pH affects the DPPH radical scavenging properties of antioxidants.

Table 3.7. DPPH radical scavenging activity (%) of HVPs obtained at hydrolysis time of 24 h (0.5% w/v) using three different buffers.

pH, buffer	Enzyme	
	Umamizyme®	Flavourzyme®
4, acetate buffer	86.73%	76.05%
7, phosphate buffer	36.51%	31.86%
9, sodium carbonate buffer	12.63%	10.11%

The DPPH radical scavenging activities of chemically hydrolyzed hempseed obtained with HCl at different acid concentration, time and temperature was also investigated. Table 3.8 shows the calculated IC_{50} values. The assay showed that the antioxidant activity of the chemical hydrolyzed is similar to that of enzymatic hydrolyzed. The highest activity is observed for peptides obtained with 1.0 M HCl at 63 °C for 48 hours. Probably these conditions allow the production of peptides with optimal sizes to antagonize the DPPH activity.

Table 3.8. DPPH radical scavenging activity of chemical HVPs obtained in different hydrolysis conditions of concentration, temperature and time.

Hydrolysis Conditions (in HCl)	IC_{50} values (mg/ml)
0.1 M, 48 h, 63 °C	2.22±0.1
1.0 M, 48 h, 63 °C	1.59±0.2
1.0 M, 6 h, 110 °C	2.68±0.3
6.0 M, 6 h, 110 °C	2.33±0.4

3.2.6. Ferrous ion-chelating potency

Iron has been found to be involved in several key pathogenic processes (such as neurodegeneration). In particular redox-active Fe(II) reacts with H_2O_2 to generate the highly reactive $^{\bullet}OH$ (hydroxyl radical) via the Fenton reaction (equation 3.3) [Wardman & Candeias, 1996]:

$$Fe(II) + H_2O_2 \rightarrow Fe(III) + OH + {^{\bullet}OH} \qquad\qquad (3.3)$$

The Fe(II)-chelating potency of a substrate is usually assessed by the ferrozine method. Ferrozine is the disodium salt of 3-(2-pyridyl)-5,6-bis(4-phenylsulfonic acid)-1,2,4-triazine (Figure 3.17). This compound binds to divalent iron and forms a stable magenta complex species which is very soluble in water and is characterized by an absorption band centred about at 562 nm, being useful for the direct determination of iron in water [Lawrence, 1970; Sanchez-Moreno, 2002]. The addition of iron chelators interferes with the ferrozine-Fe(II) complex in a concentration-dependent manner resulting in low absorbance.

Ferrozine®
3-(2-pyridyl)-5,6-diphenyl-1,2,4-triazine-4',4"-disulfonic acid disodium salt
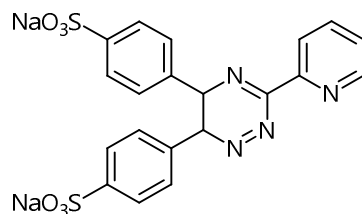
Figure 3.17.

The assay showed that samples treated with Umamizyme® at 5 hours displayed a remarkable Fe(II)-chelating potency (0.08 mg/ml). By contrast, the activity of the samples treated with Flavourzyme® is higher than the one of samples treated with Umamizyme® at each time and slightly increases with hydrolysis time up to 0.044 mg/ml.

Table 3.9 and Figures 3.18, 3.19 and 3.20 report the IC_{50} values obtained for enzymatically hydrolyzed hempseed.

Table 3.9. Fe(II)- chelating ability of HVPs obtained at hydrolysis time of 1, 5, 11 and 24 h.

Time of hydrolysis	Enzyme		Control
	Flavourzyme[®]	**Umamizyme**[®]	
1 h	0.062±0.008	0.16±0.02	0.18±0.6
5 h	0.06±0.01	0.08±0.01	0.165±0.2
11 h	0.055±0.003	0.11±0.01	0.155±0.17
24 h	0.044±0.005	0.13±0.03	0.16±0.1

Results are espressed as half maximal effective concentration (IC_{50}, mg protein/mL) ± confidence interval (CI, α=0.05), n=6.
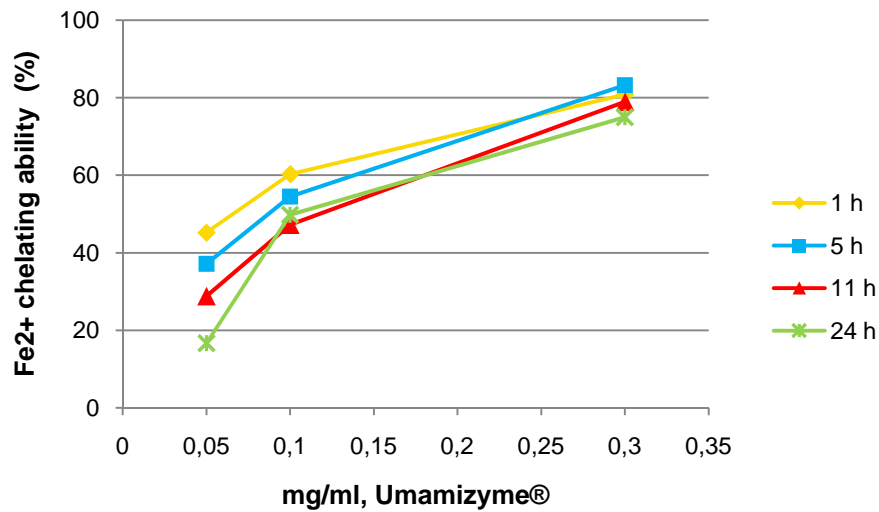
Figure 3.18. Fe(II)- chelating ability (%) calculated *versus* concentration (mg/ml) of the sample treated with Umamizyme[®].
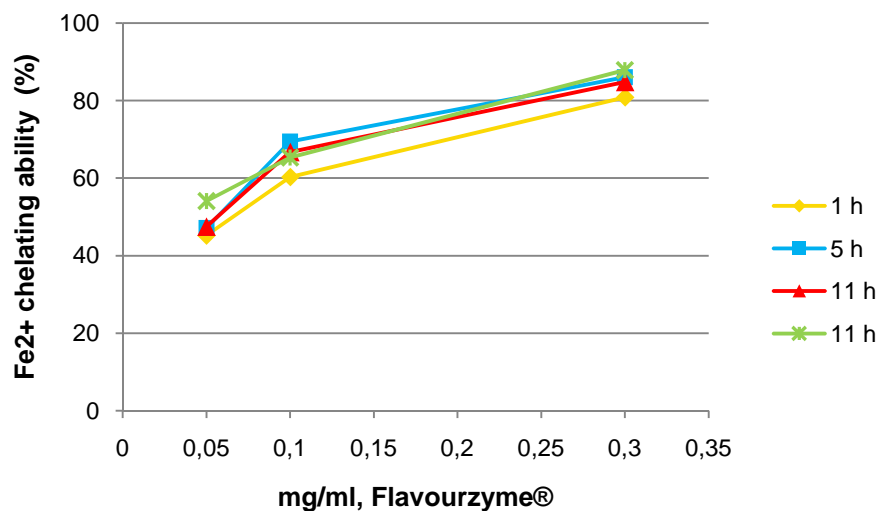
Figure 3.19. Fe(II)- chelating ability (%) calculated *versus* concentration (mg/ml) of the sample treated with Flavourzyme[®].
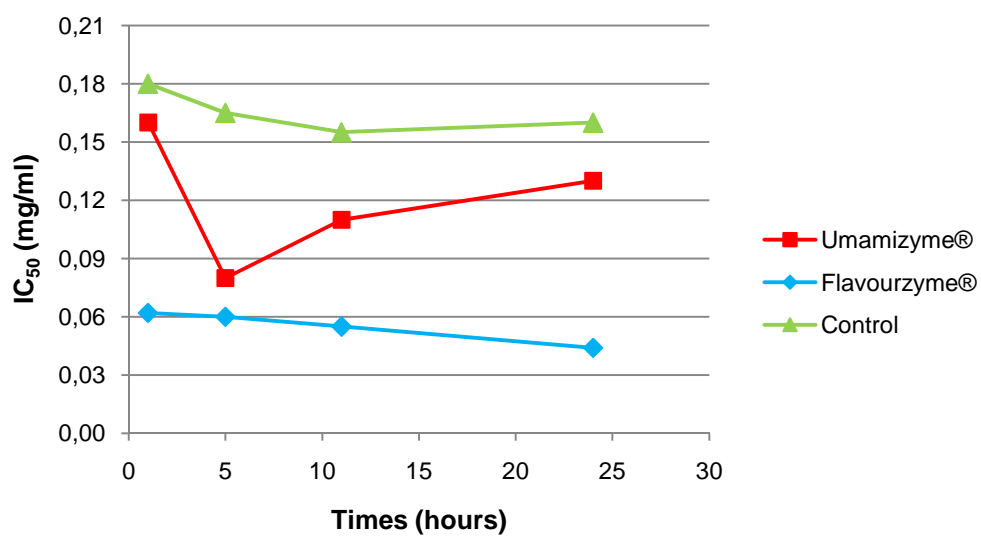
Figure 3.20. Fe(II)- chelating ability of HVPs obtained at hydrolysis time of 1, 5, 11 and 24 h.

3.2.7. Glutamate content

The determination of L-glutamate content is of utmost importance to evaluate the sensory profile of a sample. The free L-glutamate content in the fractions <10 kDa was assessed by an enzymatic assay in which L-glutamic acid is oxidised by nicotinamide-adenine dinucleotide (NAD^+) in the presence of glutamate dehydrogenase (GlDH), leading to the formation of 2-oxoglutarate and of reduced nicotinamide-adenine dinucleotide (NADH) (Figure 3.21).
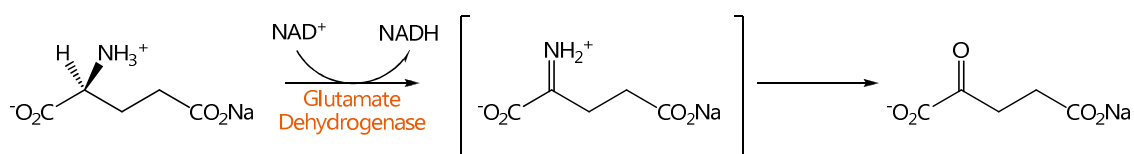
Figure 3.21. Mechanism of the glutamate dehydrogenase reaction.

The amount of reduced NADH is stoichiometric with the amount of free L-glutamic acid. This assay takes advantage of the difference in the ultraviolet absorption spectra between the oxidized (NAD^+) and reduced forms (NADH) of this coenzymes at a wavelengths of 339 nm (Figure 3.22).
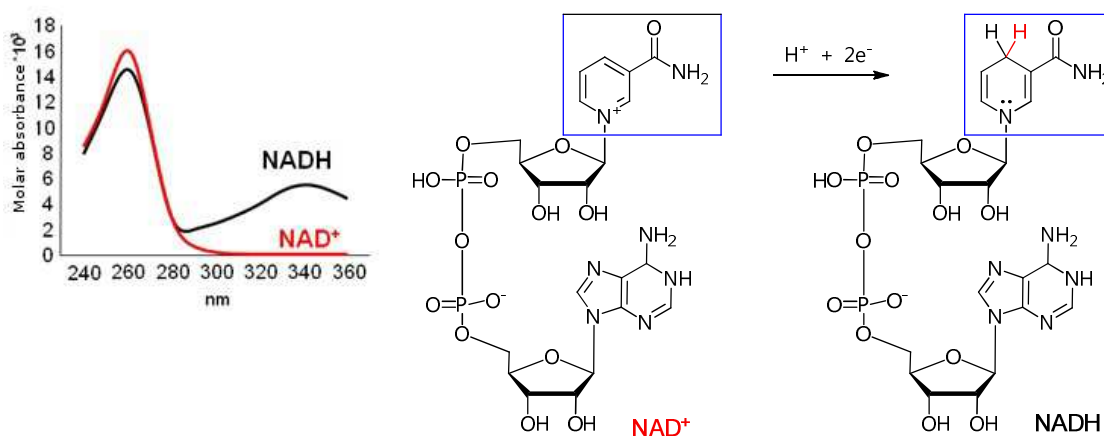
Figure 3.22. Absorbance spectra of NAD^+ and NADH.

A calibration curve was obtained using L-glutamate solutions in water at different concentrations (Figure 3.23). Defatted hempseed meal incubated under the same experimental conditions without the enzyme was used as control.

L-Glutamate		
Conc. (mM)	**μmol**	**ABS (339 nm)**
0	0	0.0565
0.025	0.05	0.1699
0.05	0.1	0.2816
0.1	0.2	0.4881
0.15	0.3	0.7189
0.25	0.5	1.2042
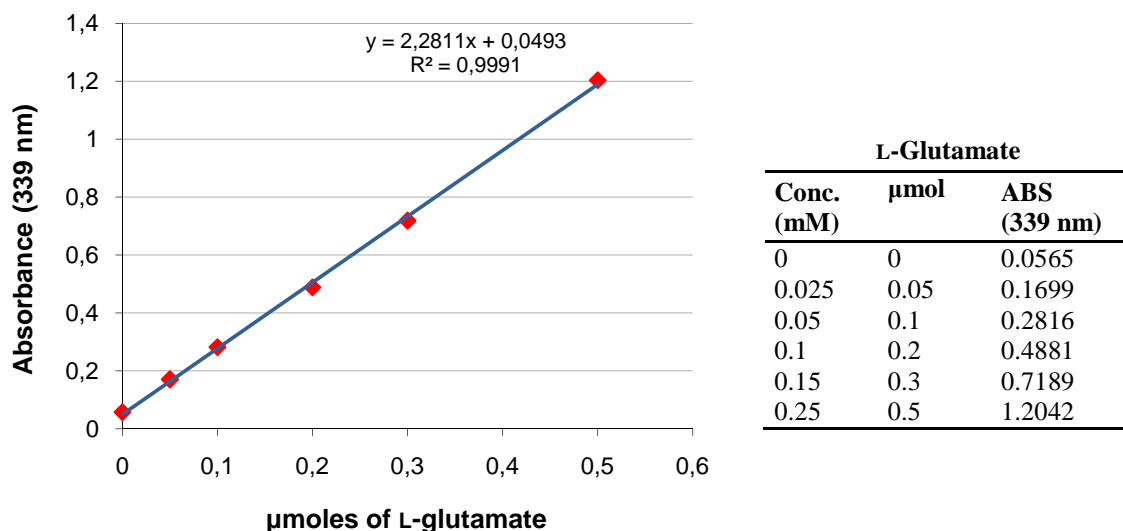
Figure 3.23. a) Standard curve obtained by plotting the change in absorbance recorded ($\lambda=339$) (Y axis), *versus* the μmoles of L-glutamate on (X axis). b) The amounts of L-glutamate used to obtain the standard curve and the recorded absorbance values are reported in the Table.

The assay shows that the free L-glutamate amount in samples treated with Flavourzyme® is not affected by the hydrolysis time, while the one in samples treated with Umamizyme® is time dependent (Figure 3.24 and Table 3.10) and increases until reaching a maximum value after 24 hours of hydrolysis.

Table 3.10. Free L-glutamate percentage in hemp protein hydrolysates obtained at hydrolysis time of 1, 5, 11 and 24 h.

Time of hydrolysis	Control	Enzyme	
		Flavourzyme®	**Umamizyme®**
1 h	0.41±0.32	0.62±0.098	1.25±0.04
5 h	0.41±0.12	0.80±0.1	1.24±0.53
11 h	0.51±0.08	0.90±0.17	1.45±0.67
24 h	0.73±0.15	0.73±0.1	3.72±1.65

Results are expressed as amount of free L-glutamate (%) ± confidence interval (CI, $\alpha=0.05$), n=6.

94
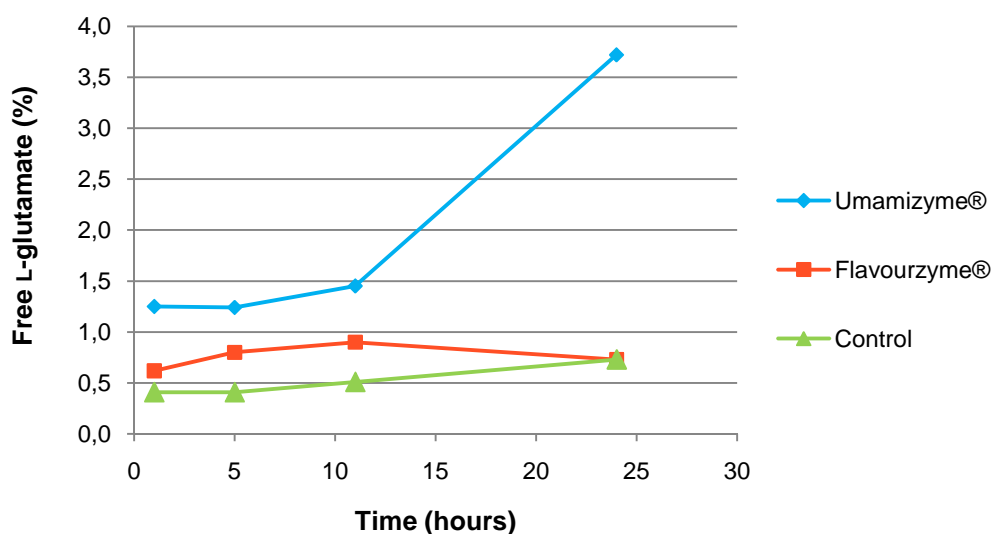
Figure 3.24. Free L-glutamate percentage in the enzymatic hydrolysates fractions and controls plotted against the hydrolysis time.

3.2.8. Sensory Profile

In order to complete the sensory profile of protein–peptide mixtures, the hempseed hydrolysates were tested by a team of selected and certified panelists, as described for rice middlings hydrolysates (section **6.2.2.3.**). Six subjects, having variable experiences of descriptive analysis, were recruited as panelists. These subjects were previously trained to evaluate the taste of aqueous solutions of the following standard taste compounds: sucrose for sweet taste (50 mmol/L); lactic acid for sour taste (20 mmol/L); NaCl for salty taste (20 mmol/L); caffeine for bitter taste (1 mmol/L); monosodium L-glutamate for umami taste (3 mmol/L).

The freeze-dried hempseed hydrolysates were dissolved in water and equilibrated at room temperature (20 ± 2 °C) to give a final concentration of 0.1 and 0.5 % (w/v). Aliquots (20 mL) of each sample were presented to the panelists. The sensory attributes were evaluated using a quantitative descriptive analysis method [Jo & Lee, 2008], based on "sip and spit" procedure, to minimize the uptake of any toxic compound.

Tables 3.11-3.12 and Figures 3.25-3.26 show the mean taste intensity ratings of the five main flavors for the analyzed hydrolysates. Data of Tables 3.11 and 3.12 indicate that

both the taste quality and intensity are strongly dependent on the concentration tested as well as on the enzyme utilized and the hydrolysis time.

Table 3.11. Taste intensity of hempseed hydrolysates water solutions (0.1% w/v) after incubation with Umamizyme and Flavourzyme. Each value represents the mean taste intensity rating scored on a 10-point category scale by six panelists.

Sample (0.1% w/v)	Bitter	Sweet	Sour	Salty	Umami
Flavourzyme 1 h	0	1.6	0	0	1.0
Flavourzyme 5 h	0	1.0	0	0	1.1
Flavourzyme 11 h	0	0.7	0	0	1.0
Flavourzyme 24 h	0	0.7	0	0	0.8
Umamizyme 1 h	0	1.0	0	0	0.6
Umamizyme 5 h	0	1.0	0	0	0.7
Umamizyme 11 h	0	1.0	0	0	1.0
Umamizyme 24 h	0	0.6	0	0	1.4

Table 3.12. Taste intensity of hempseed hydrolysates water solutions (0.5% w/v) after incubation with Umamizyme and Flavourzyme. Each value represents the mean taste intensity rating scored on a 10-point category scale by six panelists.

Sample (0.5%)	Bitter	Sweet	Sour	Salty	Umami
Flavourzyme 1 h	0	0.9	2.0	1.0	1.6
Flavourzyme 5 h	0	1.0	2.0	1.3	2.1
Flavourzyme 11 h	0	0.7	2.8	1.2	1.5
Flavourzyme 24 h	0	1.0	2.4	1.1	2.8
Umamizyme 1 h	1.0	0	1.6	0.9	1.9
Umamizyme 5 h	1.9	0	2.7	0.8	2.4
Umamizyme 11 h	1.4	0	2.5	1.2	3.5
Umamizyme 24 h	1.3	0	2.9	0	3.5
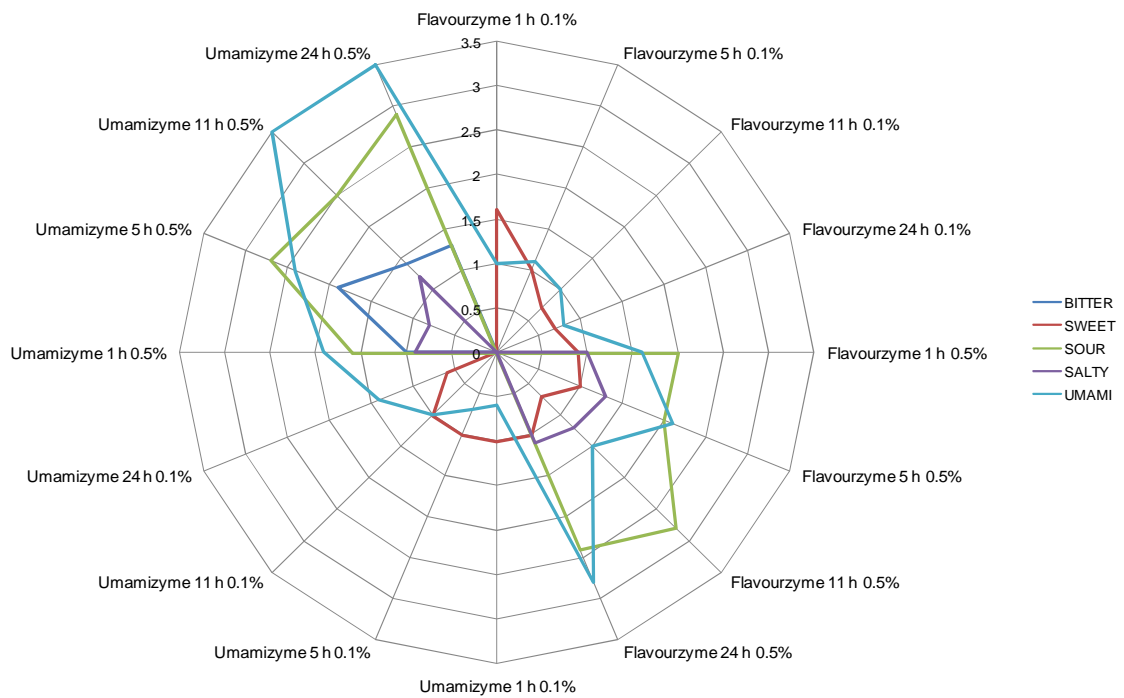
Figure 3.25. Taste profiles of hempseed hydrolysates after incubation with Umamizyme and Flavourzyme. Each value represents the mean taste intensity rating scored on a 10-point category scale by six panelists. The results are represented with a reduced scale (0-3.5) for a easier reading.

At the lower concentration (0.1% w/v) umami and sweet taste are the main attribute for each sample. In particular, umami taste was prevalent in samples incubated with Umamizyme for 24 hours. This is in agreement with the results of the glutamate assay which indicate the highest concentration of glutamate in these samples.

At the higher concentration (0.5% w/v) the umami sensation becomes more intense, particularly for the samples incubated with Umamizyme for 11 and 24 hours. At the same time also the other taste perceptions increase. This may be in agreement with the characteristic flavor enhancing activity of umami substances. In particular, a sour sensation is detect, probably due to the release of acidic aminoacids by hempseed proteins. However, the sour taste does not alter the taste sensation: it might be the basic flavor defined for the hydrolysates (as discussed for rice middlings hydrolysates in section **3.1.3.**). The bitter taste was present in the samples incubated with Umamizyme; however, it does not prevail on the umami taste. Instead, the sweet taste is present only in the hydrolyzed samples deriving from Flavourzyme.
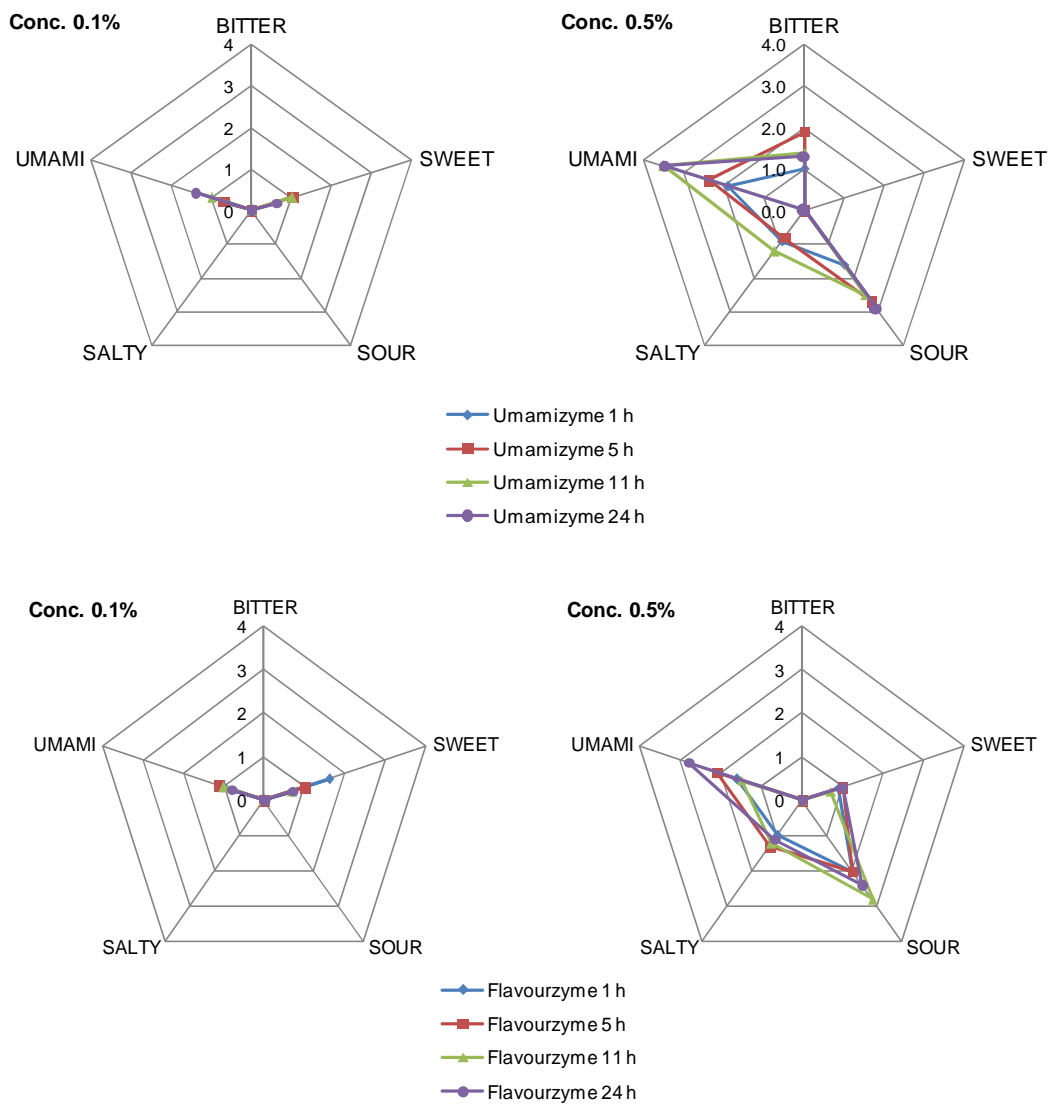
Figure 3.26. Taste profiles of MSG and rice middling hydrolysates after 24 h of incubation with Umamizyme and Flavourzyme. Each value represents the average taste intensity scored on a 10-point category scale by six panelists. Results are represented with a reduced scale for a easier reading.

3.3. Preparation of HVPs from Hempseed through Chemical Hydrolysis

Chemical hydrolysis of proteins can be carried out in either acidic or alkaline conditions.

The alkaline hydrolysis of proteins is unattractive in term of taste because it destroys key amino acids such as L-cysteine and L-arginine. Upon this process other destroyed amino acids are L-serine and L-threonine, whereas L-tryptophan is not involved.

The acidic hydrolysis is preferred and widely used in food industry because it is rapid, cheap and produces savory peptides that can be used as flavor enhancers. During this process the essential amino acids L-tryptophan, L-methionine, and L-cysteine are destroyed, whereas L-asparagine and L-glutamine are converted into aspartic and glutamic acid, respectively. Usually the biological and organoleptic properties of the end product depend on the conditions of hydrolysis (concentration and type of acid, temperature, pressure, time of hydrolysis) and on the starting material [Nagodawithana, 2010].

Hempseed proteins, extracted as described in section **6.3.2.** (*Method A*), were subjected to acidic hydrolysis according to Aaslyng [1998]. The hydrolyses were performed either in strong or weak conditions in order to obtain peptides with different molecular weight.

3.3.1. Chemical hydrolysis of hempseed proteins with Acetic Acid

The first hydrolysis on hempseed proteins was carried out with 50% acetic acid solution at 110 °C for 18 hours.

Upon this process the color of the solution did not change and few precipitate was produced. The freeze-dried product was an amber odorless amorphous solid (Figure 3.27).

The SDS-PAGE of this product could not be performed due to the high concentration of acetic acid used.

Figure 3.27. Freeze-dried hempseed protein hydrolysates.

The hempseed hydrolysates were analyzed by reverse-phase HPLC, using 0.1% TFA in water/acetonitrile as the mobile phase and a UV/VIS detector set at three different wavelengths (226, 254, 280 nm). The chromatogram showed the presence of many compounds, most of which probably are peptides with different molecular weights as shown by absorption at 226 nm. The first group of peaks, with maximum absorbance at 256 nm, is characteristic of aromatic amino acids (Figure 3.28).
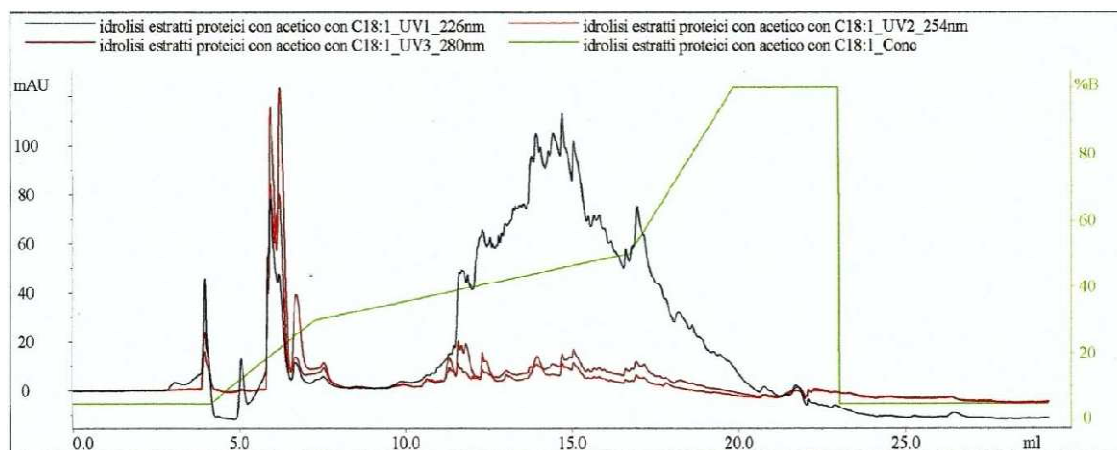
Figure 3.28. Chromatograms of hempseed protein hydrolysates obtained with acetic acid.

3.3.2. Chemical hydrolysis of hempseed proteins with Formic Acid

Formic acid (HCOOH) can be easily removed and reduces the time of hydrolysis due its higher acidity in comparison with acetic acid.

The hydrolysis was carried out with 20% HCOOH solution at 110 °C for 8 hours. The pale brown and clear starting solution did not change the color during the hydrolysis.

The freeze dried product was an amber amorphous solid with a distinct flavor of salt and a spicy note (Figure 3.29).

Figure 3.29. Freeze-dried hempseed protein hydrolysates.

The SDS-PAGE profile shows a large distribution of molecular weights, which cannot be compared with the standards (Figure 3.30).
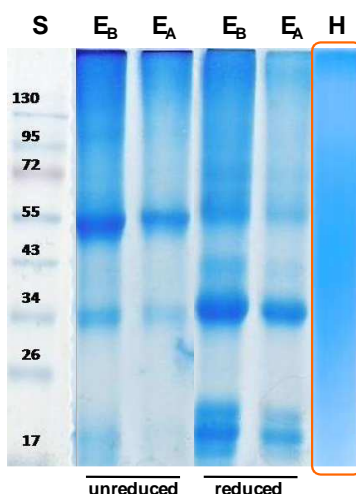
Figure 3.30. SDS-PAGE profiles of hemp proteins from defatted hempseed flour in absence (unreduced) and presence (reduced) of 2 mercaptoethanol (2-ME). S represents the protein molecular mass marker. Lanes E_B are hempseed protein extracted at pH 10.00 and analyzed in both unreduced and reduced conditions. Lanes E_A are hempseed proteins precipitated at pH 5.00 and analyzed in unreduced and reduced conditions. Lane H represents the hydrolysates obtained with HCOOH.

The RP HPLC analysis shows peaks very similar to those registered for the peptides obtained with acetic acid (Figure 3.31). However, formic acid cannot be used on industrial scale and should be present only in traces in the formulation of functional foods.
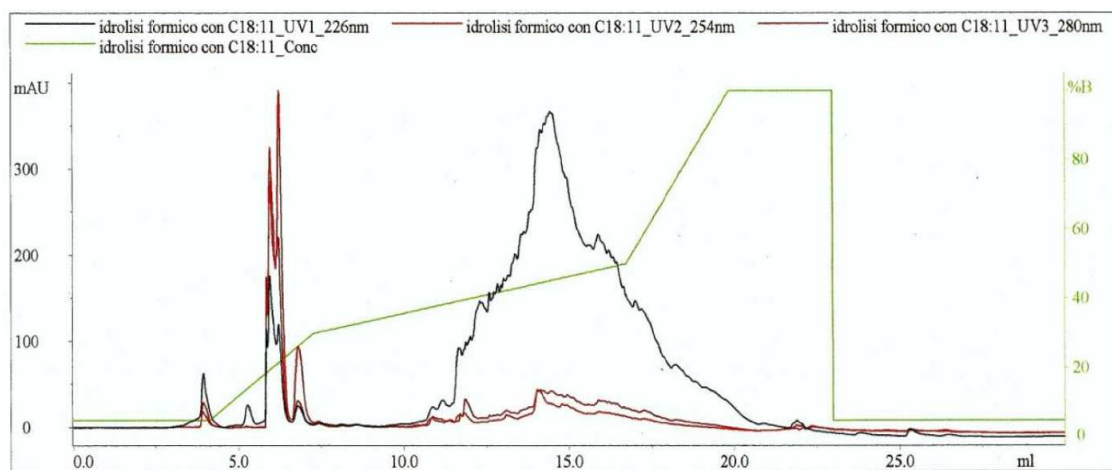
Figure 3.31. Chromatograms of hempseed protein hydrolysates obtained with formic acid.

3.3.3. Chemical hydrolysis of defatted hempseed meal with Hydrochloric Acid

To reduce the number of steps, according to Aaslyng, defatted hempseed meal was hydrolyzed with 4 M HCl at 110 °C for 6 hours [Aaslyng, 1998].

The mixture quickly became dark brown probably due to the Maillard reaction (Figure 3.32). At the end of the hydrolysis, the solution was very dark even after neutralization and filtration under vacuum. Furthermore, very dark and small clusters, which were absent in defatted hemp seed meal, were present in the undigested material (Figure 3.33). The dark solution became clear and light yellow by treatment with activated carbon followed by filtration using celite (Figure 3.34).

The lyophilization of this product was very difficult due to the high content of salts.

Figure 3.32.   *Figure 3.33.*   *Figure 3.34.*

102

The RP-HPLC analysis was not useful to separate the peptides formed during the hydrolysis, as shown by the chromatogram. Presumably, these compounds are in the salt form and hence very hydrophilic under the analysis conditions (Figure 3.35).
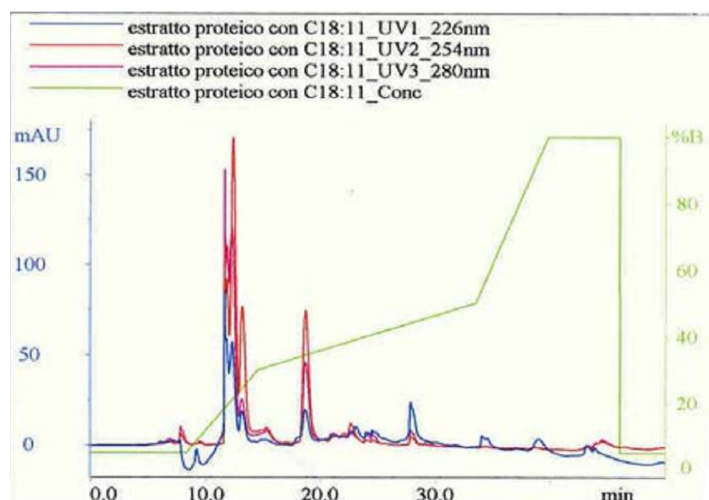
Figure 3.35. Chromatograms of hempseed hydrolysates obtained by hydrochloric acid treatment.

3.3.4. Chemical hydrolysis of hempseed proteins with Hydrochloric Acid

To reduce the problems arising from using defatted hempseed meal, we decided to perform the hydrochloric acid hydrolysis on hempseed protein extract. The hydrolyses were performed under different conditions, *i.e.* concentration, temperature, time.

✓ 0.1 M HCl for 48 hours at 63 °C;

✓ 1 M HCl for 48 hours at 63 °C;

✓ 1 M HCl for 6 hours at 110 °C

   in these cases, the solutions were neutralized using an ion-exchange resin (Amberlite 402) to reduce the pH and remove chlorides;

✓ 3 M HCl for 8 hours at 100 °C;

✓ 6 M HCl for 6 hours at 110 °C.

   the strong acidity of these solutions was reduced adding 2 M NaOH and sodium carbonate, Na_2CO_3, as the buffer. Preparative RP-HPLC was used to remove salts.

3.3.4.1. Chemical characterization

Figures 3.36-3.40 show the recorded RP-HPLC chromatograms of the hydrolysates obtained under the above conditions, using 0.1% TFA in water/acetonitrile as the mobile phase and a UV/VIS detector set at three different wavelengths (226, 254, 280 nm). The blue line corresponds to the absorption at 226 nm (typical of the peptidic bond), the red one at 254 nm and the violet one at 280 nm (typical of the aromatic compounds). The green line corresponds to the acetonitrile concentration. Each chromatogram shows a characteristic peak at short elution times, probably due to hydrophilic compounds. The maximum absorption at 254 nm is typical of aromatic amino acids.
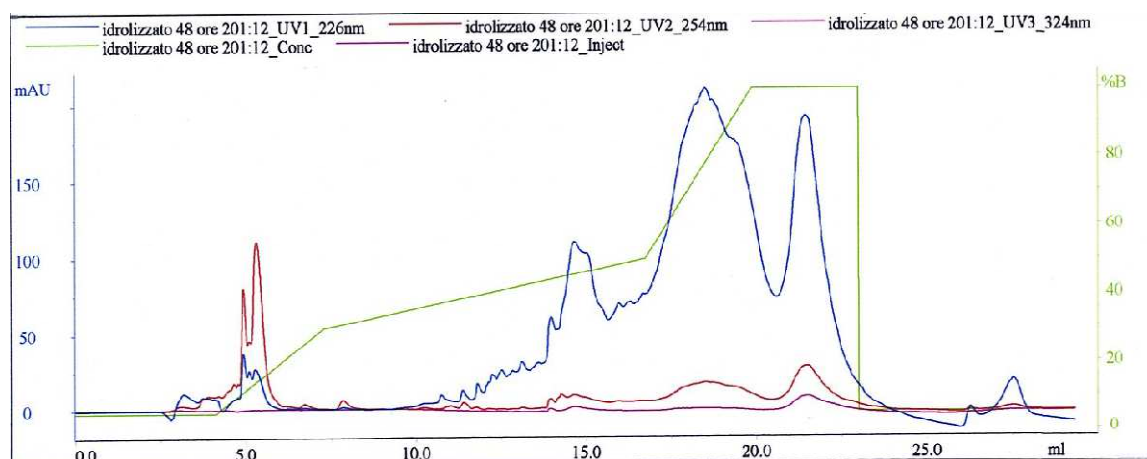
Figure 3.36. Chromatograms of hempseed protein hydrolyzed with 0.1 M HCl, at 63 °C for 48 hours.
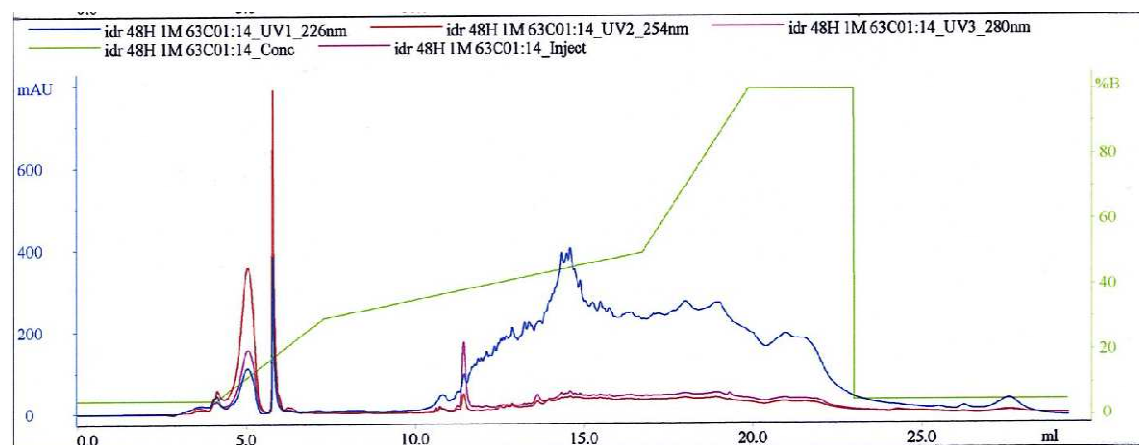
Figure 3.37. Chromatograms of hempseed protein hydrolyzed with 1 M HCl, at 63 °C for 48 hours.

104
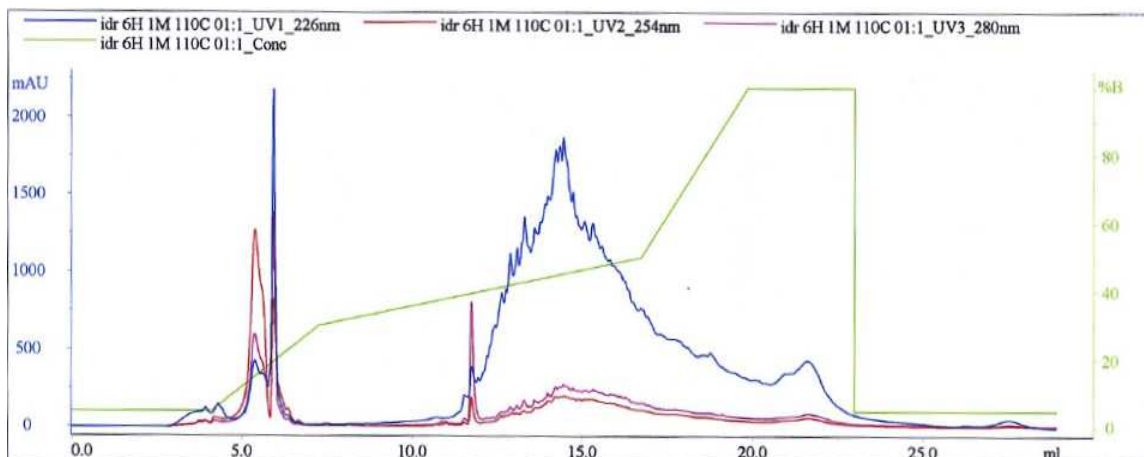
Figure 3.38. Chromatograms of hempseed protein hydrolyzed with 1 M HCl, at 110 °C for 6 hours.
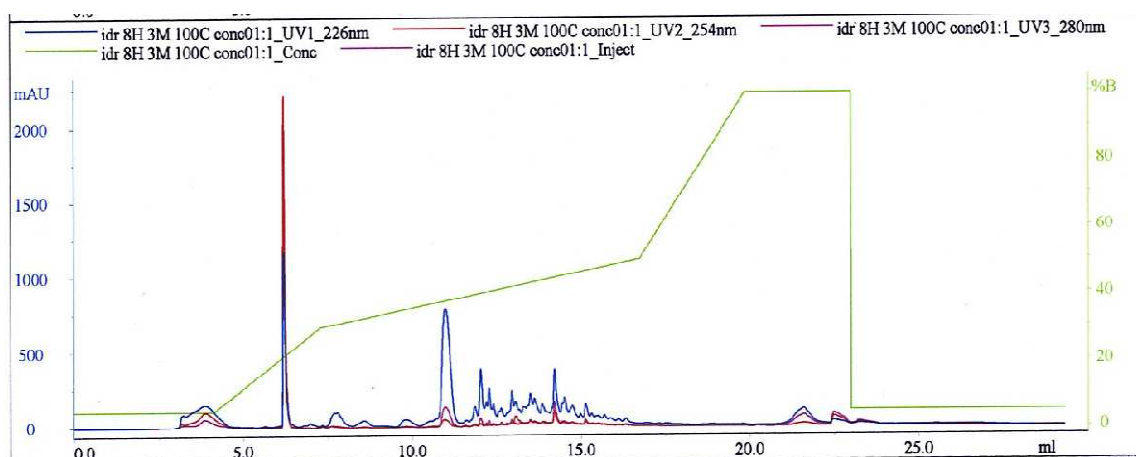
Figure 3.39. Chromatograms of hempseed protein hydrolyzed with 3 M HCl, at 100 °C for 8 hours.
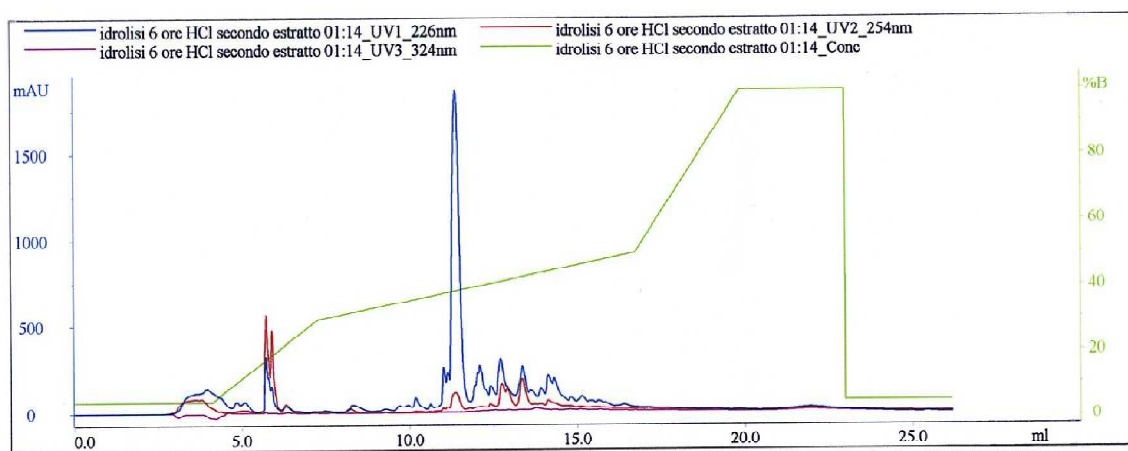
Figure 3.40. Chromatograms of hempseed protein hydrolyzed (HHI) with 6 M HCl, at 110 °C for 6 hours.

105

Figure 3.41 shows the chromatogram of peptides obtained with 3 M HCl at 100 °C for 8 hours after RP-HPLC purification.
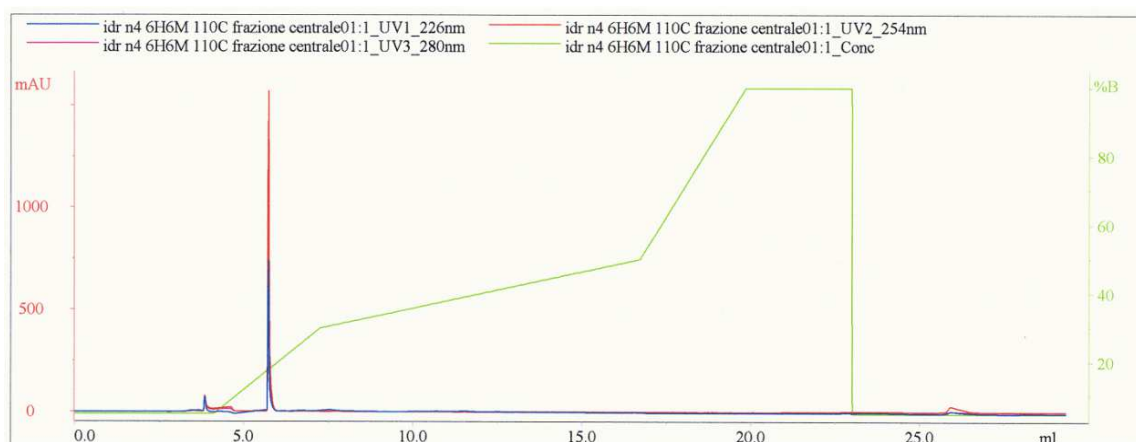
Figure 3.41. Chromatograms of hempseed protein hydrolyzed with 3 M HCl, at 100 °C for 8 hours after RP-HPLC purification.

The purified fraction was analyzed by the NMR experiments 3D DOSY (Figure 3.42) and 2D TOCSY (Figure 3.43). The NMR spectra show the presence of peptides with molecular weight of 200 Da, 500 Da and 750 Da, sugars (with molecular weight around 170 Da) and presumably a high concentration of salts.
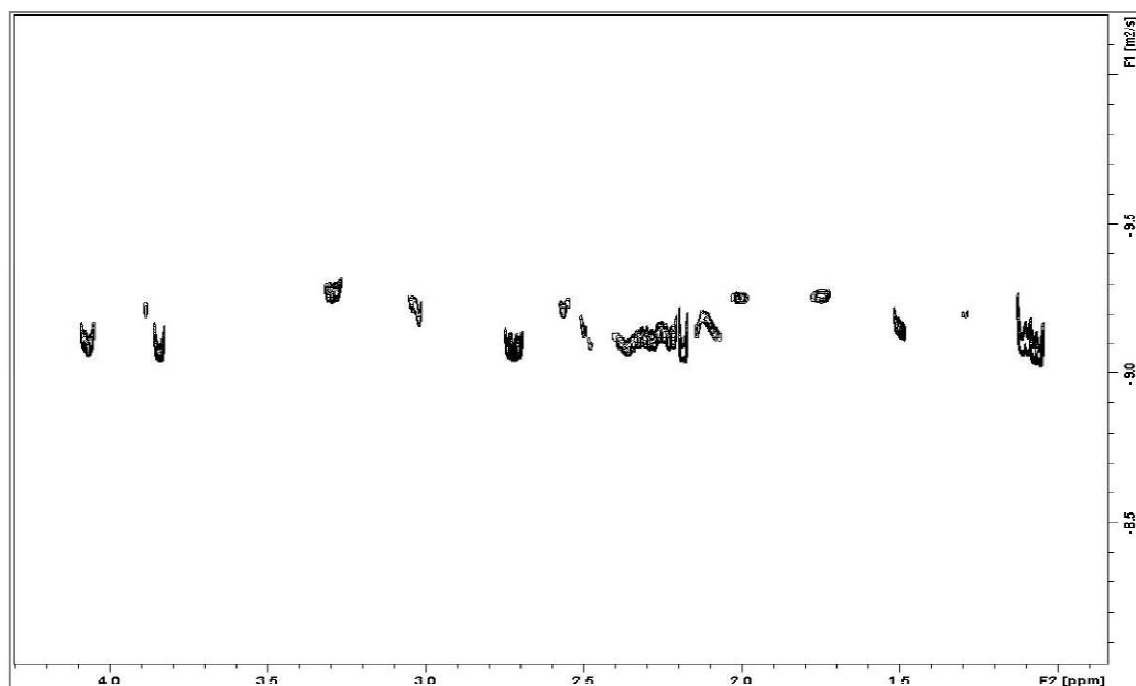
Figure 3.42. 3D DOSY spectra of hempseed protein hydrolyzed with 3 M HCl, at 100 °C for 8 hours after RP-HPLC purification.
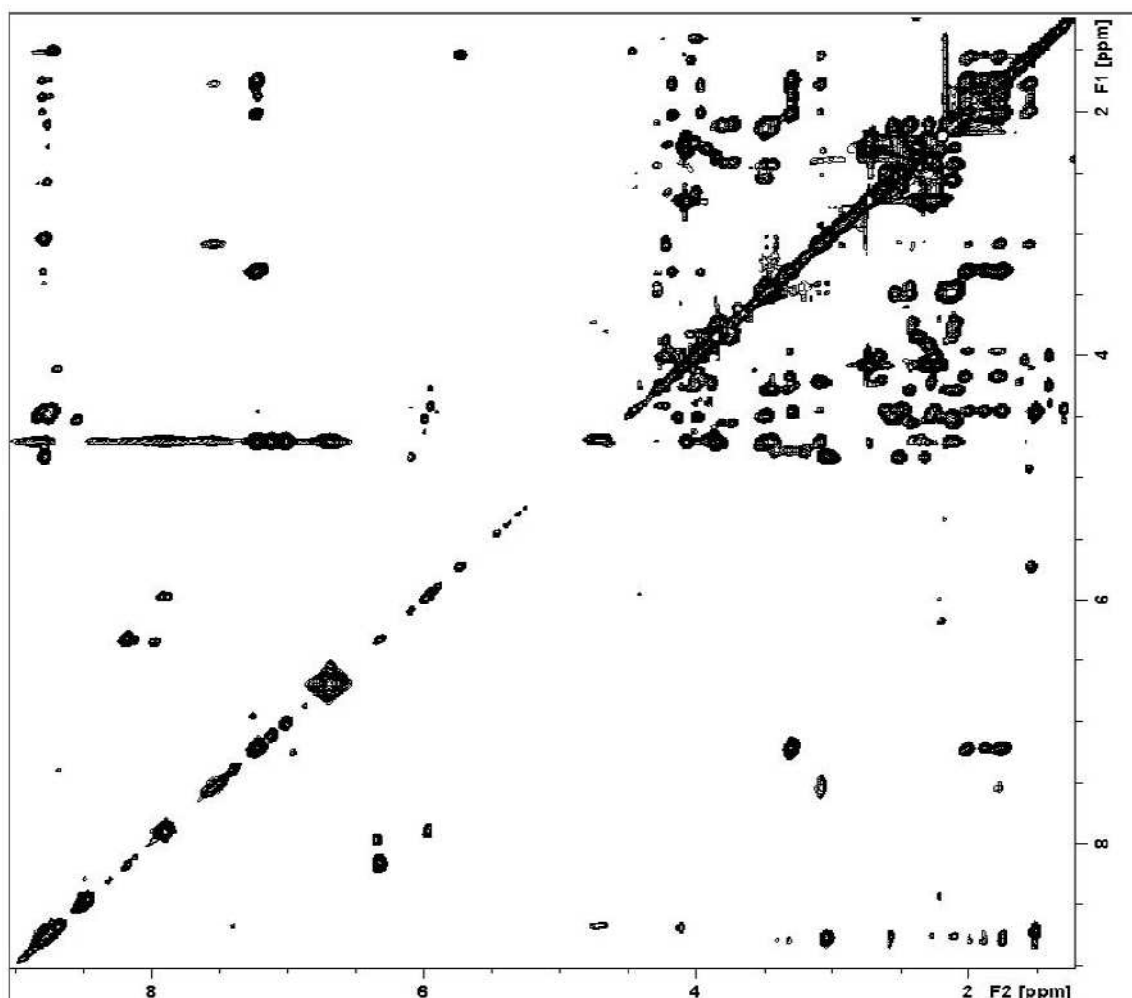
Figure 3.43. 2D TOCSY spectra of hempseed protein hydrolyzed with 3 M HCl, at 100 °C for 8 hours after RP-HPLC purification.

DOSY-NMR analysis (500 MHz, 310 K) was carried out in order to evaluate the range of molecular weights of the peptides in the reaction mixtures. However the accuracy of this analysis decreases with increasing molecular weight variability of the components. For example, Figure 3.44 shows the overlapped DOSY spectra of the mixtures obtained in the mildest (0.1 M HCl, 48 hours, 63 °C, black) and strongest (6 M HCl, 6 hours, 110 °C, red) hydrolysis conditions.

The DOSY-NMR experiments measure the diffusion coefficient values for the different components of a mixture giving a rough estimation of their molecular weight.
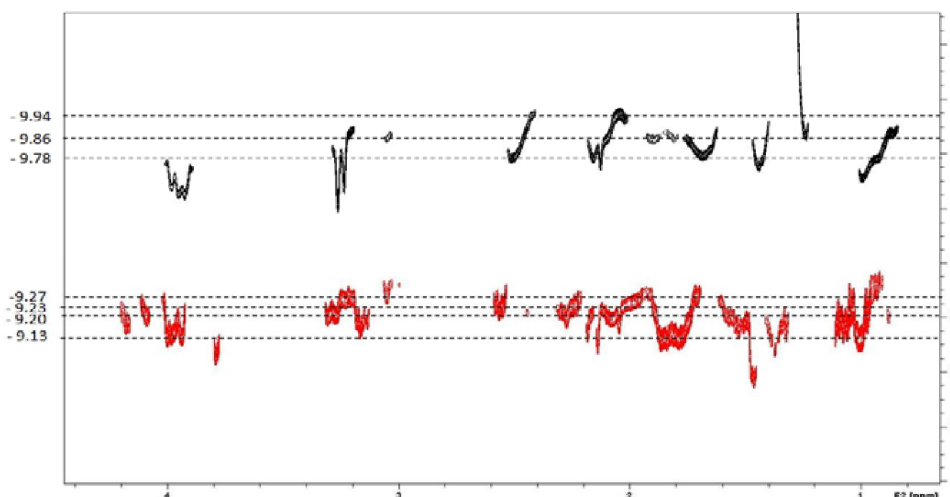
Figure 3.44. Overlapped DOSY spectra of the mixtures obtained with 0.1 M HCl for 48 hours at 63 °C (black) and 6 M HCl for 6 hours at 110 °C (red).

The following results were obtained.

(a) 0.1 M HCl, 48 h, 63 °C

Under these conditions the Maillard reaction did not take place and the mixture remained pale brown. Furthermore a small amount of dark tiny clusters, which were removed by filtration, was formed. The freeze-dried product was a brown amorphous solid (Figure 3.45).

The DOSY-NMR analysis revealed the presence of several components with molecular weights ranging from 20000 to 80000 Da, most of which ranging from 45000 (D = -9.86) to 77000 Da (D = -9.94).

Another species in low concentration with molecular weight of 25000 Da (D = -9.78) was detected.

Figure 3.45. Freeze-dried hempseed hydrolysates resulting from 0.1 M HCl at 63 °C for 48 h

(b) 1 M HCl, 48 h, 63 °C

With increasing concentration of HCl up to 1 M at the same temperature, the Maillard reaction still did not take place and the reaction mixture remained pale brown. Furthermore a higher amount of dark small clusters, which were removed by filtration, was formed. The freeze-dried product was a dark brown amorphous solid (Figure 3.46).

Figure 3.46. Freeze-dried hempseed hydro-lysates resulting from 1 M HCl at 63 °C for 48 h.

The DOSY-NMR analysis showed the presence of components with molecular weights ranging from 8000 to 27000 Da. In particular three main components with molecular weight of 11000, 13800 and 17000 Da were identified.

(c) 1 M HCl, 6 h, 110 °C

To evaluate the influence of temperature on the degree of hydrolysis the hempseed protein were reacted with 1 M HCl at a higher temperature (110 °C) for a shorter time. The freeze-dried product was a dark brown amorphous solid (Figure 3.47).

Fig 3.47. Freeze-dried hempseed hydrolysates resulting from 1 M HCl at 110 °C for 6 h.

The DOSY-NMR analysis confirmed the presence of several components with molecular weight ranging from 3000 to 10000 Da. The main components had molecular weights of about 9700 and 6000 Da.

(d) 6 M HCl, 6h, 110 °C

Increasing the HCl concentration up to 6 M under the same conditions of time and temperature, the Maillard reaction took place and the mixture became dark brown. The freeze-dried product (HHI) was a brown amorphous solid with a smell of mushroom rice. Interestingly, the chromatogram of HHI (Figure 3.40) showed a principal peak (HHP) after 11 ml of mobile phase. This fraction was purified by preparative RP-HPLC. The NMR-DOSY spectra oh HHP revealed the presences of four main component with molecular weights around 300 (D = -9.13), 470 (D = -9.20), 570 (D = -9.23), and 760 Da (D = -9.27). Another component with higher molecular weight (around 900 Da) and in lower amount was present (Figure 3.48).
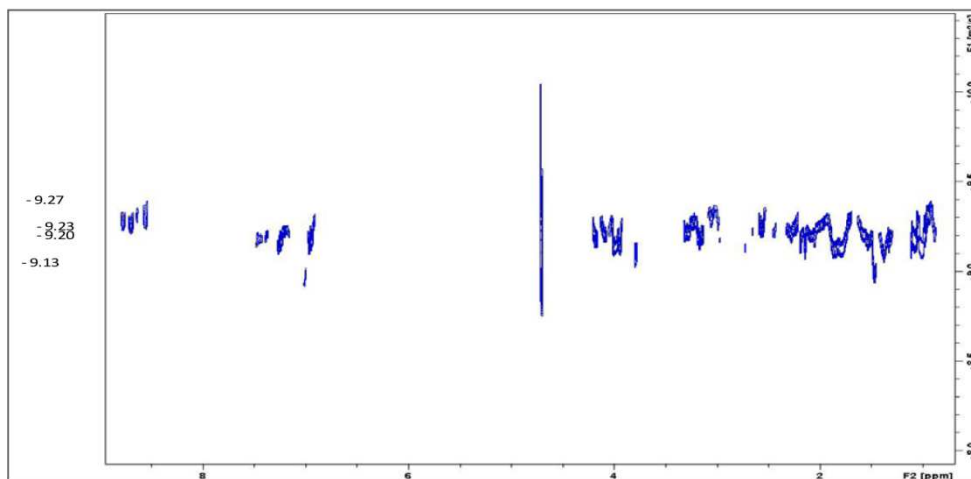
Figure 3.48. NMR-DOSY spectra of purified hempseed protein hydrolyszed (HHP) with 6 M HCl for 6 h at 110 °C.

The NMR-TOCSY spectra of HHP revealed the spin systems of L-arginine (7.21 ppm), L-lysine (7.52 ppm), L-leucine, L-alanine, L-tyrosine (6.94, 7.2 ppm). Weak signals corresponding to two L-tryptophan residues were identified as well. Other detected signals could not be unambiguously assigned to specific amino-acids (Figure 3.49).
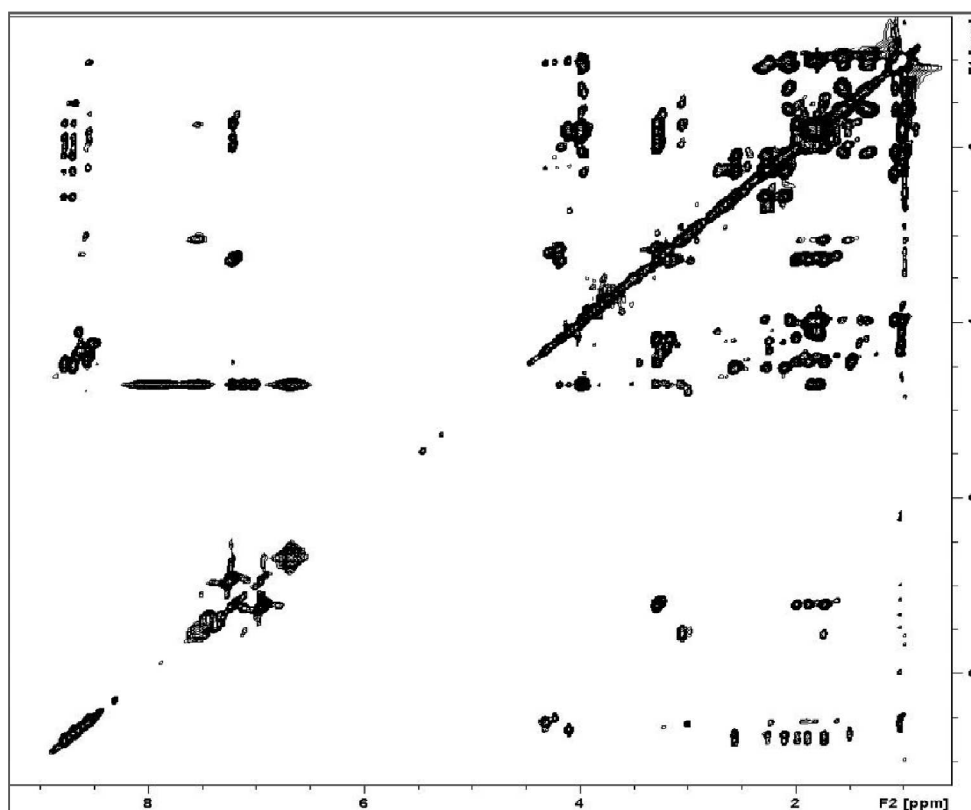
Figure 3.49. NMR-TOCSY spectra of purified hempseed protein hydrolyzed (HHP) with 6 M HCl for 6 h at 110 °C.

110

To obtain precise MW data of HHP, mass spectrometry data were recorded. The MALDI results showed the presence of a main component with molecular weight of 780 Da.

In agreement with DOSY-NMR data, other components with lower molecular weight were detected (Figure 3.50).
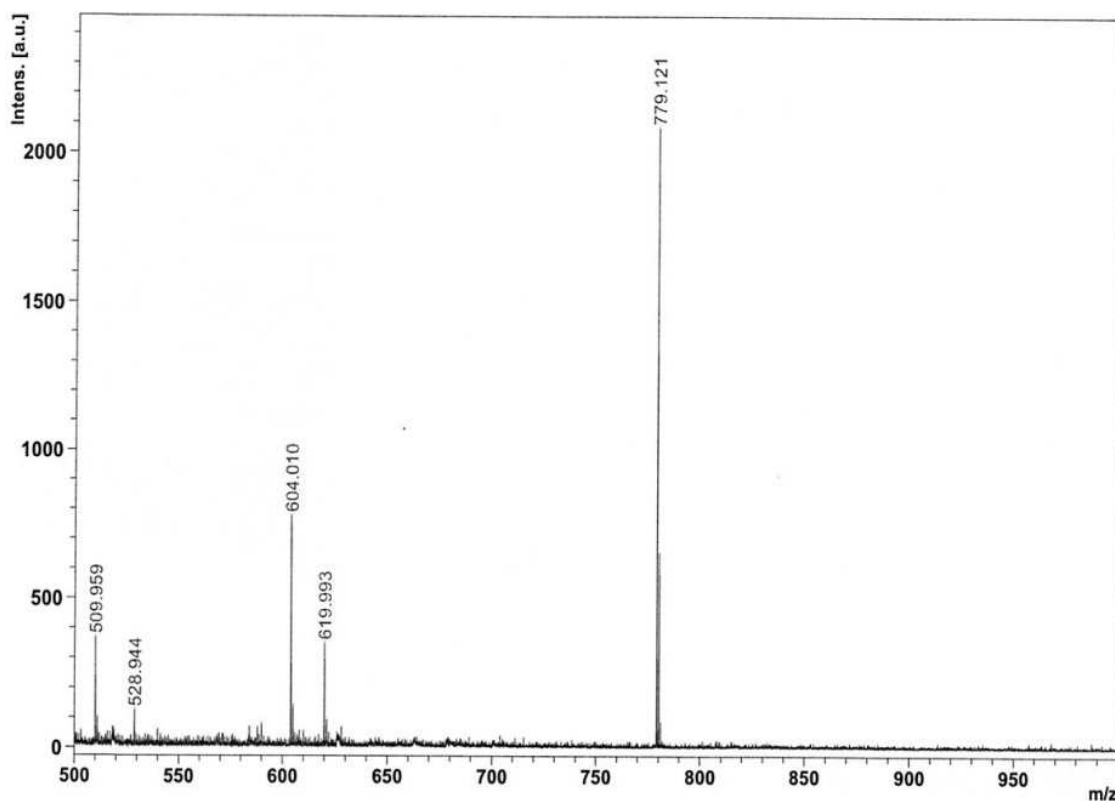
Figure 3.50. MALDI-TOF spectra of purified hempseed protein hydrolyzed (HHP) with 6 M HCl for 6 h at 110 °C.

Usually, chemical hydrolysis are not specific especially under strong conditions, thus different peptides mixtures are formed under similar hydrolysis conditions.

The hydrolysis of hempseed proteins with 6 M HCl for 6 hours at 110°C was repeated four times. Surprisingly the obtained chromatograms can be superimposed each other (Figure 3.51), showing that the obtained peptides are quite similar. Presumably these peptides belong to a repeated sequence of amino acids within proteins of the hempseed. The small differences depend on the consecutive extractions of proteins from hempseed.
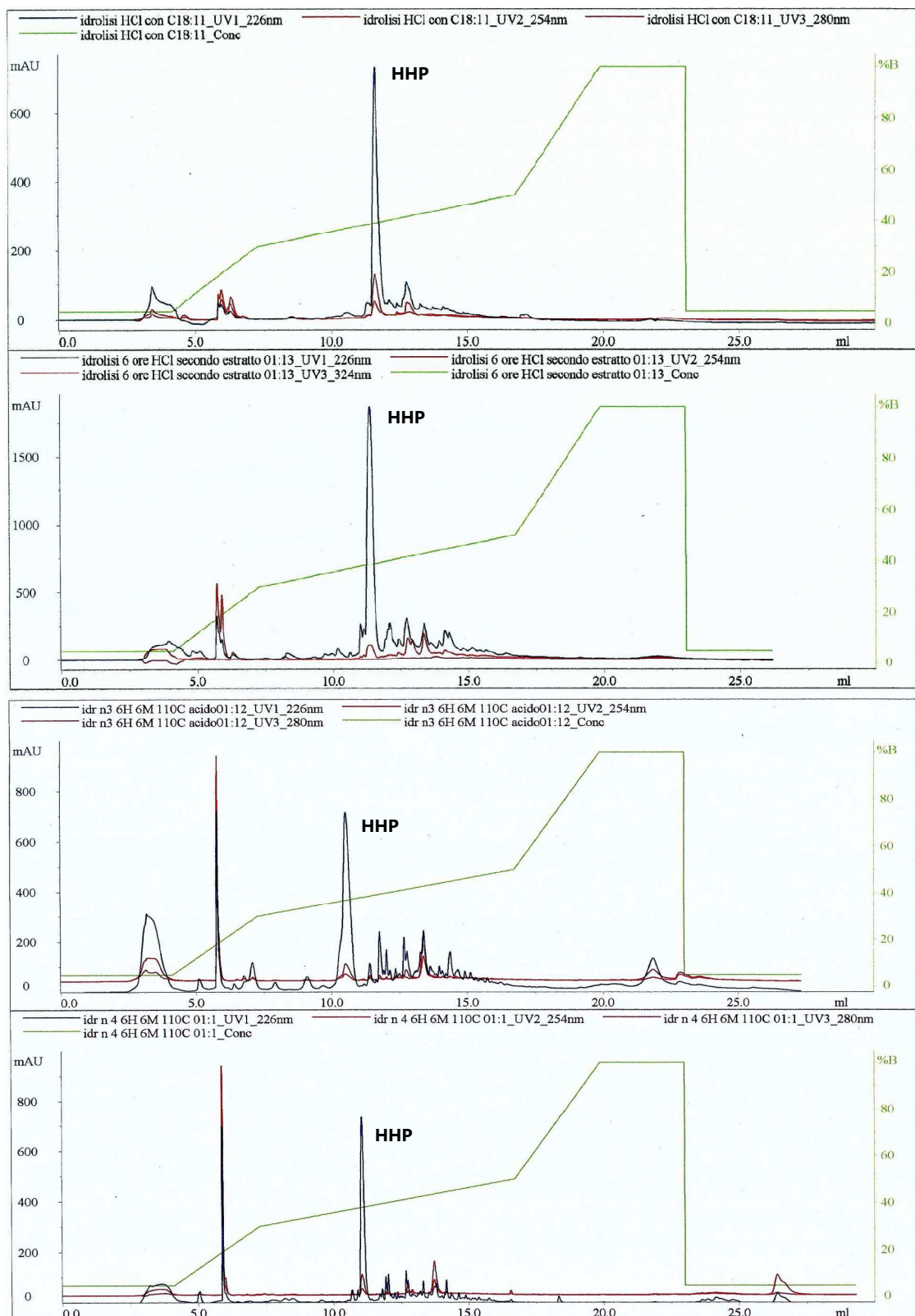
Figure 3.51. Chromatograms of hempseed hydrolyzed (HHI) with 6 M HCl for 6 hours at 110°C.

A further purification of HHP by preparative RP-HPLC, under different elution conditions, allowed the separation of two components (HHP-1 and HHP-2) as shown by the chromatogram in Figure 3.52.
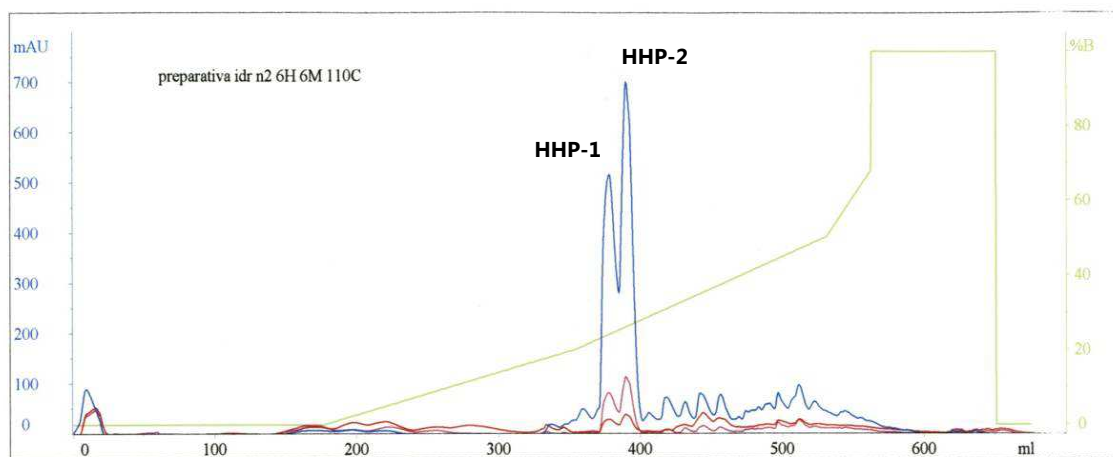
Figure 3.52. Chromatogram of HHP purified by RP-HPLC.

These components were analyzed by DOSY-NMR and TOCSY-NMR.

The DOSY-NMR analysis of the first fraction (HHP-1) showed the presence of three components with molecular weight of about 350, 470 and 800 Da. The correlations of the TOCSY-NMR analysis identified the spin systems of L-arginine, L-alanine, L-tyrosine, L-tryptophan, L-glutamic acid/glutamine (Figure 3.53). L-Glutamine cannot be identified since it is degradated to glutamic acid in the conditions of hydrolysis.

The DOSY-NMR analysis of the second fraction (HHP-2) showed the presence of three components with molecular weight of about 350, 470 and 600 Da. The TOCSY-NMR spectrum is similar to the former revealing the same spin systems with the exception of one which is not present in the first fraction and may correspond to the peptide with molecular weight of 600 Da (Figure 3.54).
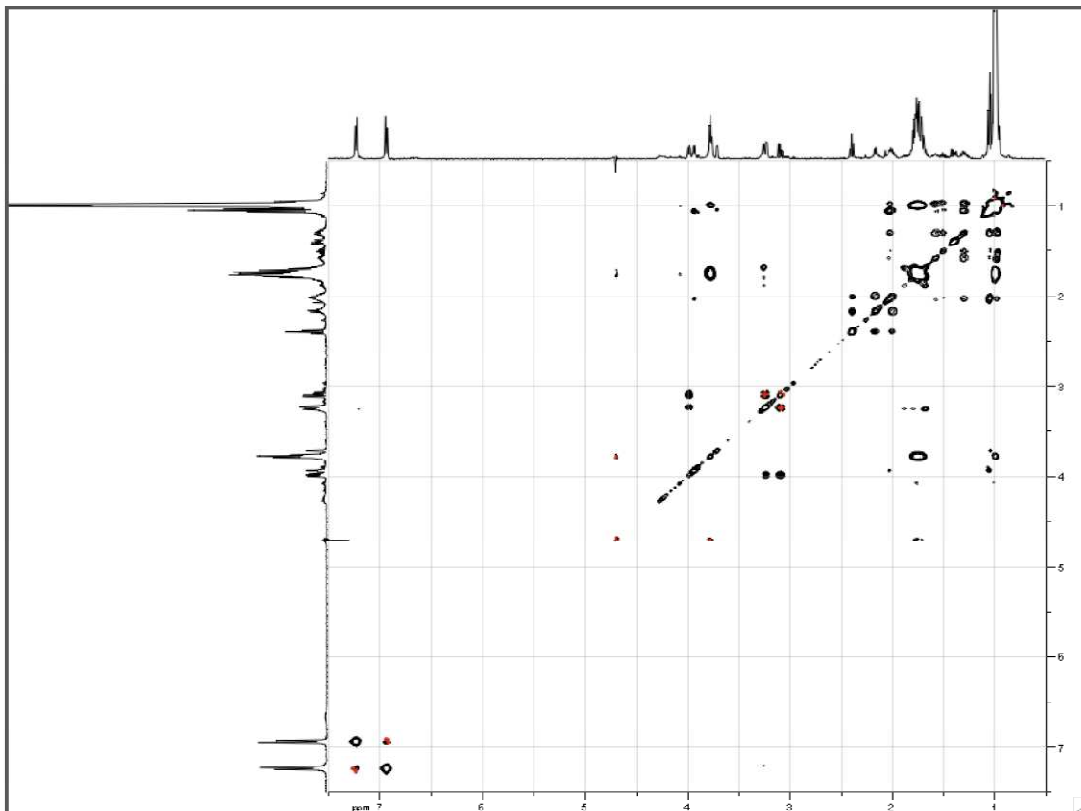
Figure 3.53. TOCSY-NMR spectra of first fraction.
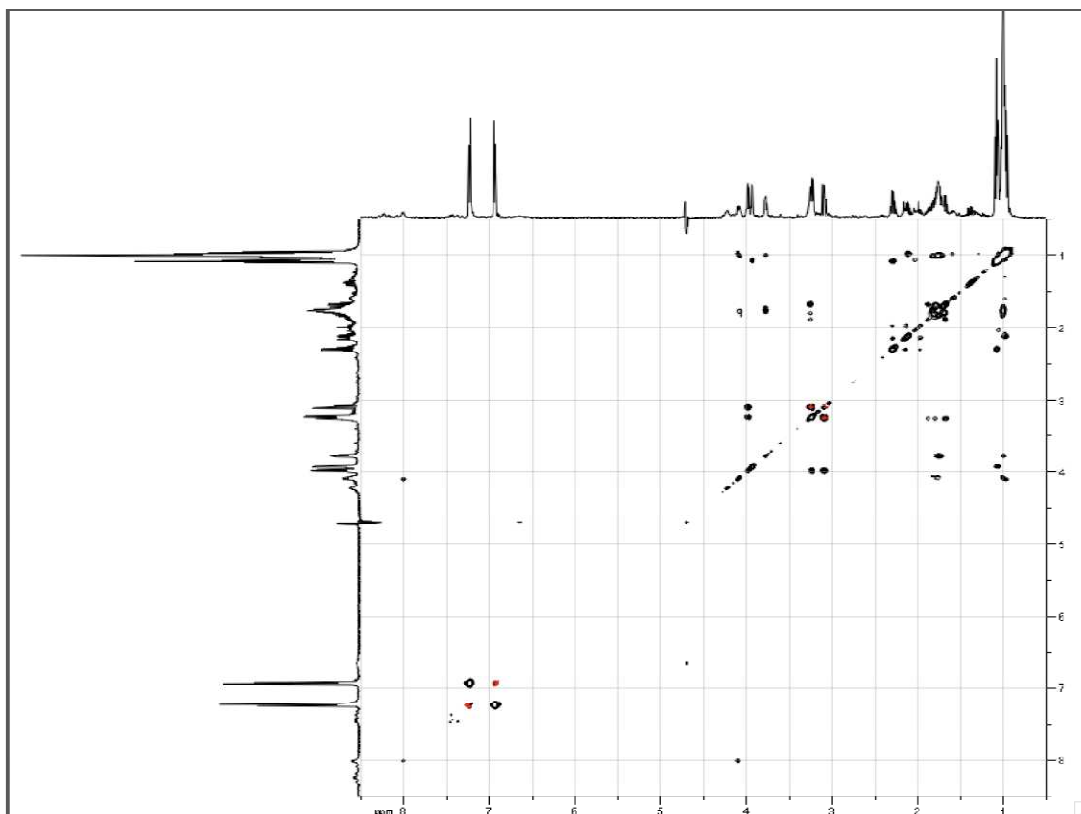
Figure 3.54. TOCSY-NMR spectra of second fraction.

114

3.3.4.2. ACE-inhibitory activity

Hypertension is one of the main risk factors of cardiovascular diseases (*i.e.* atherosclerosis, coronary heart disease, stroke, and heart failure) which are one of the leading causes of death in most industrialized countries [Boschin *et al.*, 2014].

The disease is commonly treated with blood pressure lowering drugs, in particular with the inhibitors of the angiotensin I converting enzyme (ACE; EC 3.4.15.1), which plays an important role in regulating blood pressure in the renin-angiotensin system. This enzyme catalyses the conversion of the biologically inactive angiotensin I to the potent vasoconstrictor angiotensin II, and inactivates the potent vasodilator bradykinin. Inhibitors bind tightly to the ACE active site, competing with angiotensin I for occupancy; as a consequence, ACE cannot convert angiotensin I to angiotensin II [Skeggs *et al.*, 1956]. Considering that synthetic ACE inhibitors, such as captopril, lisinopril and enalapril, may produce side effects, such as coughing, taste disturbances and skin rashes, there is interest in natural inhibitors, and numerous studies are focused on the production and isolation of ACE-inhibitory peptides from different food proteins. Food derived ACE-inhibitory peptides can be introduced into functional foods or dietary supplements. The first active peptides were obtained from milk proteins [Nakamura *et al.*, 1995], but some have been isolated from plant seeds, such as soybean [Chen *et al.*, 2004], pea [Aluko, 2008; Barbana & Boye, 2010], rice, sunflower, and wheat [Guang & Phillips, 2009]. Recently, the antihypertensive effects of enzymatic hempseed protein hydrolysates and its peptide fractions was reported by Girgih *et al.* [2011]. Several reports showed an increase in ACE-inhibitory activity with decreasing molecular weight (MW) of peptide [Benjakul & Morrissey, 1997; Jeon *et al.*, 1999].

The ACE-inhibitory activity of hempseed peptides resulting from the chemical hydrolyses was assessed according to the slightly modified method developed by Cushman & Cheung [1971]. Two samples were investigated: the crude obtained by hydrolysis with 6 M HCl for 6 hours at 110 °C (HHI) and the corresponding purified fraction by preparative RP-HPLC (HHP, Figure 3.55).
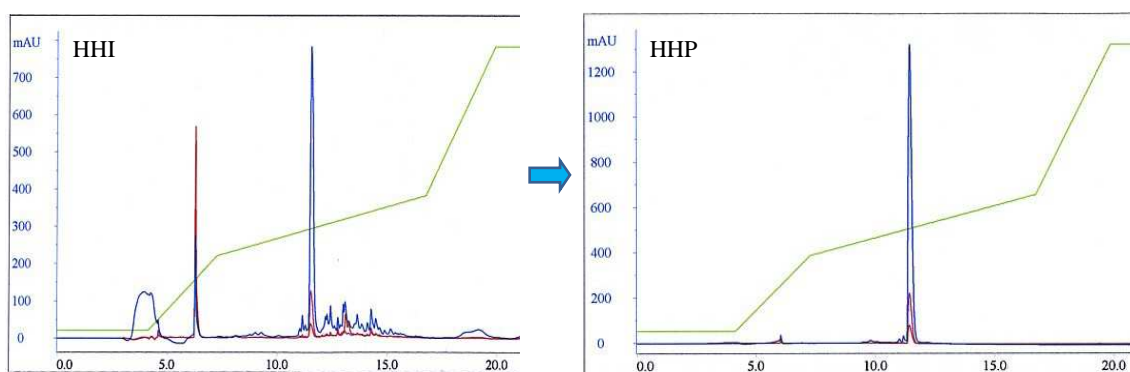
Figure 3.55. Chromatograms of hempseed peptides obtained by hydrolysis with 6 M HCl for 6 hours at 110 °C (HHI, left) and the corresponding purified fraction (HHP, right).

Figures 3.56-3.57 show the charts obtained plotting the % ACE inhibition vs. $\log_{10}$ inhibitor concentrations for both samples. Very good fits with sigmoid curves and reproducible IC_{50} values were obtained.

$$y = -27{,}219x^3 + 178{,}61x^2 - 323{,}48x + 182{,}94$$
$$R^2 = 0{,}9997$$
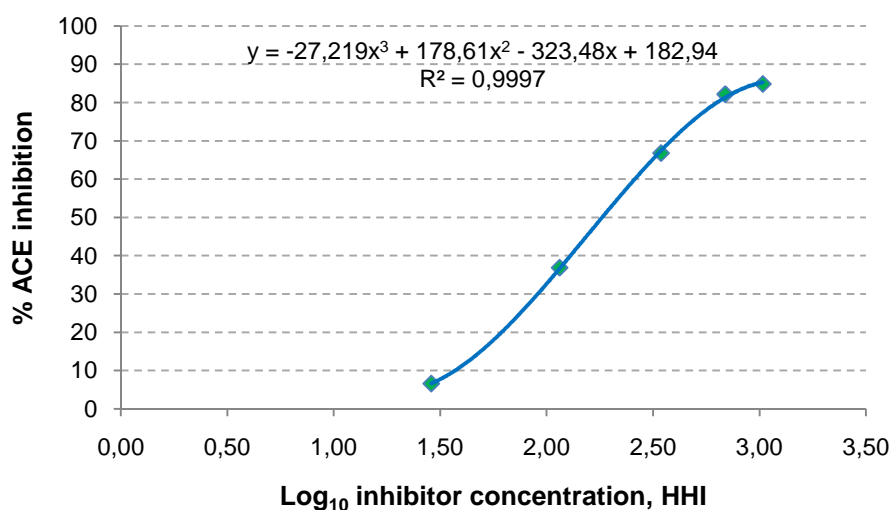
Figures 3.56 Diagrams reporting % ACE inhibition vs. $\log_{10}$ concentrations of hempseed peptides obtained by hydrolysis with 6 M HCl for 6 hours at 110 °C (HHI).

116
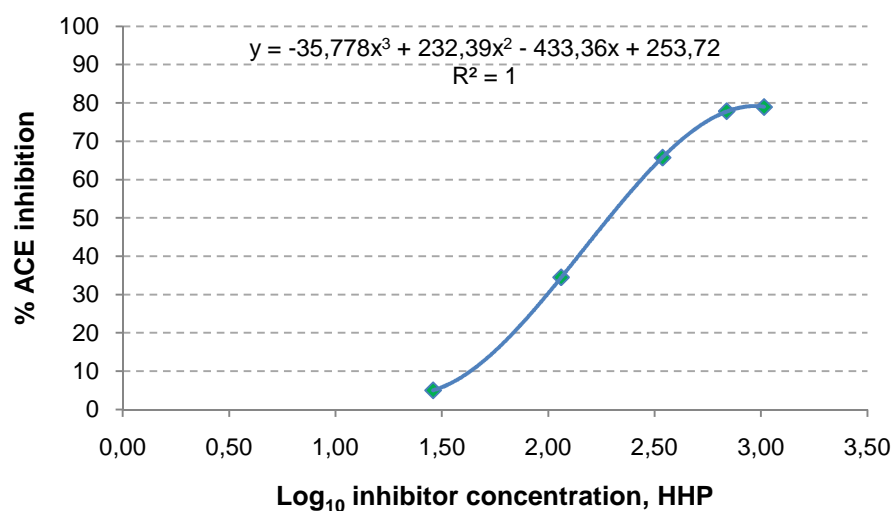
Figure 3.57. Diagrams reporting % ACE inhibition vs. $\log_{10}$ concentrations of hempseed peptides obtained by hydrolysis with 6 M HCl for 6 hours at 110 °C and purified with RP-HPLC (HHP).

The maximum percentage of ACE inhibition and the IC_{50} values are reported in Table 3.13.

Table 3.13. Values of highest inhibitor concentration (μg/ml), maximum percentage of ACE-inhibition and IC_{50} (μg/ml) for hempseed peptides resulting from hydrolysis with 6 M HCl for 6 hours at 110 °C. Values are reported as mean value ± standard deviation of three independent experiments; values with different letters are significantly different ($p < 0.05$).

Sample	Highest inhibitor concentration (μg/ml)	Max ACE inhibition (%)	IC_{50} (μg/ml)
HHI	1035.9	85	180.11 ± 3.07
HHP	1035.9	79	191.62 ± 1.57

Both samples show similar IC_{50} values. The slowly reduced ACE-inhibitory activity of the purified fraction HHP suggests that there was some synergistic effect in the crude product HHI. These results are in agreement with the values reported in a previous study performed on enzymatic hempseed hydrolysates HVPs [Girgih *et al.*, 2001]. However, the comparison of our data with those obtained by other authors is a complex task, since the observed differences in the ACE-inhibitory activity may be related to a

variety of causes, such as the sample and the protein extraction procedure, as well as the differences in the peptide mixture composition, related to changes in the parameters of the digestion process, *i.e.* enzyme, pH, time, temperature, substrate/enzyme ratio [Barbana & Boye, 2010], or the different analytical method used for the determination of the ACE-inhibitory activity.

Our data indicate that chemical hempseed hydrolysates may become a valuable source of ACE-inhibitory peptides, which in the future may be used for the formulation of functional foods or dietary supplements for the prevention or treatment of hypertension.

3.4. Preparation of HVPs from Flaxseed through Enzyme-catalyzed Hydrolysis

Production and characterization of HVPs from flaxseed *by-products* is currently under investigation. In particular, four Italian *cultivar* of flax (*Linum usitatissimum* L.), namely, Solal, Merlin Linoal and Natural are being considered.

Flaxseed (*Linum usitatissimum* L., family: *Linaceae*) has been cultivated since antiquity, mainly for the use of its oil and fiber. Whole flaxseed is rich in lipids, dietary fibre, proteins and lignans [Oomah & Mazza, 1993]. The main product obtained from flaxseed is oil, which is the richest known plant source of the ω-3 fatty acid α-linolenic acid [Sammour, 1999]. Flaxseed meal is the main by-product from the flaxseed oil extraction process. This product, traditionally used as animal feed, contains three important fractions: proteins (about 35-40%), essential amino acids; mucilage, which is a mixture of neutral arabinoxylans and rhamnogalacturonans with good water-holding capacities and high viscosity [Ribeiro *et al.*, 2013]. In particular, the amino acid composition of flaxseed proteins is comparable to that of soy with high amounts of glutamic acid (about 40%), aspartic acid, leucine, arginine, lysine and branch-chain amino acids [Marambe *et al.*, 2008].

Because of these properties, flaxseed meal has recently received much attention as a functional food constituent. Moreover, flaxseed HVPs appear to be valuable component for human nutrition as well as for the production of flavor enhancers.

3.4.1. Removal of Mucilage

The procedure of hydrolysis described for both rice middlings and hempseeds meal could not be performed on flaxseed due to the high amount of mucilage that hampered the hydrolysis of proteins. Flaxseed mucilage contains about 50–80% carbohydrates and 4–20% proteins and ash. The major constituent consists of two polysaccharide components, neutral and acidic, that largely contribute to the soluble fiber fraction of flaxseed and are suggested to have a hypoglycemic effect in humans [Cunnane *et al.*, 1993]. Moreover, mucilage appears to play a role in reducing diabetes and coronary heart disease, preventing colon and rectal cancer and reducing the incidence of obesity [Singer *et al.*, 2011]. Flaxseed mucilage is commonly employed in the cosmetic industry as texturing agents; however, in food industry, its application as functional food has not yet been extensively examined. Recently, Kaewmanee *et al.* [2014] evaluated the chemical composition, physicochemical, functional and sensory properties of flaxseed mucilage supporting their use for industrial applications.

To perform the hydrolysis, we decided to remove mucilage by shaking defatted flaxseed meal in water [Kaewmanee *et al.*, 2014]. The resulting viscous solutions containing the dissolved polysaccharides were filtered and precipitated with ethanol. Mucilage was then recovered by centrifugation. The pellet was dissolved in distilled water and freeze-dried.

In order to evaluate the presence of protein in the extracted mucilage, SDS-analysis was performed. However these results are still preliminary and the characterization of mucilage protein profile of all the flaxseed cultivar is under investigation.

3.4.2. Enzymatic Hydrolysis

The enzymatic hydrolysis of de-mucilagenated and defatted flaxseed meal was performed in semi-preparative scale according to the method described for hempseed meal in section **6.3.3.** [Bagnasco *et al.*, 2013]. Briefly, enzymatic hydrolysis of defatted and de-mucilagenated flaxseed meal was performed using two commercial food grade protease cocktails (Flavourzyme® and Umamizyme®), in ammonium bicarbonate as a

buffer. Defatted and de-mucilagenated flaxseed meal was incubated under the same experimental conditions without the enzyme as a control. The reaction was stopped after 1, 5, 11 and 24 h by addition of formic acid to the mixture, and finally centrifuged.

3.4.3 Chemical Characterization of Flaxseed HVPs

Total nitrogen of defatted flaxseed meal was assessed by Kjeldahl method performed by Centro di Ricerca per le Produzioni Foraggere e Lattiero-Casearie (CRA) of Lodi. Crude protein content was estimated by multiplying total nitrogen content by the conversion factor 6.25 (Table 4.14).

Table 4.14.

Number of analysis	N total g/100g of meal	% Protein (N total * 6.25)
25	5.18	32.4

The SDS-PAGE as well as the characterization of flaxseed hydrolysates are in progress. Current studies are being focused on assessment of the sensory profile as well as of the nutraceutical properties (such as antioxidant and ACE activities) of both flaxseed hydrolysates and extracted mucilage.

4. RESULTS AND DISCUSSION
PART 2

4.1. Alkylation of N^2 of guanosine
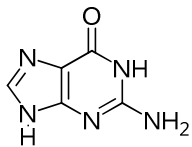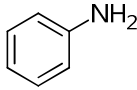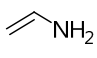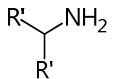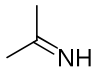
The reactivity of the exocyclic amino group in position 2 of the guanosine ring is significantly different from that of a -NH$_2$ on an aromatic ring. Indeed, the carbonyl group in position 6 pulls the electrons of the purine ring substituents, especially those of the nitrogen in position 2 (Scheme 4.1). The preferred tautomeric form in guanosine is the keto form, making the guanosine ring electron-poor.
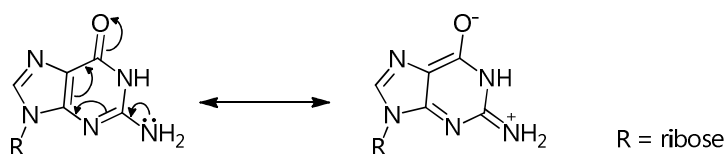
Scheme 4.1.

The prevalence of the keto-amino tautomer makes the C_2-NH$_2$ bond significantly shorter than a typical single C^{arom}-NH$_2$ bond, as confirmed by measuring the length of the C-N bond in various structural contexts (Table 4.1).

Table 4.1.

	Observed bond lenght [Å]	Calculated bond lenght [Å]	Ref.
C^2-NH$_2$	1.336	1.377	*JACS* **1970**, *92*, 2929-2936
	1.341	–	http://ndbserver.rutgers.edu/archives/proj/valence/bases8.html (nucleic acid database)
	1.330		*ActaCryst. C* **2006**, *62*, 515-517
C^{arom}-NH$_2$	1.426		
C^{sp2}-NH$_2$	1.322		
C^{sp3}-NH$_2$	1.472		F. Taddei "Il legame chimico", UTET, 1976
C^{sp2}=NH$_2$	1.340		

The length of the C^2-NH$_2$ bond in guanosine nucleus (1.336 Å) is more similar to a double C=N bond (1.322 Å) than an amino group of an aromatic ring (1,426 Å) and the electron-withdrawing properties of the guanosine nucleus render the amino group scarcely reactive as a nucleophile. For this reason, specific strategies have been developed for its alkylation.

A procedure for the alkylation of the exocyclic amino group of guanosine was described in 1980 by Kemal and Reese [1980]. This strategy requires two steps. The first step involves the reaction of the nucleoside with an aldehyde and *p*-thiocresol in refluxing ethanol, affording a N^2-[1-(*p*-tolylthio)alkyl] guanosine through the intermediacy of an imine. Reduction of the resulting *p*-tolylthioalkyl derivative with NaBH$_4$ in the second step gives the desired alkylated product. However, the recovery of the final product is difficult and sometimes the protection of the ribose hydroxyl groups is required.

Through a modification of this procedure, our group succeeded in synthesizing the derivatives shown in Table 4.2 [Cairoli *et al.*, 2008]. The starting material was 2',3'-*O*-

isopropylideneguanosine and the reduction step was carried out without prior purification of intermediate thio adduct (Scheme 4.2).

Conditions
(i) *p*-TsOH, *2,2*-dimetossipropano, acetone, rt, 4-6h
(ii) RCHO, p-tiocresolo, EtOH, AcOH, reflux, 24h
(iii) NaBH$_4$, EtOH,reflux, 1-2h
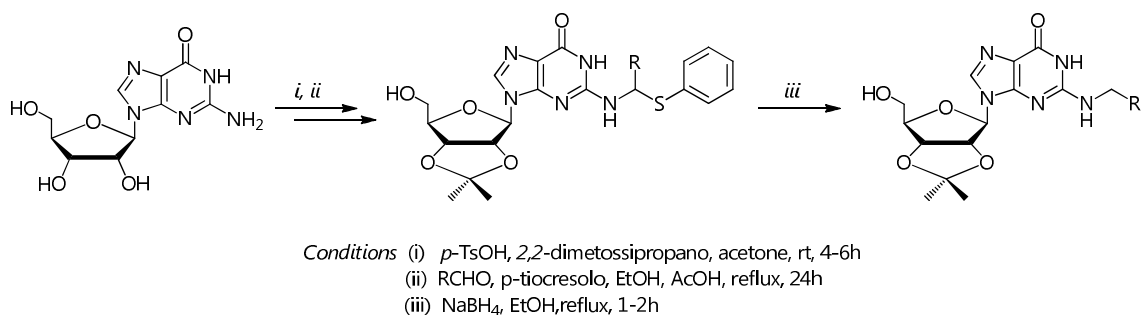
Scheme 4.2.

Table 4.2.

RCHO	NHCH2R	yield
HCHO	NHCH$_3$	23%
CH$_3$CHO	NHCH$_2$CH$_3$	23%
CH$_3$SCH$_2$CHO	NHCH$_2$CH$_2$SCH$_3$	36%
CH$_3$SCH$_2$CH$_2$CHO	NHCH$_2$CH$_2$CH$_2$SCH$_3$	49%
CH$_3$CH$_2$CH$_2$CHO	NHCH$_2$CH$_2$CH$_2$CH$_3$	46%
CH$_3$(CH$_2$)$_6$CHO	NH(CH$_2$)$_7$CH$_3$	35%
PhCH$_2$CH$_2$CHO	NHCH$_2$CH$_2$CH$_2$Ph	48%

4.2. 2-halogeno purine

Since the exocyclic amino group of guanosine has proved to be scarcely reactive, we decided to pursue an alternative approach based on the activation of the position 2 of the purine ring as halo-derivative, followed by the displacement of the halogen with diamines, as shown in the retrosynthetic plan reported in Scheme 4.3. The resulting intermediates carry a free amino group at the end of the side chain, which should be condensed with the gamma carboxylic group of glutamic acid. Two different approaches were attempted in order to achieve this goal.
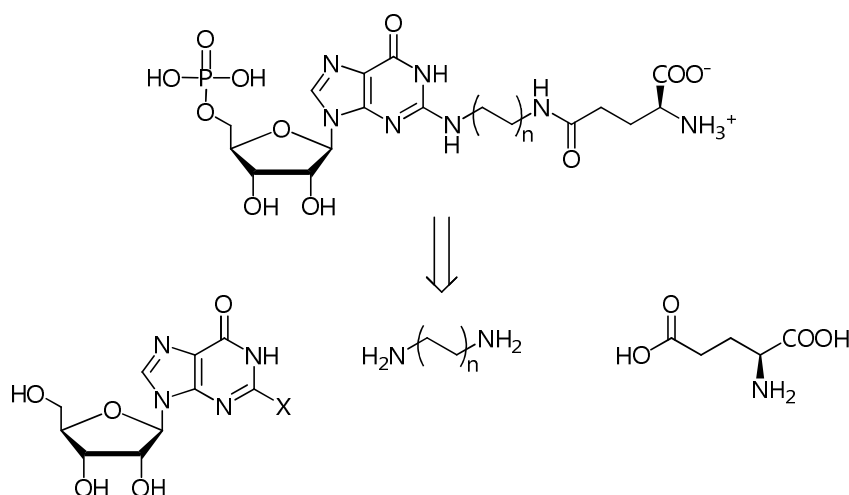
Scheme 4.3.

4.2.1. First Strategy (through 6-chloro-2-iodo-purine)

According to evidences from the literature, the replacement of the amino group in position 2 of the guanosine nucleus by a halogen atom was at first carried out on derivatives in which the amido function in positions 1 and 6 of the guanosine was masked (Scheme 4.4). The hydroxyl groups of commercial guanosine **4.1** were protected as acetyl derivatives using acetic anhydride in the presence of triethylamine (TEA) and *p*-(dimethylamino)-piridine (DMAP) affording derivative **4.2** [Bridson *et al.*, 1977]. Then 2',3',5'-tri-*O*-acetylguanosine **4.2** was converted into 2-amino-6-chloro-9-

(2',3',5'-tri-*O*-acetyl-β-D-ribofuranosyl)-purine **4.3** by reaction with phosphorus oxychloride (POCl₃) in the presence of tetraethylammonium chloride and *N,N*-dimethylaniline (DMA) in refluxing acetonitrile (CH₃CN) [Robins&Uznasnski,1981]. Since decomposition of the 6-chloro derivative **4.3** could occur during the reaction, Robins and Uznasnski studied this reactionby ³¹P NMR spectroscopy reproducing the chlorination conditions in an NMR tube containingPOCl₃, DMA andtri-*O*-acetylguanosine **4.2** in CD₃CN at 70°C. The authors concluded that the first step of the reaction involves the phosphorylation of **4.2** to give an aromatic phosphorodichloridate intermediate **B**, followed by the attack of chloride at position 6 of **B** to give **4.3** and dichlorophosphate **C** (Scheme 4.5). A higher concentration of external chloride anions should favor conversion of **B** in **4.3** before decomposition occurs. Indeed, the addiction of tetraethylammonium chloride to the reaction mixture in a cognate experiment resulted in the faster disappearance of intermediate **B** and in an increased yield of **4.3**.
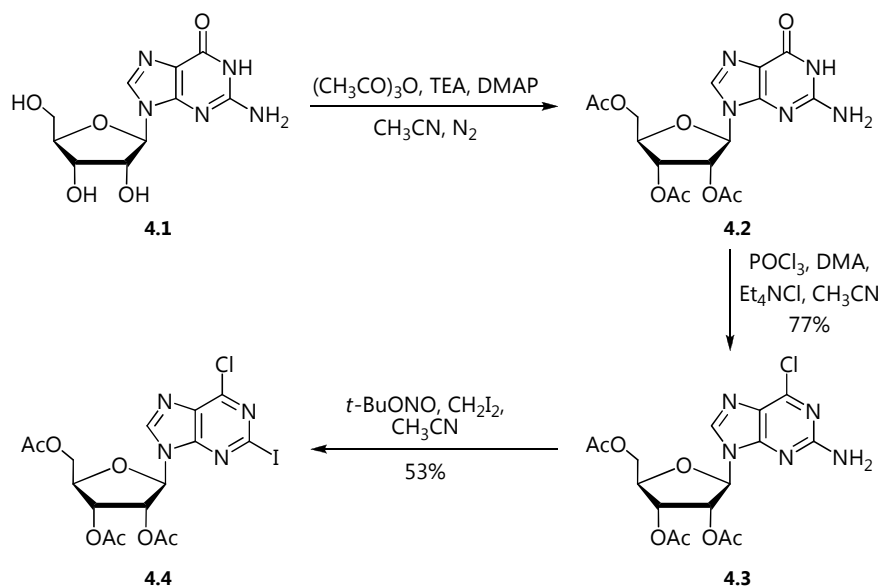
Scheme 4.4.
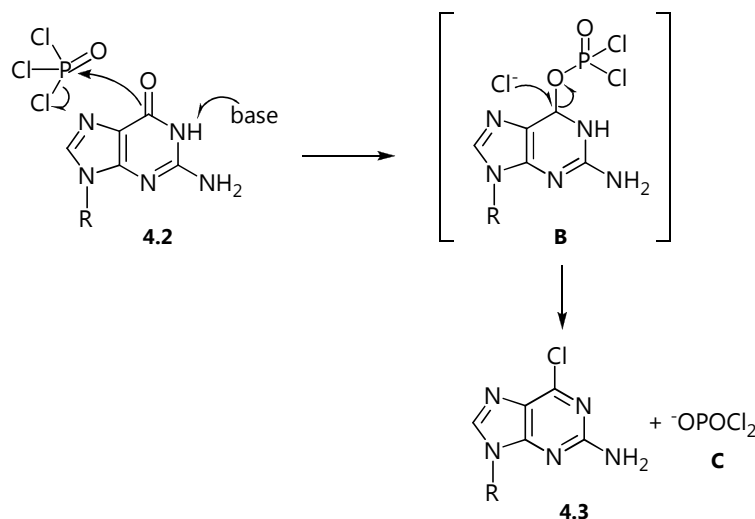
Scheme 4.5.

The iodine atom in position 2 of derivate **4.3** was introduced by reaction with *t*-butylnitrite and diiodomethane to give compound **4.4** [Ohno *et al.*, 2004]. The mechanism of this reaction (Sandmeyer's reaction) involves a purinyl radical which was generated transiently through the thermal homolysis of the 2-diazonium intermediate [Nair & Fasbender, 1993].

Introduction of an alkoxy group in position 6 of **4.4** can be achieved by nucleophilic substitution of the chorine atom with the proper alcoholate. The reaction outcome is strongly dependent on the temperature as well as on the structure of the alcoholate. The introduction of a methoxy group in position 6 was achieved by reaction of the derivative **4.4** with sodium methoxyde at room temperature. Indeed, at room temperature the desired mono-substituted product **4.5a** is preferentially formed because position 6 is more reactive than the position 2, although in position 2 there is a better leaving group. By raising the temperature up to 60 °C, the di-substituted product in positions 2 and 6 (**4.6a**) is formed (Scheme 4.6) [Nair *et al.*, 1988]. The introduction of a benzyloxy group in position 6 to give derivative 5b (Scheme 4.7) was carried out by using sodium benzyloxide according to the method described by Casu *et al*. [2012].This reaction is more sensitive to the temperature than the first one. Indeed, at room temperature the di-substituted product in positions 2 and 6 (**4.6b**) was obtained as the major product. The desired mono-substituted derivative (**4.5b**) was obtained by adding a stoichiometric amount of sodium benzyloxyde to a DMF solution of **4.4** at 0 °C. Sodium benzyloxyde

was previously generated by adding a stoichiometric amount of sodium to benzyl alcohol.

In both cases (compounds **4.5a** and **4.5b**), the alkaline environment determined the cleavage of the acetyl protecting groups of the ribose.
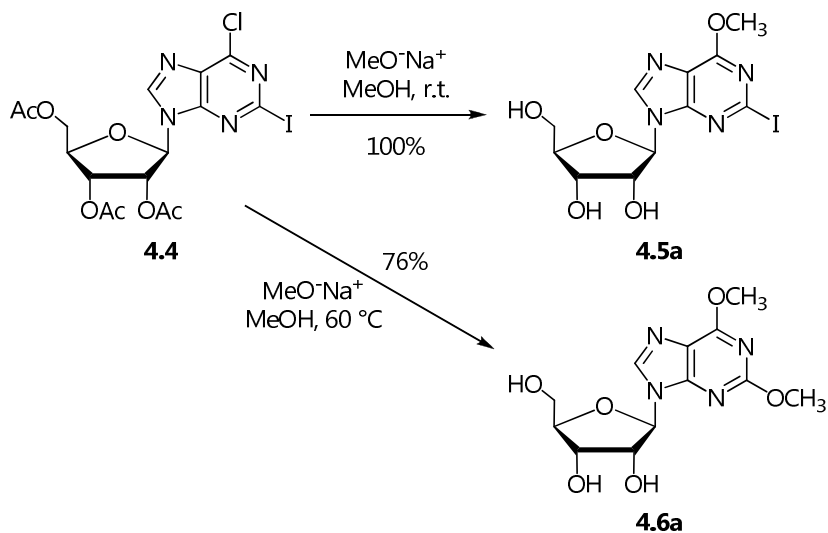
Scheme 4.6.
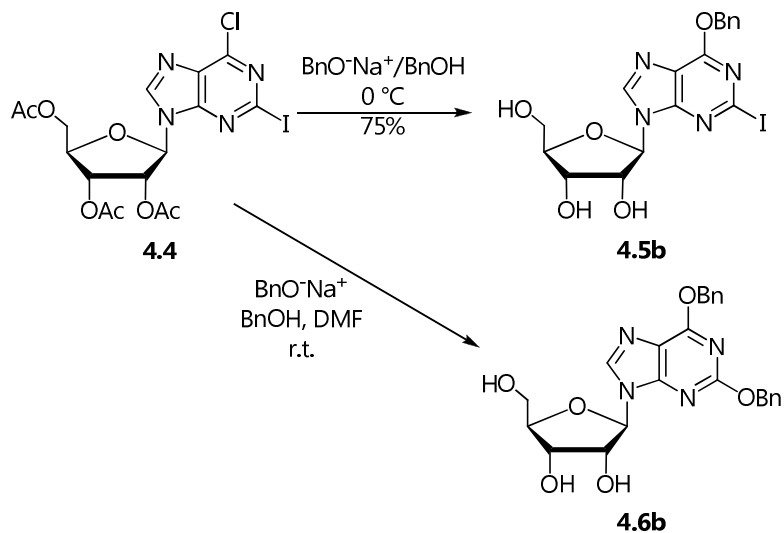
Scheme 4.7.

The presence of a reactive iodine atom in position 2 of derivatives **4.5a** and **4.5b** paved the way to a further functionalization of the purine moiety.

The 2' and 3' hydroxyl groups of compound **4.5a** and **4.5b** were reprotected by reaction with 2,2-dimethoxypropane (DMP) in acetone in the presence of a catalytic amount of *p*-toluenesulfonic acid, affording compounds **4.7a** and **4.7b** (Scheme 4.8).

4.5a R=Me
4.5b R=Bn

4.7a R=Me, 79%
4.7b R=Bn, 100%
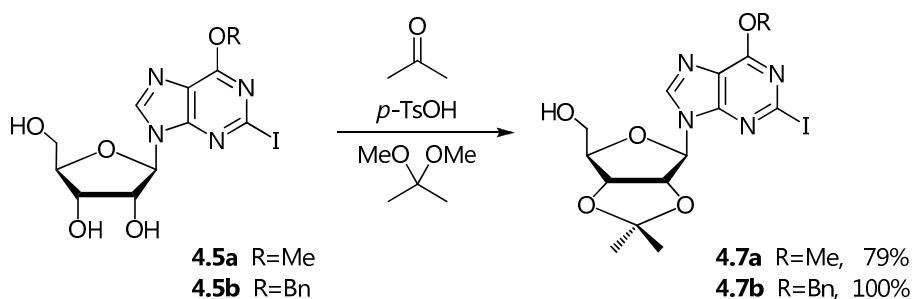
Scheme 4.8.

Displacement of iodine atom of derivative **4.7a** was carried out at high temperature using hexamethylenediamine **A** in DMF [Gunic *et al.*, 2004]. Two products were obtained: the desired product **4.8a** as minor component of the reaction mixture and a principal product, the structure of which is not yet univocally attributed. However, NMR spectra of this compound showed the presence of the diamine moiety and the lack of the methoxy group in position 6.

Since the purification of derivative **4.8a** was proved to be very difficult due to its high polarity, which hampered column chromatography separation, we tried to use the monocarbamate of 1,6-hexamethylenediamine **A1** as the nucleophile for the displacement of the iodine atom of intermediate **4.7a** (Scheme 4.9). Monocarbamate **A1** was obtained by the dropwise addition of a CH_2Cl_2 solution of di-*tert*-butyl dicarbonate (Boc$_2$O) to an excess of 1,6-hexamethylenediamine at 0 °C. Then, displacement of iodine atom of derivatives **4.7a** was carried out using monocarbamate **A1** according to the procedure described above. Even in this case two principal products were formed and the desired derivative **4.8b** was isolated as minor component. Furthermore, the conversion of the methoxy group at position 6 into a carbonyl group was unsuccessful. The reaction was performed according to Nair *et al.* [1988] by treatment with trimethylsilyliodide, generated in situ from trimethylsilylchloride and potassium iodide, in the presence of a catalytic amount of acetonitrile followed by addition of few drops of water to hydrolyze all the silyl groups.
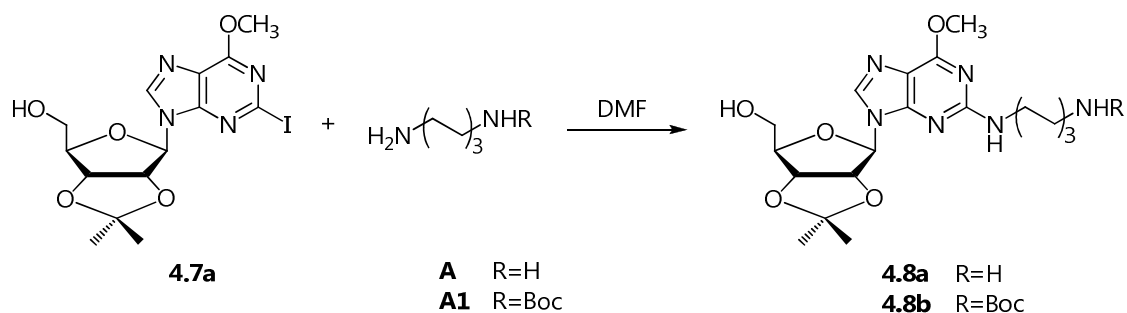
Scheme 4.9.

The synthetic plan so far described revealed some drawbacks up to this point: low solubility of intermediates; high polarity of the involved compounds, which rendered the chromatographic separations difficult or even impossible; unusual stability of the protecting group in position 6 of the purine nucleus, which proved to be difficult to remove. For all these reasons we set up an alternative approach based on the protectionsof the 5' hydroxyl group of ribose as *tert*-butyldimethylsilylether andof the position 6 of the purine ring as benzyloxy derivative. Reaction of intermediate **4.7b** with *tert*-butyldimethylsilylchloride in DMF in the presence of imidazole afforded the protected derivative **4.9** (Scheme 4.10).Displacement of the iodine atom in position 6 of derivative **4.9** was then carried out at high temperature using an excess of hexamethylenediamine in 2-ethoxyethanol [Bressi *et al.*, 2000]. Even in this case, two principal products were formed and the desired product **4.10** was isolated as the minor component.

The coupling of **4.10** with the γ-carboxylic group of glutamic acid, protected at the α-carboxy- and α-amino positions, was carried out in the presence of DCC at room temperature to give the hybrid compound **4.11** (Scheme 4.10).
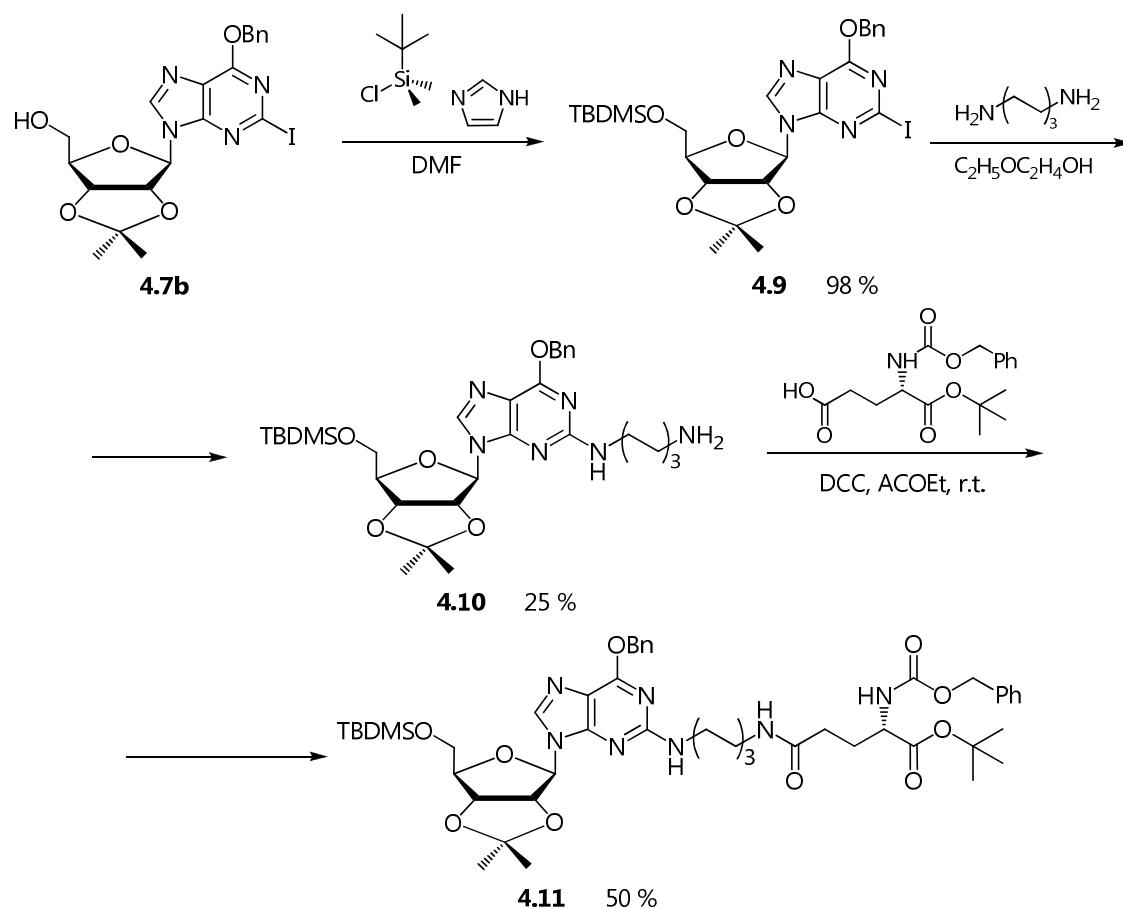
Scheme 4.10.

The critical step of this strategy appeared to be the reaction of the iodo-derivatives with the diamine. Reaction mixtures became indeed dark-red and many compounds were detected by TLC analysis. Presumably, some radical species were formed, even when the reactions were carried out in the dark. Consequently, the isolation of the desired products was in many cases very difficult. In addition, every attempt to remove the benzyloxy function in position 6results to be unsuccessful.

For these reasons we decided to pursue an alternative approach, based on the activation of position 2 of the purine-ring as halo-derivative, but leaving the amido function in positions 1 and 6 of the purine nucleus untouched.

4.2.2. Second Strategy (through 2-halogeno-6-oxopurine)

4.2.2.1. 2-Iodo-purine

In 2007 Nair *et al.* [2007] reported the synthesis of 2-iodo-6-oxo-9-(2',3',5'-tri-*O*-acetyl-*β*-D-ribofuranosyl) purine **4.12** (Scheme 4.11) by reaction with isoamyl nitrite in the presence of an excess of iodoform (CHI$_3$) in dryCH$_3$CN in 72% yield. However, no experimental details were given and also the characterization of the formed product was lacking. When we tried to reproduce those experiment, the desired product **4.12** was isolated in very low yield. Moreover, the high amount of CHI$_3$ used made purification of product **4.12** very difficult. Finally, the major product of the reaction was compound **4.13**, which probably arises from a radical reaction involving the CH$_3$CN used as the solvent [Matsuda *et al.*, 1992].
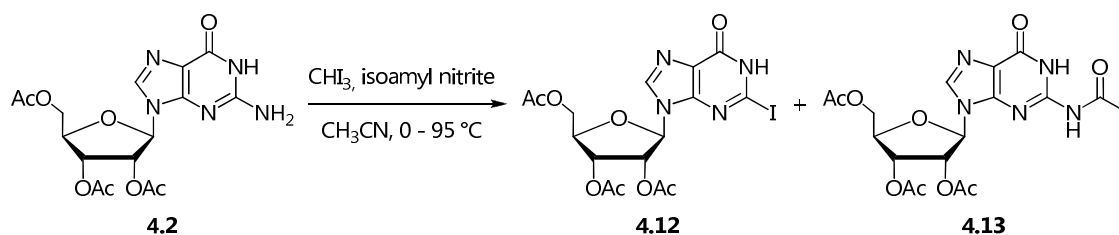
Scheme 4.11.

For these reasons we undertook a detailed study of the reaction, by varying solvent and temperature, in order to achieve better yields and to minimize the formation of by-products (Scheme 4.12 and Table 4.3).
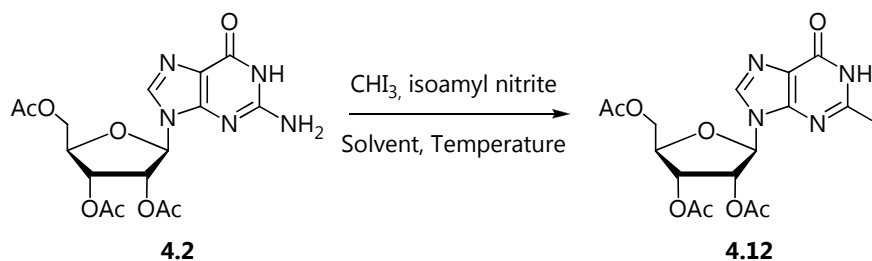
Scheme 4.12.

Table 4.3.

Entry	Solvent	Temperature
12a	CH_3CN	0 °C → 95 °C
12b	CH_3CN	65 °C
12c	DMF	65 °C
12d	$ClCH_2CH_2Cl$	0 °C → 65 °C
12e	$ClCH_2CH_2Cl$	r.t. → 65 °C
12f	$ClCH_2CH_2Cl$	65 °C

The best results were obtained using 1,2-dichloroethane as the solvent at the fixed temperature of 65°C. Also in this case, however, the yield did not exceed 30%.

As the acetyl protecting groups of the ribose moiety would interfere in the reaction with the diamine at a later stage of the synthesis, we tried also different protective groups using compound **4.14** as the starting material, as shown in Scheme 4.13. The yields remained however low.
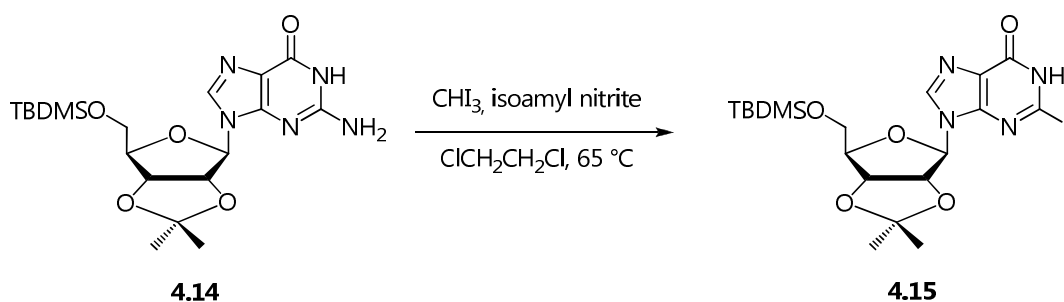
Scheme 4.13.

The scarce results obtained up to this point and the observed low stability of the iodo derivative **4.12** prompted us to consider the use of halogens other than iodine.

4.2.2.2. 2-Bromo- and 2-Chloro-purine

A procedure by Quian and Glaser [2005] (Scheme 4.14) reported the introduction of a bromine atom in the position 2 of the purine nucleoside **4.16**, protected in position 6 as benzyloxy derivative. Compound **4.17** was obtained in 62% yield by a diazotization-halogenation reaction in the presence of *tert*-butyl nitrite and antimony bromide (SbBr$_3$) in methylene bromide (CH$_2$Br$_2$)at low temperature.
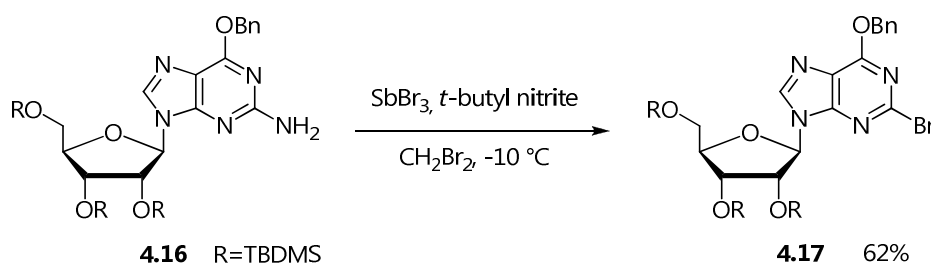
*Scheme 4.14.*Procedure by Quian and Glaser [2005].

We tried the reaction using the protected guanosine **4.14**, without masking the oxo group in position 6 of the purine nucleus, obtaining the desired, stable bromo derivative **4.18** in 60% yield (Scheme 4.15).
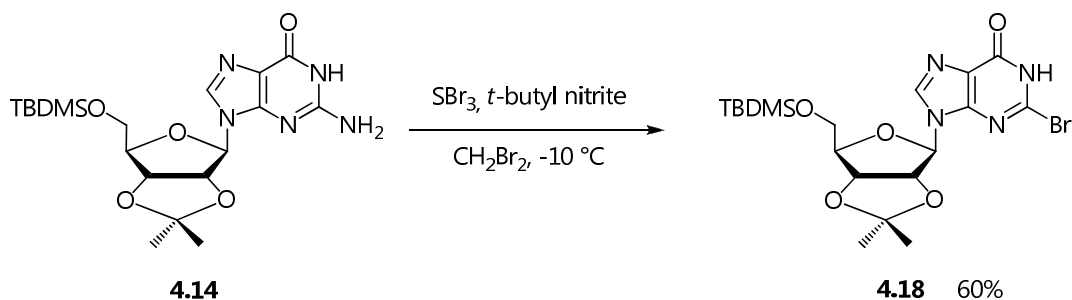
Scheme 4.15.

On the basis of this good result, the same procedure was repeated using antimony trichloride in dichloromethane, affording the 2-chloro derivative **4.19**. However, in this case the yield dropped to 30% (Scheme 4.16).

4.14 → **4.19** 30%

SCl₃, *t*-butyl nitrite

CH₂Br₂, -10 °C
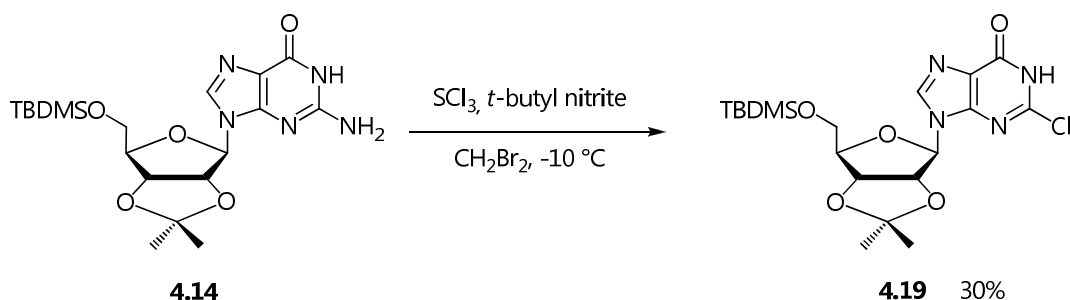
Scheme 4.16.

Antimony (III) halides are effective catalysts for diazotization reaction [Quian & Glaser, 2005] and have Lewis acidic properties as well as serving as halogen donors. Because antimony compounds are toxic and $SbCl_3$ has been shown to bind to DNA [Huang *et al.*, 1998], efficient halo-dediazoniation procedures that do not employ SbX_3 are preferred. Nitrosyl chloride (NOCl) in the presence of Lewis acids such as $AlCl_3$, PCl_3, $AsCl_3$, or $TiCl_4$ has been used for the in situ diazotization of aliphatic amines [Doyle *et al.*, 1978]. Generation of NOCl from silicon chlorides and alkyl nitrites is reported in early patent literature [Beckman *et al.*, 1951] and trimethylsilyl chloride (TMS-Cl)-$NaNO_2$ have been used for halo-dediazoniation [Ku *et al.*, 1981].

Francom and Robins [2003] reported the treatment of 6-chloro-9-(2',3',5'-tri-*O*-acetyl-β-D-ribofuranosyl)-2-aminopurine **4.3** with TMS-Br and *tert*-butyl nitrite (TBN) in dibromomethane to give the crystalline 2-bromo-6-chloropurine **4.20b** in 85% yield. It is also described a procedure to insert a chlorine atom. TMS-Cl and benzyltriethylammonium nitrite (BTEA-NO_2) gave the crystalline 2,6-dichloropurine nucleoside **4.20a** (83%) and acetyl chloride/BTEA-NO_2 was equally affective (86%) (Scheme 4.17).

a) TMSCl, BTEA-NO₂
   CH₂Cl₂   or
   AcCl, BTEA-NO₂
   CH₂Cl₂, 0-5 °C

b) TMSBr, *t*-butyl nitrite
   CH₂Br₂, 0-5 °C

4.3

4.20a X=Cl 83-86%
4.20b X=Br 85%
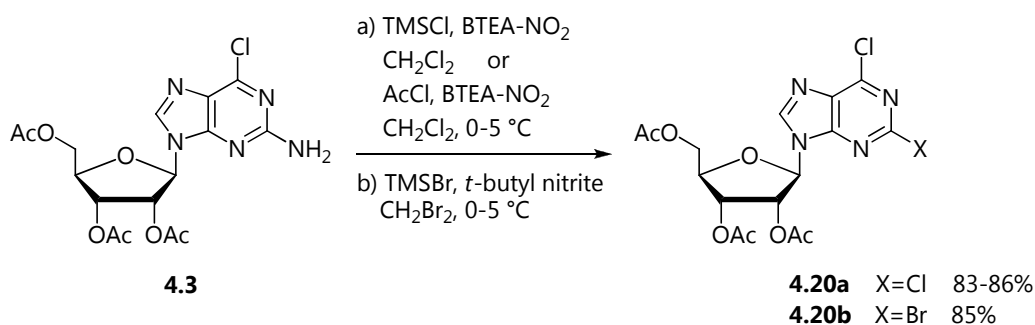
Scheme 4.17. Procedure by Francom and Robins [2003].

138

On the basis of this evidences [Francom & Robins, 2003] we reacted the protected guanosine derivative **4.14** with *t*-butylnitrite in the presence of trimethylbromosilane in dibromomethane at low temperature (Scheme 4.18). The 2-bromoderivative **4.18** was obtained in a satisfactory 70% isolated yield.
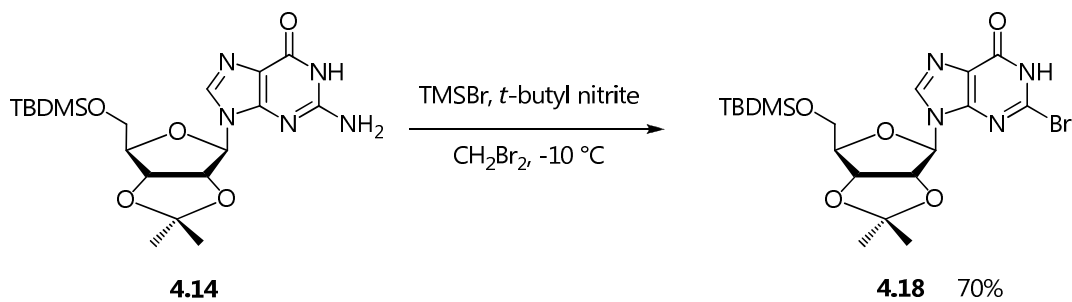
Scheme 4.18.

4.3. Introduction of the spacer: Nucleophilic aromatic substitution on the purine ring of guanosine

The spacer was then linked to position 2 of the protected guanosine activated as halogen derivative. The selected linkers were represented by terminal diamines of variable lengths:

A 1,6-diaminohexane $H_2N(CH_2)_6NH_2$

B 1,4-diaminobutane $H_2N(CH_2)_4NH_2$

C 1,2-diaminoethane $H_2N(CH_2)_2NH_2$

In a first experiment we carried out a nucleophilic aromatic substitution on the crude iodo derivative **4.12** with 1,4 diaminobutane **B**.
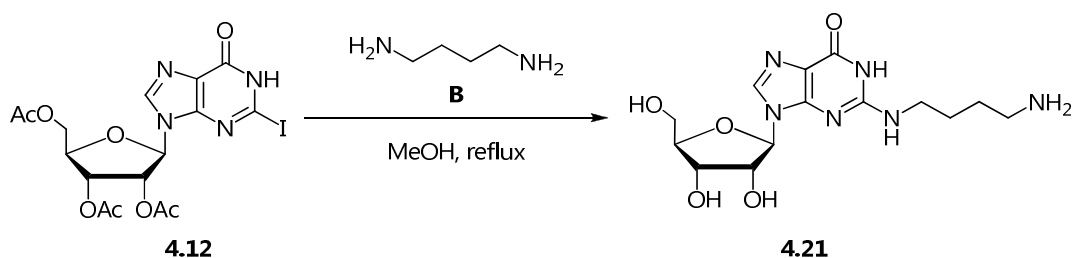
Scheme 4.19.

The reaction was carried out in refluxing MeOH (Scheme 4.19). The progress of the reaction proved to be difficult to monitor by TLC, thus we observed only the disappearance of the starting material **4.12**. The product **4.21** was not isolated, but evidences of its formation came from ESI-MS spectra of the reaction crude.

As the acetyl protecting groups of the ribose moiety do not tolerate the treatment with the nucleophilic diamine in boiling methanol, we evaluated the possibility of using other protecting groups from the beginning of the synthetic plan. The reaction was therefore repeated using the iodo derivative **4.15** as the starting material (Scheme 4.20).
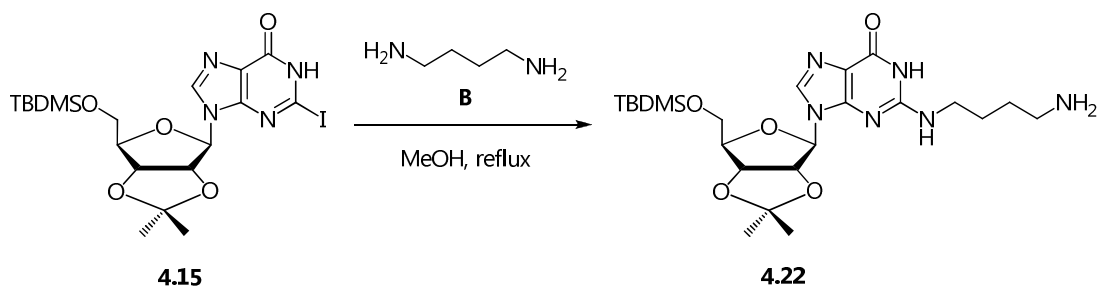
Scheme 4.20.

Evidence of the formation of the desired product **4.22** came once again from ESI-MS spectra, but **4.22** was not purified, although different techniques, such as precipitation and ion exchange chromatography, were attempted. Reactions in Schemes 4.19 and 4.20 required very long times for completion, up to 5-6 days, so we decided to change the solvent, in order to raise the temperature. Using DMF (Scheme 4.21) compound **4.23**, different from that we expected, was obtained as the major reaction product.
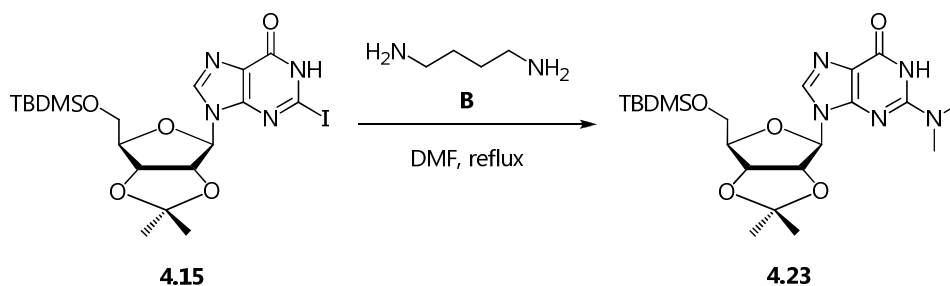
Scheme 4.21.

Finally, by using 2-methoxyethanol (Scheme 4.22), the product **4.22** was formed, as shown by ESI-MS analysis, but we did not succeed in purifying it through the usual laboratory techniques (silica gel chromatography, ion exchange chromatography, crystallization etc).
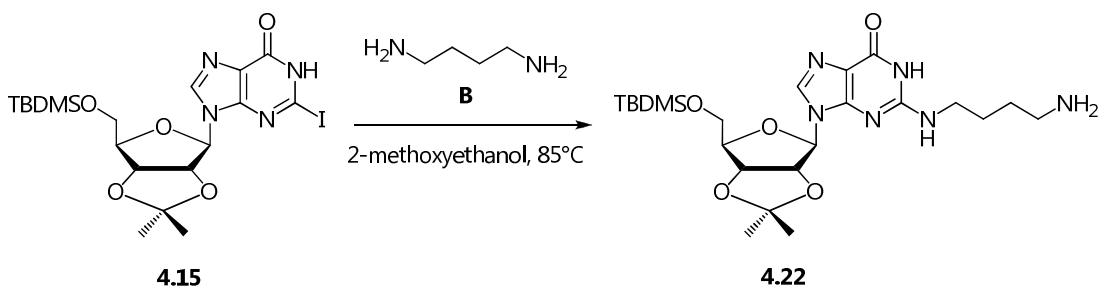
Scheme 4.22.

According to these results, we carried out nucleophilic aromatic substitutions also on the chloro- and bromo derivatives **4.18** and **4.19**, using diamines of different lengths (**A**, **B** and **C**). All these reactions were carried out in 2-methoxyethanol as the solvent at 85 °C (Schemes 4.23-4.25).
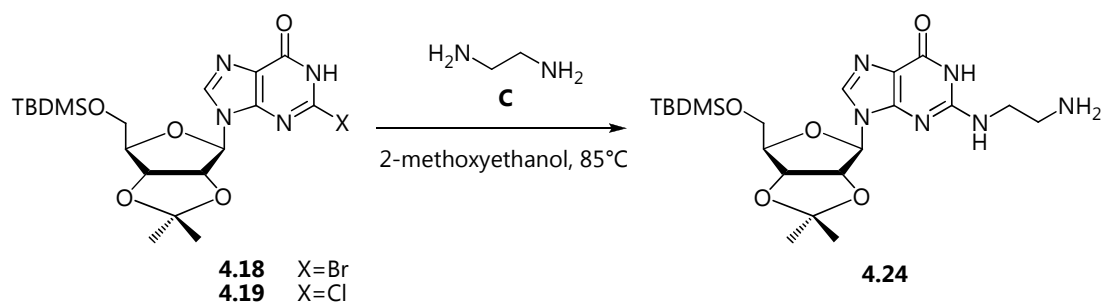
Scheme 4.23.
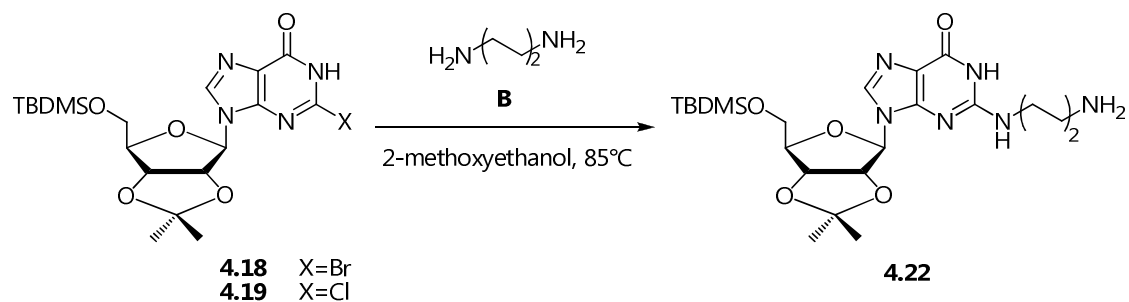
Scheme 4.24.
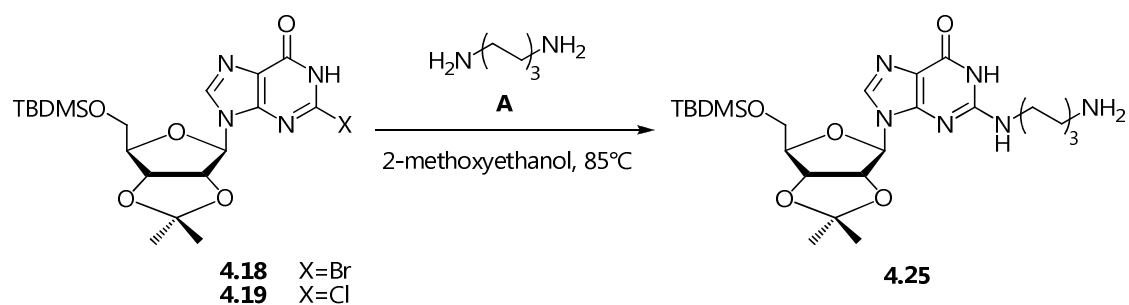
Scheme 4.25.

Even in this cases, isolation of the products was difficult. We had evidence of the formation of the product by ESI-MS and NMRspectra. In particular, inspection of the ^{1}H NMR spectra showed that the obtained compounds were ca 80-90% pure and they have been obtained in ca 70% yield.

In order to prove the identity of compound **4.22**, its free amino group was reacted di-*tert*-butyl dicarbonate (Boc₂O) affording compound **4.26** (Scheme 4.26), which was fully characterized by ESI-MS and 1D and 2D-NMR spectroscopy.
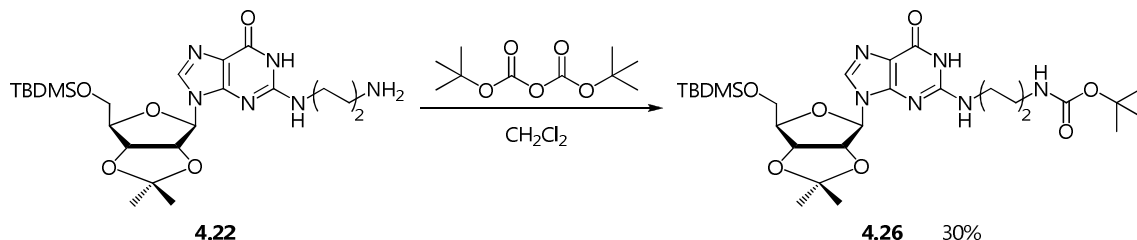
Scheme 4.26.

Due to the easier purification of 26, we decided to use the Boc-protected 1,4-diaminobutane **B1** as the nucleophile in the halogen-displacing reaction (Scheme 4.27). The reaction of **B1** and either bromo **4.18** or chloro **4.19** derivative gave the desired product in 63% and 82% yield, respectively.
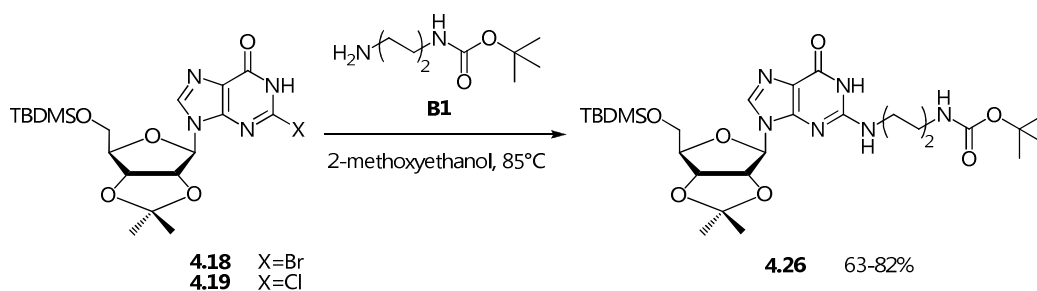
Scheme 4.27.

However, the cleavage of the N-Boc-protecting group in the next stage of the synthesis gave unsatisfactory results, due to the partial cleavage of the hydroxyl-protecting groups of the ribose moiety (Scheme 4.28).
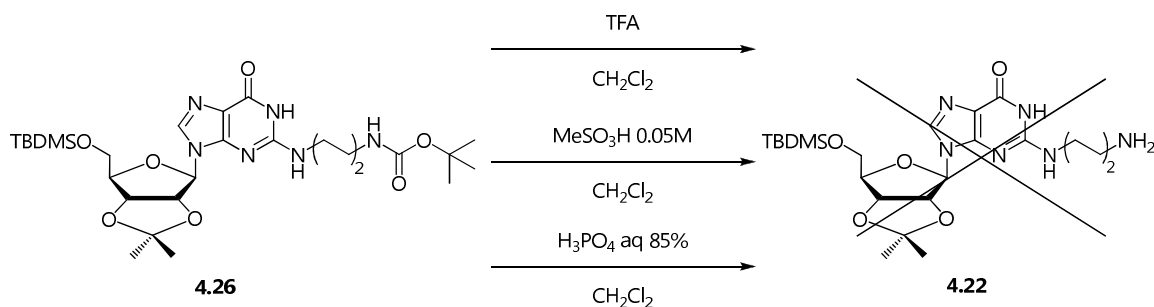
Scheme 4.28.

We concluded that the use of the mono-Boc derivatives of the nucleophilic diamines was not convenient, at least for two reasons. First, the removal of the Boc-protecting group revealed to be a non-selective reaction, forcing us to protect the ribose hydroxyl groups once again. Secondly, this approach required the use of huge amounts of diamines. A large excess of diamine is indeed requested in order to assure the mono-Boc protection in the preparation of reactant **B1**, and the mono-Boc amine **B1** is in turn used in large excess in the nucleophilic aromatic substitution reaction. On the basis of these evidences, we concluded that a better strategy could involve the use of the crude, unpurified derivatives **4.22**, **4.24** and **4.25**, which were obtained with a satisfactory degree of purity (vide supra).

Derivatives **4.22**, **4.24** and **4.25** were then reacted with L-glutamic acid protected at the α-carboxyl- and α-amino positions (z-Glu-OtBu-γOH) in the presence of DCC at room temperature, to give the hybrid compounds **4.27**, **4.28** and **4.29** (Scheme 4.29).
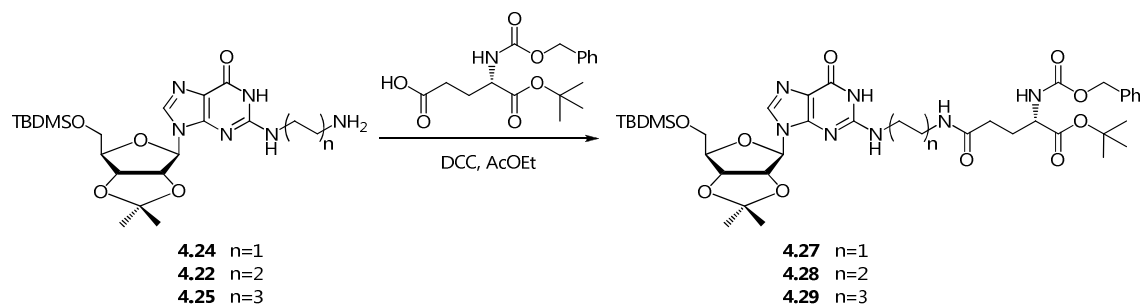
Scheme 4.29.

The hybrid compounds **4.27**, **4.28** and **4.29** were obtained in satisfactory yields (Table 4.4) after flash column chromatography.

144

Table 4.4

	Hybrid compound	Chain lenght	Yield[1]
4.27		CH$_2$=2	64%
4.28		CH$_2$=4	47%
4.29		CH$_2$=6	50%

1) overall yield after two steps

4.4. Phosphorylation of the position 5' of ribose

In order to phosphorylate the hybrid compound **4.27**, **4.28**, **4.29**, the TBDMS groups in position 5' of such derivatives were cleaved by using tetra-*n*-butylammonium fluoride (TBAF • 3H$_2$O) in THF at room temperature (Scheme 4.30). The products were purified by flash chromatography (table 4.5).
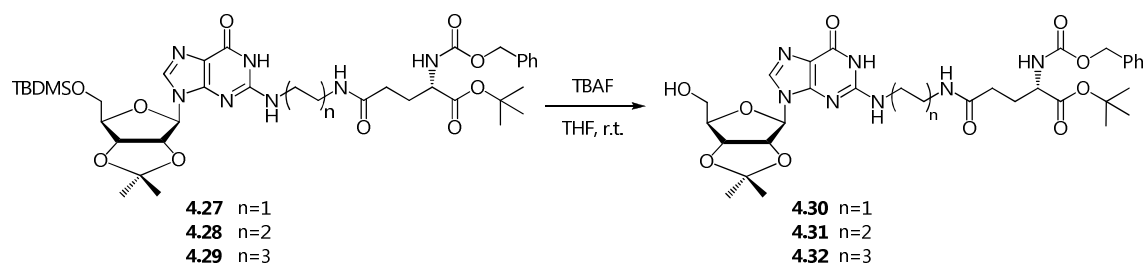
Scheme 4.30.

Table 4.5

Hybrid compound	Chain lenght	Yield
4.30	CH$_2$=2	84%
4.31	CH$_2$=4	82%
4.32	CH$_2$=6	58%

146

The subsequent phosphorylation of the free position 5' of the ribose was obtained following the procedure described by Yoshikawa *et al.* [1969], using phosphorus oxychloride ($POCl_3$) as the phosphorylating agent and triethylphosphate (TEP) as the solvent.

The reaction proceeds through the intermediacy of a guanosine-triethylphosphate complex (Figure 4.1), as described by Ikemoto *et al.* [1995]. This Guo-TEP complex showed excellent selectivity and high reactivity toward phosphorus oxychloride compared with those of free guanosine. After the activation of the 5'-hydroxyl group of guanosine through the formation of the complex, attack of the phosphorylating agent $POCl_3$ occurs and the $O^{5'}$-$POCl_2$ bond is formed (intermediate **4.34** in Scheme 4.31). Hydrolysis of intermediate **4.34** at pH 2-3 at 70 ºC furnished the phosphorylated compound **4.35**, in which the isopropylidene protection on the 2',3' positions of the ribose has been removed.
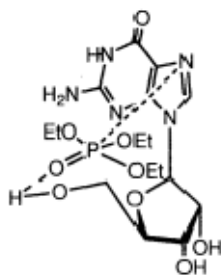
Figure 4.1.
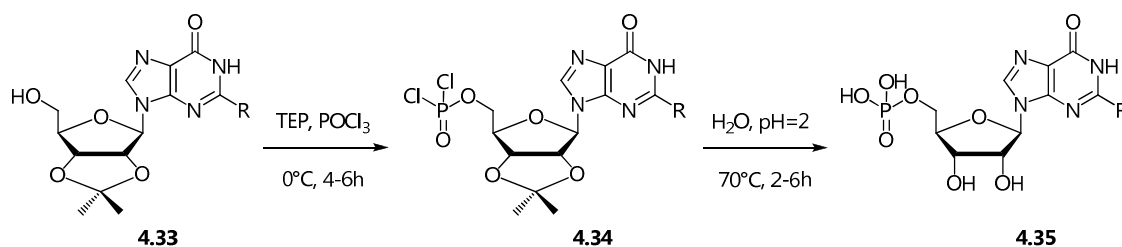
Scheme 4.31.

This procedure was applied on the hybrid compounds previously synthesized **4.31** and **4.32** (Schemes 4.32 and 4.34). The obtained products were purified by preparative HPLC.

In the phosphorylation step of hybrid compound **4.31** some difficulties were encountered (Scheme 4.32). While the formation of the O-P bond takes place without any apparent problems (formation of a single spot on TLC plate), during the successful hydrolytic step a series of by-products appeared in the reaction mixture.

The by-products were isolated by preparative HPLC (Figure 4.2). As results, the desired compound **4.36a** was obtained in 42% yield.
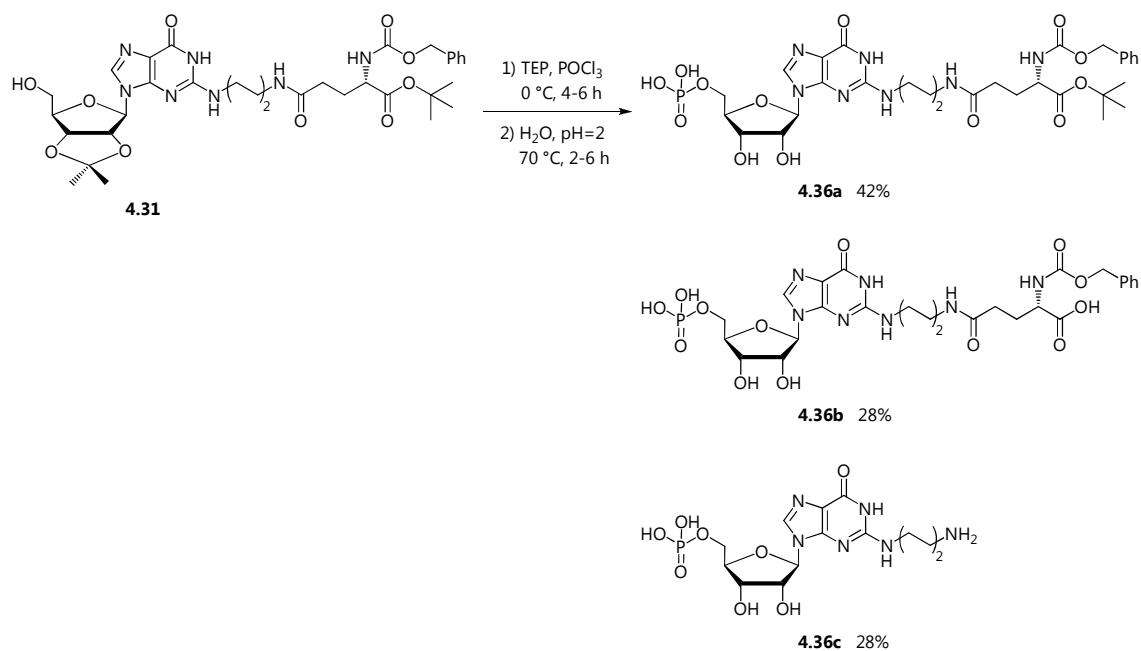
Scheme 4.32.
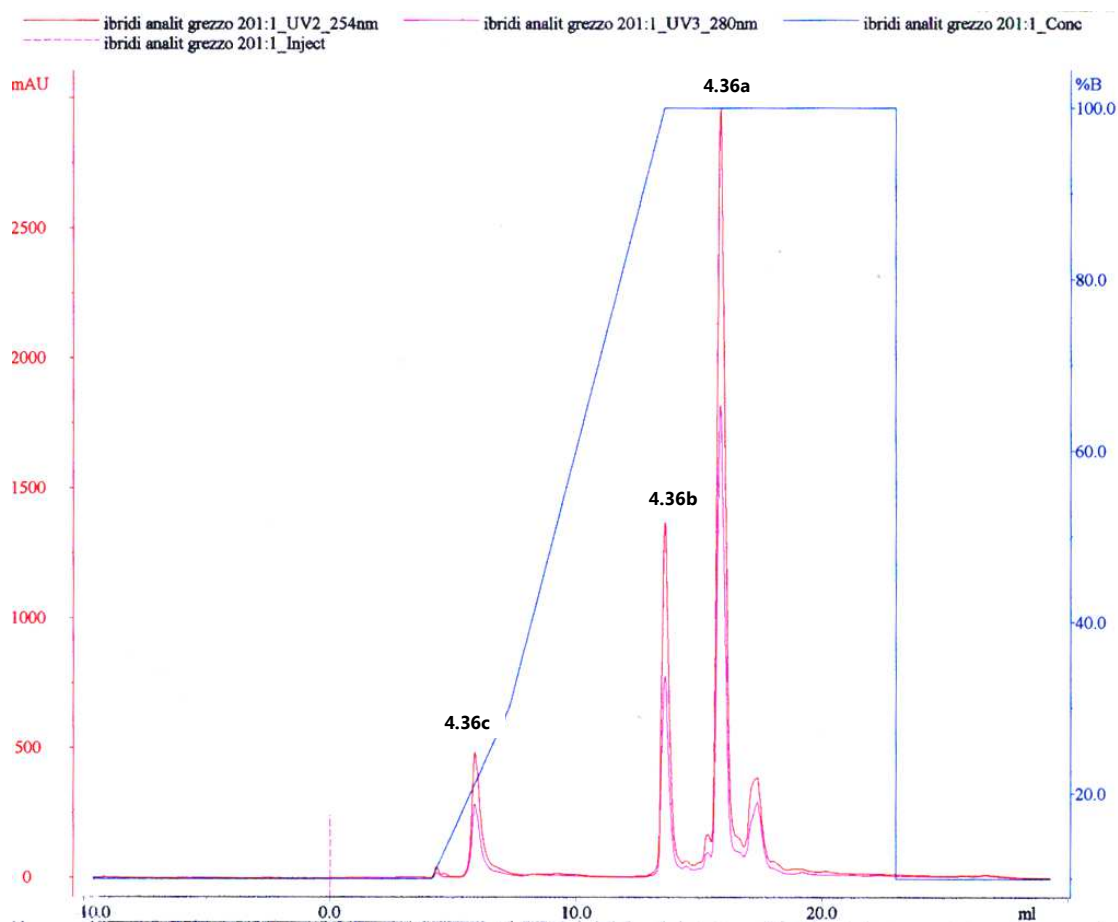
Figure 4.2.

Indeed the conditions of the hydrolytic step determined the cleavage of the linker-glutamic acid bond as well as the Boc protection on the glutamic acid moiety.

Formation of compound **4.36b** could be rationalized on the basis of the removal of the *t*-butyl ester group [Green & Wuts, 1999] during the hydrolytic step following the phosphorylation (Scheme 4.32).

Among the by-products, compound **4.36c** was detected too. Its origin can be rationalized assuming the cleavage of the *N*-protecting benzyloxycarbonyl group [Green & Wuts, 1999] followed by an intramolecular attack of the amino group of the glutamic acid moiety on the γ-carboxyl, affording pyroglutamates **4.37a** and/or **4.37b** (not detectable in HPLC), and derivative **4.36c** (Scheme 4.33).

4.36a R = tBoc
4.36b R = H

4.36c

4.37a R = tBoc
4.37b R = H
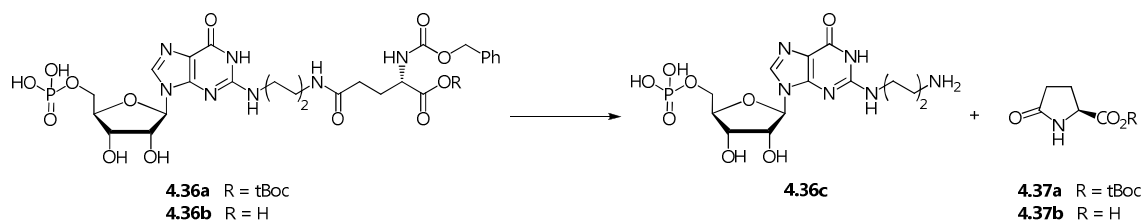
Scheme 4.33.

We tried the same reaction on hybrid compound **4.32**, but we encountered the same problems (Scheme 4.34 and Figure 4.3).

4.32

1) TEP, POCl$_3$
   0 °C, 4-6 h

2) H$_2$O, pH=2
   70 °C, 2-6 h

4.38a 60%

4.38b 10%

4.38c 10%

Scheme 4.34.

150
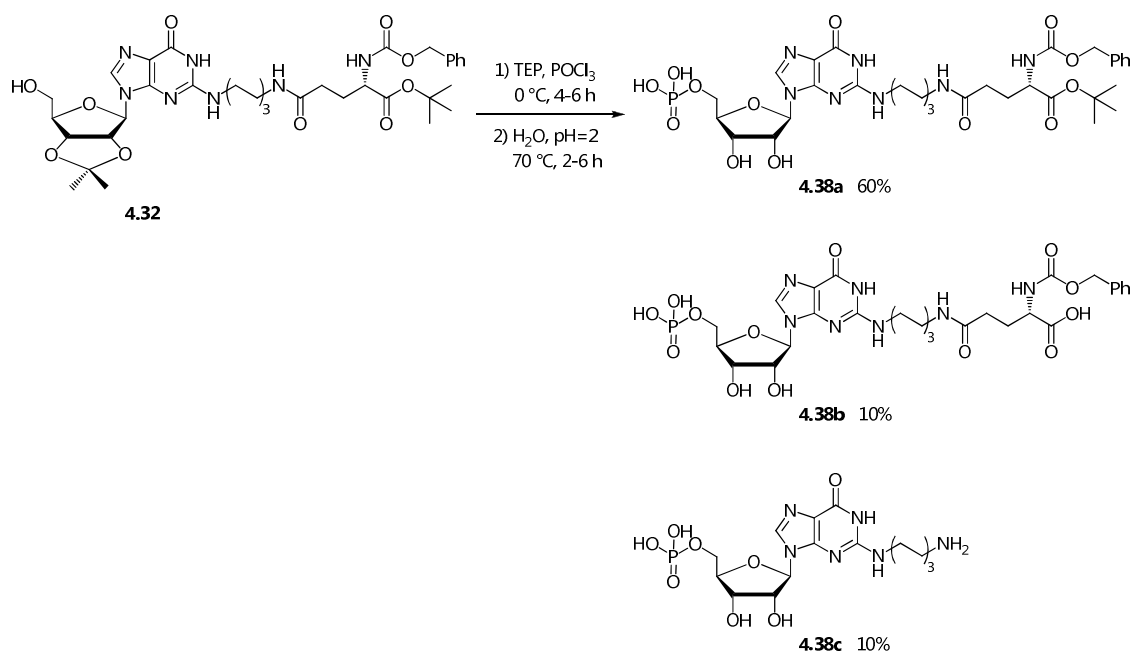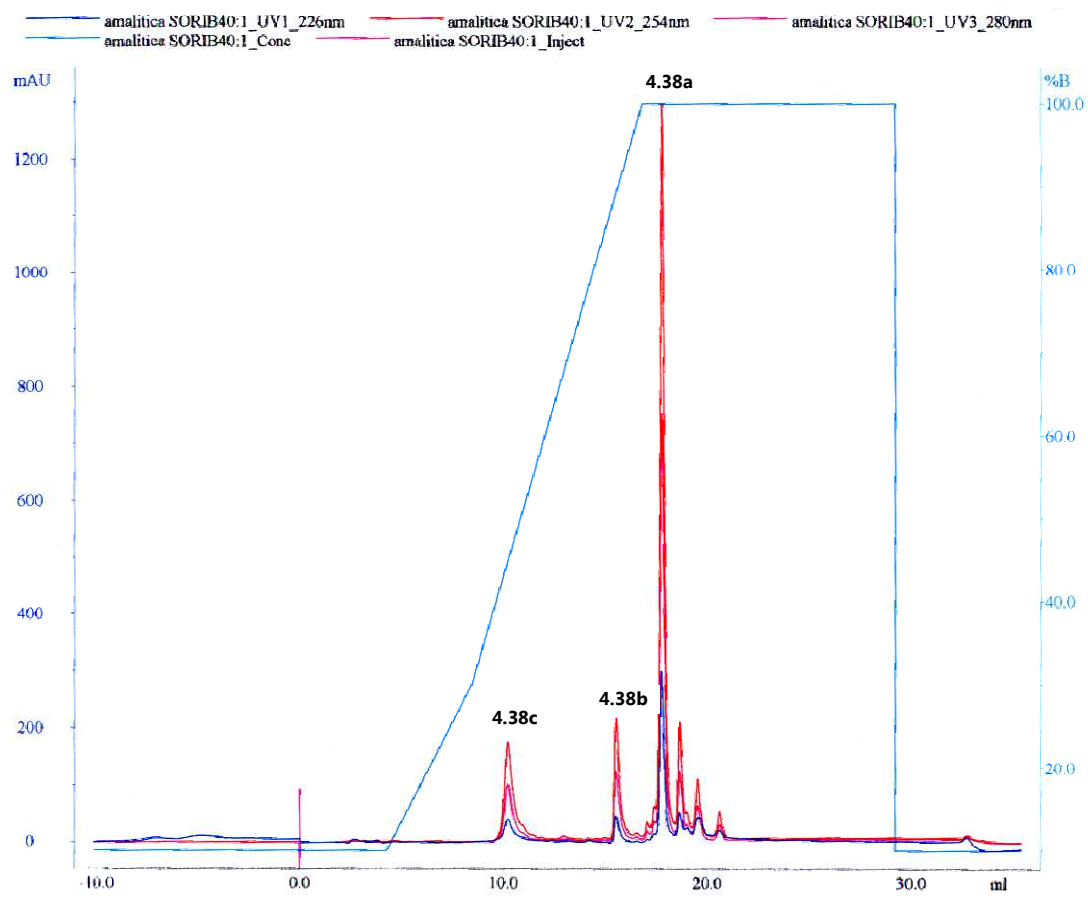
Figure 4.3.

Removal of the glutamic acid moiety protecting groups from compound **4.38a** was achieved in almost quantitative yield by reaction in neat trifluoroacetic acid (TFA) at low temperature for few minutes (Scheme 4.35).
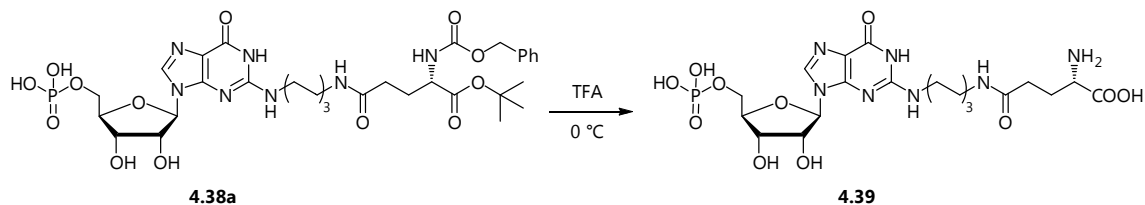
Scheme 4.35.

On the basis of this result, we decided to change slightly our strategy, avoiding the HPLC purification step after the phosphorylation reaction. The protected hybrid compound **4.30** was thus phosphorylated as previously reported (Scheme 4.36), but the reaction crude was not purified. Instead, it was desalted by the use of a XAD-4 resin. XAD-4 resin is a polystyrene-based polimer able to bind aromatic compounds through hydrophobic interactions when the products are solubilized in water. Resin-adsorbed compounds can then be recovered by elution with methanol.
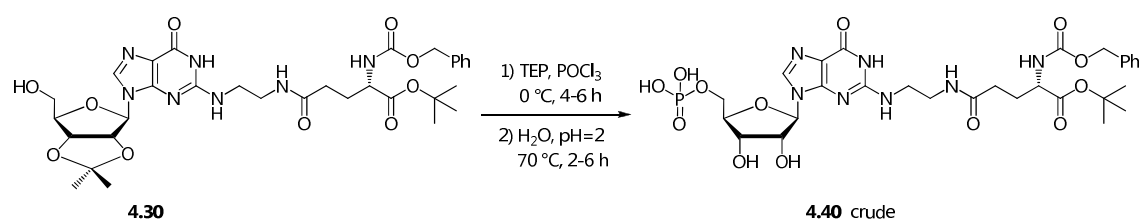
Scheme 4.36.

Attempts to deprotect the desalted intermediate **4.40** with trifluoroacetic acid gave unsatisfactory results, but the addition of a trace amount of trifluoromethanesulfonic acid (TFMS) to a trifluoroacetic acid solution of **4.40** at 0 °C afforded rapidly the desired product **4.41** (Scheme 4.37). A single preparative HPLC purification could therefore be carried out at the level of the final product **4.41**.
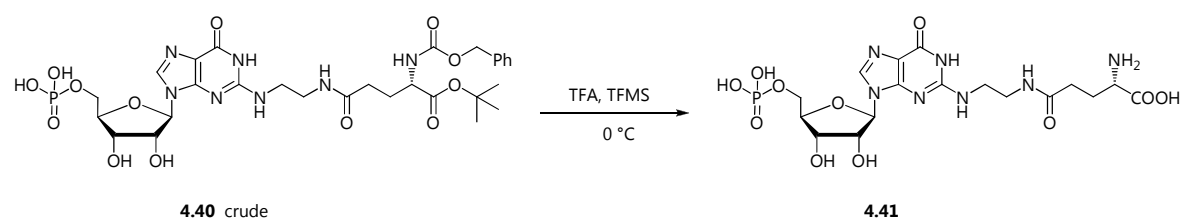
Scheme 4.37.

The overall synthetic plan is shown in Scheme 4.38.
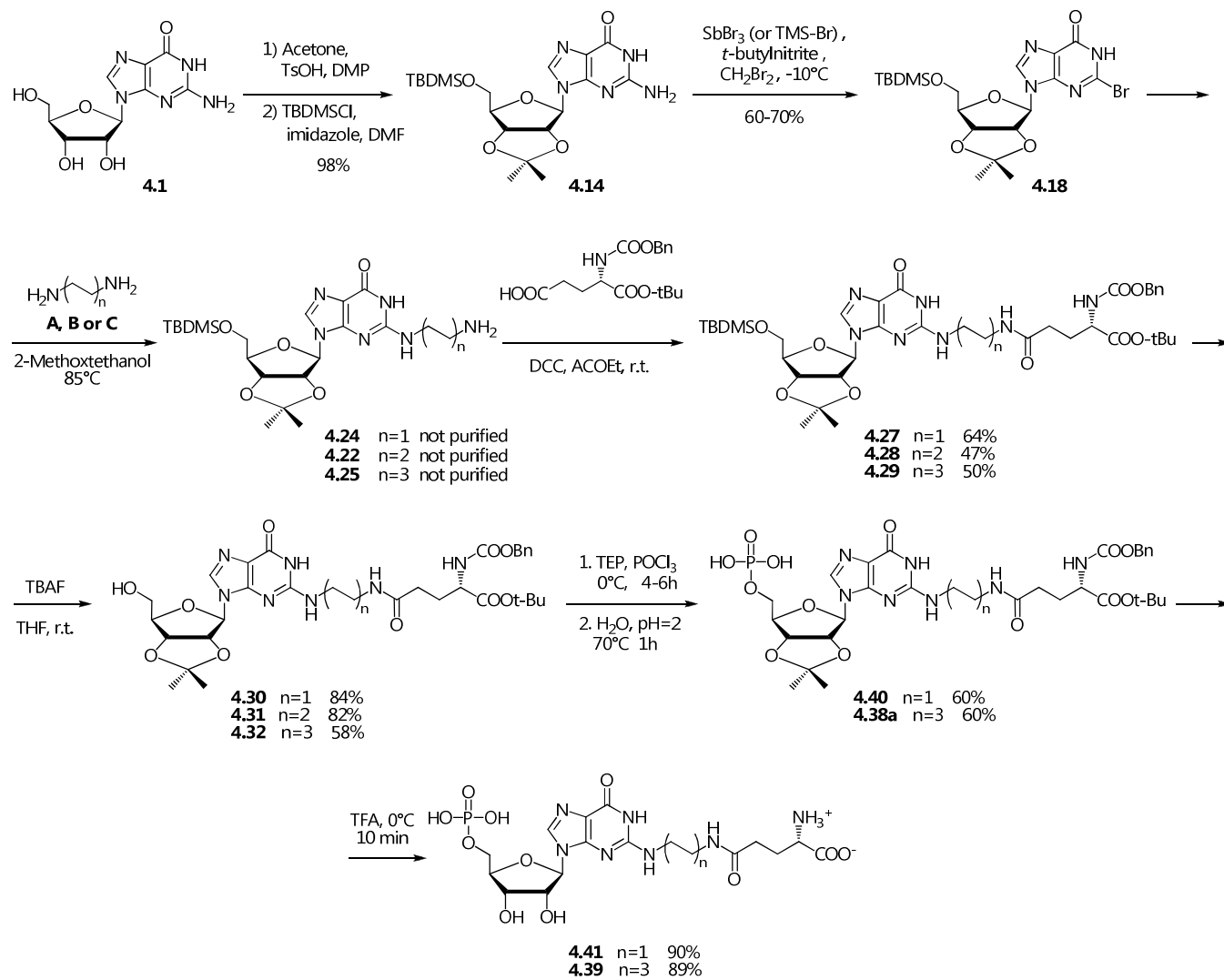
Scheme 38.

5. CONCLUSIONS AND FUTURE PERSPECTIVES

In conclusion:

1. By-products from food industry can be exploited as valuable sources of bioactive peptides. In addition, the mixture of peptides obtained from rice middlings and hemp seeds through enzymatic hydrolysis were shown to elicit intense glutamate-like umami taste. Such hydrolyzed vegetable proteins could then potentially be used as ingredients in culinary products. The same hydrolytic protocol will be applied to proteins of flax seeds.

2. The synthesis of two hybrid compounds in which the umami moieties (glutamate and purine 5'-ribonucleotide) are covalently connected through flexible linkers (**4.39** and **4.41**) was carried out. We plan to apply the same synthetic protocol to the preparation of other hybrids with different linker lengths.

Using the T1R1 extracellular VFTD obtained by homology modeling [Mouritsen, 2012] and the hybrids **4.39** and **4.41** and those which will be synthesized as ligands, molecular dynamics simulation will be performed in order to verify the optimal length of the linker to reach both receptor sites and to unravel the molecular mechanism behind the synergistic effect of the two ligands on the dynamics of the receptor.

In addition, to assess the binding affinity constant of the hybrids and of potential ligands for the umami receptor we aim at developing a biochromatographic system through immobilization of this receptor on a chromatographic support, taking advantage of the accumulated experience of the group of Pharmaceutical Analysis from the University of

Pavia (Italy) and of a recent joint collaboration about the immobilization of a purine nucleoside phosphorylase (from *Aeromonas hydrophila*) as an on-line enzyme reactor for biocatalytic applications [Calleri *et al.*, J. Chromatography B, accepted with revisions].

This task represents a future perspective of the work in the view to take on structure–activity relationship (SAR) studies on umami receptor ligands.

Development of new technologies to facilitate and speed up the screening of ligand libraries is raising considerable interest, particularly in drug discovery. Current screening assays typically rely on function- or affinity-based assays. Following the former approach, the "event" triggered by ligand-receptor binding can be measured, for example, through the quantification of a released second messanger, or by experiments performed on isolated tissues.

On the other hand, binding assays, frequently performed with radioligands, allow to estimate ligand-receptor affinity. The binding affinity for a ligand can be described by measuring several parameters such as K_i (equilibrium dissociation constant of a ligand determined in inhibition studies), K_d (equilibrium dissociation constant), and IC_{50} (molar concentration of an antagonist that reduces the response to an agonist by 50%).

In this frame, affinity chromatography is a quite recent method used to assess interactions between a ligand and its protein target [Schiel *et al.*, 2010]. Basically, the assay is performed in HPLC systems where a column contains the protein immobilized on a stationary phase or on the inner surface of silica capillaries [Sanghvi *et al.*, 2011]. In this technique the retention of analytes depends on the same type of specific, reversible interactions that are encountered in biological systems, as is the case of the ligand-receptor binding. Another evident advantage of such a system relies on the repeated use of the column without a significant loss of properties of immobilized protein, and on the possibility of automation of the analytical assay to assist in the high-throughput screening of a large number of candidates.

Two general formats can be applied in affinity chromatography: zonal elution and frontal analysis. While in zonal elution a small plug of analyte is injected to get information on the interaction of the analyte with the immobilized target, frontal analysis uses the continuous infusion of analyte through a column. Although frontal

158

analysis requires a larger volume of sample than zonal elution, this method has the advantage to provide more information per analysis. Frontal affinity chromatography (FAC) can be used to measure binding constants of the analyte for the immobilized biomolecule with accuracy and precision and to rank potential ligands for a specific receptor [Hage & Tweed, 1997; Moaddel *et al.*, 2002].

Frontal affinity chromatography coupled online to an electrospray mass spectrometer (FAC/MS) is a recently developed screening method for high-throughput screening of combinatorial libraries and compound mixtures [Schriemer, 2004; Calleri *et al.*, 2009]. In this approach, a sample consisting of a mixture of compounds is continuously infused through the column and the order of elution, monitored by the specific *m/z* values, parallels the order of affinity, with the strongest ligand eluting the latest [Calleri *et al.*, 2009; Calleri *et al.*, 2011. Ranking affinity studies may represent a rapid and convenient method for the selection of new potential candidates.

Such a biochromatographic tool has been successfully applied to assess the binding affinity constant of potential ligands for the A_{2A} adenosine receptor subtype [Temporini *et al.*, 2013], for the gamma isoform ligand binding domain (LBD) of peroxisome proliferator-activated receptor (PPAR-γ) belonging to the nuclear receptor superfamily of ligand-activated transcription factors [Calleri *et al.*, 2012], and for the G-protein-coupled receptor (GPCR) GPR17 [Calleri *et al.*, 2010].

It is worth mentioning that two out of the three mentioned applications above involve adenine related compounds [Temporini *et al.*; 2013] or purine nucleotide analogues as well [Calleri *et al.*, 2010], that is molecules structurally related to newly here synthesized potential flavor enhancers.

6. EXPERIMENTAL SECTION
PART 1

6.1. General - Enzymatic and Chemical Hydrolyses

Unless otherwise stated, all reagents were purchased from Sigma-Aldrich (Milan, Italy) and were of analytical grade. All the solvents were of HPLC grade.

Umamizyme (declared activity of 74.3 U/g) was a gift from Amano Enzyme Inc. (Nagoya, Japan) and Flavourzyme (declared activity of 500 U/g) was purchased from Sigma (Milan, Italy).

These are fungal food-grade protease/peptidase complexes produced by submerged fermentation of a strain of Aspergillus oryzae. They exhibit both endoprotease and exopeptidase activities. These enzymes were selected on the basis of their ability to debitter bitter protein hydrolysates at low degrees of hydrolysis (10% to 20%) and to enhance flavor for high degrees of hydrolysis (50% or above) [Hamada, 2000a]. Their optimum activity occurs at 45 °C and pH 7 for Umamizyme$^{®}$ and at 50 °C and pH 8 for Flavourzyme$^{®}$, respectively.

HPLC Analysis: Each chemical hydrolyzed solution was analyzed and purified by RP HPLC using an Amersham pharmacia biotech (P900) liquid chromatographer connected to a UV-vis detector; chromatographic conditions were as follows: column for analytical HPLC, Jupiter RP-18 (4μ proteo 90A size: 250x4.60 mm, Phenomenex); column for semipreparative HPLC, Jupiter- RP-18 (10 μm, size:250x10 mm, Phenomenex); flow rate, 0,5 ml/min; detector, λ 226 and 254 nm; mobile phase: A (0,1% TFA (v/v) in water) and B (80% acetonitrile/ 20% water with 0,1% of TFA), gradient elution from 5% to 100% B in 45 min.

NMR Spectroscopy: NMR analysis was performed by ISMAC-CNR and was used to characterize the hydrolyzed compounds by recording homonuclear 2D TOCSY, NOESY and ROESY spectra and diffusion experiments (DOSY). From scalar and dipolar NMR experiments an indication of the kind of amino-acids present in the peptides was derived, while DOSY experiments allowed to define the range of peptide molecular weights present in the samples obtained with different hydrolysation-conditions.

Mass Spectrometry: Mass spectra were obtained with a Bruker ion-trap Esquire 3000 or 6000 apparatus (ESI ionization) and Microflex apparatus (MALDI ionization) from Bruker.

Other Analytical Methodos: *UV measurements* were carried out with a Jasco V-360 UV-Vis Spectrophotometer (Jasco International, Tokyo, Japan) equipped with software Spectramenager (Fixed Wavelength Measurement).

6.2. Preparation of HVPs from Rice Middlings through Enzyme-catalyzed Hydrolysis

Rice middlings were kindly provided by a local milling factory (Curti Riso, Valle Lomellina, Pavia, Italy). Rice middlings defatting was achieved as previously described [Van Der Borght *et al.*, 2006], by stirring continuously for 1 hour at room temperature a suspension of bran with *n*-hexane (1:5 w/v). The defatting matrix was recovered using a Buchner funnel and air dried under a hood overnight. The protein content of defatted rice middlings was determined by the Kjeldahl method [AOAC, 1990]. The value of 5.95 was used as protein conversion factor.

6.2.1. Enzymatic Hydrolysis

The protein hydrolysates from rice middlings were obtained according to the method of Hamada [1999], with some modifications. Four reactor system (PolyBLOCK, Hel, UK) interfaced to a PC by means of WinISO software (Hel, Borehamwood, UK) was employed. For any reactor, defatted rice middlings (3 g of matrix corresponding to 540 mg of proteins) were suspended in 100 mM ammonium bicarbonate buffer (final concentration 10% w/v) by adjusting pH to the optimal value for any enzyme, as indicated by manufacturers. Any suspension was pre-incubated for 25 min at the desired temperature. The specific protease was added to the reaction mixture in order to give a final enzyme/substrate ratio (E/S) of 5% w/w and the mixture was stirred at 400 rpm during reaction. Proteolysis was stopped at time interval of 1, 5, 11, and 24 h and immediately the enzyme was inactivated by addition of formic acid up to pH 3.5. After proteolysis, the suspensions of rice middlings were subjected to sonication processing in

a water-bath. The solubilized proteins and peptides were recovered after centrifugation at 3000 rpm and 20 °C for 30 min. Controls of the proteolysis experiments were prepared by repeating the above reported procedure without enzyme.

6.2.2. Characterization of protein hydrolysates

6.2.2.1. Protein electrophoresis

SDS-PAGE was performed on a discontinuous buffered system according to the method of Laemmli [Laemmli, 1970] using 17 % separating gel and 5 % stacking gel. Electrophoresis was performed with a Mini-PROTEAN Tetra Cell apparatus (Biorad) connected to a power supply PowerPac HC (Biorad). Fractions (25μl) of protein hydrolysates were diluted using loading sample buffer solution, namely 60% glycerol, 12% SDS, 0.2% bromophenol blue in 250 mM Tris–HCl buffer pH 6.6, and heated at 97 °C for 3 min. After a short centrifugation, samples were subjected to SDS-PAGE. Before the sample entered the separating gel, electrophoresis was performed at 100 V and after-wards it was performed at 150 V until the tracking dye reached the bottom of the gel. Electrophoresis of each protein sample was carried out in duplicate. The gels were fixed with 45% methanol and 10% acetic acid for 20 min, stained with Coomassie Brillant Blue R-250 blue–picric acid solution and destained with water. For protein pattern characterization by densitometric scanning, the individual lanes of the stained gels were scanned by an Image Scanner (Amersham Pharmacia Biotech) and analyzed by the Lazarsoftware and NIH software. Image analysis software calculated integrated optical density (IOD) for bands resolved in each lane, thereby generating a total lane IOD values corrected for background. Total lane IOD was used to estimate a global value of protein degradation [Frazer & Bucci, 1996]. Changes in the relative amount of each protein bands present in successive samples were estimated from their respective percent area on the densitograms against the percentage area of the same band at time zero [Alarcón et al., 2001]. The rate of hydrolysis was expressed by a numerical value obtained considering both the percentage of reduction in optical density for each band after the reaction time, and the relative proportion such band represented to total

proteins. Only those bands representing at least 10% of total protein in the sample at the beginning of the assay were considered for estimations. The value obtained was named Coefficient of Protein Degradation (CPD) and it was estimated using the following mathematical expression [Alarcón *et al.*, 1999; Alarcón *et al.*, 2001]:

$$CPD = \Sigma^{n}_{i=1} [(OD_i(t_0) - OD_i(t) / OD_i(t_0)] \; x \; [OD_i(t_0) / \Sigma^{n}_{i=1} OD_i(t_0)] \qquad (eq. \; 6.1)$$

where i = major protein bands identified from 1 to n; OD_i = optical density of the protein band i; t = time of reaction.

6.2.3. Functional properties

6.2.3.1. Emulsifying properties

The emulsifying activity index (EAI) and emulsion stability index (ESI) of the samples were determined according to the method of Pearce and Kinsella [1978], with minor modifications made by Yin *et al.* [2008]. For the emulsion formation, 3 ml of 0.2% protein hydrolysate dispersion (in deionized water adjusted to pH 3.0, 5.0, 7.0 and 9.0 with 1 N NaOH or HCl) and 1 ml of corn oil were homogenized by manual agitation for 1 min. One hundred microliters of emulsion were taken from the bottom of the homogenized-emulsion, immediately (0 min) or 10 min after homogenization, and diluted (1:100, v/v) in 0.1% (w/v) SDS solution. After shaking in vortex mixer for about 5 s, the absorbance of diluted emulsions was read at 500 nm in the spectrophotometer. EAI and ESI values were calculated by the following equations:

$$EAI(m^2/g) = [2*2.303*A_0*DF/c*\varphi*(1-\theta)*10000] \qquad (eq. \; 6.2)$$

$$ESI \; (min) = (A_0 / A_0 - A_{10})*10 \qquad (eq.6.3)$$

where DF is the dilution factor (100), c the initial concentration of protein (g/ml), φ the optical path (0.01 m), θ the fraction of oil used to form the emulsion (0.25), and A_0 and

A_{10} the absorbance of the diluted emulsions at 0 and 10 min. Measurements were performed in duplicate.

6.2.3.2. Foaming properties

Foaming properties including foaming capacity (FC) and foam stability (FS) were determined according to the method of Fernandez and Macarulla [1997] with minor modifications made by Yin et al. [2008]. Aliquots (5 ml) of protein hydrolysate solutions (1%, w/v, pH 7.0) were homogenized in a measuring cylinder (15 ml) by manual agitation for 2 min. FC was calculated as the percent increase in volume of the protein dispersion upon mixing, while FS was estimated as the percentage of foam remaining after 30 min. Measurements were performed in duplicate.

6.2.4. Sensory analysis

The sensory profiling was carried out at the Sensory Laboratory at Special Company for Professional Training and Technological and Commercial Promotion of the Chamber of Commerce of Savona (Albenga, Italy). Five subjects participated in the descriptive analysis as panelists. The subjects had variable experiences of descriptive analysis. Five samples were prepared as 0.5% solutions in deionized water consisting of protein hydrolysates selected in the SDS-PAGE experiment. A 0.5% MSG solution was presented as a reference. Aliquots (20 ml) of each sample, equilibrated with room temperature (20 ± 2 °C), were presented to the panelists in a disposable plastic cup coded with random numbers. The presentation order of the samples was randomized to minimize the presentation order effect. The subjects were previously trained until consensus was reached to evaluate the five basic tastes (sweet, bitter, sour, salty and umami). The sensory attributes were evaluated using a quantitative descriptive analysis method [Jo & Lee, 2008], based on "sip and spit" procedure. The subjects rinsed their mouths with filtered water before tasting and between tasting samples. The subjects rated the intensity of stimulus using a 10-point category scale whose left and right ends

were labeled "weak" and "strong", respectively. Each sample was evaluated 2 times in different sessions. Odor references were also determined in order to obtain the characteristic flavor for each protein hydrolysate.

6.2.5. Statistical analysis

Statistical analyses were performed with the Origin Pro 8 software (Origin Lab Inc., Northampton, MA). The data were expressed as mean ± SE and evaluated using one-way analysis of variance followed by Tukey's post-hoc test. A level ofpb0.05 was used as a criterion for statistical significance.

6.3. Preparation of HVPs from Hempseed through Enzyme-catalyzed Hydrolysis

6.3.1. Defatted Hempseed Meal

Hemp (*Cannabis sativa* L., var. Futura) seeds, harvested in Cavriana (MN) and Treviglio (BG), were provided by CNR-Institute of Biology and Biotechnology (IBBA) of Milan, Italy, during 2011/2012. A voucher specimen is stored and preserved in our laboratory at Department of Chemistry at University of Milan. Seeds were stored at 4 °C in the dark until use.

Hempseeds were defatted by stirring a suspension of seeds with *n*-hexane (1:4 w/v) at room temperature for 3 hours and overnight with renewed *n*-hexane (1:6 w/v). The defatted seeds were recovered using a Buchner funnel, air dried under a hood overnight, and ground with a home-style grinder (Braun Multiquick System 2K100). The obtained flour was again defatted with the same procedure described above. After vacuum filtration of the defatted matrix, the organic phase was concentrated under reduced pressure and the flour was air dried under a hood overnight. Both defatted hempseed flour and extracted hemp oil were stored at -20 °C until use.

Commercial hempseed samples were kindly provided from Exhemplara® - Prodotti Biologici in Canapa (Roma, Italy). Hempseeds were defatted and ground as described above. The obtained flour was used to provide hempseed hydrolysates for sensory profiling.

The protein contents of both defatted hempseed flours were determined according to the Kjeldahl method, which was performed by Centro di Ricerca per le Produzioni Foraggere e Lattiero-Casearie (CRA) of Lodi, by measuring the nitrogen content with a

CNH analyzer [AOAC, 1980]. The value of 6.25 was used as conversion factor to determine the protein content.

6.3.2. Protein Extraction

Hempseed protein extraction was carried out by alkali solubilization/acid-precipitation procedures using two different methods.

Method A (NaOH/HCl). According to Wang *et al.* [2009], defatted hempseed meal was suspended in distilled water (in ratio 1:20 v/w, dry weight basis) and the pH was adjusted to 10.00 with 1 M NaOH at 37 °C. The mixture was stirred for 3 h to extract the proteins and then centrifuged at 8000 rpm for 30 min. to recover both supernatant and the residue. The residue was subjected to one more protein extraction followed by centrifugation using the same procedure described above. The latter residue was discarded and the combined alkali extracts were adjusted to pH 5.0 with 1 M HCl at room temperature to precipitate the proteins. Recovered protein precipitate was collected by centrifugation (8000rpm, 30 min, rt), suspended again in distilled water and pH was adjusted to 7.0 using 1 M NaOH.

Method B (NH₃/HCCOH). The same procedure was followed for the method B where NH_3 was used for the alkali-extraction and HCOOH was used for the acid-precipitation. In both cases, the protein solution was dialyzed against distilled water (MWCO 3500, Spectra/Por®) at 4 °C for 48 h to remove small molecules, such as salts, and finally lyophilized. The freeze-dried hemp seed protein isolate was stored at -20 °C until use. An aliquot of this product was analyzed by ^{1}H NMR spectroscopy (1D 500 MHz, pH 7, 37 °C).

To analyze the protein extract by SDS-PAGE the procedure of extraction was slightly modified by using two different approaches. In the first one defatted hempseed meal (75 g) was subjected to the same protein extraction reported in Method A. After centrifugation, the obtained precipitate was washed with pre-cooled deionized water, dispersed in 50 mM Tris/0.05% SDS pH 8.0 (1.5 ml), stirred in termomixer (1000 rpm, 20 °C, 1h 30 min) and subjected to sonication processing in a water-bath.

In the second one defatted hempseed meal (75 g) was mixed with 2% SDS/6 M urea (1.5 ml) and with 2% SDS/6 M urea/1% DTT (1:20 w/v, 1.5 ml). After continuously stirring for 2 h at 37 °C, the suspension was centrifuged at 8000 rpm for 30 min and the residue discarded. Both protein solutions were preserved at -20 °C until use.

6.3.3. Enzymatic Hydrolysis

The enzymatic hydrolysis of defatted hempseed meal was performed according to the method described by Bagnasco *et al.* [2013]. Four reactor system (PolyBLOCK, Hel, UK) interfaced to a PC by means of WinISO software (Hel, Borehamwood, UK) was employed on hemp seeds provided by CNR-IBBA of Milan. A semi-preparative scale protocol was used for commercial hempseed samples.

Defatted hempseed flour (3 g of harvest matrix and 30 g of commercial matrix corresponding to 675 mg and 6.750 g of proteins, respectively) were suspended in 100 mM ammonium bicarbonate buffer (final concentration 10% w/v) by adjusting pH to the optimal value for any enzyme, as indicated by manufacturers. Any suspension was preincubated for 20 minutes at the desired temperature. The specific protease was added to the reaction mixture in order to give a final enzyme/substrate ratio (E/S) of 5% w/w and the mixture was stirred at 400 rpm.

Hydrolyses were carried out in the above conditions and stopped after 1, 5, 11 and 24 hours by addition of formic acid up to pH 3.5 to inactivate the enzyme. Subsequently the suspensions were sonicated in a water-bath for 10 minutes and centrifuged at 8000 rpm for 30 min at room temperature to recover solubilized proteins and peptides and remove the undigested materials. The supernatants, containing HVPs, were collected, freeze-dried and stored at -20 °C before further analysis. Controls of the proteolysis experiments were obtained by repeating the above procedure without the enzymes.

6.3.4. Ultrafiltration

The freeze-dried hydrolysates (350 mg) were resuspended in bi-distilled water (50 ml), sonicated for 15 minutes and passed through an Amicon stirred ultrafiltration cell (Stirred Cell - Millipore) using a 10000-Da Molecular Weight Cutoff (MWCO) membrane, to remove the molecules (peptides and undigested proteins) larger than the membrane pores. The permeate, containing low-MW peptides (<10000 Da), was freeze-dried and stored at -20 °C until needed.

6.3.5. SDS-PAGE (sodium dodecyl sulfate-polyacrylamide gel electrophoresis)

6.3.5.1. SDS-PAGE of protein extract

SDS-PAGE was performed on a discontinuous buffered system according to the method of Laemmli [1970] using 12% separating gel and 4% stacking gel. Electrophoresis was performed with a Mini-PROTEAN Tetra Cell apparatus (Biorad) connected to a power supply PowerPac HC (Biorad). Fractions of protein extract, corresponding to 60 μg of proteins, determined with 2-D Quant Kit (Amersham Biosciences), were diluted using loading sample buffer solution, namely 60% glycerol, 12% SDS, 0.2% bromophenol blue in 250 mM Tris–HCl buffer (pH 6.6), and heated at 97 °C for 3 min. After a short centrifugation, samples were subjected to SDS-PAGE. Before the sample entered the separating gel, electrophoresis was performed at 100 V and afterwards it was performed at 150 V until the tracking dye reached the bottom of the gel. Electrophoresis of each protein sample was carried out in duplicate. The gels were stained with Coomassie Brillant Blue R-250 in 40% ethanol and 10% acetic acid solution and destained with 40% ethanol and 10% acetic acid solution. For protein pattern characterization by densitometric scanning, the individual lanes of the stained gels were scanned by an Image Scanner (Amersham Pharmacia Biotech) and analyzed by the Lazarsoftware. The relative protein amount of each subunit (protein band) of protein was calculated from their respective percent area on the densitograms against the total subunits area of

protein. Only the main bands, representing at least 10% of total proteins, were considered for estimations.

6.3.5.2. SDS-PAGE of protein hydrolysates

SDS-PAGE was performed on a discontinuous buffered system according to the method of Laemmli [1970] using 17% separating gel and 4% stacking gel. Electrophoresis was performed with a Mini-PROTEAN Tetra Cell apparatus (Biorad) connected to a power supply PowerPac HC (Biorad). Fractions (20 μl) of protein hydrolysates were diluted using loading sample buffer solution, namely 60% glycerol, 12% SDS, 0.2% bromophenol blue in 250 mM Tris–HCl buffer (pH 6.6), and heated at 97 °C for 3 minutes. After a short centrifugation, samples were subjected to SDS-PAGE. Before the sample entered the separating gel, electrophoresis was performed at 100 V and afterwards it was performed at 150 V until the tracking dye reached the bottom of the gel. Electrophoresis of each protein sample was carried out in duplicate. The gels were stained with Coomassie Brillant Blue R-250 in 40% ethanol and 10% acetic acid solution and destained with 40% ethanol and 10% acetic acid solution. For protein pattern characterization by densitometric scanning, the individual lanes of the stained gels were scanned by an Image Scanner (Amersham Pharmacia Biotech) and analyzed by the Lazarsoftware and NIH software.

Image analysis software calculated integrated optical density (IOD) for bands resolved in each lane, thereby generating a total lane IOD values corrected for background. Total lane IOD was used to estimate a global value of protein degradation [Frazer & Bucci, 1996]. Changes in the relative amount of each protein bands present in successive samples were estimated from their respective percent area on the densitograms against the percentage area of the same band at time zero [Alarcón *et al.*, 2001].

The rate of hydrolysis was expressed by a numerical value obtained considering both the percentage of reduction in optical density for each band after the reaction time, and the relative proportion such band represented to total proteins. Only those bands representing at least 10% of total protein in the sample at the beginning of the assay were considered for estimations. The value obtained was named Coefficient of Protein

Degradation (CPD) and it was estimated using the following mathematical expression [Alarcón *et al.*, 1999; Alarcón et al., 2001]:

$$CPD = \Sigma^n_{i=1} [(OD_i(t_0) - OD_i(t) / OD_i(t_0)] \times [OD_i(t_0) / \Sigma^n_{i=1} OD_i(t_0)] \qquad (eq.\ 6.1)$$

where i = major protein bands identified from 1 to n; OD_i = optical density of the protein band i; t = time of reaction.

6.3.6. Protease activity assay

The activity of Flavourzyme® and Umamizyme® was determined according to Cupp-Enyad with some modifications (Cupp-Enyad, 2008).

The assay was performed with the following reagents:

A. A 50 mM K_2HPO_4 buffer, pH 7.5, placed at 37 °C until use.

B. Casein in buffer A (0.65% w/v) at pH 7.5 prepared by stirring 650 mg of casein with 1 ml of buffer A and gradually increasing the temperature up to 80-85 °C in 10 minutes. The solution was finally placed at 37 °C until use.

C. 110 mM trichloroacetic acid (TCA).

D. Folin & Ciolcaltea's reagent (Sigma-Aldrich) diluted in water (1:4 v/v).

E. 500 mM Na_2CO_3.

F. 10 mM sodium acetate + 5 mM calcium acetate at pH 7.5, placed at 37 °C until use.

G. 1.1 mM L-tyrosine standard.

H. Protease solutions of Flavourzyme® and Umamizyme® in F

A calibration curve was obtained by measuring the absorbances of four solutions containing increasing volumes of a 1.1 mM solution of L-tyrosine **G** (0.03, 0.06, 0.08 and 0.12 ml), 0.25 ml of the F-C reactive solution **D**, 1.25 ml of 500 mM Na_2CO_3 **E**, and water up to 1 ml (Table 6.1). A sample containing the same reagents without L-tyrosine was used as blank.

Table 6.1.

Reagent	Blank	Sample 1	Sample 2	Sample 3	Sample 4
1.1 mM l-tyrosine (G)	/	30 μl	60 μl	80 μl	120 μl
H₂O	500 μl	470 μl	440 μl	420 μl	380 μl
500 mM Na₂CO₃ (E)	1.25 ml	1.25 ml	1.25 ml	1.25 ml	1.25 ml
F-C reactive solution (D)	250 μl	250 μl	250 μl	250 μl	250 μl

Calculated ε = 10979

The absorbances of the standard solutions were measured with a spectrophotometer at a wavelength of 750 nm. The calibration curve was obtained with a graphing program by plotting the amount (μmol) of L-tyrosine solution **G** on the Y axis, versus the change in absorbance recorded on the X axis.

The assay is performed at 25 °C in two steps. In the first one blank, sample, and control solutions are prepared. The sample solution was obtained by adding the protease solution **H** (0.1 ml) to casein **B** (0.5 ml) in a plastic microcentrifuge tube. After 5 minutes TCA **C** (0.5 ml) was added to inactivate the enzyme. The control solution was prepared with the same procedure but adding the buffer **F** (0.1 ml) instead of the protease solution **H**. The blank solution was prepared by adding in a plastic microcentrifuge tube the protease solution **H**, TCA **C** (0.5 ml) and casein **B** (0.5 ml) at the same time. Afterwards each tube was centrifuged at 13200 rpm for 1 minute.

In the second step 500 mM Na₂CO₃ **E** (0.625 ml) and the F-C reactive **D** (0.125 ml) were added to each supernatant (0.25 ml) in a plastic microcentrifuge tube. After 15 minutes each solution was centrifuged at 13200 rpm for 1 minute and the supernatant absorbances were read at 750 nm in disposable plastic cuvettes.

The μmoles of tyrosine equivalents released were determinate using the calibration curve. The activity of Flavourzyme® was obtained by the equation:

$$U/ml\ enzyme = \frac{(\mu mol\ of\ tyrosine\ equivalents\ released) x (ml\ used\ in\ step\ 1)}{(ml\ of\ enzyme) x (reaction\ time,\ min) x (ml\ used\ in\ step\ 2)} \quad (eq.\ 6.4)$$

As Umamizyme® is a solid protease, the enzymatic activity was obtained by the equation:

$$U/mg\ enzyme = \frac{U/ml\ enzyme}{mg\ protein/ml\ enzyme} \qquad (eq.\ 6.5)$$

6.3.7. 1,1-Diphenyl-2-picrylhydrazyl (DPPH) radical scavenging activity

DPPH radical scavenging activity was evaluated as described by Li *et al.* [2007] with slightly modification. In disposable plastic cuvettes each *hydrolyzed sample* dissolved in water (400 μl) was mixed with 99.5% ethanol (400 μl) and 0.02% DPPH (w/v) in 99.5% ethanol (100 μl). The resulting solutions was incubated in the dark at room temperature for 60 minutes, then absorbance at 339 nm was recorded (A_s) using a UV-visible spectrophotometer. A lower absorbance A_s of the reaction mixture suggested a higher free radical scavenging ability. A mixture containing distilled water (400 μl) instead of the hydrolyzed samples was used as control (A_c). A mixture containing hydrolyzed sample solution (400 μl) and 99.5% ethanol (500 μl) without DPPH was used as blank (A_b). The percentage of the DPPH scavenging activity was calculated by the equation:

$$Radical\ scavenging\ activity\ (\%) = \frac{A_c + A_b - A_s}{A_c}\ x\ 100 \qquad (eq.\ 6.6)$$

Defatted hempseed meal incubated under the same experimental conditions without the enzyme was used as negative control; whereas reduced glutathione (GSH, 0.005% - 0.015% w/v) and butylated hydroxytoluene (BHT, 0.0005% - 0.0025% w/v) were used as positive control.

The IC_{50} value was determined at three different concentrations (0.1%, 0.3%, 0.5% w/v) of the hydrolyzed fractions by plotting the calculated free radical scavenging activity (%) against the sample concentration [Udenigwe *et al.*, 2009].

To investigate the effect of buffers and pH on the scavenging activities, the hydrolyzed fractions at 24 hours (60 μl at final concentration of 0,5 % w/v) was mixed with 40 μl of

0.1 M acetate buffer (pH 4.0), 0.1 M phosphate buffer (pH 7.0) and sodium carbonate buffer (pH 9.0). The assay was performed as described above.

All assays were performed in triplicate.

6.3.8. Ferrous ion-chelating potency

The iron (II) chelating potency was determined as described by Blat *et al.* [2008] with slight modifications. Reactions were carried out in distilled water. In a plastic microcentrifuge tube each *hydrolyzed sample* (800 µl) was incubated with 2 mM $FeCl_2$ (10 µl) for 30 minutes, followed by addition of 5 mM ferrozine (20 µl, Sigma-Aldrich). The resulting solution was kept at room temperature for 1 hour, then the absorbance at 562 nm (A_s) was recorded using a UV-visible spectrophotometer. A complex of $FeCl_2$/ferrozine has a strong absorbance at 562 nm. A high ferrous ion-chelating ability in the test sample results in a low absorbance. A solution of 2 mM $FeCl_2$ (10 µl) in distilled water (800 µl), instead of the hydrolyzed samples, was used as control (A_c). A water solution of each hydrolyzed sample (800 µl) without $FeCl_2$ was used as blank (A_b). The percentage of the Fe(II)-chelating ability was calculated by the following equation:

$$Chelating\ effect\ (\%) = \frac{A_c + A_b - A_s}{A_c}\ x100 \qquad\qquad (eq.\ 6.7)$$

Defatted hempseed meal incubated under the same experimental conditions without the enzyme was used as negative control, whereas the disodium salt of the ethylenediaminetetraacetic acid (EDTA(Na_2), at various concentration from 0.0001% to 0.03% w/v) was used as a standard metal chelating agent. All assays were performed in triplicate.

The IC_{50} value was determined at three different concentrations (0.005%, 0.01%, 0.03% w/v) of the hydrolyzed fractions by plotting the reciprocal of the calculated chelating effects (%) against that of the sample concentrations (Double Reciprocal plot method).

6.3.9. Glutamate content

The amount of free L-glutamate in hempseed hydrolysates was assessed by a L-glutamate determination kit (GLN-1, Sigma, Milan - Italy).

The assay was performed using a buffer containing 1 ml of Hydrazine Hydrate (64% Hydrazine) and 19 ml of Tris (100 mM)-EDTA (2 mM) at pH 9.0. A calibration curve was obtained using water solutions at different concentrations of L-glutamate (25, 50, 100, 150 and 250 μM).

In disposable plastic cuvettes containing 500 μl of buffer were added in succession 30 mM β-Nicotinamide Adenine Dinucleotide (NAD, 50 μl); 100 mM Adenosine 5'-Diphosphate (ADP, 5 μl) and the hydrolysate solution (125 μl). The volume was adjusted to 1.0 mL with water (320 μl).

After mixing by inversion, the absorbance of the resulting solutions was recorded at 339 nm to obtain background reading. Afterward Glutamate Dehydrogenase (L-GLDH; 1200 U/ml, 10 μl) was added to each solution. The cuvettes were mixed by inversion and kept at 37 °C for 1 h, then absorbance at 339 nm was recorded. Net absorbance was calculated by subtracting the background absorbance. A solution containing the same reagents without hydrolysates was used as blank.

6.3.10. Sensory analysis

The sensory profiling was carried out at the Sensory Laboratory of the Special Company for Professional Training and Technological and Commercial Promotion of the Chamber of Commerce of Savona (Albenga, Italy). At least six subjects participated in the descriptive analysis as panelists. The subjects had variable experiences of descriptive analysis. Each sample was prepared as 0.1% and 0.5% solutions in deionized water. Aliquots (20 mL) of each sample, equilibrated at room temperature (20 ± 2 °C), were presented to the panelists in a disposable plastic cup coded with random numbers. The presentation order of the samples was randomised to minimize the presentation order effect. The subjects were previously trained until consensus was reached to evaluate the five basic tastes (sweet, bitter, sour, salty and umami). The

sensory attributes were evaluated using a quantitative descriptive analysis method [Jo & Lee, 2008], based on "sip and spit" procedure. In more detail, the subjects rinsed their mouths with filtered water before tasting each sample. The subjects rated the intensity of stimulus using a 10-point category scale whose limits were labelled as "weak" and "strong", respectively. Each sample was evaluated 2 times in different sessions.

6.3.11. Statistical analysis

Statistical analyses were performed with the Origin Pro 8 software (Origin Lab Inc., Northampton, MA). The data were expressed as mean±SE and evaluated using one-way analysis of variance followed by Tukey's post-hoc test. A level of $p<0.05$ was used as a criterion for statistical significance.

6.4. Preparation of HVPs from Hempseed through Chemical Hydrolysis

6.4.1. Chemical hydrolysis with Acetic Acid

In a flask 50% acetic acid (60 ml) was added to hempseed proteins (100 mg) extracted with Method A (section 6.3.2.). The mixture (pH 2.0) was stirred at 110 °C for 18 h, then allowed to cool to room temperature and freeze-dried. The freeze-dried product was analyzed by reverse-phase HPLC under the following conditions. *Flow rate*: 0.5 ml/min. Detection λ: 226, 254, 280 nm. *Mobile phase*: solvent A, 0.1% TFA in water; solvent B, 0.1% TFA in water/acetonitrile (20/80). Gradient elution from 5% to 100% solvent B:

1. column equilibration 0,3 CV + wash out unbound sample 1 CV (corresponding to 1.3 CV with 5% B)
2. gradient 1: from 5% to 30% B in 1 CV
3. gradient 2: from 30% to 50% B in 3 CV
4. gradient 3: from 50% to 100% B in 1 CV
5. clean after gradient 1: 100% B for 1 CV
6. re-equilibration: 5% B for 2 CV

6.4.2. Chemical hydrolysis with Formic Acid

In a flask 20% formic acid (60 ml) was added to hempseed proteins (100 mg) extracted with Method A (section 6.3.2.). The mixture was stirred at 110 °C for 6 hours, then at room temperature overnight, and finally freeze-dried. The freeze-dried product was analyzed by reverse-phase HPLC and by SDS-PAGE under the conditions described in **6.4.1.** and **6.3.5.2** sections, respectively.

6.4.3. Chemical hydrolysis of defatted hempseed flour with Hydrochloric Acid

Hydrolysis of defatted hempseed flour with hydrochloric acid was performed according to Aaslyng [Aaslyng, 1998]. In a three-necked flask, a solution of 4 M HCl (150 ml) was added to defatted hemp seed flour (3.0 g). The mixture was stirred at 110 °C for 6 hours, then was allowed to cool to room temperature, neutralized with 4 M NaOH and vacuum filtered on a sintered glass filter. The undigested material formed very dark and small clusters. After treatment with active carbon, followed by filtration trough celite, the dark solution became clear and light yellow in color. The product was stored at - 20 °C.

6.4.4. Chemical hydrolysis of hempseed proteins with 6 M HCl for 6 h at 110 °C

In a round bottom flask, a solution of 6 M HCl (150 ml) was added to hempseed proteins (1.5 g). The mixture was stirred at 110 °C for 6 hours, then was allowed to cool to room temperature. Finally it was neutralized with 4 M NaOH, adding Na_2CO_3 as a buffer, at 0 °C up to pH 5.8. The solution was diluted with water (1:20) and freeze-dried. The freeze-dried product was analyzed and purified by RP HPLC.
Analytical RP HPLC was performed under the conditions described in **6.4.1.** section. Preparative RP HPLC was performed under the following conditions. *Flow rate*: 0.5

ml/min. *Detection* λ: 226, 254, 280 nm. *Mobile phase*: solvent A, 0.1% TFA in water; solvent B, 0.1% TFA in water/acetonitrile (20/80). *Gradient elution* from 5% to 100% solvent B:

1. column equilibration 0,3 CV + wash out unbound sample 1 CV (corresponding to 1.3 CV with 5% B)
2. gradient 1: from 5% to 30% B in 2 CV
3. gradient 2: from 30% to 50% B in 6 CV
4. gradient 3: from 50% to 100% B in 1 CV
5. clean after gradient 1: 100% B for 1 CV
6. reequilibration: 5% B for 2 CV

The fractions purified by RP-HPLC were analyzed by ^{1}H-NMR, DOSY and TOCSY (at 500 MHz and 310 K). NMR analysis was performed by ISMAC-CNR of Milan. The major peak was also analyzed by MS-MALDI.

Moreover, the ACE-inhibitory activity was assessed.

6.4.5. Chemical hydrolysis of hempseed proteins with 0.1 M HCl for 48 h at 63 °C

In a round bottom flask, a solution of 0.1 M HCl (100 ml) was added to hempseed proteins (1.11 g). The mixture (pH 4.0) was stirred at 63 °C for 48 hours, then was allowed to cool to room temperature. To remove salts, activated AMBERLITE 402 resin (2.0 g) was added to the mixture. After stirring for 2 hours, the resin was filtered under vacuum and the solution was freeze-dried. A brown amorphous solid (1.0 g) was obtained.

Analytical RP HPLC was performed under the conditions described in **6.4.1.** section. The freeze-dried product was analyzed by ^{1}H-NMR, DOSY and TOCSY (at 500 MHz and 310 K). NMR analysis was performed by ISMAC-CNR of Milan.

6.4.6. Chemical hydrolysis of hempseed proteins 1 M HCl M for 6 h at 110 °C

In a two-necked bottom flask, a solution of 1 M HCl (150 ml) was added to hempseed proteins (1.50 g). The mixture was stirred at 110 °C for 6 hours, then was allowed to cool to room temperature. To remove salts, activated AMBERLITE 402 resin (30.0 g) was added to the mixture. After stirring for 2 hours, the resin was filtered under vacuum and the solution was freeze-dried.

Analytical and preparative RP HPLC were performed under the conditions described in **6.4.1.** section. The freeze-dried product was analyzed by ^{1}H-NMR, DOSY and TOCSY (at 500 MHz and 310 K). NMR analysis was performed by ISMAC-CNR of Milan.

6.4.7. Chemical hydrolysis of hempseed proteins with 1 M HCl for 48 h at 63 °C

In a two-necked bottom flask, a solution of 1 M HCl (100 ml) was added to hempseed proteins (1.00 g). The mixture was stirred at 63 °C for 48 hours, then was allowed to cool to room temperature. To remove salts, activated AMBERLITE 402 resin (30.0 g) was added to the mixture. After stirring for 1 hours, the resin was filtered under vacuum and the solution was freeze-dried. A brown amorphous solid (400 mg) was obtained.

Analytical and preparative RP HPLC were performed under the conditions described in **6.4.1.** section. The freeze-dried product was analyzed by ^{1}H-NMR, DOSY and TOCSY (at 500 MHz and 310 K). NMR analysis was performed by ISMAC-CNR of Milan.

6.4.8. Chemical hydrolysis of hempseed proteins with 3 M HCl for 8 h at 100 °C

In a two-necked bottom flask, a solution of 3 M HCl (200 ml) was added to hempseed proteins (2.00 g). The mixture was stirred at 100 °C for 8 hours, then was allowed to cool to room temperature. To remove salts, activated AMBERLITE 400 resin (15.0 g)

was added to the mixture. After stirring for 3 hours, the resin and insoluble product were filtered under vacuum. The solution was neutralized with 4 M NaOH, adding Na_2CO_3 as a buffer, up to pH 5.8 and freeze-dried.

Analytical and preparative RP HPLC were performed under the conditions described in **6.4.1.** section.

6.4.9. ACE-inhibitory activity assay

The assay was performed by using Hippuryl-Histidyl-Leucine (HHL) as substrate [Cushman & Cheung, 1971] and HPLC DAD for the detection of Hippuric Acid (HA) [Wu *at al.*, 2002]. Some modifications were introduced, as described below. A volume of 100 µl of 2.5 mM HHL in buffer 1 (100 mM tris-HCOOH, 300 mM NaCl pH 8.3) was mixed with 30 µl of "inhibitor" in buffer 1 at different concentrations.

The "inhibitor" is a peptide mixture obtained from the digestion of proteins, *i.e.* TPEs, industrial isolates, or laboratory purified proteins. Usually, at least 6 concentrations were used for each inhibitor, and each solution was tested twice: the highest concentration used in the assays was 1035.9 µg/ml; serially dilutions were performed to obtain the other concentrations (Table 6.2).

Table 6.2.

Conc. Inib (µg/ml)
0.00
28.75
115.02
345.07
690.13
1035.9

HHL solution was daily prepared because, in line with our experience and literature data [Shalaby *et al.*, 2006], it is not very stable. Samples were pre-incubated at 37 °C for 15 min, then 15 µl of ACE solution, corresponding to 3 mU of enzyme in buffer 2 (100 mM tris-HCOOH, 300 nM NaCl, 10 µM $ZnCl_2$, pH 8.3), were added; samples were then incubated for 60 min at 37 °C. The reaction was stopped with 125 µl of 0.1 M

HCl. The aqueous solution was extracted twice with 600 μl of ethyl acetate, and the solvent was evaporated at 95 °C, the residue was then dissolved in 500 μl of buffer 1 and analyzed by HPLC. In our experiments, the direct injection in HPLC did not give optimal results regarding peak shape and baseline for a reliable and accurate quantification. For this reason, we decided to perform the extraction step, using ethyl acetate and a double step of extraction followed by the evaporation of solvent in glass vials. The evaporation conditions greatly influenced the results of the assay: a trace of residual solvent results in abnormally high absorbance values [Lam *et al.*, 2007]. Obviously the sample preparation requires one more step, but the extraction assures good reproducibility in the quantification of the HA chromatographic peak and the absence of interfering peaks due to peptides. Sigmoid curves (Figure 2) fit very well the data points representing the ACE inhibition in function of inhibitor concentration, as pointed out by the correlation coefficient (R^2).

HPLC analyses were performed with a HPLC 1200 Series equipped with an autosampler (Agilent Technologies, Santa Clara, US) with a Lichrospher 100, C18 column (4.6-250 mm, 5 lm; Grace, Italy). Water and acetonitrile were used as solvents with the following gradient: 0 min 5% acetonitrile, 10 min 60% acetonitrile, 12 min 60% acetonitrile, 15 min 5% acetonitrile. Injection volume was 10 μl, wavelength 228 nm, flow 0.5 ml/min. The retention time of hippuric acid (HA) was 4.2 min. The detector response for standard HA was linear in the range 1–100 μg/ml. The relative standard deviation for determination of the 10 μg/ml HA solution was 2.5% (n = 8), very similar to already published data [Wu *et al.*, 2002].

ACE inhibition measurement

The evaluation of ACE inhibition was based on the comparison between the concentrations of HA in the presence or absence of an inhibitor (inhibitor blank). The phenomenon of autolysis of HHL to give HA was evaluated by a reaction blank, i.e. a sample with the higher inhibitor concentration and without the enzyme.

The percentage of ACE inhibition was computed considering the area of HA peak with the following formula:

% ACE inhibition = [(A_{IB} - A_N)/ [(A_{IB} - A_{RB})]x10   *(eq. 6.8)*

188

where A_{IB} is the area of HA in Inhibitor Blank (IB) sample (i.e. sample with enzyme but without inhibitor), A_N is the area of HA in the samples containing different inhibitor amounts and ARB is the area of HA in the reaction blank (RB) sample (i.e. sample without enzyme and with inhibitor in the highest concentration).

The percentages of ACE inhibition were plotted vs. $\log_{10}$ inhibitor concentrations, obtaining a sigmoid curve; IC_{50} was defined as the inhibitor concentration needed to observe a 50% inhibition of the ACE activity. Only when the ACE-inhibitory activity was more than 50%, the IC_{50} value was calculated. The IC_{50} values were obtained independently testing each inhibitor three times.

6.5. Preparation of HVPs from Flaxseed through Enzyme-catalyzed Hydrolysis.

Four Italian cultivars of flax (*Linum usitatissimum* L.) seeds, namely, Solal, Merlin Linoal and Natural, harvested in Cavriana (MN) and Treviglio (BG), were provided by CNR -Institute of Biology and Biotechnology (IBBA) of Milan, Italy, during 2011/2012. A voucher specimen is stored and preserved in our laboratory at Department of Chemistry at University of Milan. Seeds were stored at 4 °C in the dark until use.

6.5.1. Defatted Flaxseed Meal

According to the method described for hemp seeds in section **6.3.1**, defatted flaxseed flour was obtained by stirring with *n*-hexane and milling the flax seeds. Both defatted flaxseed flour and extracted hemp oil were stored at -20 °C until use.

The protein contents of defatted flaxseed flour was determined according to the Kjeldahl method, which was performed by Centro di Ricerca per le Produzioni Foraggere e Lattiero-Casearie (CRA) of Lodi, by measuring the nitrogen content with a CNH analyzer [AOAC, 1980]. The value of 6.25 was used as conversion factor to determine the protein content.

6.5.2. Extraction of Mucilage

Mucilage of defatted flaxseed flour was extracted according to the slightly modified method of Bagnasco et al. (2013). Each cultivar of defatted flaxseed flour was

suspended with distilled water (ratio 1:10 w/v) and kept under shaking for 12 h in a shaker at room temperature. The suspension was centrifuged at 8000 rpm for 30 min to recover both supernatant and the residue. The residue, containing de-mucilaginated and defatted flaxseed flour, was dried in an oven at 50-70 °C for two days. The resulting viscous solutions containing the dissolved polysaccharides was filtered through a sterile gauze and precipitated with ethanol (in ration 1:1.5 v/v) for 1 hour at 4 °C. Mucilage was then recovered by centrifuging at 8000 rpm for 30 min at room temperature. The pellet was dissolved in distilled water and freeze-dried. Both freeze-dried mucilage and dried flaxseed flour were stored at -20 ° C until use.

6.5.3. Enzymatic Hydrolysis

The enzymatic hydrolysis of defatted flaxseed flour was performed in semi-preparative scale according to the method described for hemp seeds in section **6.3.3.**.

Defatted hempseed flour (20 g corresponding to 3.5 g of proteins) was suspended in 100 mM ammonium bicarbonate buffer (final concentration 10% w/v) by adjusting pH to the optimal value for any enzyme, as indicated by manufacturers. Any suspension was preincubated for 20 minutes at the desired temperature. The specific protease was added to the reaction mixture in order to give a final enzyme/substrate ratio (E/S) of 5% w/w (135 μl of Flavourzyme® and 200 mg of Umamizyme® were used, respectively) and the mixture was stirred at 400 rpm.

Hydrolyses were carried out in the above conditions and stopped after 1, 7, 14 and 24 hours by addition of formic acid up to pH 3.5 to inactivate the enzyme. Subsequently the suspensions were sonicated in a water-bath for 10 minutes and centrifuged at 8000 rpm for 30 min at room temperature to recover solubilized proteins and peptides and remove the undigested materials. The supernatants, containing HVPs, were collected, freeze-dried and stored at -20 °C before further analysis. Controls of the proteolysis experiments were obtained by repeating the above procedure without the enzymes.

6.5.4. SDS-PAGE

The SDS-PSGE analysis of flaxseed mucilage was carried out according to the method described for hemp seeds in section **6.3.5.**.

7. EXPERIMENTAL SECTION
PART 2

7.1 General - Synthesis of modified nucleosides

All reagents were purchased from Sigma-Aldrich (Milan, Italy) and/or from VWR International and were used without further purification. All the solvents were of HPLC grade.

Analytical Thin Layer Chromatography TLC was performed on silica gel 60 F_{254} or 60 RP-18 F254s precoated aluminum sheets (0.2 mm layer; Merck, Darmstadt, Germany); components were detected under an UV lamp (λ 254 nm), by spraying with a ceric sulfate/ammonium molybdate solution or with a ninhydrin solution [5% (w/v) ninhydrin in ethanol], followed by heating at about 150 °C. Hybrid compounds were detected by exposing the TLC sheets to iodine vapors.

Puritication Methods: Amberlite XAD-4 was purchased from Supelco (Sigma-Aldrich). Purification of products was accomplished either by flash chromatography (silica gel 60, 40–63 mm, Merck) or by preparative HPLC using an Amersham pharmacia biotech (P900) liquid chromatographer connected to a UV-vis detector; chromatographic conditions were as follows: column, Jupiter RP-18 (4μ, proteo 90 A size: 25x2.12 cm, Phenomenex); flow rate, 0,5 ml/min; detector, λ 226 and 254 nm; mobile phase: A (0,1% TFA (v/v) in water) and B (80% acetonitrile/ 20% water with 0,1% of TFA), gradient elution from 5% to 100% B in 45 min.

NMR Spectroscopy: ^{1}H, ^{13}C and ^{13}P NMR spectra were acquired at 400.13, 100.61 and 161.96 MHz, respectively, on a Bruker Advance 400 spectrometer (Bruker, Karlsruhe, Germany) interfaced with a workstation running a Windows operating system and

equipped with a TOPSPIN software package. ^{1}H and ^{13}C chemical shifts (δ) are given in parts per million (ppm) and are referenced to the solvent signals [δ_H 7.25, δ_C 77.00; δ_H 2.50 and δ_C 39.50 ppm from Tetramethylsilane (TMS) for CDCl$_3$ and DMSO-d_6, respectively]. ^{31}P chemical shifts (ppm) are referred to 85% H$_3$PO$_4$ as the external standard (δ 0.00 ppm). ^{13}C NMR signal multiplicities were based on attached proton test (APT) spectra. ^{1}H signals were assigned with the aid of ^{1}H–^{1}H correlation spectroscopy (^{1}H–^{1}H COSY). ^{13}C NMR signals were assigned on the basis of heteronuclear multiple-quantum correlation (HMQC) and heteronuclear multiple-bond correlation (HMBC) experiments.

Mass Spectrometry: Electrospray ionization mass (ESI-MS) spectra were recorded on a Thermo Finnigan LCQ Advantage spectrometer (Hemel Hempstead, Hertfordshire, UK).

7.2. Synthesis of 1,6-Diamino-*N*-*tert*-butyloxycarbonylhexane (A1)
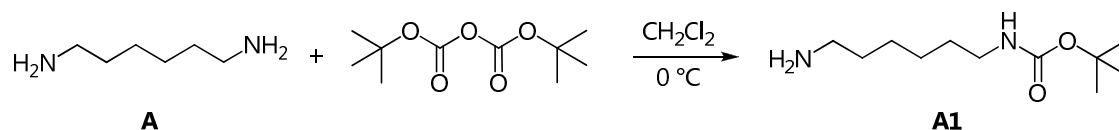
A solution of (Boc)$_2$O (764 mg, 3.5 mmol) in CH$_2$Cl$_2$ (30 ml) was added dropwise over 1 hto a stirred solution of 1,6-diaminohexane **A** (2.034 g, 17.5 mmol) in CH$_2$Cl$_2$ (70 ml) at 0 °C. The mixture was stirred at 0 °C for 2 h, then at room temperature for another 1 h (TLC monitoring, eluent MeOH/30% NH$_3$ 9:1, R$_f$ product = 0.36).

The mixture was filtered trough celite and the filtrate was evaporated under reduced pressure. The colorless oily residue was taken up with AcOEt (80 ml) and washed with brine (20 ml x 5). The aqueous layer was extracted with AcOEt (50 ml). The combined organic layers were dried over Na$_2$SO$_4$ and the solvent was evaporated under reduced pressure to give 1,6-Diamino-*N*-tert-butyloxycarbonylhexane **A1** (725 mg, 3.35 mmol) as a slightly coloured oil.

Yield = 96%

^{1}H NMR (400 MHz, CDCl$_3$):

δ 1.14 (s, 2H, -NH$_2$), 1.26-1.37 (m, 4H, -CH$_2$-), 1.37-1.52 (s + m, 9H + 4H, *t*-Bu + -CH$_2$-), 2.67 (t, 2H; NCH$_2$-), 3.09 (q, 2H, -C(O)NCH$_2$-); 4.60 (bs, 1H, -C(O)NH-).

^{13}C NMR (100 MHz, CDCl$_3$):

δ 26.4 (2C, CH$_2$^{3,4}); 26.5 (CH$_2$^{2}); 28.3 (3C, -COOC(**CH$_3$**)$_3$); 29.9 (CH$_2$^{5}); 33.6 (CH$_2$^{6}); 42.0 (**CH$_2$**^{1}NHCO-); 78.8 (**C**(CH$_3$)$_3$); 155.9 (-**C**OOC(CH$_3$)$_3$).

Mass spectrum

ESI-MS positive mode, *m/z*: 217 [M+H$^+$].

[Pons, 1998]

7.3. Synthesis of 1,4-diamino-*N*-*tert*-buthoxycarbonylbutane (B1)
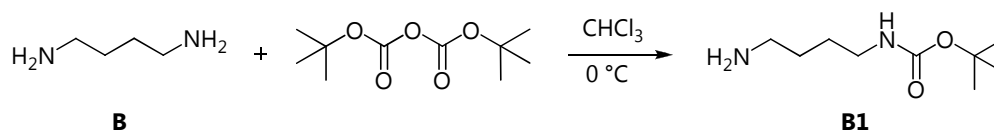
A solution of (Boc)$_2$O (1.59 g, 7.3 mmol) in CHCl$_3$ (15 ml) was added dropwise over 4 h to a stirred solution of 1,4-diaminobutane **B** (3.82 ml, 38.0 mmol) in CHCl$_3$ (30 ml) at 0 °C. The resulting solution was stirred at room temperature overnight monitoring the progress of the reaction by TLC (eluent ammonia-saturated CH$_2$Cl$_2$/MeOH 9:1, R$_f$ product = 0.34).

Then, the resulting slurry mixture was diluted in CHCl$_3$ (30 ml) and washed with 1 N NaHCO$_3$ (30 ml x 2) and brine (30 ml). The organic layer was dried over Na$_2$SO$_4$ and concentrated under reduced pressure to obtain compound **B1** as a clear yellow oil (5.84 g, 31.0 mmol).

Yield: 80%

^{1}H NMR (400 MHz, CDCl$_3$):

δ 4.88 (br s, 1H); 3.12 (m, 2H); 2.72 (m, 2H); 1.49 (m, 4H); 1.45 (s, 9H); 1.18 (m, 2H).

^{13}C NMR (100 MHz, CDCl$_3$):

δ 155.79; 41.54; 40.11; 30.64; 28.14; 27.19.

Mass spectrum

ESI-MS positive mode, *m/z:*189.0 [M+H]$^+$.

[Pons, 1998]

200

7.4. Synthesis of 2',3',5'-Tri-*O*-acetylguanosine (4.2)
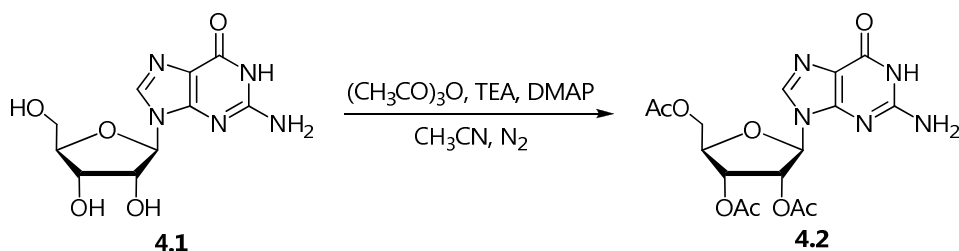
In a three-necked round-bottom flask, to a suspension of guanosine **4.1** (5.0 g, 17.66 mmol) in dry acetonitrile (100 ml) dimethylaminopyridine (DMAP 130 mg, 1.06 mmol) and triethylamine (TEA 8.8 ml, 63.56 mmol) were added under nitrogen atmosphere. The mixture was stirred for some minutes and acetic anhydride (5.8 ml, 61.81 mmol) was added dropwise at 0 °C. Then the mixture was allowed to cool to room temperature under stirring. The reaction progress was monitored the by TLC analysis (eluent CH_2Cl_2/MeOH 9:1, R_f product = 0.45).

After the complete dissolution of **4.1** (about 30 minutes), methanol (150 ml) was added and the solution was evaporated under reduced pressure. The crude yellow oil residue was recrystallizated adding 2-propanol (20 mL). This mixture was stored at 4 °C overnight, filtered and washed with 2-propanol and *n*-hexane to give compound **4.2** (6.8 g, 17.66 mmol) as a white soft solid.

Yield = 94%

^{1}H NMR (400 MHz, DMSO-*d_6*):
δ 2.04 (s, 9H, -COCH$_3$); 4.28 (m, 2H, $CH_2^{5'a/b}$); 4.36 (dd, *J* = 3.7 Hz, 1H, $CH^{4'}$); 5.49 (dd, *J* = 6 Hz, 1H, $CH^{3'}$); 5.78 (dd, *J* = 6 Hz, 1H, $CH^{2'}$); 5.98 (d, *J* = 6 Hz, 1H, $CH^{1'}$); 6.59 (br s, 2H, NH_2); 7.93 (s, 1H, CH^8); 10.85 (br s, 1H, N^1H).

^{13}C NMR (100 MHz, DMSO-*d_6*):
δ 20.09-20.27-20.42 (3 -$C_{acetyl}H_3$) ; 63.02 ($C^{5'}$); 70,29 ($C^{3'}$); 72.07 ($C^{2'}$); 79.51 ($C^{4'}$); 84.53 ($C^{1'}$); 116.85 (C^5); 135.59 (C^8); 151.05 (C^4); 153.83 (C^2); 156.60 (C^6); 169.6-169.8-170.4 (3 -CO_{acetyl}).

Mass spectrum

ESI-MS positive mode, *m/z***:** 410.1 [M+H$^+$]; 432.2 [M+Na$^+$]; 841.1 [2M+Na$^+$]; 1249.8 [3M+Na$^+$]; 1659.5 [4M+Na$^+$].

[Bridson, 1977]

7.5. Synthesis of 2',3',5'-*O*-triacetyl-6-chloroguanosine (4.3)
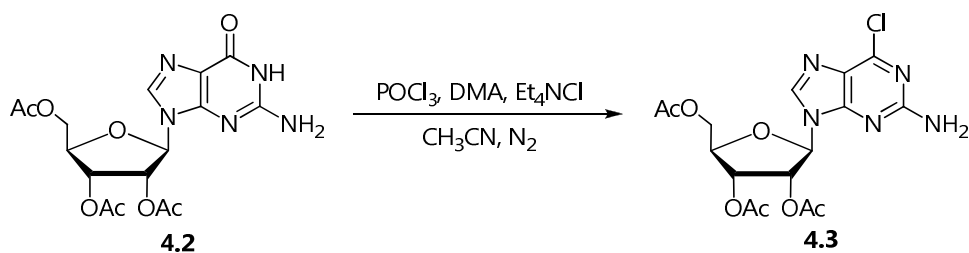
In an anhydrous two-necked round-bottom flask to a mixture of pre-dried 2',3',5'-tri-*O*-acetylguanosine **4.2** (10.233 g, 25 mmol) and Et_4NCl (8.288 g, 50 mmol, pre-dried in vacuo at 80°C for one day over P_2O_5), acetonitrile (50 mL, distilled from P_2O_5 under an argon atmosphere) and *N,N*-dimethylaniline (DMA 3.16 ml, 25 mmol, pre-distilled from CaH_2 under a nitrogen atmophere) were added under a stream of dry nitrogen. The solution was stirred for 2 min and phosphoryl chloride (13.7 ml, 15 mmol) were added dropwise at room temperature. The flask was placed in an oil bath preheated to 100 °C and the solution was stirred at reflux for 35 min until TLC showed the complete disappearance of **4.2** (eluent CH_2Cl_2/MeOH 9.5:0.5, R_f product = 0.45).

Volatiles were evaporated immediately under reduced pressure. The resulting yellow foam was dissolved in $CHCl_3$ (150 ml) and stirred vigorously with crushed ice for 15 min. The layers were separated and the aqueous phase was extracted with $CHCl_3$ (4 x 50 ml). The combined organic phase was washed with cold water (3 x 60ml), 5% $NaHCO_3$/H_2O up to pH 7 (3 x 50 ml) and brine (2 x 50 ml), dried over Na_2SO_4, filtered, and concentrated to 1/2 of the starting volume. 2-Propanol (60 ml) was added and the solution was slowly concentrated under reduced pressure to 40 ml. The mixture was stored at 4 °C overnight. The crystalline product was filtered and washed with 2-propanol to give crude **4.3** (8.50 g, 19.9 mmol, 79%). This product was recrystallized with 2-propanol to give purified **4.3** (8.10 g, 19 mmol) as a white crystalline solid.

Yield = 76 %

^{1}H NMR (400 MHz, CDCl$_3$):

δ 2.11-2.12-2.17 (3s, 9H, -COCH$_3$); 4.36-4.51 (m, 2H, CH$_2$$^{5'a/b}$); 4.36 (m, 1H, CH$^{4'}$); 5.25 (br s, 2H, NH$_2$); 5.77 (dd, J = 5.00 Hz, 1H, CH$^{3'}$); 5.98 (dd, J = 5.2 Hz, 1H, CH$^{2'}$); 6.03 (d, J = 5.2 Hz, 1H, CH$^{1'}$); 7.90 (s, 1H, CH^8).

^{13}C NMR (100 MHz, CDCl$_3$):

δ 20.38-20.49-20.66 (3 -C$_{acetyl}$H$_3$) ; 62.91 (C$^{5'}$); 70,53 (C$^{3'}$); 72.78 (C$^{2'}$); 80.06 (C$^{4'}$); 86.66 (C$^{1'}$); 125.88 (C^5); 140.67 (C^8); 151.95 (C^6); 153.11 (C^4); 159.12 (C^2); 169.29-169.51-170.42 (3 -CO$_{acetyl}$).

Mass spectrum

ESI-MS positive mode, *m/z:* 428.2 [M+H]$^+$; 450.4 [M+Na]$^+$; 259.2 [M$^+$-nitrogen base].

[Robins *et al.*, 1981]

7.6. Synthesis of 2-iodo-6-chloro-9-(2',3',5'-tri-*O*-acetyl-*β*-d-ribofuranosyl)-purine (4.4)

In an anhydrous three-necked flask to a suspension of 6-chloro-2',3',5'-*O*-triacetylguanosine **4.3** (855 mg, 2 mmol) in dried acetonitrile (2.5 ml, distilled from P_2O_5 under an argon atmosphere) CH_2I_2(0.8 ml, 10 mmol) was added under a stream of dry nitrogen. The solution was stirred for 2 min and *t*-butyl nitrite (0.36 ml, 3 mmol) were added dropwise at room temperature. The flask was placed in an oil bath preheated to 100 °C and the solution was stirred at reflux for 20 min, until TLC showed the complete disappearance of **4.3** (eluent AcOEt/*n*-hexane 6.5:3.5, R_f product = 0.4).

Volatiles were evaporated immediately under reduced pressure. The resulting deep red residue was dissolved in AcOEt (50 ml) and stirred vigorously with an aqueous saturated NaS_2O_3 solution (50 ml) for some minutes. The layers were separated and the aqueous phase was extracted with AcOEt (3 x 50 ml). The combined organic phase was washed with brine (4 x 50ml), dried over Na_2SO_4, filtered, and concentrated under reduced pressure. The residue was purified by flash chromatography (eluent AcOEt/*n*-hexane = 6.5:3.5). The yellow crude was taken up in AcOEt (8 ml) and precipitated with cold *n*-hexane to give 2-iodo-6-chloro-9-(2',3',5'-tri-*O*-acetyl-*β*-D-ribofuranosyl)-purine **4.4** as a white solid (625 mg, 1.16 mmol).

Yield = 58 %

^{1}H NMR (400 MHz, CDCl$_3$):

δ 2.13 (s, 3H, 3'-COCH$_3$); 2.16 (s, 3H, 5'-COCH$_3$); 2.20 (s, 3H, 2'-COCH$_3$); 4.40 (m, 2H, H$^{5'}$); 4.49 (m, 1H, H$^{4'}$); 5.61 (dd, *J* = 5.6 Hz, 1H, H$^{3'}$); 5.80 (dd, *J* = 5.6 Hz, 1H, H$^{2'}$); 6.22 (d, *J* = 5.2 Hz, 1H, H$^{1'}$); 8.22 (s, 1H, H^8).

¹³C NMR (100 MHz, CDCl₃):

δ 20.38 (2'-$C_{acetyl}H_3$); 20.52 (5'-$C_{acetyl}H_3$); 20.82 (3'-$C_{acetyl}H_3$); 62.92 ($C^{5'}$); 70.61($C^{3'}$); 73.38 ($C^{2'}$); 80.91 ($C^{4'}$); 86.69 ($C^{1'}$); 116.97 (C^2); 132.27 (C^5); 143.07 (C^8); 151.06 (C^6); 151.96 (C^4); 169.34 (2'-CO_{acetyl}); 169.50 (3'-CO_{acetyl}); 170.15 (5'-CO_{acetyl}).

Mass spectrum

ESI-MS positive mode, *m/z***:** 561.2, 562.2 [M+Na]⁺ (relative peak height ratio = 3:1)

[Ohno *et al.*, 2004]

7.7. Synthesis of 2-iodo-6-methoxy-9-(*β*-D-ribofuranosyl)-purine (4.5a)

In a two-necked, round-bottom flask dry methanol (24 ml) was charged. Under a stream of dry nitrogen, sodium (214 mg, 9.3 mmol) was added slowly in pieces. After the complete dissolution of the metal, the solution was allowed to cool to room temperature and 2-iodo-6-chloro-9-(2',3',5'-tri-*O*-acetyl-*β*-D-ribofuranosyl)-purine **4.4** (500 mg, 0.93 mmol) was added. The mixture was stirred for 20 min at room temperature until TLC showed the complete disappearance of **4.4** (eluent CH_2Cl_2/MeOH 6:1, R_f product = 0.5).

The reaction was quenched with NH_4Cl (498 mg, 9.3 mmol) and the resulting mixture was stirred for some minutes. After vacuum filtration the solution was mildly concentrated under reduced pressure to obtain a white solid, which was dissolved in distilled water and adsorbed on Amberlite XAD-4 resin 20-50 Mesh (1 g of product: 30 g of resin) at room temperature over night. The mixture was vacuum filtered, and the product was desorbed from the resin with methanol. Finally methanol was evaporated under reduced pressure to give 2-iodo-6-methoxy-9-(*β*-D-ribofuranosyl)-purine **4.5a** as a white solid (374 mg, 0.92 mmol).

Yield = 99 %

^{1}H NMR (400 MHz, CD$_3$OD):

δ 3.79 (dd, J_1 = 12.3, J_2 = 3.4 Hz, 1H, CH$^{5'}$); 3.91 (dd, J_1 = 12.3, J_2 = 3.0 Hz, 1H, CH$^{5'}$); 4.14-4.20 (m, 1H, CH$^{4'}$); 4.18 (s, 3H, -OCH$_3$); 4.36 (dd, J_1 = 4.9, J_2 = 3.9 Hz, 1H, CH$^{3'}$); 4.68 (dd, J_1 = 5.3 Hz, J_2 = 5.3 Hz, 1H, CH$^{2'}$); 6.04 (d, J = 5.5 Hz, 1H, CH$^{1'}$); 8.48 (s, 1H, CH^8).

¹³C NMR (100 MHz, CD₃OD):

δ 54.42 (-OCH₃); 61.53 (C⁵'); 70.67 (C³'); 74.36 (C²'); 86.15 (C⁴'); 89.41 (C¹'); 117.04 (C²); 121.23 (C⁵); 142.18 (C⁸); 151.85 (C⁴); 159.61 (C⁶).

Mass spectrum

ESI-MS positive mode, *m/z*: 431.4 [M+Na]⁺.

ESI-MS negative mode, *m/z*: 275.7 [M-ribose moiety]; 815.7 [2M-H⁺]

[Robins *et al.*, 1981]

7.8. Synthesis of 2-iodo-6-benzyloxy-9-(β-D-ribofuranosyl)-purine (4.5b)

4.4 → **4.5b** Bn = CH₂Ph

In a two-necked, round-bottom flask dry benzyl alcohol (4 mL) was charged. Under a stream of dry nitrogen, sodium (184 mg, 4 mmol) was added slowly in pieces. After the complete dissolution of the metal, the solution was allowed to cool to room temperature. The obtained solution was then added under stirring to a cooled (0 °C) mixture of 2-iodo-6-chloro-9-(2',3',5'-tri-*O* -acetyl-*β*-D-ribofuranosyl)-purine **4.4** (1.077 g, 2.00 mmol) in dry DMF (8.5 ml), under an argon atmosphere. The mixture was stirred at 0 °C monitoring the progress of the reaction by TLC analysis (eluent CH_2Cl_2/MeOH 9.5:0.5, R_f product = 0.32).

After 40 minutes the reaction was quenched with NH_4Cl (498 mg, 6 mmol) and was stirred for 10 minutes. The resulting mixture was diluited with water (10 ml) and extracted with ethyl acetate (4 x 10 ml). The combined organic phase were washed with brine (15 ml), dried on sodium sulfate, and concentrated under reduced pressure. The residue was purified by flash chromatography (CH_2Cl_2/MeOH 9.5:0.5) to give 2-iodo-6-benzyloxy-9-(*β*-D-ribofuranosyl)-purine **4.5b** as a white crystalline solid(720 mg, 1.49 mmol).

Yield = 75%

¹H NMR (400 MHz, CD₃OD):

δ 3.78 (dd, J_1 = 12.3, J_2 = 3.4 Hz, 1H, CH⁵'); 3.90 (dd, J_1 = 12.3, J_2 = 3.0 Hz, 1H, CH⁵'); 4.16 (dd, J_1 = 6.7, J_2 = 3.3 Hz, 1H, CH⁴'); 4.35 (dd, J_1 = 5.0, J_2 = 3.7 Hz, 1H, CH³'); 4.67 (dd, J_1 = 5.3 Hz, J_2 = 5.3 Hz,1H, CH²'); 5.63 (s, 2H, -CH₂Ph); 6.04 (d, J = 5.5 Hz, 1H, CH¹'); 7.38-7.59 (m, 5H); 8.48 (s, 1H, CH⁸).

¹³C NMR (100 MHz, CD₃OD):

δ 62.16 ($C^{5'}$); 70.08 (**C**H$_2$Ph); 71.31 ($C^{3'}$); 75.04 ($C^{2'}$); 86.79 ($C^{4'}$); 90.08 ($C^{1'}$); 117.49 (C^2); 121.92 (C^5); 128.20-128.31-128.60-128.81-129.15-136.26 (-C$_6$H$_5$); 142.18 (C^8); 152.75 (C^4); 159.61 (C^6).

Mass spectrum

ESI-MS positive mode, *m/z:* 507.4 [M+Na]$^+$; 991.3 [2M+Na]$^+$, 375 [M-ribofuranosyl moiety]$^+$.

[Casu *et al.*, 2012]

7.9. Synthesis of 2-iodo-6-methoxy-9-(β-D-2',3'-O-isopropyliden)-purine (4.7a)

To a suspension of 2-iodo-6-methoxy-9-(β-D-ribofuranosyl)-purine **4.5a** (1.22 g, 3 mmol) in acetone (30 ml), p-toluensulphonic acid (285 mg, 1.5 mmol) and 2,2-dimethoxypronane (4.00 ml, 30 mmol) were added, under an argon atmosphere. The mixture was stirred at room temperature until TLC showed the complete disappearance of **4.5a** (eluent AcOEt$_2$/n-hexane = 7:3). After 6 h n-hexane was added in order to obtain a white precipitate. The mixture was stored at 4 °C overnight and filtered. Compound **4.7a** was obtained as a white solid (1.062 g, 2.37 mmol).

Yield: 79%

^{1}H NMR (400 MHz, DMSO-d_6):

δ 1.35 (s, 3H, C(CH$_3$)); 1.56 (s, 3H, C(CH$_3$)); 3.54 (td, J_1 = 5.2 Hz, J_2 = 1.4 Hz, 2H, CH$_2$[5'a/b]); 4.09 (s, 3H, -OCH$_3$); 4.24 (dd, J_1 = 7.5 Hz, J_2 = 4.8 Hz, 1H, CH[4']); 4.96 (dd, J_1 = 6.1 Hz, J_2 = 2.7 Hz, 1H, CH[3']); 5.06(t, J = 5.3 Hz, 1H, -OH[5']); 5.33 (dd, J_1 = 6.1 Hz, J_2 = 2.5 Hz, 1H, CH[2']); 6.17 (d, J = 2.4 Hz, 1H, CH[1']); 8.52 (s, 1H, CH[8]).

^{13}C NMR (100 MHz, DMSO-d_6):

δ 25.69 (C(**CH$_3$**)$_2$); 27.48 (C(**CH$_3$**)$_2$); 55.30 (-OCH$_3$); 61.90 (C[5']); 81.77 (C[3']); 84.14 (C[2']); 87.68 (C[4']); 90.06 (C[1']); 113.58 (**C**(CH$_3$)$_2$); 118.97 (C[2]); 121.51 (C[5]); 142.68 (C[8]); 152.65 (C[4]); 159.92 (C[6]).

Mass spectrum

ESI-MS positive mode, *m/z***:** 277.2 [M$^+$-nitrogen base]; 449.1 [M+H$^+$]; 471.2 [M+Na$^+$].

7.10. Synthesis of 2-iodo-6-benzyloxy-9-(β-ᴅ-2',3'-*O*-isopropyliden)-purine (4.7b)

To a suspension of 2-iodo-6-benzyloxy-9-(β-D-ribofuranosyl)-purine **4.5b** (660 mg, 1.36 mmol) in acetone (15 ml), *p*-toluensulphonic acid (258 mg, 1.36 mmol) and 2,2-dimethoxypronane (1.67 ml, 13.60 mmol) were added, under an argon atmosphere. The mixture was stirred at room temperature until complete dissolution of **4.5b** (about 30 minutes) monitoring the reaction progress by TLC (CH_2Cl_2/MeOH 9.6:0.4, R_f product = 0.4). The solvent was evaporated under reduced pressure. The yellow foam residue was taken up in ethyl acetate (10 ml), washed with $NaHCO_3$ (2 x 5ml) and brine (5 ml). The organic phase was dried on Na_2SO_4, concentrated under reduced pressure to 1/3 of the starting volume and *n*-hexane (1 ml) was added in order to obtain compound **4.7b** as a white foam solid (510 mg, 1.36 mmol).

Yield: 100%

^{1}H NMR (400 MHz, CDCl$_3$):

δ 1.40 (s, 3H, CH$_3$);1.66 (s, 3H, CH$_3$);3.84 (dd, J_1 = 12.8, J_2 = 2.0 Hz, 1H, CH$^{5'}$); 4.02 (dd, J_1 = 12.8, J_2 = 1.6 Hz, 1H, CH$^{5'}$); 4.54 (d, J = 1.4 Hz, 1H, CH$^{4'}$); 5.14 (dd, J_1 = 6.0 Hz, J_2 = 1.3 Hz, 1H, CH$^{3'}$); 5.17-5.22 (m, 1H, CH$^{2'}$); 5.66 (d, J = 2.0 Hz, 2H, -**CH$_2$**Ph); 5.86 (d, J = 4.9 Hz, 1H, CH$^{1'}$); 7.33-7.58 (m, 5H, -C$_6$H$_5$); 7.90 (s, 1H, CH^8).

^{13}C NMR (100 MHz, CDCl$_3$):

δ 25.91-28.29 (2 –C(**CH$_3$**)$_2$); 64.03 (C$^{5'}$); 70.53 (**CH$_2$**Ph); 82.18 (C$^{3'}$); 83.45 (C$^{2'}$); 86.58 (C$^{4'}$); 94.63 (C$^{1'}$); 115.00 (-**C**(CH$_3$)$_2$); 117.85 (C^2); 123.79 (C^5); 129.20-129.28-129.75-135.71 (-C$_6$H$_5$); 142.52 (C^8); 152.16 (C^4); 160.30 (C^6).

Mass spectrum

ESI-MS positive mode, *m/z***:** 547.2 [M+Na]⁺; 1070.9 [2M+Na]⁺.

7.11. Synthesis of 2-(1,6-diaminohexane)-6-methoxy-9-(*β*-D-2',3'-*O*-isopropyliden)-purine (4.8a)

To a solution of 2-iodo-6-methoxy-9-(*β*-d-2',3'-*O*-isopropyliden)-purine **4.7a** (224 mg, 0.5 mmol) in DMF (2 ml), 1,6-diaminohexane (291 mg, 2.5 mmol) dissolved in DMF (1.0 ml) was added under an argon atmosphere. The reaction mixture was stirred at 70 °C until TLC showed the complete disappearance of **4.7a** (eluent CH_2Cl_2/MeOH 9:1). After 17 h the solution was allowed to cool to room temperature and AcOEt (5 ml) was added. The mixture was washed with distilled water (3 x 3ml),an aqueous saturated NaS_2O_3 solution (4 ml) and brine (3 ml), dried over Na_2SO_4, filtered, and concentrated under reduced pressure. The residue was purified by flash chromatography (eluent CH_2Cl_2/MeOH 9.5:0.5) to give 2-(1,6-diaminohexane)-6-methoxy-9-(*β*-D-2',3'-*O*-isopropyliden)-purine **4.8a** as a yellow oil (30 mg, 0.06 mmol).

Yield = 14%

^{1}H NMR (400 MHz, CD$_3$OD):

δ 1.43 (s, 3H, C(CH$_3$)); 1.45-1.54 (m, 4H, CH$_2$^{12,13}); 1.58 (dd, J_1 = 13.7, J_2 = 6.9 Hz, 2H, CH$_2$^{14}); 1.64 (s, 3H, C(CH$_3$)); 1.73 (dd, J_1 = 14.0 Hz, J_2 = 6.9 Hz, 2H, CH$_2$^{11}); 3.26 (t, J = 7.0 Hz, 2H, CH$_2$^{15}-NH$_2$); 3.57 (t, J = 6.5 Hz, 2H, CH$_2$^{10}); 3.75 (qd, J_1 = 11.6 Hz, J_2 = 5.2 Hz, 2H, CH$_2$$^{5'a/b}$); 4.06 (s, 3H, -OCH$_3$); 4.30 (dd, J_1 = 8.0 Hz, J_2 = 5.0 Hz, 1H, CH$^{4'}$); 5.11 (dd, J_1 = 6.1 Hz, J_2 = 2.9 Hz, 1H, CH$^{3'}$);5.58 (dd, J_1 = 6.2 Hz, J_2 = 2.4 Hz, 1H, CH$^{2'}$); 6.10 (d, J = 2.4 Hz, 1H, CH$^{1'}$); 7.88 (s, 1H, CH^8).
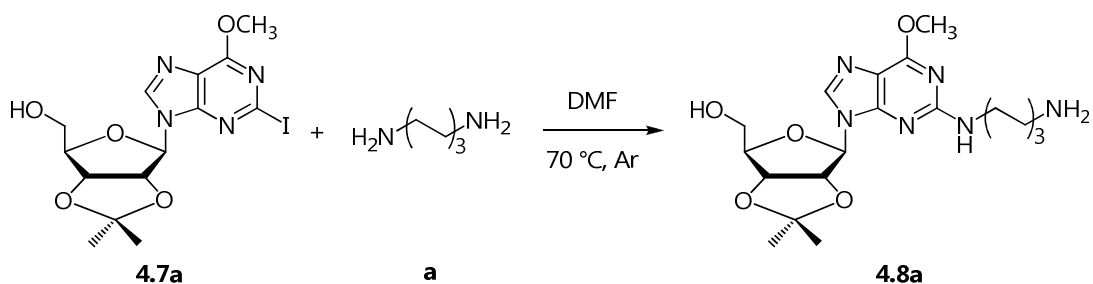
¹³C NMR (100 MHz, CH₃OD):

δ24.17 (C(**CH**$_3$)); 26.15 (C(**CH**$_3$));26.25-26.26 (C^{12,13}); 29.10 (C^{11}); 30.71 (C^{14}); 37.51 (CH$_2$^{15}); 39.72 (C^{10}); 52.61 (-OCH$_3$); 62.12 (CH$_2$$^{5'a/b}$); 81.66 (CH$_2$$^{3'}$); 83.69 (CH$_2$$^{2'}$); 87.03 (CH$_2$$^{4'}$); 90.51 (CH$_2$$^{1'}$); 113.71 (**C**(CH$_3$)$_2$); 113.72 (C^5); 138.54 (C^8); 152.93 (C^4); 159.59 (C^2); 161.04 (C^6).

Mass spectrum

ESI-MS positive mode, *m/z***:** 437.2 [M+H$^+$]; 459.4 [M+Na$^+$]; 895.5 [2M+Na$^+$].

[Bressi*et al.*, 2000].

7.12. Synthesis of 2-(1,6-diamino-*N*-*tert*-butyloxycarbonylhexane)-6-methoxy-9-(*β*-D-2',3'-*O*-isopropyliden)-purine (4.8b)

To a solution of 2-(1,6-diaminohexane)-6-methoxy-9-(β-D-2',3'-O-isopropyliden)-purine **4.7a** (224 mg, 0.5 mmol) in DMF (1 ml), 1,6-diamino-N-tert-butyloxycarbonylhexane **A1** (216 mg, 1mmol) dissolved in DMF (1.0 ml) and triethylamine (TEA, 0.139 ml, 1 mmol) were added under an argon atmosphere.The reaction mixture was stirred at 80 °C monitoring the progress by TLC analysis (eluent CH_2Cl_2/MeOH 9:1, R_f product = 0.5).

After 36 h the solution was allowed to cool to room temperature and AcOEt (5 ml) was added. The mixture was washed with 0.5 M HCl (3 x 2 ml), distilled water (1 x 3ml),an aqueous saturated NaS_2O_3 solution (3 ml) and brine (3 x 3 ml), dried over Na_2SO_4, filtered, and concentrated under reduced pressure. The orange oil residue (205 mg) was purified by preparative TLC (eluent CH_2Cl_2/MeOH 9.5:0.5) to give the desired product **4.8b** as a yellow oil (41 mg, 0.08 mmol).

Yield = 16%

^{1}H NMR (400 MHz, DMSO-*d_6*):
δ 1.20-1.42 (m, 4H, $CH_2^{12,13}$); 1.49-1.60 (m, 4H, $CH_2^{11,14}$);1.32 (s, 3H, $C(CH_3)_2$); 1.36 (s, 9H, -$OC(CH_3)_3$); 1.53 (s, 3H, $C(CH_3)_2$);2.89 (dt, 2H, CH_2^{15}); 3.26 (m, 2H, CH_2^{10}); 3.50 (m, 2H, $CH_2^{5'}$); 3.97 (s, 3H, -OCH_3); 4.13 (m, 1H, $CH^{4'}$);4.96-5.01 (m, 2H, $CH^{3'}$, N^2H); 5.39 (m, 1H, $CH^{2'}$); 6.06 (m, 2H, $CH^{1'}$); 6.75 (s, 1H, OH); 7.08 (br s, 1H, -NHBoc); 8.04 (s, 1H, CH^8).

¹³C NMR (100 MHz, DMSO-*d₆*):

δ 26.23 (-C(**CH₃**)₂); 27.28-27.46 (CH₂^{12,13}); 28.11 (-COOC(**CH₃**)₃); 29.37 (-C(**CH₃**)₂); 30.09 (CH₂^{14}); 30.65 (CH₂^{11}); 40.00 (CH₂^{15}); 42.27 (CH₂^{10});54.23 (-OCH₃); 62.72 (C$^{5'}$); 78.40 (**C**(CH₃)₃); 82.51 (C$^{3'}$); 84.23 (C$^{2'}$); 87.84 (C$^{4'}$); 89.81 (C$^{1'}$);114.05 (**C**(CH₃)₂); 114.96 (C^5);139.83 (C^8); 154.36 (C^4); 156.69 (-**C**OOC(CH₃)₃); 159.95 (C^2); 161.70 (C^6).

Mass spectrum

ESI-MS positive mode, *m/z***:** 459.4 [M$^+$–Boc+Na$^+$]; 559.3 [M+Na$^+$]; 1095.1 [2M+Na$^+$].

[Bressi *et al.*, 2000]

7.13. Synthesis of 2-iodo-6-benzyloxy-9-(*β*-D-5'-*tert*butyldimethylsilyl-2',3'-*O*-isopropyliden)-purine (4.9)

To a solution of 2-iodo-6-benzyloxy-9-(*β*-D-2',3'-*O*-isopropyliden)-purine **4.7b** (721 mg, 1.38 mmol) in DMF (2.5 mL)at room temperature under an argon atmosphere, imidazole (206 mg, 3.31 mmol) and *tert*-butyldimethylsilylchloride (250 mg, 1.66 mmol) were added. The reaction mixture was stirred until TLC showed the complete disappearance of **4.7b** (eluent AcOEt/*n*-hexane = 3:7, R_f product = 0.37).

After 1 h AcOEt (20 ml) was added and the solution was washed with 0.5 M HCl (2 x 10 ml), water (2 x 10 ml) and brine (10 ml). The organic phase was dried on Na_2SO_4 and concentrated at reduced pressure. The residue was purified by flash chromatography (AcOEt/*n*-hexane = 3:7) to afford 2-iodo-6-benzyloxy-9-(*β*-D-5'-*tert*-butyldimethylsilyl-2',3'-*O*-isopropyliden)-purine **4.9** as a white foam solid (869 mg, 1.36 mmol).

Yield: 98%

^{1}H NMR (400 MHz, CDCl$_3$):

δ 0.11 (s, 6H, Si(CH$_3$)$_2$); 0.90 (s, 9H, -C(CH$_3$) $_3$); 1.41 (s, 3H, -C(CH$_3$) $_2$); 1.65 (s, 3H, -C(CH$_3$) $_2$);3.81 (dd, J_1 = 11.2, J_2 = 4.3 Hz, 1H, CH$^{5'}$); 3.90 (dd, J_1 = 11.2, J_2 = 3.8 Hz, 1H, CH$^{5'}$); 4.39 (dd, J_1 = 6.9, J_2 = 3.8 Hz, 1H, CH$^{4'}$); 4.97 (dd, J_1 = 6.1 Hz, J_2 = 2.8 Hz, 1H, CH$^{3'}$); 5.14 (dd, J_1 = 6.1 Hz, J_2 = 2.6 Hz, 1H, CH$^{2'}$); 5.64 (s, 2H, -**CH$_2$**Ph); 6.19 (d, J = 2.6 Hz, 1H, CH$^{1'}$); 7.31-7.65 (m, 5H, -C$_6$H$_5$); 8.10 (s, 1H, CH^8).

¹³C NMR (100 MHz, CDCl₃):

δ -5.41 (Si(CH₃)₂); -5.32 (Si(CH₃)₂);18.42 (Si**C**(CH₃)₃); 25.49 (C(**C**H₃)₂); 25.95 (C(**C**H₃)₃); 27.32 (C(**C**H3)₂); 63.52 (C⁵'); 69.52 (**C**H₂Ph); 81.27 (C³'); 84.86 (C²'); 87.28 (C⁴'); 90.64 (C¹'); 114.33 (-**C**(CH₃)₂); 117.35 (C²); 121.95 (C⁵); 128.45-129.01-135.44 (-C₆H₅); 140.92 (C⁸); 152.21 (C⁴); 159.32 (C⁶).

Mass spectrum

ESI-MS positive mode, *m/z*: 639.5 [M+H]⁺; 661.5 [M+Na]⁺; 662.5 [M+H+Na]⁺; 663.6 [M+2H+Na]⁺; 664 [M+3H+Na]⁺; 1299.2 [2M+Na]⁺; 1300.3 [2M+H+Na]⁺; 1301.4 [2M+2H+Na]⁺; 1302.4[2M+3H+Na]⁺.

7.14. Synthesis of 2-(1,6-diaminohexane)-6-methoxy-9-(β-D-2',3'-O-isopropyliden)-purine (4.10)

4.9 → **4.10**

To a solution of 2-iodo-6-benzyloxy-9-(*β*-D-5'-*tert*butyldimethylsilyl-2',3'-*O*-isopropyliden)-purine **4.9** (255 mg, 0.43 mmol) in 2-ethoxyethanol (2.5 ml), 1,6-diaminohexane (139 mg, 1.2 mmol) was added under an argon atmosphere. The reaction mixture was stirred at 80 °C until TLC showed the complete disappearance of **4.9** (eluent ammonia-saturated CH_2Cl_2/MeOH 9.5:0.5 R_f product = 0.55).

After 17 h the solution was allowed to cool to room temperature and concentrated under reduced pressure. The residue was purified by flash chromatography (eluent ammonia-saturated CH_2Cl_2/MeOH 9.5:0.5) to give the desidered product **4.10** (67 mg, 0.108 mmol) as a yellow oil.

Yield = 25%

^{1}H NMR (400 MHz, CDCl$_3$):

δ 0.09 (s, 6H, Si(CH$_3$)$_2$); 0.88 (s, 9H, -C(CH$_3$)$_3$); 1.34-1.54 (m, 4H, CH$_2^{12,13}$); 1.54-1.80 (m, 4H, CH$_2^{11,14}$); 1.41 (s, 3H, C(CH$_3$)$_2$); 1.64 (s, 3H, C(CH$_3$)$_2$); 2.72 (t, *J* = 6.8 Hz, 2H, CH$_2^{15}$); 3.42 (dt, *J$_1$* = 12.7, *J$_2$*= 6.5 Hz 2H, CH$_2^{10}$); 3.73-3.83 (m, 2H, CH$^{5'}$); 4.33 (dd, *J$_1$*= 7.7, *J$_2$*= 4.5 Hz 1H, CH$^{4'}$); 4.94-5.03 (m, 1H, CH$^{3'}$); 5.30 (d, *J* =2.7 Hz, 1H, CH$^{2'}$); 5.57 (s, 2H, -CH$_2$Ph); 6.07 (d, *J* = 1.9 Hz, 1H, CH$^{1'}$); 7.30-7.56 (m, 5H, -C$_6$H$_5$); 7.76 (s, 1H, CH^8).

^{13}C NMR (100 MHz, CDCl$_3$):

δ -4.75 (Si(CH$_3$)$_2$); 1.67 (Si(CH$_3$)$_2$); 19.03 (Si**C**(CH$_3$)$_3$); 26.14 (C(**CH$_3$**)$_2$); 26.57 (C(**CH$_3$**)$_3$); 27.39-27.64 (CH$_2^{12,13}$); 27.92 (-**C**(CH$_3$)$_2$); 30.36 (CH$_2^{14}$); 34.06 (CH$_2^{11)}$;

42.65 (CH$_2^{15}$); 42.75 (CH$_2^{10}$); 64.15 (C$^{5'}$); 68.40 (**C**H$_2$Ph); 82.11 (C$^{3'}$); 85.03 (C$^{2'}$); 87.61 (C$^{4'}$); 90.71 (C$^{1'}$); 114.53 (**C**(CH$_3$)$_2$); 115.99 (C^5); 128.52-128.80-128.99-129.19-129.39-137.39 (-C$_6$H$_5$); 138.30 (C^8); 154.24 (C^4); 159.75 (C^2); 161.39 (C^6).

Mass spectrum

ESI-MS positive mode, *m/z***:** 627.6 [M+H$^+$]; 649.5 [M+Na$^+$]; 1253.4 [2M+H$^+$]; 1275.5 [2M+H$^+$Na$^+$]

[Bressi, 2000].

7.15. Synthesis of compound 4.11

To a solution of product **4.10** (118 mg, 0.19 mmol) in AcOEt (1.5 ml), Z-Glu-*O*-tBu-γOH (64 mg, 0.19 mmol) and DCC (39 mg, 0.19 mmol) were added under an argon atmosphere.The mixture was stirred at room temperature overnight monitoring the progress of the reaction by TLC analysis (eluent ammonia-saturated CH_2Cl_2/MeOH 9.6:0.4, R_f product = 0.32).

The mixture was filtered under vacuumand concentrated under reduced pressure.Finally, the residue was purified by flash chromatography (eluent AcOEt/*n*-hexane = 9.6:0.4) to give the desidered product **4.11** (67 mg, 0.108 mmol) as a yellow oil.

Yield = 50%

^{1}H NMR (400 MHz, CDCl$_3$):

δ 0.02 (s, 3H, Si(CH$_3$)); 0.03 (s, 3H, Si(CH$_3$)); 0.09 (s, 9H, SiC(CH$_3$)$_3$); 1.01-1.22 (m, 2H, CH$_2$^{13}); 1.30-1.42 (m, 2H, CH$_2$^{12});1.40 (s, 3H, C(CH$_3$)$_2$); 1.46 (OC(CH$_3$)$_3$); 1.49-1.56 (m, 2H, CH$_2$^{14}); 1.63 (s, 3H, C(CH$_3$)$_2$); 1.70 (dt, J_1 = 13.5 Hz, J_2 4.04 = Hz, 2H, CH$_2$^{11}); 1.88-1.99 (m, 2H, CH$_2$^{17}); 2.11-2.30 (m, 2H, CH$_2$^{16}); 3.24 (dd, J_1 = 11.85 Hz, J_2 = 5.8 Hz, 2H, CH$_2$^{15});3.36-3.45 (m, 2H, CH$_2$^{10}); 3.79 (qd, J_1 = 11.0 Hz, J_2 = 4.7 Hz, 2H, CH$_2$$^{5'a/b}$); 4.17-4.25 (m, 1H, CHGlu); 4.32 (dd, J_1 = 7.5 Hz, J_2 = 4.4 Hz, 1H, CH$^{4'}$); 4.97 (dd, J_1 = 6.1 Hz, J_2 = 2.8 Hz, 1H, CH$^{3'}$); 5.04 (br t, J = 5.2 Hz, 1H, N^{2}H); 5.11 (s, 2H, -OCH$_2$Ph); 5.28 (d, J = 4.5 Hz, 1H, CH$^{2'}$); 5.56 (s, 2H, COOCH$_2$Ph); 6.07 (d, J = 2.2 Hz, 1H, CH$^{1'}$); 5.64 (br d, J = 7.7 Hz, 1H, **H**NCOOCH$_2$Ph); 6.09 (br s, 1H, NHCOGlu); 7.26-7.53 (m, 10H, 2 -C$_6$H$_5$); 7.76 (s, 1H, H8).
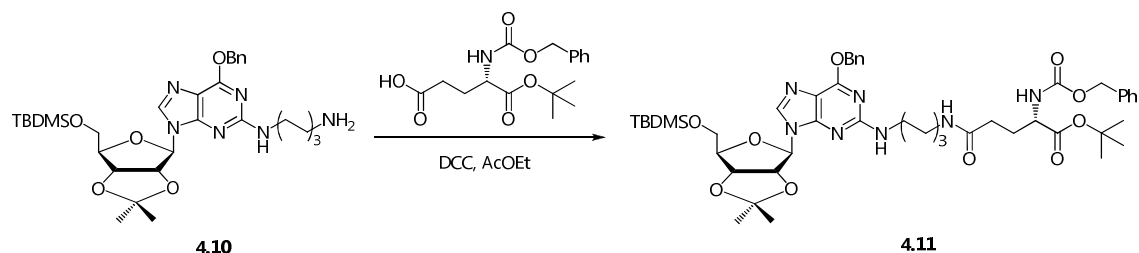
^{13}C NMR (100 MHz, CDCl$_3$):

δ-6.46 (Si(CH$_3$)); 0.00 (Si(CH$_3$)); 17.35 (SiC(CH$_3$)$_3$);24.89 (C(CH$_3$)$_2$); 24.61 (CH$_2$^{13}); 24.83 (CH$_2$^{11});25.72 (SiC(CH$_3$)$_3$); 26.24 (C(CH$_3$)$_2$); 26.55 (CH$_2$^{12}); 26.94 (OC(CH$_3$)$_2$); 29.24 (CH$_2$^{16}); 29.56 (CH$_2$^{14}); 32.92 (CH$_2$^{17}); 38.52 (CH$_2$^{15}); 40.90 (CH$_2$^{10}); 53.01 (CHGlu); 62.46 (C$^{5'}$); 65.96, 66.72 (2 CH$_2$Ph); 80.39 (C$^{3'}$);81.46 (OC(CH$_3$)$_3$); 83.40 (C$^{2'}$); 85.89 (C$^{4'}$); 88.98 (C$^{1'}$); 114.25 (C^5); 126.85, 127.03, 127.10, 127.15, 127.32, 127.50, 127.83, 127.94, 128.02, 135.22, 135.68 (2 -C$_6$H$_5$); 136.58 (C^8); 152.54 (C^4);155.40 (NHCOOCH$_2$Ph); 158.05 (C^2); 159.69 (C^6);170.05 (COOC(CH$_3$)$_3$); 170.88 (NHCOGlu).

Mass spectrum

ESI-MS positive mode, *m/z*: 946.7 [M+H$^+$]; 968.6 [M+Na$^+$]; 1913.3 [2M+Na$^+$]

7.16. Synthesis of 2-iodo-9-(2',3',5'-tri-*O*-acetyl-*β*-D-ribofuranosyl)-purine (4.12)
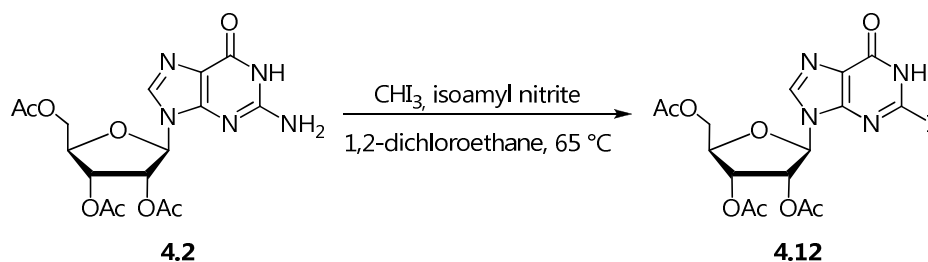
Under argon atmosphere, to a suspension of 2',3',5'-tri-*O*-acetylguanosine **4.2** (0.204 g, 0.5 mmol) in 1,2-dichloroethane (4 ml) CH_3I (0.787 g, 2.0 mmol) and isoamyl nitrite (0.67 ml, 5.0 mmol), both dried before use, were added at room temperature. The reaction mixture stirred at 65°C for 2 h. The reaction was monitored by TLC (eluent CH_2Cl_2/MeOH 9.5:0.5). After completion, the solvent was removed under reduced pressure and the resulting residue, dissolved in CH_2Cl_2, was purified by column chromatography (eluent CH_2Cl_2/MeOH 9.5:0.5) to afford 2-iodo-9-(2',3',5'-tri-*O*-acetyl-*β*-d-ribofuranosyl)-purine **4.12** (0.08 g, 0.15 mmol) as a yellow solid.

Yield: 30%

^{1}H NMR (400 MHz, DMSO-*d₆*):

δ ^{1}H NMR (400 MHz, DMSO): δ 2.06 – 2.04 – 2.21 (s, 9H, -OCOCH$_3$); 4.26 (m, 2H, $CH_2^{5'a/b}$); 4.38 (dd, J = 5.6 Hz, 1H, $CH^{4'}$); 5.57 (dd, *J* = 5.6 Hz, 1H, $CH^{3'}$); 5.81 (dd, *J* = 5.6 Hz, 1H, $CH^{2'}$); 6.13 (d, *J* = 5.6 Hz, 1H, $CH^{1'}$); 8.24 (s, 1H, CH^8); 13.09 (s, 1H, NH^1).

^{13}C NMR (100 MHz, DMSO-*d₆*):

δ 20.70 – 20.84 – 21.03 (-OCH$_3$) ; 63.16 ($C^{5'}$); 70,77 ($C^{3'}$); 72.86 ($C^{2'}$); 80.14 ($C^{4'}$); 86.05 ($C^{1'}$); 124.79 (C^5); 138.00 (C^8); 148.45 (C^4); 157.31 (C^2-C^6); 169.46 (OCOCH$_3^{2'}$); 169.84 (OCOCH$_3^{3'}$); 169.70 (OCOCH$_3^{5'}$).

Mass spectrum
ESI-MS positive mode, *m/z:* 543.2 [M+Na]$^+$; 1063.1 [2M+Na]$^+$.

7.17. Synthesis of 2-*N*-acetyl-9-(2',3',5'-tri-*O*-acetyl-*β*-D-ribofuranosyl)-purine (4.13)
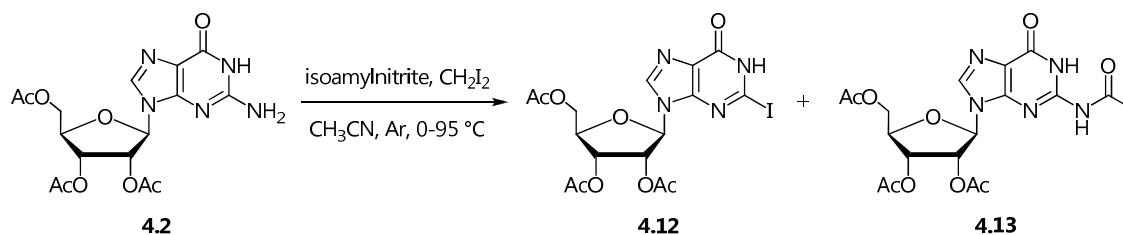
Under an argon atmosphere and in anhydrous conditions, to a solution of 2',3',5'-tri-*O*-acetylguanosine **4.2** (0.41 g, 1.0 mmol) in CH_3CN (15 ml) CH_2I_2 (1.57 g, 4.0 mmol) and isoamyl nitrite (1.33 ml, 10.02 mmol), both dried before use, were added at 0°C. After 30 minutes the reaction mixture was allowed to come to room temperature and stirred at 95°C for 2 h. The reaction was monitored by TLC (eluent CH_2Cl_2/MeOH 9.5:0.5). After completion, the solvent was removed under reduced pressure and the resulting residue, dissolved in CH_2Cl_2, was purified by column chromatography (eluent CH_2Cl_2/MeOH 9.5:0.5) to afford 2-*N*-acetyl-9-(2',3',5'-tri-*O*-acetyl-*β*-d-ribofuranosyl)-purine **4.13** (0.207 g, 0.46 mmol) as a yellow solid. Product **4.12** was not purified.

Yield: 47%

^{1}H NMR (400 MHz, DMSO-*d₆*) product 4.13:

δ 2.04 (s, 9H, -$OCOCH_3$); 3.33 (s, 3H, -$NHCOCH_3$), 4.28 (m, 2H, $CH_2^{5'a/b}$); 4.36 (dd, J = 3.7 Hz, 1H, $CH^{4'}$); 5.49 (dd, *J* = 6 Hz, 1H, $CH^{3'}$); 5.78 (dd, *J* = 6 Hz, 1H, $CH^{2'}$); 6.13 (d, *J* = 6.13 Hz, 1H, $CH^{1'}$); 8.24 (s, 1H, CH^8); 13.09 (s, 1H, NH^1).

^{13}C NMR (100 MHz, DMSO-*d₆*) product 4.13:

δ 21.35 – 21.50 – 21.69 (-OCH_3) ; 63.82 ($C^{5'}$); 71,04 ($C^{3'}$); 73.62 ($C^{2'}$); 80.79 ($C^{4'}$); 86.68 ($C^{1'}$); 111.37 (C^5); 125.44 (C^8); 149.11 (C^4); 155.94 (C^2); 157.97 (C^6); 171.12 – 170.50 – 170.36 ($OCOCH_3$); 174.66 ($NHCOCH_3$).

Mass spectrum

ESI-MS positive mode, *m/z***:** 452.3 [M+H]$^{+}$, 474.4 [M+Na]$^{+}$, 925.5 [2Mx2+Na]$^{+}$ (product **4.13**); 543.3 [M+Na]$^{+}$, 1063.2 [2M+Na]$^{+}$ (product **4.12** as impurity).

[Nair *et al.*,2007]

7.18. Synthesis of 5'-*tert*-butyldimethylsilyl-2',3'-*O*-isopropylidene-2-bromo-guanosine (4.14)
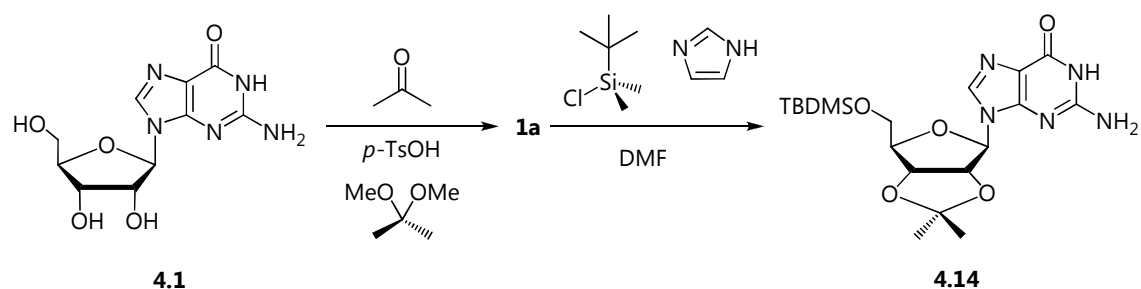
2',3'-*O*-isopropylidenguanosine **1a**. To a suspension of guanosine **4.1** (7.3 g, 25.78 mmol) in acetone (250 ml), *p*-toluenesulfonic acid (5.35 g, 28.12 mmol) and 2,2-dimethoxypronane (25 ml, 204.03 mmol) were added under inert atmosphere. The mixture was stirred overnight at room temperature. The solvent was removed under reduced pressure and the crude was dissolved in H_2O (150 ml) and NH_3 (15 ml). The solution was kept overnight at 4 °C. The resulting precipitate was filtered to afford 2',3'-*O*-isopropylidenguanosine **1a** as a white solid (6.7 g, 20.73 mmol).

Yield: 80%

^{1}H NMR (400 MHz, DMSO-d_6):

δ(ppm): 1.31 (s, 3H, CH_3); 1.51 (s, 3H, CH_3); 3.53 (m, 2H, $CH_2^{5'}$); 4.12 (m 1H, $CH^{4'}$); 4.96 (dd, J= 5.0, 6.2 Hz, 1H, $CH^{3'}$); 5.11 (t, J= 5.4 Hz, 1H, OH); 5.18 (dd, J = 2.8, 6.4 Hz, 1H, $CH^{2'}$); 5.92 (d, J=2.8 Hz, 1H, $CH^{1'}$); 6.52 (s, 2H, NH_2); 7.91 (s, 1H, CH_8); 10.71 (s, 1H, NH_1).

^{13}C NMR (100 MHz, DMSO-d_6):

δ(ppm): 25.6, 27.5 (CH_3); 62.0 ($C^{5'}$); 81.6 ($C^{3'}$) 84.0.0 ($C^{2'}$); 87.1 ($C^{4'}$); 88.9 ($C^{1'}$); 113.6 ((CH_3)$_2$C); 117.1 (C^5); 136.5 (C^8); 151.2 (C^4); 154.1 (C^2); 157.3 (C^6).

Mass spectrum

ESI-MS positive mode, *m/z*: 324.0 [M+H]$^+$; 347.4 [M+Na]$^+$; 324.0 [M+H]+; 647.1 [2M]$^+$; 669.2 [2M+Na]$^+$; 969.4 [3M]$^+$; 992.1 [3M+Na]$^+$; 1315.3 [4M+Na]$^+$; 1616.8 [5M]$^+$; 1638.0 [5M+Na]$^+$.

2',3'-*O*-isopropyliden-5'-*tert*-butyldimethylsilylguanosine **4.14**. Under nitrogen atmosphere, to a suspension of 2',3'-*O*-isopropylidenguanosine **1a** (1.09 g, 3.37 mmol) in DMF (10 ml), imidazole (0.51 g, 7.56 mmol) and *tert*-butyldimethylsilylchloride (0.60 g, 3.98 mmol) were added at room temperature. The reaction was monitored by TLC (eluent CH_2Cl_2/MeOH 12.5:1, R_f product = 0.38). After 4h the reaction mixture was extracted with CH_2Cl_2 (50 mL), washed with H_2O (2x40 ml) and brine. The organic layer was dried over Na_2SO_4 and the solvent was removed under reduced pressure. The crude was purified by flash chromatography (eluent CH_2Cl_2/MeOH 12.5:1) to afford the desired compound **4.14** as a white solid (1.39 g, 3.20 mmol).

Yield: 95%

^{1}H NMR (400 MHz, CDCl$_3$):

δ 0.12 (s, 6H, Si(CH$_3$)$_2$); 0.89 (s, 9H, C(CH$_3$)$_3$); 1.42 (s, 3H, C(CH$_3$)$_2$); 1.66 (s, 3H, C(CH$_3$)$_2$); 3.78-3.88 (m, 2H, $CH_2^{5'a/b}$); 4.37 (dd, J = 3.7 Hz, 1H, $CH^{4'}$); 4.95 (dd, *J* = 3.0, 6.2 Hz, 1H, $CH^{3'}$); 5.32 (dd, *J* = 2.2, 6.2 Hz, 1H, $CH^{2'}$); 6.02 (d, *J* = 2.4 Hz, 1H, $CH^{1'}$); 6.29 (s, 2H, NH$_2$); 7.79 (s, 1H, CH^8); 12.05 (s, 1H, NH^1).

^{13}C NMR (100 MHz, CDCl$_3$):

δ **-**5.45 (Si(CH$_3$)$_2$); -5.35 (Si(CH$_3$)$_2$); 18.38 (SiC(CH$_3$)$_3$); 25.63 (C(CH$_3$)$_2$); 25.92 (C(CH$_3$)$_3$); 27.28 (C(CH$_3$)$_2$); 63.48 ($C^{5'}$); 81.25 ($C^{3'}$); 84.71 ($CH^{2'}$); 87.01 ($C^{4'}$); 90.34 ($C^{1'}$); 114.10 (C(CH$_3$)$_2$); 117.36 (C^5); 136.0 (C^8); 151.3 (C^4); 153.60 (C^2); 159.05 (C^6).

Mass spectrum

ESI-MS positive mode, *m/z*: 438.3 [M+H]$^+$; 874.4 [2M]$^+$; 897.4 [2M+Na]$^+$; 1312.4 [3M]$^+$; 1771.8 [4M+Na]$^+$.

7.19.   Synthesis   of   2-iodo-9-(*β*-D-2',3'-*O*-isopropyliden-5'-*tert*-butyldimethylsilyl)purine (4.15)
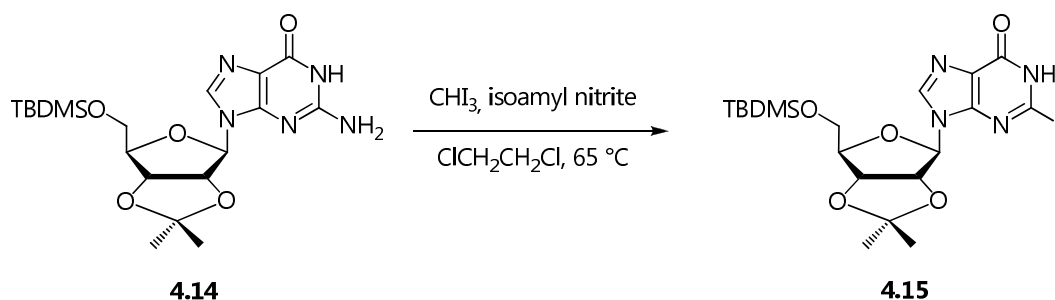
4.14   **4.15**

Under argon atmosphere, to a suspension of 2',3'-*O*-isopropyliden-5'-*tert*-butyldimethylsilylguanosine **4.14** (0.219 g, 0.5 mmol) in 1,4-dichloroethane (4 ml) CH_3I (0.787 g, 2.0 mmol) and isoamyl nitrite (0.67 ml, 5.0 mmol), both dried before use, were added at room temperature. The reaction mixture was stirred for 30' at room temperature and at 95°C for 5 h. Progress of the reaction was monitored by TLC (eluent CH_2Cl_2/MeOH 9.5:0.5, R_f product = 0.24). Volatiles were removed under reduced pressure.Product **4.15** was not isolated.

Mass spectrum

ESI-MS positive mode, *m/z***:** 549.1 [M+H]$^+$; 571.3 [M+Na]$^+$; 1119.1 [2M+Na]$^+$.

7.20. Synthesis of 2-bromo-9-(*β*-D-2',3'-*O*-isopropyliden-5'-*tert*-butyldimethylsilyl)purine (4.18)

Method A
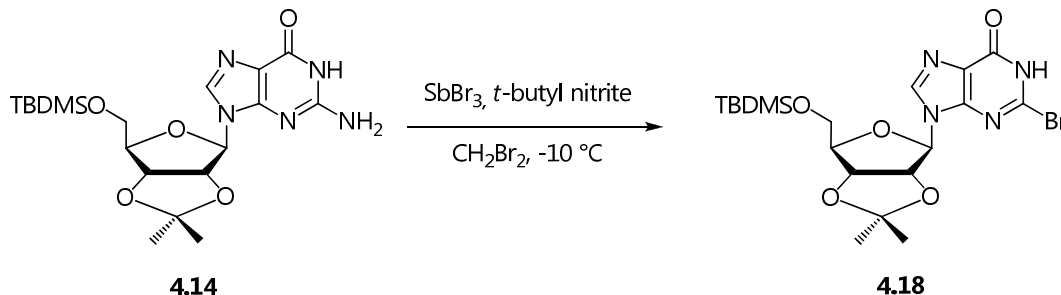
2',3'-*O*-isopropyliden-5'-*tert*-butyldimethylsilylguanosine **4.14** (0.437 g, 1.0 mmol) and SbBr$_3$ (0.506 g, 1.4 mmol) were suspended in dry CH$_2$Cl$_2$ (10 ml) at 0 °C. After cooling the mixture to 0 °C, *tert*-butylnitrite (0.42 ml, 3.5 mmol) was added dropwise. The reaction was stirred at -10°C for 1 h and then diluted with a mixture of crushed ice, water (32.5 ml) and NaHCO$_3$ (1.32 g). The resulting precipitate was filtered and the filtrate was extracted with CH$_2$Cl$_2$. The organic phase was dried over Na$_2$SO$_4$, the solvent was removed under reduced pressure and the crude yellow oil was purified by flash chromatography (eluent CH$_2$Cl$_2$/MeOH 9.5:0.5, R$_f$ product = 0.38) to obtain 2-bromo-9-(*β*-D-2',3'-*O*-isopropyliden-5'-*tert*-butyldimethylsilyl)purine **4.18** as a pale yellow solid (0.3 g, 0.6 mmol).

Yield: 60%

[Quian & Glaser, 2005]

Method B

4.14   TMSBr, *t*-butyl nitrite   **4.18**
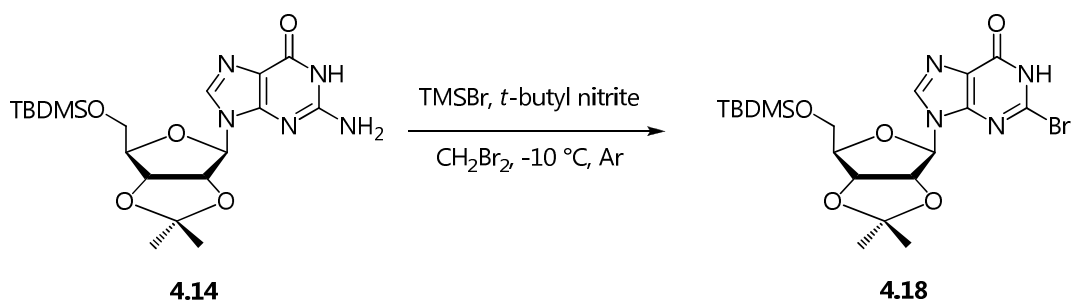
To a stirred solution of 5'-*tert*-butyldimethylsilyl-2',3'-*O*-isopropylidene guanosine **4.14** (438 mg, 1 mmol) in CH_2Br_2 (7 mL), cooled at -10 °C under argon atmosphere, trimethylbromosilane (1.2 mL, 1.38 g, 9 mmol) and *tert*-butylnitrite, (2.4 mL, 2.06 g, 20 mmol) were added dropwise . The dark brown solution was stirred at -10 °C for 2 h and at 0-10 °C (TLC control, CH_2Cl_2/MeOH=9.5:0.5, R_f product = 0.42).

After 5 h the solution was added dropwise to a cold, vigorously stirred mixture of saturated $NaHCO_3$:H_2O (150 mL)//CH_2Cl_2(150 mL). The aqueous layer was extracted with CH_2Cl_2 (70 mL), and the combined organic phase was washed with H_2O (70 mL) and brine (70 mL) and then dried on Na_2SO_4. Volatiles were evaporated in vacuo, and the yellow oil was purified by flash chromatography on silica gel (CH_2Cl_2/MeOH 9.5/0.5) to give 5'-*tert*-butyldimethylsilyl-2',3'-*O*-isopropylidene-2-bromo-guanosine **4.18** (350 mg, 70%) as yellow crystalline solid.

Yield = 70%

¹H NMR (400 MHz, CDCl₃):

δ 0.09 (s, 6H, Si(CH₃)₂); 0.91 (s, 9H, SiC(CH₃)₃); 1.41 (s, 3H, C(CH₃)₂); 1.67 (s, 3H, C(CH₃)₂); 3.83-3.91 (dd, J = 3.6, 3.2, 2H, CH₂$^{5'a/b}$); 4.40 (dd, J = 3.2 Hz, 1H, CH$^{4'}$); 4.94 (dd, *J* = 2.8, 6.2 Hz, 1H, CH$^{3'}$); 5.07 (dd, *J* = 2.8, 6.2 Hz, 1H, CH$^{2'}$); 6.15 (d, *J* = 2.8 Hz, 1H, CH$^{1'}$); 8.08 (s, 1H, CH^8); 12.85 (br s, 1H, NH^1).

¹³C NMR (100 MHz, CDCl₃):

δ -5.46 (Si(CH₃)₂); -5.35 (Si(CH₃)₂); 18.42 (SiC(CH₃)₃); 25.45 (C(CH₃)₂); 25.96 (SiC(CH₃)₃); 27.31 (C(CH₃)₂); 63.51 (C$^{5'}$); 81.13 (C$^{3'}$); 85.22 (CH$^{2'}$); 86.91 (C$^{4'}$);

90.71 ($C^{1'}$); 114.42 ($\mathbf{C}(CH_3)_2$); 123.85 (C^5); 137.60 (C^8); 148.35 (C^4); 133.15 (C^2); 158.91 (C^6).

Mass spectrum

ESI-MS positive mode, *m/z:* 523.4 [M ^{79}Br +Na]$^+$; 525.4 [M ^{81}Br +Na]$^+$; 1023.3 [Mx2 ^{79}Br +Na]$^+$; 1025.3 [Mx2 ^{81}Br+Na]$^+$

[Francom & Robins, 2003].

7.21. Synthesis of 2-chloro-9-(*β*-D-2',3'-*O*-isopropyliden-5'-*tert*-butyldimethylsilyl)purine (4.19)

4.14 → **4.19**

Reagents: SbCl₃, *t*-butyl nitrite, CH₂Cl₂, -10 °C
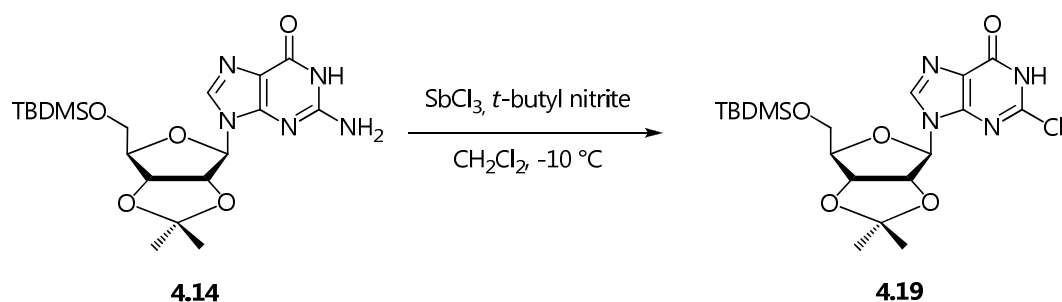
2',3'-*O*-isopropyliden-5'-*tert*-butyldimethylsilylguanosine **4.14** (0.144 g, 0.33 mmol) and $SbCl_3$ (0.105 g, 0.46 mmol) were suspended in dry CH_2Cl_2 (10 ml) at 0°C. After cooling the mixture to 0 °C, *tert*-butylnitrite (0.14 ml, 1.15 mmol) was added dropwise. The reaction was stirred at -10 °C for 1 h and then diluted with a mixture of crushed ice, water (32.5 ml) and $NaHCO_3$ (1.32 g). The resulting precipitate was filtered and the filtrate was extracted with CH_2Cl_2. The organic phase was dried over Na_2SO_4, the solvent was removed under reduced pressure and the crude was purified by flash chromatography (eluent CH_2Cl_2/MeOH 9.5:0.5, R_f product = 0.38) to obtain 2-chloro-9-(*β*-D-2',3'-*O*-isopropyliden-5'-*tert*-butyldimethylsilyl)purine **4.19** as a pale yellow solid (0.048 g, 0.10 mmol).

Yield: 31%

¹H NMR (400 MHz, CDCl₃)

δ 0.09 (s, 6H, Si(CH₃)₂); 0.91 (s, 9H, SiC(CH₃)₃); 1.41 (s, 3H, C(CH₃)₂); 1.65 (s, 3H, C(CH₃)₂); 3.83 – 3.91 (dd, J = 3.6, 3.2, 2H, $CH_2^{5'a/b}$); 4.42 (dd, *J* = 3.2 Hz, 1H, $CH^{4'}$); 4.95 (dd, *J* = 2.8, 6.2 Hz, 1H, $CH^{3'}$); 5.06 (dd, *J* = 2.8, 6.2 Hz, 1H, $CH^{2'}$); 6.14 (d, *J* = 2.8 Hz, 1H, $CH^{1'}$); 8.10 (s, 1H, CH^8); 12.85 (br s, 1H, NH^1).

¹³C NMR (100 MHz, CDCl₃)

δ -4.71 (Si(CH₃)₂); -4.82 (Si(CH₃)₂); 19.09 (Si**C**(CH₃)₃); 26.10 (C(**CH₃**)₂); 26.61 (Si**C**(**CH₃**)₃); 27.98 (C(**CH₃**)₂); 64.18 (C$^{5'}$); 81.78 (C$^{3'}$); 85.94 (CH$^{2'}$); 87.69 (C$^{4'}$); 91.47 (C$^{1'}$); 115.07 (**C**(CH₃)₂); 124.12 (C^5); 137.60 (C^8); 148.85 (C^4); 144.83 (C^2); 159.51 (C^6).

Mass spectrum

ESI-MS positive mode, *m/z*: 457.3 [M+H]$^+$; 479.5 [M+Na]$^+$; 495.5 [M+K]$^+$; 935.4 [2M+Na]$^+$.

[Quian & Glaser, 2005]

7.22. Synthesis of 2-(1,4-diaminobutane)-9-(2',3',5-tri-*O*-acetyl-*β*-D-ribofuranosyl)purine (4.21)

4.12   **4.21**
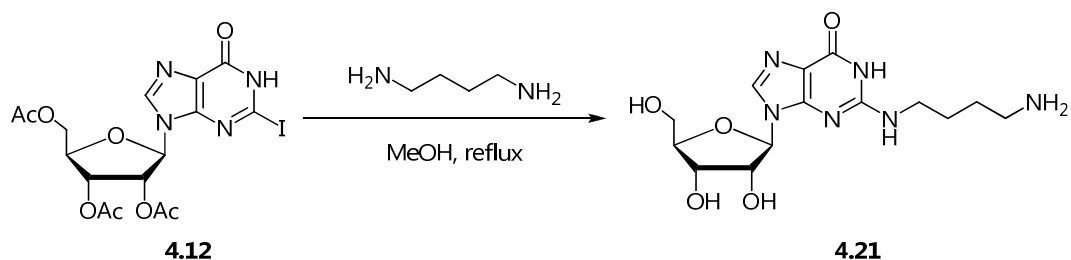
2-iodo-9-(2',3',5'-tri-*O*-acetyl-*β*-D-ribofuranosyl)-purine **4.12** (0.10g, 0.19 mmol) and 1,4-diaminobutane (0.14 ml, 1.4 mmol) were dissolved in MeOH (2 ml) and the resulting solution was refluxed for 2 h. Progress of the reaction was monitored by TLC (eluent CH_2Cl_2/MeOH 9:1 or AcOH:*n*BuOH:H_2O = 1:4:1). Volatiles were removed under reduced pressure.

2-(1,4-diaminobutane)-9-(2',3',5-tri-*O*-acetyl-*β*-D-ribofuranosyl)purine **4.21** was not isolated.

Mass spectrum

ESI-MS positive mode, *m/z*: 355.3 [M+H]$^+$; 377.5 [M+Na]$^+$.

[Bressi, 2000].

236

7.23. Synthesis of 2-(1,4-diaminobutane)-9-(*β*-D-2',3'-*O*-isopropyliden-5'-*tert*-butyldimethylsilyl)purine (4.22)

4.15 → **4.22**

(H₂N—(CH₂)₄—NH₂, MeOH, reflux)
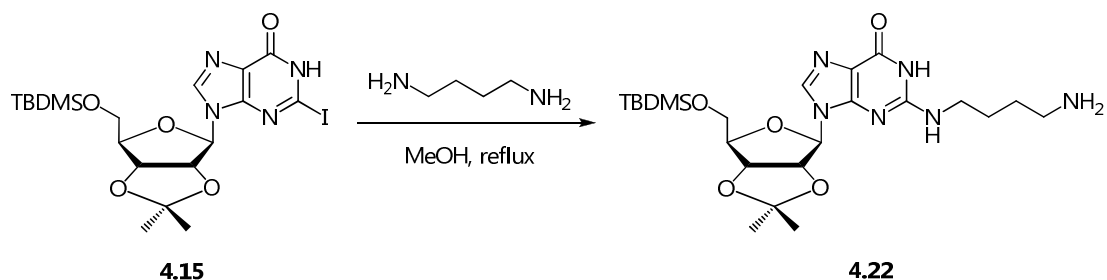
2-iodo-2',3'-*O*-isopropyliden-5'-*tert*-butyldimethylsilylguanosine **4.15** (0.44 g, 0.79 mmol) and 1,4-diaminobutane (0.16 ml, 1.6 mmol) were dissolved in MeOH (4 ml) and the resulting solution was refluxed for two days. Progress of the reaction was monitored by TLC (eluent CH₂Cl₂/MeOH 9:1 or AcOH/*n*BuOH/H₂O 1:4:1). 2-(1,4-diaminobutane)-9-(*β*-D-2',3'-*O*-isopropyliden-5'-*tert*-butyldimethylsilyl)purine **4.22** was not isolated.

Mass spectrum

ESI-MS positive mode, *m/z*: 509.4 [M+H]⁺; 531.5 [M+Na]⁺; 1017.5 [2M+H]⁺.

7.24. Synthesis of 2-*N,N*-dimethyl-9-(*β*-D-2',3'-*O*-isopropyliden-5'-*tert*-butyldimethylsilyl)purine (4.23)

4.15   **4.23**
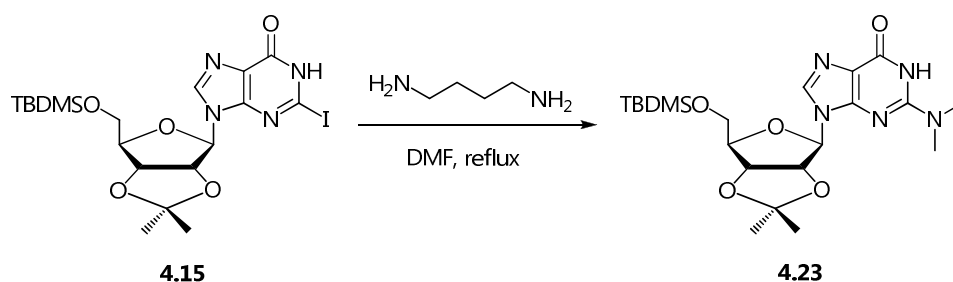
2-iodo-2',3'-*O*-isopropyliden-5'-*tert*-butyldimethylsilylguanosine **4.15** (0.07 g, 0.13 mmol) and 1,4-diaminobutane (0.04 ml, 0.38 mmol) were dissolved in DMF (3 ml) and the resulting solution was refluxed for one day. Progress of the reaction was monitored by TLC (eluent CH_2Cl_2/MeOH 9:1 or AcOH/*n*BuOH/H_2O 1:4:1). The reaction mixture was diluted in AcOEt (5 ml) and washed with H_2O (2 x 2.5 ml). The organic phase was dried over Na_2SO_4 and the solvent was removed under reduced pressure to obtain 2-*N,N*-dimethyl-9-(*β*-D-2',3'-*O*-isopropyliden-5'-*tert*-butyldimethylsilyl)purine **4.23** as a yellow solid (0.018 g, 0.04 mmol).

Yield: 30%

^{1}H NMR (400 MHz, DMSO-d_6)

δ -0.03 (s, 6H, Si(CH$_3$)$_2$); 0.81 (s, 9H, C(CH$_3$)$_3$); 1.32 (s, 3H, C(CH$_3$)$_2$); 1.52 (s, 3H, C(CH$_3$)$_2$); 3.07 (s, 6H, C(CH$_3$)$_2$); 3.67-3.69 (m, 2H, CH$_2^{5'a/b}$); 4.12 (dd, J = 3.2, 6 Hz, 1H, CH$^{4'}$); 4.93 (dd, *J* = 2.8, 6 Hz, 1H, CH$^{3'}$); 5.39 (dd, *J* = 2, 6 Hz, 1H, CH$^{2'}$); 6.04 (d, *J* = 2 Hz, 1H, CH$^{1'}$); 7.97 (s, 1H, CH^8); 11.05 (s, 1H, NH^1).

^{13}C NMR (100 MHz, DMSO-d_6)

δ -5.45 (Si(CH$_3$)$_2$); -5.35 (Si(CH$_3$)$_2$); 19.11 (Si**C**(CH$_3$)$_3$); 26.27 (C(**C**H$_3$)$_2$); 26.85 (C(**C**H$_3$)$_3$); 28.04 (C(**C**H$_3$)$_2$); 38.95 (N(CH$_3$)$_2$); 64.26 (C$^{5'}$); 82.21 (C$^{3'}$); 84.26 (CH$^{2'}$); 87.73 (C$^{4'}$); 89.83 (C$^{1'}$); 114.07 (**C**(CH$_3$)$_2$); 117.41 (C^5); 137.3 (C^8); 151.08 (C^4); 154.22 (C^2); 158.64 (C^6).

Mass spectrum

ESI-MS positive mode, *m/z***:** 466.3 [M+H]$^{+}$; 953.3 [2M+Na]$^{+}$.

7.25. Synthesis of 2-(1,2-diaminoethane)-9-(*β*-D-2',3'-*O*-isopropyliden-5'-*tert*-butyldimethylsilyl)purine (4.24), 2-(1,4-diaminobutane)-9-(*β*-D-2',3'-*O*-isopropyliden-5'-*tert*-butyldimethylsilyl)purine (4.22) and 2-(1,6-diaminohexane)-9-(*β*-D-2',3'-*O*-isopropyliden-5'-*tert*-butyldimethylsilyl)purine (4.25)
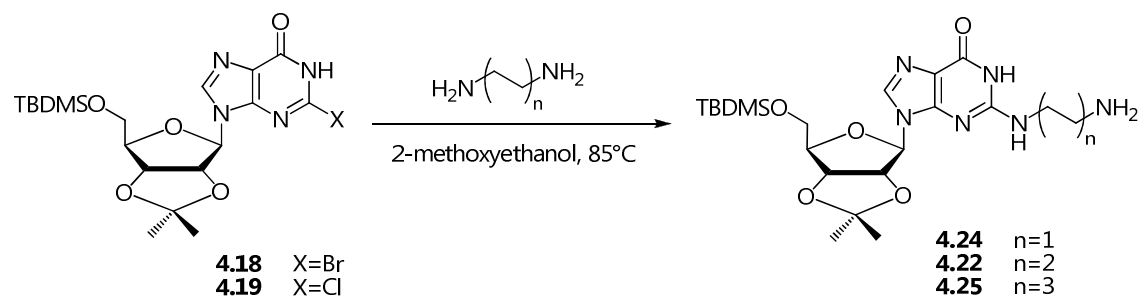
Substrate **4.18** or **4.19** (1 mmol) and the proper diamine (5 mmol) were dissolved in 2-methoxyethanol (5 ml) and the resulting solution was stirred at 85°C for four-six days. The reaction was monitored by TLC (eluent CH_2Cl_2/MeOH 9.5:0.5 or AcOH/*n*BuOH/H_2O 1:4:1). The mixture was then diluted in AcOEt (10 ml) and washed with H_2O (2 x 5 ml). The organic phase was dried over Na_2SO_4 and the solvent was removed under reduced pressure to obtain **4.24**, **4.22** or **4.25** as a crude product, which was not further purified.

Mass spectrum

ESI-MS positive mode, *m/z*:

4.24)481.3 [M+H]$^+$; 504.3 [M+Na]$^+$; 519.3 [M+K]$^+$, 961.6 [2M]$^+$, 983.6 [2M+Na]$^+$.

4.22)509.7 [M+H]$^+$; 531.7 [M+Na]$^+$; 1017.7 [2M]$^+$, 1039.9 [2M+Na]$^+$, 1325.9 [3M]$^+$.

4.23)537.3 [M+H]$^+$; 559.3 [M+Na]$^+$·

240

7.26. Synthesis of 2-(1,4-diamino-N^6-*tert*-buthoxycarbonylbutane)-9-(*β*-D-2',3'-*O*-isopropyliden-5'-*tert*-butyl dimethylsilyl)purine (4.26)

Method A

4.22   **4.26**
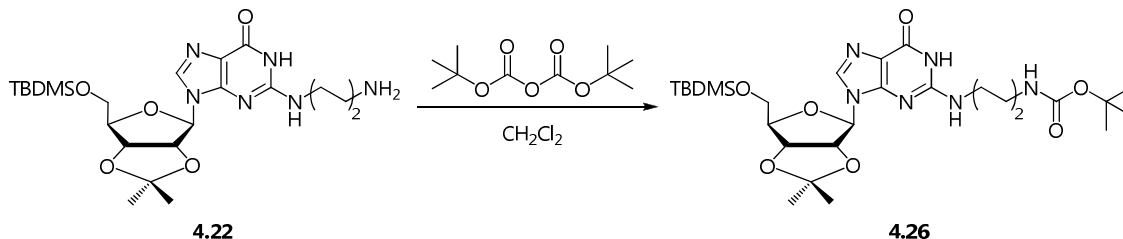
To a solution of 2-(1,6-diaminobutane)-9-(*β*-D-2',3'-*O*-isopropyliden-5'-*tert*-butyldimethylsilyl-2',3'-*O*-isopropyliden)purine **4.22** in CH_2Cl_2 (2 ml) Boc_2O (0.07 g, 0.33 mmol) was added dropwise. The reaction was monitored by TLC (eluent CH_2Cl_2/MeOH 9.5:0.5, R_f product = 0.46), then the solvent was removed under reduced pressure. The crude was purified by flash chromatography (eluent CH_2Cl_2/MeOH 19:1) to afford 2-(1,6-diamino-N^6-*tert*-buthoxycarbonylbutane)-9-(*β*-D-2',3'-*O*-isopropyliden-5'-*tert*-butyldimethylsilyl-2',3'-*O*-isopropyliden) purine **4.26** as a pale yellow solid (0.06 g, 0.098 mmol).

Yield: 30%

Method B

4.18   X=Br   **4.26**
4.19   X=Cl
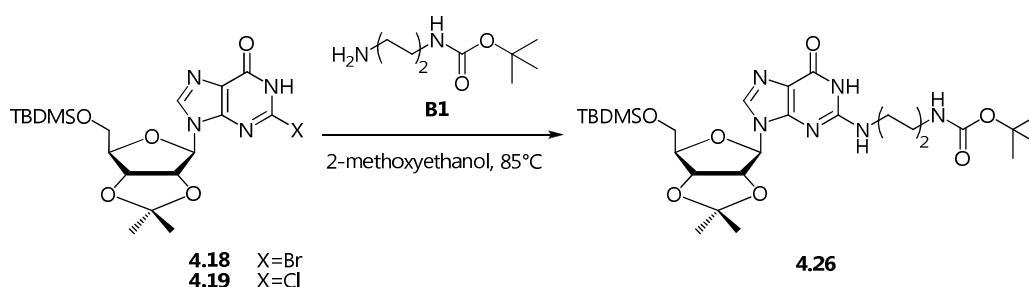
Substrate **4.18** or **4.19** (0.28 mmol) and 1,4-diamino-*N*-*tert*-buthoxycarbonylbutane **E** (1.32 mmol) were dissolved in 2-methoxyethanol (2 ml) and the resulting solution was stirred at 85 °C for four-six days. The reaction was monitored by TLC (eluent CH_2Cl_2/MeOH 9.5:0.5, R_f product = 0.46, or AcOH/*n*BuOH/H_2O 1:4:1). The mixture

was then diluted in AcOEt (5 ml) and washed with H_2O (2 x 2 ml). The organic phase was dried over Na_2SO_4 and the solvent was removed under reduced pressure a crude which was purified by flash chromatography (eluent CH_2Cl_2/MeOH 9.5:0.5) to afford 2-(1,4-diamino-N^6-*tert*-buthoxycarbonylbutane)-9-(β-D-2',3'-*O*-isopropyliden-5'-*tert*-butyl dimethylsilyl)purine **4.26** as a pale yellow solid.

Yield:

from **18**) 82%

from **19**) 63%

^{1}H NMR (400 MHz, CDCl$_3$)

δ 0.14 (s, 6H, Si(CH$_3$)$_2$); 0.89 (s, 9H, SiC(CH$_3$)$_3$); 1.45 (s, 9H, OC(CH$_3$)$_3$); 1.41 (s, 3H, C(CH$_3$)$_2$); 1.66 (s, 3H, C(CH$_3$)$_2$); 1.76 – 1.64 (m, 4H, CH$_2^{11,12}$); 3.49 – 3.21 (m, 4H, CH$_2^{10,13}$); 3.78-3.87 (m, 2H, CH$_2^{5'a/b}$); 4.34 (dd, J = 3.2, 6 Hz, 1H, CH$^{4'}$); 4.95 (dd, J = 2.8, 6 Hz, 1H, CH$^{3'}$); 5.28 (dd, J = 2, 6 Hz, 1H, CH$^{2'}$); 6.04 (d, J = 2 Hz, 1H, CH$^{1'}$); 7.77 (s, 1H, CH^8); 11.60 (br s, 1H, NH^1).

^{13}C NMR (100 MHz, CDCl$_3$)

δ -5.38 (Si(CH$_3$)$_2$); -5.38 (Si(CH$_3$)$_2$); 18.37 (Si**C**(CH$_3$)$_3$); 25.46 (C(**C**H$_3$)$_2$); 25.90 (Si**C**(CH$_3$)$_3$); 27.25 (C(**C**H$_3$)$_2$); 27.34 (O**C**(CH$_3$)$_3$); 28.48 (OC(**C**H$_3$)$_3$); 26.38 – 29.70 (CH$_2^{11,12}$); 40.29 – 41.02 (CH$_2^{10,13}$); 63.57 (C$^{5'}$); 78.93 (C$^{3'}$); 84.57 (CH$^{2'}$); 87.01 (C$^{4'}$); 90.26 (C$^{1'}$); 113.96 (**C**(CH$_3$)$_2$); 117.04 (C^5); 138.0 (C^8); 151.50 (C^4); 152.81 (C^2); 156.13 (**C**OO(CH$_3$)$_3$); 159.16 (C^6).

Mass spectrum

ESI-MS positive mode, *m/z*: 609.5 [M+H]$^+$; 631.5 [M+Na]$^+$; 1239.6 [2M+Na]$^+$; ms/ms 509.2 (M-Boc).

7.27. Synthesis of compounds 4.27, 4.28, 4.29

4.24 n=1
4.22 n=2
4.25 n=3

4.27 n=1
4.28 n=2
4.29 n=3
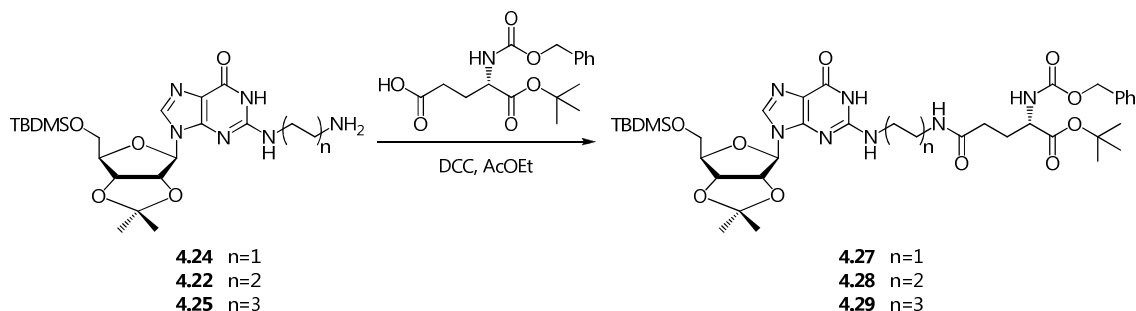
To a solution of substrate **4.24**, **4.22** or **4.25** (0.39 mmol) in AcOEt (2 ml), N^{α}-benzyloxycarbonyl-γ-L-glutamic acid O^{α}-*tert*-butyl ester (0.51 mmol) and DCC (0.39 mmol) were added. Progress of the reaction was monitored by TLC (eluent CH_2Cl_2/MeOH 9.5:0.5).

Then the mixture was filtered under vacuum, and washed with HCl 0.5 M (2 ml), $NaHCO_3$ (2 ml), and brine (2 ml). The combined organic phases were dried over Na_2SO_4 and concentrated under reduced pressure. The crude was purified by flash chromatography (eluent CH_2Cl_2/MeOH 9.5:0.5) to afford **4.27**, **4.28** or **4.29** as pale yellow solids.

Compound 4.27
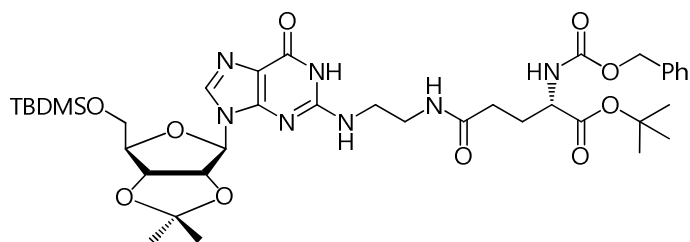
Yield = 64 %

¹H NMR (400 MHz, CDCl₃)

δ 0.05 (s, 3H, Si(CH₃)₂); 0.06 (s, 3H, Si(CH₃)₂); 0.89 (s, 9H, SiC(CH₃)₃); 0.91 (s, 3H, C(CH₃)₂); 1.41 (s, 9H, OC(CH₃)₃); 1.64 (s, 3H, C(CH₃)₂); 1.95 – 2.04 (m, 1H, CH₂^{13a}); 2.12 – 2.20 (m, 1H, CH₂^{13b}); 2.24 – 2.37 (m, 2H, CH₂^{12}); 3.45 – 3.66 (m, 4H, CH₂^{10,11}); 3.78 – 3.90 (m, 2H, CH₂$^{5'a/b}$); 4.15 – 4.20 (m, 1H, CHGlu); 4.33 – 4.36 (dd, 1H, CH$^{4'}$); 4.93 – 4.95 (dd, 1H, CH$^{3'}$); 5.02 – 5.12 (m, 2H, CH₂Ph); 5.24 – 5.25 (dd, 1H, CH$^{2'}$);

5.67 – 5.69 (br d, 1H, **NH**CHGlu); 6.06 (d, 1H, CH$^{1'}$); 7.29 – 7.31 (m, 5H, Ph); 7.51 (br s, 1H, **NH**COCH$_2$CH$_2$); 8.08 (s, 1H, CH^8); 11.05 (br s, 1H, NH^1).

^{13}C NMR (100 MHz, CDCl$_3$)

δ -5.42 (Si(CH$_3$)$_2$); 1.00 (Si(CH$_3$)$_2$); 18.35 (Si**C**(CH$_3$)$_3$); 25.57 (C(**C**H$_3$)$_2$); 25.88 (SiC(**C**H$_3$)$_3$); 27.33 (C(**C**H$_3$)$_2$); 24.93 (O**C**(CH$_3$)$_3$); 27.91 (OC(**C**H$_3$)$_3$); 28.33 (CH$_2$^{13}); 32.01 (CH$_2$^{12}); 41.15 – 38.59 (CH$_2$^{10,11}); 54.41 (CHGlu); 63.55 (C$^{5'}$); 66.70 (**C**H$_2$Ph); 81.16 (C$^{3'}$); 81.29 (C$_q$Ph); 84.54 (CH$^{2'}$); 87.10 (C$^{4'}$); 90.40 (C$^{1'}$); 114.12 (**C**(CH$_3$)$_2$); 116.74 (C^5); 128.40 – 128.18 – 127.94 (Ph); 136.41 (C^8); 151.63 (C^4); 152.96 (C^2); 156.20 (**C**OOCH$_2$Ph);158.31 (C^6); 171.12 (**C**OO(CH$_3$)$_3$); 173.20 (NH**C**OGlu).

Mass spectrum

ESI-MS positive mode, *m/z*: 800.7 [M+H]$^+$; 822.9 [M+Na]$^+$; 1622.1 [2M+Na]$^+$·

Compound 4.28
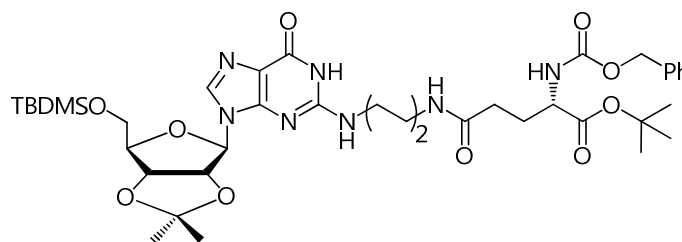
Yield = 47 %

^{1}H NMR (400 MHz, CDCl$_3$)

δ0.01 (s, 3H, Si(CH$_3$)$_2$); 0.02 (s, 3H, Si(CH$_3$)$_2$); 0.83 (s, 9H, SiC(CH$_3$)$_3$); 1.26 – 1.29 (m, 2H, CH$_2$^{11}); 1.37 (s, 3H, C(CH$_3$)$_2$); 1.42 (s, 9H, OC(CH$_3$)$_3$); 1.60 (s, 3H, C(CH$_3$)$_2$); 1.68 – 1.72 (m, 2H, CH$_2$^{12}); 1.91 – 1.95 (m, 1H, CH$_2$^{15a}); 2.12 – 2.17 (m, 1H, CH$_2$^{15b}); 2.24 – 2.26 (m, 2H, CH$_2$^{14}); 3.27 – 3.28 (m, 2H, CH$_2$^{13}); 3.44 – 3.92 (m, 2H, CH$_2$^{10}); 3.83 – 3.73 (m, 2H, CH$_2$$^{5'a/b}$); 4.15 – 4.20 (m, 1H, CHGlu); 4.30 (dd, 1H, CH$^{4'}$); 4.91 (dd, 1H, CH$^{3'}$); 5.07 (dd, 2H, CH$_2$Ph); 5.20 (dd, 1H, CH$^{2'}$); 5.83 (br d, 1H, **NH**CHGlu); 6.02 (d, 1H, CH$^{1'}$); 6.84 (br s, 1H, **NH**COCH$_2$CH$_2$); 7.28 – 7.31 (m, 5H, Ph); 7.73 (s, 1H, CH^8); 11.35 (br s, 1H, NH^1).

¹³C NMR (100 MHz, CDCl₃)

δ-5.29 (Si(CH₃)₂); -5.25 (Si(CH₃)₂); 18.47 (Si**C**(CH₃)₃); 25.57 (C(**CH₃**)₂); 26.00 (SiC(**CH₃**)₃); 26.33 (**CH₂**^{12}); 26.93 (O**C**(CH₃)₃); 27.38 (C(**CH₃**)₂); 28.05 (OC(**CH₃**)₃); 28.89 (**CH₂**^{15}); 31.69 (**CH₂**^{11}); 32.64 (**CH₂**^{14}); 39.15 (**CH₂**^{13}); 40.98 (**CH₂**^{10}); 54.35 (**CH**Glu); 63.64 (C$^{5'}$); 67.00 (**CH₂**Ph); 81.46 (C$^{3'}$); 82.36 (C$_q$Ph); 84.66 (**CH**$^{2'}$); 86.96 (C$^{4'}$); 90.11 (C$^{1'}$); 114.08 (**C**(CH₃)₂); 117.10 (C^5); 128.56 – 128.16 – 128.05 (Ph); 136.41 (C^8); 151.50 (C^4); 152.81 (C^2); 156.49 (NH**C**OCH₂Ph); 159.13 (C^6); 171.26 (**C**OO(CH₃)₃); 172.31 (NH**C**OGlu).

Mass spectrum

ESI-MS positive mode, *m/z:* 850.9 [M+Na]⁺; 826.4 [M-H]⁺; 1653.0 [2M-H]⁺; 1679.0 [2M+Na]⁺.

Compound 4.29

Yield = 50 %

¹H NMR (400 MHz, CDCl₃)

δ0.01 (s, 3H, Si(CH₃)₂); 0.02 (s, 3H, Si(CH₃)₂); 0.86 (s, 9H, SiC(CH₃)₃); 1.26 – 1.29 (m, 2H, CH₂^{11}); 1.37 (s, 3H, C(CH₃)₂); 1.43 (s, 9H, OC(CH₃)₃); 1.53 – 1.47 (m, 2H, CH₂^{12}); 1.66 (s, 3H, C(CH₃)₂); 1.61 – 1.65 (m, 2H, CH₂$^{10-15}$); 1.89 – 1.97 (m, 2H, CH₂$^{15-10}$); .1.89 – 1. 97 (m, 1H, CH₂^{17a}); 2.14 – 2.25 (m, 1H, CH₂^{17b}); 2.21 – 2.28 (m, 2H, CH₂^{16}); 3.20 – 3.24 (m, 2H, CH₂^{13}); 3.34 – 3.45 (m, 2H, CH₂^{10}); 3.83 – 3.74 (m, 2H, CH₂$^{5'a/b}$); 4.17 – 4.22 (m, 1H, CHGlu); 4.29 (dd, 1H, CH$^{4'}$); 4.92 (dd, 1H, CH$^{3'}$); 5.08 (dd, 2H, CH₂Ph); 5.21 (dd, 1H, CH$^{2'}$); 5.80 (br d, 1H, N**H**CHGlu); 6.02 (d, 1H, CH$^{1'}$); 6.53 (br s, 1H, N**H**COCH₂CH₂); 7.30 – 7.33 (m, 5H, Ph); 7.73 (s, 1H, CH^8); 11.74 (br s, 1H, NH^1).

¹³C NMR (100 MHz, CDCl₃)

δ -6.39 (Si(CH$_3$)$_2$); -6.39 (Si(CH$_3$)$_2$); 17.37 (SiC(CH$_3$)$_3$); 24.46 (C(CH$_3$)$_2$); 24.90 (SiC(CH$_3$)$_3$); 26.33 (CH$_2$^{12}); 26.93 (OC(CH$_3$)$_3$); 26.26 (C(CH$_3$)$_2$); 26.95 (OC(CH$_3$)$_3$); 28.89 (CH$_2$^{15}); 31.69 (CH$_2$^{11}); 32.64 (CH$_2$^{14}); 39.15 (CH$_2$^{13}); 40.98 (CH$_2$^{10}); 53.13 (CHGlu); 62.56 (C$^{5'}$); 65.94 (CH$_2$Ph); 80.43 (C$^{3'}$); 83.48 (CH$^{2'}$); 85.92 (C$^{4'}$); 88.89 (C$^{1'}$); 112.88 (C(CH$_3$)$_2$); 116.18 (C^5); 126.98 – 127.11 – 127.47 (Ph); 135.25 (C^8); 150.20 (C^4); 151.75 (C^2); 155.45 (NHCOCH$_2$Ph); 158.09 (C^6); 170.09 (COO(CH$_3$)$_3$); 171.26 (NHCOGlu).

Mass spectrum

ESI-MS positive mode, *m/z*: 878.4 [M+Na]$^+$.

7.28. Synthesis of compounds 4.30, 4.31, 4.32

4.27 n=1
4.28 n=2
4.29 n=3

4.30 n=1
4.31 n=2
4.32 n=3

To a solution of substrate **4.27**, **4.28** or **4.29** (0.17 mmol) in THF (2 ml), TBAF·3H$_2$O (0.34 mmol) was added. Progress of the reaction was monitored by TLC (eluent CH$_2$Cl$_2$/MeOH 1:1). After 6 h, the mixture was diluted in CH$_2$Cl$_2$(3 ml) and washed with H$_2$O (2 x 2 ml). The combined organic phases were dried over Na$_2$SO$_4$ and concentrated under reduced pressure. The crude was purified by flash chromatography (eluent CH$_2$Cl$_2$/MeOH 9:1) to afford **4.30**, **4.31** or **4.32** as pale yellow solids.

Compound 4.30

Yield = 84 %

^{1}H NMR (400 MHz, CDCl$_3$)

δ 1.32 (s, 3H, C(CH$_3$)$_2$); 1.38 (s, 9H, OC(CH$_3$)$_3$); 1.52 (s, 3H, C(CH$_3$)$_2$); 1.70 – 1.79 (m, 2H, CH$_2$^{13a}); 1.89 – 1.98 (m, 1H, CH$_2$^{13b}); 2.14 – 2.18 (m, 2H, CH$_2$^{12}); 3.86 – 3.91 (m, 2H, CH$_2$^{10}); 3.86 – 3.91 (m, 2H, CH$_2$^{11}); 3.47 – 3.56 (m, 2H, CH$_2$$^{5'a/b}$); 3.89 (br s, 1H, CHGlu); 4.12 (dd, 1H, CH$^{4'}$); 4.91 (m, 1H, CH$^{3'}$); 5.02 (m, 2H, CH$_2$Ph); 5.29 (dd, 1H, CH$^{2'}$);5.98 (d, 1H, CH$^{1'}$); 6.48 (br d, 1H, N**H**CHGlu); 7.32 (m, 5H, Ph); 7.58 (br s, 1H, N**H**COCH$_2$); 7.92 (s, 1H, CH^8); 11.72 (br s, 1H, NH^1).
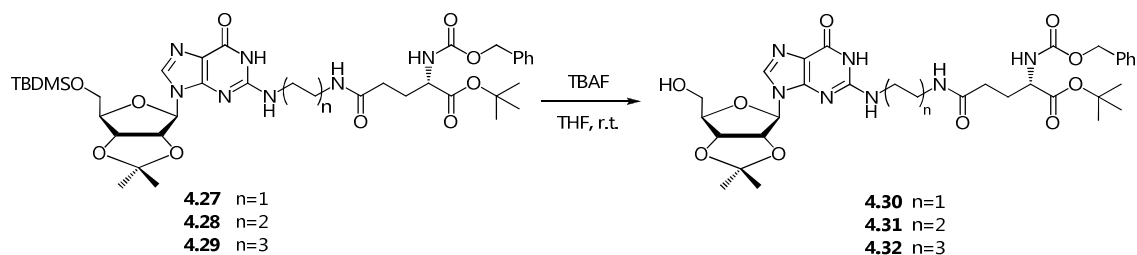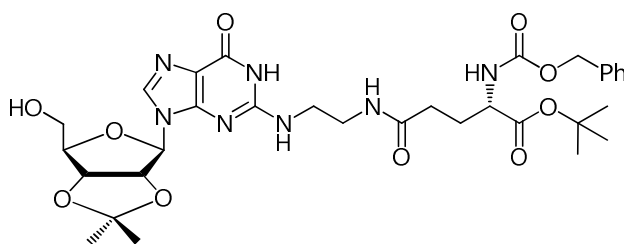
^{13}C NMR (100 MHz, CDCl$_3$)

δ 25.63 (C(**CH$_3$**)$_2$); 27.10 (**CH$_2$**^{13}); 27.51 (C(**CH$_3$**)$_2$); 27.52 (OC(**CH$_3$**)$_3$); 28.10 (O**C**(CH$_3$)$_3$); 32.05 (**CH$_2$**^{12}); 38.45 (**CH$_2$**^{11}); 41.06 (**CH$_2$**^{10}); 54.69 (**CH**Glu); 62.02 (C$^{5'}$); 65.90 (**CH$_2$**Ph); 81.74 (C$^{3'}$); 81.03 (C$_q$Ph); 83.66 (**CH**$^{2'}$); 86.87 (C$^{4'}$); 89.12 (C$^{1'}$); 113.50 (**C**(CH$_3$)$_2$); 117.38 (C^5); 128.21 – 128.29 – 128.80 (Ph); 137.46 (C^8); 151.59 (C^4); 153.07 (C^2); 156.55 (**C**OOCH$_2$Ph); 157.11 (C^6); 171.80 (**C**OO(CH$_3$)$_3$); 172.05 (NH**C**OOGlu).

Mass spectrum

ESI-MS positive mode, *m/z*: 686.8 [M+H]$^+$; 708.9 [M+Na]$^+$; 724.0 [M+K]$^+$; 1393.8 [2M+Na]$^+$.

Compound 4.31
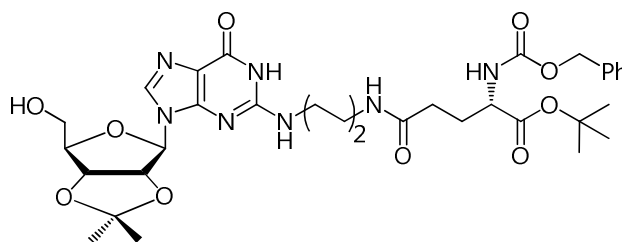
Yield = 82 %

^{1}H NMR (400 MHz, CDCl$_3$)

δ 1.27 (m, 2H, CH$_2$^{11}); 1.39 (s, 3H, C(CH$_3$)$_2$); 1.44 (s, 9H, OC(CH$_3$)$_3$); 1.63 (s, 3H, C(CH$_3$)$_2$); 1.69 (m, 2H, CH$_2$^{12}); 1.91 – 2.00 (m, 1H, CH$_2$^{15a}); 2.13 – 2.21 (m, 1H, CH$_2$^{15b}); 2.27 – 2.29 (m, 2H, CH$_2$^{14}); 3.23 – 3.33 (m, 2H, CH$_2$^{13}); 3.37 – 3.46 (m, 2H, CH$_2$^{10}); 3.77 – 3.92 (m, 2H, CH$_2$$^{5'a/b}$); 4.19 (br s, 1H, CHGlu); 4.39 (dd, 1H, CH$^{4'}$); 5.05 (m, 1H, CH$^{3'}$); 5.05 (m, 2H, CH$_2$Ph); 5.29 (dd, 1H, CH$^{2'}$); 5.92 (d, 1H, CH$^{1'}$); 6.93 (br d, 1H, N**H**CHGlu); 7.08 (br s, 1H, N**H**COCH$_2$CH$_2$); 7.32 (m, 5H, Ph); 7.84 (s, 1H, CH^8); 11.41 (br s, 1H, NH^1).

^{13}C NMR (100 MHz, CDCl$_3$)

δ 25.41 (C(**CH$_3$**)$_2$); 26.25 (**CH$_2$**^{12}); 26.62 (OC(**CH$_3$**)$_3$); 27.44 (C(**CH$_3$**)$_2$); 27.94 (O**C**(CH$_3$)$_3$); 28.79 (**CH$_2$**^{15}); 32.60 (**CH$_2$**^{11}); 32.64 (**CH$_2$**^{14}); 39.14 (**CH$_2$**^{13}); 41.06

(CH$_2$^{10}); 54.31 (CHGlu); 62.58 (C$^{5'}$); 66.94 (CH$_2$Ph); 81.20 (C$^{3'}$); 82.37 (C$_q$Ph); 83.49 (CH$^{2'}$); 86.07 (C$^{4'}$); 91.32 (C$^{1'}$); 114.12 (**C**(CH$_3$)$_2$); 117.37 (C^5); 127.97 – 128.11 – 128.48 (Ph); 136.25 (C^8); 151.07 (C^4); 153.02 (C^2); 156.47 (**C**OOCH$_2$Ph);158.59 (C^6); 171.23 (**C**OO(CH$_3$)$_3$); 172.51 (NH**C**OGlu).

Mass spectrum

ESI-MS positive mode, *m/z***:** 714.4 [M+H]$^+$; 736.4 [M+Na]$^+$·

Compound 4.32

Yield = 58 %

^{1}H NMR (400 MHz, CDCl$_3$)

δ 1.26 – 1.29 (m, 2H, CH$_2$^{11}); 1.37 (s, 3H, C(CH$_3$)$_2$); 1.43 (s, 9H, OC(CH$_3$)$_3$); 1.53 – 1.47 (m, 2H, CH$_2$^{12}); 1.66 (s, 3H, C(CH$_3$)$_2$); 1.61 – 1.65 (m, 2H, CH$_2$$^{10-15}$); 1.89 – 1.97 (m, 2H, CH$_2$$^{15-10}$); .1.89 – 1. 97 (m, 1H, CH$_2$^{17a}); 2.14 – 2.25 (m, 1H, CH$_2$^{17b}); 2.21 – 2.28 (m, 2H, CH$_2$^{16}); 3.20 – 3.24 (m, 2H, CH$_2$^{13}); 3.34 – 3.45 (m, 2H, CH$_2$^{10}); 3.83 – 3.74 (m, 2H, CH$_2$$^{5'a/b}$); 4.17 – 4.22 (m, 1H, CHGlu); 4.29 (dd, 1H, CH$^{4'}$); 4.92 (dd, 1H, CH$^{3'}$); 5.08 (dd, 2H, CH$_2$Ph); 5.21 (dd, 1H, CH$^{2'}$); 5.80 (br d, 1H, N**H**CHGlu); 6.02 (d, 1H, CH$^{1'}$); 6.53 (br s, 1H, N**H**COCH$_2$CH$_2$); 7.30 – 7.33 (m, 5H, Ph); 7.73 (s, 1H, CH^8); 11.74 (br s, 1H, NH^1).
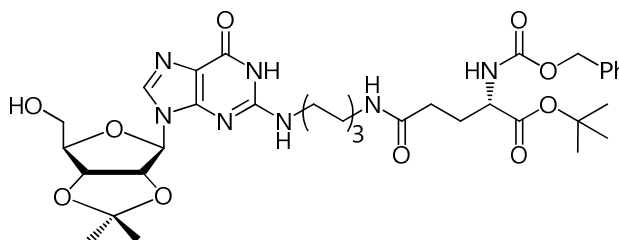
^{13}C NMR (100 MHz, CDCl$_3$)

δ 24.46 (C(**C**H$_3$)$_2$); 26.33 (CH$_2$^{12}); 26.93 (O**C**(CH$_3$)$_3$); 26.26 (C(**C**H$_3$)$_2$); 26.95 (OC(**C**H$_3$)$_3$); 28.89 (CH$_2$^{15}); 31.69 (CH$_2$^{11}); 32.64 (CH$_2$^{14}); 39.15 (CH$_2$^{13}); 40.98 (CH$_2$^{10}); 53.13 (CHGlu); 62.56 (C$^{5'}$); 65.94 (CH$_2$Ph); 80.43 (C$^{3'}$); 83.48 (CH$^{2'}$); 85.92 (C$^{4'}$); 88.89 (C$^{1'}$); 112.88 (**C**(CH$_3$)$_2$); 116.18 (C^5); 126.98 – 127.11 – 127.47 (Ph);

135.25 (C^8); 150.20 (C^4); 151.75 (C^2); 155.45 (NH**C**OCH$_2$Ph); 158.09 (C^6); 170.09 (**C**OO(CH$_3$)$_3$); 171.26 (NH**C**OGlu).

Mass spectrum

ESI-MS positive mode, *m/z***:** 742.4 [M+H]$^+$; 764.4 [M+Na]$^+$; 780.4 [M+K]$^+$.

7.29. Synthesis of compounds 4.36a, 4.36b, 4.36c
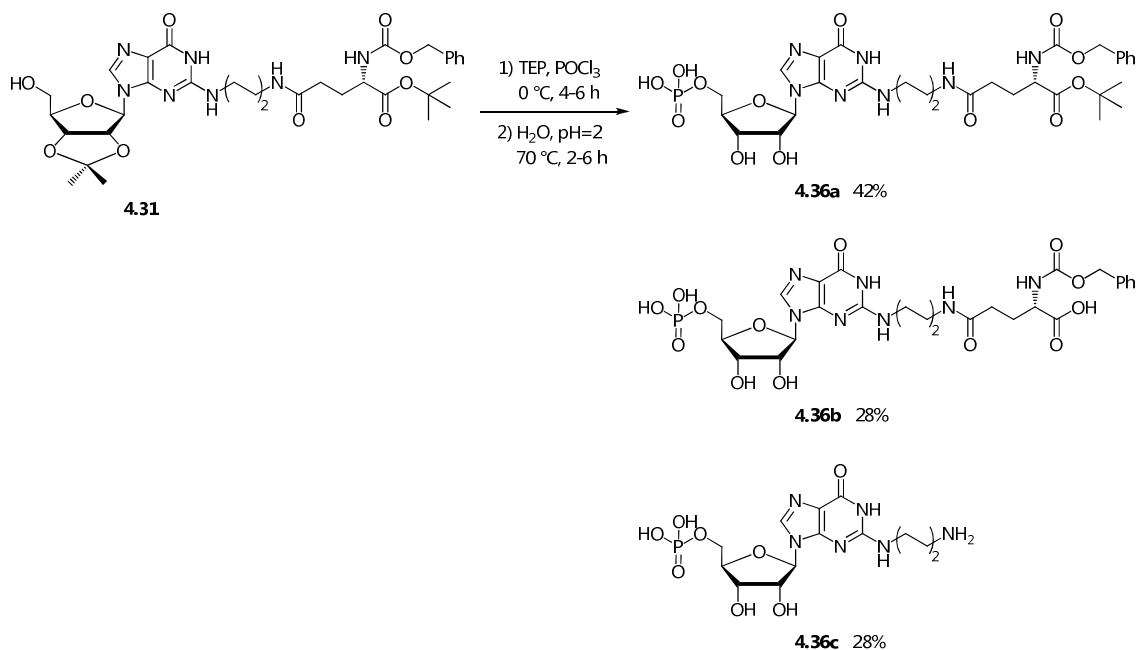
Under inert atmosphere, to a stirred solution of compound **4.31** (0.13 mmol) in TEP (1.5 ml), POCl$_3$ (0.65 mmol) was added dropwise at 0°C. The mixture was then stirred at 0°C, monitoring progress of the reaction by reverse phase TLC (eluent MeOH/H$_2$O 4:1). After 3 h, the mixture was diluted with H$_2$O (2 ml) and NaOH 2N was carefully added to pH 2. The resulting solution was stirred for 4 h at 70°C, then pH was adjusted to 7.0. The solvent was removed by lyophilization and products **4.36a**, **4.36b** and **4.36c** were afforded isolated by reverse phase HPLC.

Compound 4.36a
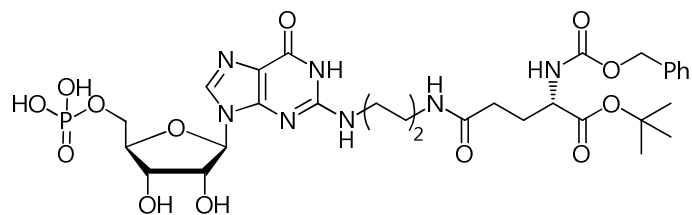
Yield = 41 %

^{1}H NMR (400 MHz, D$_2$O)

δ 1.13 (s, 9H, OC(CH$_3$)$_3$); 1.29 (m, 2H, CH$_2$^{11}); 1.45 (m, 2H, CH$_2$^{12}); 1.71 – 1.83 (m, 1H, CH$_2$^{15a}); 1.99 – 2.04 (m, 1H, CH$_2$^{15b}); 2.15 – 2.22 (m, 2H, CH$_2$^{14}); 2.99 – 3.07 (m, 2H, CH$_2$^{13}); 3.15 – 3.19 (m, 2H, CH$_2$^{10}); 3.80 – 3.89 (m, 2H, CH$_2$$^{5'a/b}$); 3.80 – 3.89 (br s, 1H, CHGlu); 4.09 (dd, 1H, CH$^{4'}$); 4.17 (m, 1H, CH$^{3'}$); 4.47 (dd, 1H, CH$^{2'}$); 4.91 – 5.02 (m, 2H, CH$_2$Ph); 5.72 (d, 1H, CH$^{1'}$); 7.18 – 7.25 (m, 5H, Ph); 7.90 (s, 1H, CH^8).

^{13}C NMR (100 MHz, D$_2$O)

δ 25.78 (CH$_2$^{12}); 26.35 (CH$_2$^{11}); 27.84 (OC(CH$_3$)$_3$); 27.74 (CH$_2$^{15}); 29.58 (OC(**C**H$_3$)$_3$); 32.54 (CH$_2$^{14}); 39.22 (CH$_2$^{13}); 41.10 (CH$_2$^{10}); 55.98 (CHGlu); 64.18 (C$^{5'}$); 66.88 (CH$_2$Ph); 71.41 (C$^{3'}$); 82.37 (C$_q$Ph); 75.28 (CH$^{2'}$); 84.31 (C$^{4'}$); 87.13 (C$^{1'}$); 117.09 (C^5); 127.59 – 128.23 – 128.64 (Ph); 136.31 (C^8); 152.09 (C^4); 157.71 (C^2); 161.37 (**C**OOCH$_2$Ph);168.22 (C^6); 175.37 (**C**OO(CH$_3$)$_3$); 179.07 (NH**C**OGlu).

^{31}P NMR (161.98 MHz, D$_2$O)

δ 0.45

Mass spectrum

ESI-MS positive mode, *m/z***:** 754.3 [M+H]$^+$; 776.3 [M+Na]$^+$; 792.3 [M+K]$^+$.

Compound 4.36b

Yield = 28 %

^{1}H NMR (400 MHz, D$_2$O)

δ 1.43 – 1.46 (m, 4H, CH$_2$$^{11-12}$); 1.71 – 1.77 (m, 1H, CH$_2$^{15a}); 1.98 – 2.06 (m, 1H, CH$_2$^{15b}); 2.15 – 2.19 (m, 2H, CH$_2$^{14}); 2.99 – 3.09 (m, 2H, CH$_2$^{13}); 3.15 – 3.21 (m, 2H, CH$_2$^{10}); 3.79 – 3.90 (m, 2H, CH$_2$$^{5'a/b}$); 3.79 – 3.90 (br s, 1H, CHGlu); 4.11 (dd, 1H, CH$^{4'}$); 4.19 (m, 1H, CH$^{3'}$); 4.48 (dd, 1H, CH$^{2'}$); 4.92 – 5.03 (m, 2H, CH$_2$Ph); 5.73 (d, 1H, CH$^{1'}$); 7.20 – 7.26 (m, 5H, Ph); 7.91 (s, 1H, CH^8).

^{13}C NMR (100 MHz, D$_2$O)

δ 25.78 (CH$_2$$^{11-12}$); 26.35 (CH$_2$$^{11-12}$); 27.84 (CH$_2$^{15}); 32.56 (CH$_2$^{14}); 39.23 (CH$_2$^{13}); 41.11 (CH$_2$^{10}); 55.99 (CHGlu); 64.18 (C$^{5'}$); 64.15 (C$_q$Ph); 66.89 (CH$_2$Ph); 71.40 (C$^{3'}$); 75.26 (CH$^{2'}$); 84.32 (C$^{4'}$); 87.12 (C$^{1'}$); 117.10 (C^5); 128.23 – 128.65 – 128.74 (Ph); 136.31 (C^8); 152.09 (C^4); 157.71 (C^2); 161.37 (**C**OOCH$_2$Ph);168.23 (C^6); 175.37 (**C**OO(CH$_3$)$_3$); 179.07 (NH**C**OGlu).

^{31}P NMR (161.98 MHz, D$_2$O)

δ 0.34

Mass spectrum

ESI-MS positive mode, *m/z*: 698.3 [M+H]$^+$; 720.4 [M+Na]$^+$; 736.4 [M+K]$^+$.

Compound 4.36c

Yield = 28 %

^{1}H NMR (400 MHz, D$_2$O):

δ 1.61 (m, 4H, CH$_2$$^{11\text{-}12}$); 2.96 (m, 2H, CH$_2$^{13}); 3.30 (m, 2H, CH$_2$^{10}); 3. 96 – 4.05 (m, 2H, CH$_2$$^{5'a/b}$); 4.24 (dd, 1H, CH$^{4'}$); 4.43 (m, 1H, CH$^{3'}$); 4.74 (dd, 1H, CH$^{2'}$); 5.88 (d, 1H, CH$^{1'}$); 7.96 (s, 1H, CH^8).

^{13}C NMR (100 MHz, D$_2$O):

δ 24.19 (CH$_2$$^{11\text{-}12}$); 25.51 (CH$_2$$^{11\text{-}12}$); 39.29 (CH$_2$^{13}); 40.22 (CH$_2$^{10}); 64.69 (C$^{5'}$); 70.60 (C$^{3'}$); 73.43 (CH$^{2'}$); 83.79 (C$^{4'}$); 87.46 (C$^{1'}$); 115.99 (C^5); 136.31 (C^8); 152.89 (C^4); 159.36 (C^2); 180.71 (C^6).

^{31}P NMR (161.98 MHz, D$_2$O):

δ 0.64

Mass spectrum

ESI-MS positive mode, *m/z***:** 435.2 [M+H]$^+$; 869.3 [2M]$^+$.

7.30. Synthesis of compounds 4.38a, 4.38b, 4.38c

Under inert atmosphere, to a stirred solution of compound **4.32** (0.13 mmol) in TEP (1.5 ml), $POCl_3$ (0.65 mmol) was added dropwise at 0 °C. The mixture was then stirred at 0 °C, monitoring progress of the reaction by reverse phase TLC (eluent $MeOH/H_2O$ 4:1). After 3 h, the mixture was diluted with H_2O (2 ml) and NaOH 2N was carefully added to pH 2. The resulting solution was stirred for 4 h at 70 °C, then pH was adjusted to 7.00. The solvent was removed by lyophilization and products **4.38a**, **4.38b** and **4.38c** were afforded isolated by reverse phase HPLC.

Compound 4.38a

Yield = 60 %

^{1}H NMR (400 MHz, D_2O):

δ 1.43 (s, 9H, $OC(CH_3)_3$); 1.26 – 1.29 (m, 4H, CH_2^{12-13}); 1.53 – 1.47 (m, 2H, CH_2^{11-14}); 1.42 – 1.47 (m, 2H, CH_2^{11-14}); 1.72 – 1. 79 (m, 1H, CH_2^{17a}); 1.98 – 2.06 (m, 1H,

CH$_2$^{17b}); 2.14 – 2.17 (m, 2H, CH$_2$^{16}); 2.92 – 3.06 (m, 2H, CH$_2$^{10}); 3.12 – 3.23 (m, 2H, CH$_2$^{15}); 3.90 – 3.78 (m, 2H, CH$_2$$^{5'a/b}$); 3.90 – 3.78 (m, 1H, CHGlu); 4.06 (dd, 1H, CH$^{4'}$); 4.11 (dd, 1H, CH$^{3'}$); 4.45 (dd, 1H, CH$^{2'}$); 4.93 – 5.04 (dd, 2H, CH$_2$Ph); 5.70 (d, 1H, CH$^{1'}$); 7.23 – 7.28 (m, 5H, Ph); 7.90 (s, 1H, CH^8).
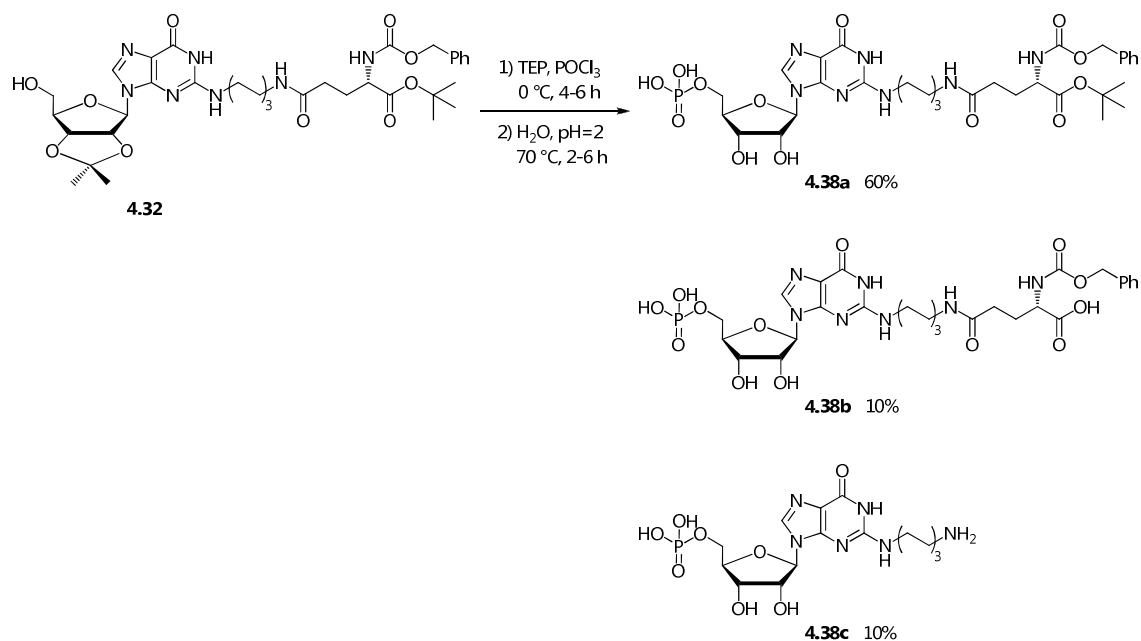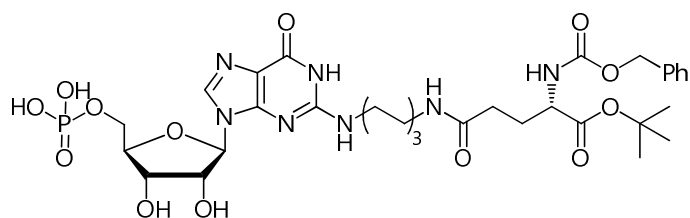
^{13}C NMR (100 MHz, D$_2$O):

δ 26.93 (OC(CH$_3$)$_3$); 25.85 – 27.87 – 28.13 – 28.84 (CH$_2$$^{11-12-13-14}$); 28.85 (CH$_2$^{16}); 35.53 (CH$_2$^{17}); 39.38 (CH$_2$^{15}); 41.53 (CH$_2$^{10}); 55.93 (CHGlu); 64.43 (C$^{5'}$); 66.88 (CH$_2$Ph); 71.67 (C$^{3'}$); 75.78 (CH$^{2'}$); 84.46 (C$^{4'}$); 87.49 (C$^{1'}$); 112.88 (C(CH$_3$)$_2$); 117.08 (C^5); 127.61 – 128.26 – 127.61 (Ph); 136.34 (C^8); 152.16 (C^4); 157.68 (C^2); 161.50 (NHCOCH$_2$Ph); 168.24 (C^6); 175.27 (COO(CH$_3$)$_3$); 179.05 (NHCOGlu).

^{31}P NMR (161.98 MHz, D$_2$O):

δ -0.42

Mass spectrum

ESI-MS positive mode, *m/z*: 782.3 [M+H]$^+$; 804.3 [M+Na]$^+$; 820.4 [M+K]$^+$.

Compound 4.38b

Yield = 10 %

^{1}H NMR (400 MHz, D$_2$O):

δ 1.18 – 1.34 (m, 4H, CH$_2$$^{12-13}$); 1.35 – 1.45 (m, 2H, CH$_2$$^{11-14}$); 1.46 – 1.56 (m, 2H, CH$_2$$^{11-14}$); 1.75 – 1.82 (m, 1H, CH$_2$^{17a}); 2.00 – 2.11 (m, 1H, CH$_2$^{17b}); 2.15 – 2.27 (m, 2H, CH$_2$^{16}); 2.96 – 3.05 (m, 2H, CH$_2$^{10b}); 3.05 – 3.15 (m, 2H, CH$_2$^{10a}); 3.19 – 3.30 (m, 2H, CH$_2$^{15}); 3.81 – 3.86 (m, 1H, CHGlu); 3.95 – 4.05 (m, 2H, CH$_2$$^{5'a/b}$); 4.22 (dd, 1H, CH$^{4'}$); 4.41 (dd, 1H, CH$^{3'}$); 4.64 (dd, 1H, CH$^{2'}$); 4.90 – 5.02 (dd, 2H, CH$_2$Ph); 5.87 (d, 1H, CH$^{1'}$); 7.23 – 7.28 (m, 5H, Ph); 7.98 (s, 1H, CH^8).

³¹P NMR (161.98 MHz, D₂O):

δ 1.03

Mass spectrum

ESI-MS positive mode, *m/z***:** 726.3 [M+H]⁺; 748.4 [M+Na]⁺); 864.3[M+K]⁺

Compound 4.38c

Yield = 10 %

¹H NMR (400 MHz, D₂O):

δ 1.23 – 1.33 (m, 6H, CH$_2$$^{12\text{-}13}$); 1.45 – 1.50 (m, 2H, CH$_2$$^{11\text{-}14}$); 2.44 – 2.49 (m, 2H, CH$_2$^{10}); 3.14 – 3.22 (m, 2H, CH$_2$^{15}); 3.78 – 3.88 (m, 2H, CH$_2$$^{5'a/b}$); 4.09 (dd, 1H, CH$^{4'}$); 4.13 (dd, 1H, CH$^{3'}$); 4.50 (dd, 1H, CH$^{2'}$); 5.70 (d, 1H, CH$^{1'}$); 7.92 (s, 1H, CH^{8}).
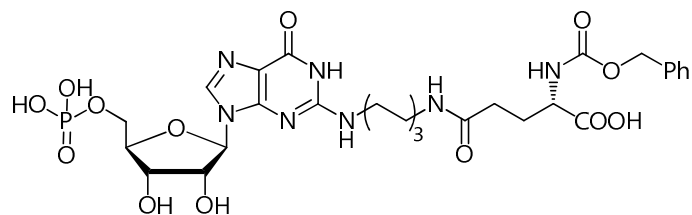
³¹P NMR (161.98 MHz, D₂O):

δ 3.96

Mass spectrum

ESI-MS positive mode, *m/z***:** 463.2 [M+H]⁺; 531.6 [M+3Na]⁺

7.31. Synthesis of compound 4.39
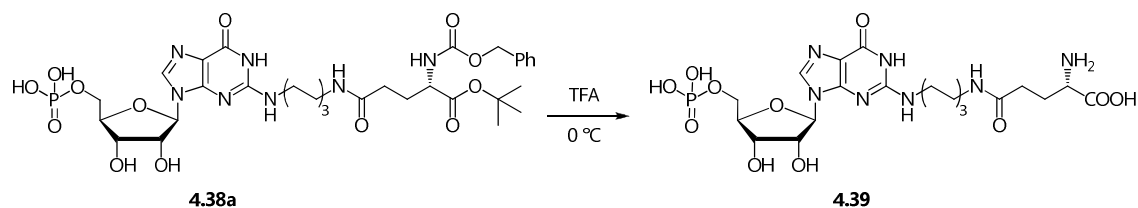
Compound **4.38a** (75 mg, 0.096 mmol) was dissolved in Trifluoroacetic acid (TFA, 1.5 ml) at 0 °C. The solution was stirred at 0 °C for 15 minutes, monitoring the course of the reaction by inverse phase TLC (MeOH/H$_2$O·0,1%TFA 1:1, R_f product = 0.46). TFA was removed under reduced pressure and the product was triturated with Et$_2$O. The supernatant was removed and the solid was resuspended diethyl ether (5 ml) and collected by filtration. The white solid was washed with ether (3 x 5 ml) and dried under reduced pressure.

Yield = 95 %

^{1}H NMR (400 MHz, D$_2$O):

δ 1.25 – 1.31 (m, 4H, CH$_2^{12-13}$); 1.53 – 1.46 (m, 2H, CH$_2^{11-14}$); 1.41 – 1.52 (m, 2H, CH$_2^{11-14}$); 1.72 – 1. 79 (m, 1H, CH$_2^{17a}$); 2.00 – 2.07 (m, 1H, CH$_2^{17b}$); 2.14 – 2.17 (m, 2H, CH$_2^{16}$); 2.87 – 3.11 (m, 2H, CH$_2^{10}$); 3.10 – 3.19 (m, 2H, CH$_2^{15}$); 3.89 – 3.71 (m, 2H, CH$_2^{5'a/b}$); 3.90 – 3.81 (m, 1H, CHGlu); 4.07 (dd, 1H, CH$^{4'}$); 4.13 (dd, 1H, CH$^{3'}$); 4.46 (dd, 1H, CH$^{2'}$); 5.69 (d, 1H, CH$^{1'}$); 7.92 (s, 1H, CH^8).

^{13}C NMR (100 MHz, D$_2$O):

δ 25.86 – 28.23 – 28.53 – 28.84 (CH$_2^{11-12-13-14}$); 29.12 (CH$_2^{16}$); 24.12 (CH$_2^{17}$); 39.31 (CH$_2^{15}$); 41.03 (CH$_2^{10}$); 57.49 (CHGlu); 64.22 (C$^{5'}$); 70.15 (C$^{3'}$); 76.90 (CH$^{2'}$); 85.16 (C$^{4'}$); 88.01 (C$^{1'}$); 117.08 (C$^{5'}$); 137.28 (C^8); 152.22 (C^4); 158.98 (C^2); 167.23 (C^6); 176.98 (**C**OOH); 181.69 (NH**C**OGlu).

^{31}P NMR (161.98 MHz, D$_2$O):

δ -0.47

Mass spectrum

ESI-MS positive mode, *m/z***:** 536.2 [M+H]$^+$; 558.1 [M+Na]$^+$; 574.1 [M+K]$^+$

7.32. Synthesis of compound 4.40
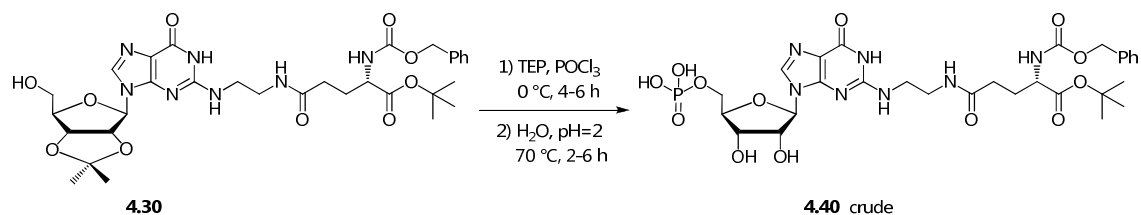
Under inert atmosphere, to a stirred solution of compound **4.30** (154.5 mg, 0.225 mmol) in TEP (1.5 ml), POCl$_3$ (0.1 ml, 1.125 mmol) was added dropwise at 0 °C. The mixture was then stirred at 0 °C, monitoring the progress of the reaction by reverse phase TLC (eluent MeOH/H$_2$O 4:1, R$_f$ product = 0.5). After 3 h, the mixture was diluted with H$_2$O (2 ml) and the pH was adjusted to 2.0 by careful addition of 2 N NaOH. The resulting solution was stirred for 4 h at 70 °C, then pH was adjusted to 7.0 with 2 N NaOH. The solvent was removed by lyophilisation; the residue was taken up in water and added to a suspension of XAD-4 resin (1 g of resin/20 mg of crude) in acidic water at pH ca 2 (HCl). The suspension was stirred until disappearance of the product in the supernatant (RP TLC monitoring). The resin was then charged into a glass column, and washed with water until negative assay for chloride ion (1% AgNO$_3$). The resin pad was then eluted with methanol and the eluate was collected in fractions. Fractions containing the product (RP TLC) were combined and evaporated under reduced pressure. The residue was re-dissolved with water and lyophilized. White solid (132 mg, 0.196 mmol).

Yield = 87 %

^{1}H NMR (400 MHz, D$_2$O):
δ 1.41 (s, 9H, OC(CH$_3$)$_3$); 1.71 – 1. 84 (m, 1H, CH$_2^{13a}$); 2.01 – 2.11 (m, 1H, CH$_2^{13b}$); 2.14 – 2.17 (m, 2H, CH$_2^{12}$); 2.88 – 3.16 (m, 2H, CH$_2^{10}$); 3.88 – 3.77 (m, 2H, CH$_2^{5'a/b}$); 3.88 – 3.75 (m, 1H, CHGlu); 4.06 (dd, 1H, CH$^{4'}$); 4.12 (dd, 1H, CH$^{3'}$); 4.51 (dd, 1H, CH$^{2'}$); 4.96 (dd, 2H, CH$_2$Ph); 5.81 (d, 1H, CH$^{1'}$); 7.21 – 7.32 (m, 5H, Ph); 7.92 (s, 1H, CH^8).

¹³C NMR (100 MHz, D₂O):

δ 27.94 (O**C**(CH₃)₃); 28.84 (CH₂^{11}); 28.85 (CH₂^{12}); 35.53 (CH₂^{13}); 43.00 (CH₂^{10}); 57.03 (CHGlu); 65.55 (C$^{5'}$); 67.75 (CH₂Ph); 72.36 (C$^{3'}$); 79.97 (CH$^{2'}$); 85.54 (C$^{4'}$); 91.94 (C$^{1'}$); 113.77 (**C**(CH₃)₂); 119.09 (C⁵); 127.60 – 129.78 – 131.61 (Ph); 139.64 (C⁸); 151.83 (C⁴); 158.98 (C²); 162.48 (NH**C**OCH₂Ph); 169.28 (C⁶); 175.29 (**C**OO(CH₃)₃); 183.09 (NH**C**OGlu).
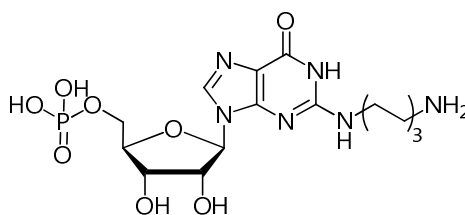
³¹P NMR (161.98 MHz, D₂O):

δ -0.39

Mass spectrum

ESI-MS positive mode, *m/z:* 726.3 [M+H]$^+$; 748.2 [M+Na]$^+$; 764.7 [M+K]$^+$

7.33. Synthesis of compound 4.41
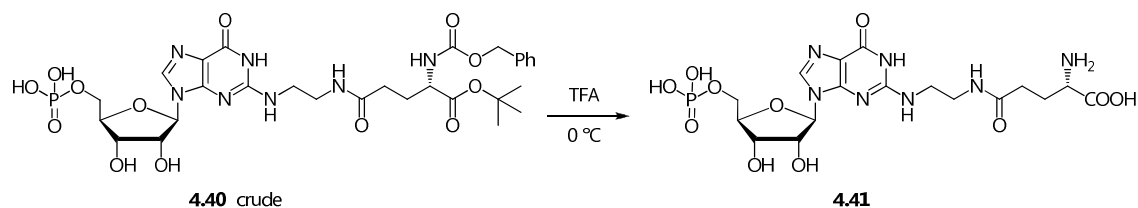
The crude compound **4.40** (132 mg, 0.196 mmol) was dissolved in Trifluoroacetic acid (TFA, 1.5 ml) in presence of a trace amount of trifluoromethanesulfonic acid (TFMS) at 0 °C. The solution was stirred at 0 °C for 15 minutes, monitoring the course of the reaction by inverse phase TLC (MeOH/H₂O·0,1%TFA 1:1).

TFA was removed under reduced pressure and the product was triturated with Et₂O. The supernatant was removed and the solid was resuspended diethyl ether (5 ml) and collected by filtration. The white solid was washed with ether (3 x 5 ml) and dried under reduced pressure.

Yield = 95 % crude product (to be purified by HPLC)

^{1}H NMR (400 MHz, D$_2$O):

δ 1.67 – 1. 83 (m, 1H, CH$_2^{13a}$); 2.02 – 2.09 (m, 1H, CH$_2^{13b}$); 2.14 – 2.17 (m, 2H, CH$_2^{12}$); 2.89 – 3.21 (m, 2H, CH$_2^{10}$); 3.89 – 3.77 (m, 2H, CH$_2^{5'a/b}$); 3.90 – 3.76 (m, 1H, CHGlu); 4.06 (dd, 1H, CH$^{4'}$); 4.12 (dd, 1H, CH$^{3'}$); 4.53 (dd, 1H, CH$^{2'}$); 5.80 (d, 1H, CH$^{1'}$); 7.92 (s, 1H, CH^8).

^{13}C NMR (100 MHz, D$_2$O):

δ 27.19 (CH$_2^{11}$); 28.79 (CH$_2^{12}$); 33.21 (CH$_2^{13}$); 46.02 (CH$_2^{10}$); 57.05 (CHGlu); 66.97 (C$^{5'}$); 72.36 (C$^{3'}$); 79.97 (CH$^{2'}$); 85.55 (C$^{4'}$); 92.36 (C$^{1'}$); 121.01 (C^5); 141.89 (C^8); 151.55 (C^4); 159.00 (C^2); 168.54 (C^6); 176.98 (**C**OOH); 183.11 (NH**C**OGlu).

^{31}P NMR (161.98 MHz, D$_2$O):

δ -0.39

Mass spectrum

ESI-MS positive mode, *m/z***:** 535.2 [M+H]$^+$; 558.1 [M+Na]$^+$); 574.2 [M+K]$^+$·

8. REFERENCES

A.O.A.C., Official Methods of Analysis, 13th ed. Association of Official Analytical Chemists. Washington D. C., **1980**, pp. 376-384.

Adebiyi, A. P.; Adebiyi, A. O.; Ogawa, T.; Muramoto, K. Purification and characterisation of antioxidative peptides from unfractionated rice bran protein hydrolysates, *Int. J. Food Sci. Technol.*, **2008**, *43*, 35-43.

Alarcón, F. J.; Moyano, F. J.; Díaz, M. Use of SDS-page in the assessment of protein hydrolysis byfish digestive enzymes, *Aquaculture International*, **2001**, *9*, 255-267.

Alarcón, F. J.; Moyano, F. J.; Díaz, M.; Fernández-Díaz, C.; Yúfera, M. (1999). Optimization of the protein fraction of microcapsules used in feeding of marine fish larvae using in vitro digestibility techniques, *Aquaculture Nutrition*, **1999**, *5*, 107-113.

Aluko, R. E. Determination of nutritional and bioactive properties of peptides in enzymatic pea, chickpea, and mung bean protein hydrolysates, *J. AOAC Int.*, **2008**, *91*, 947-956.

An, H.; Smith, D. The Bicinchoninic Acid (BCA) for determination of total protein, In *Handbook of Food Analytical Chemistry, Water, Proteins, Enzymes, Lipids, and Carbohydrates*, Wrolstad, R. E. *et al.* Eds, Wiley, **2005**, pp. 83-86.

Anderson, A. K.; Guraya, H. S. Extractability of protein in physically processed rice bran, *J. Am. Oil Chem. Soc.*, **2001**, *78*, 969-972.

Anson, M. L. The estimation of pepsin, trypsin, papain, and cathepsin with hemoglobin, *J. Gen Physiol.*, **1938**, *22*, 79-89.

Arai, S.; Yamashita, M.; Fujimaki, M. Tastes of l-glutamyl oligopeptides in relation to their chromatographic properties, *Agric. Biol. Chem.*, **1973**, *37*, 151-156.

Arzu, A.; Mayorga, H.; Gonzales, J.; Rolz, C. Enzymatic hydrolysis of cottonseed protein. *J. Agric. Food Chem.*, **1972**, *20*, 805-809.

Bagnasco, L.; Pappalardo, V. M.; Meregaglia, A.; Kaewmanee, T.; Ubiali, D.; Speranza, D.; Cosulich, M. E. Use of food-grade proteases to recover umami protein–peptide mixtures from rice middlings, *Food Res. Int.*, **2013**, *50*, 420-427.

Barbana, C.; Boye, J. I. Angiotensin I-converting enzyme inhibitory activity of chickpea and pea protein hydrolysates, *Food Res. Int.*, **2010**, 43, 1642-1649.

Beckham, L. J.; Fessler, W. A.; Kise, M. A. Nitrosyl Chloride, *Chem. Rev.*, **1951**, *48*, 319-396.

Behrens, M.; Meyerhof, W.; Hellfritsch, C.; Hofmann, T. Sweet and umami taste: natural products, their chemosensory targets, and beyond, *Angew. Chem. Int. Ed.*, **2011**, *50*, 2220-2242.

Benjakul, S.; Morrissey, M. T. Protein hydrolysates from pacific whiting solid wastes, *J. Agric. Food. Chem.*, **1997**, *45*, 3423-3430.

Blat, D.; Weiner, L.; Youdim, M. B. H.; Fridkin, M. A novel Iron-Chelating Derivate of the neuroprotective Peptide NAPVSIPQ shows superior antioxidant and autoneurodegenerative capabilities, *J. Med. Chem.*, **2008**, *51*, 126-134.

Bo, L.; Chen, F.; Wang, X.; Ji, B.; Wu, Y. Isolation and identification of antioxidative peptides from porcine collagen hydrolysate by consecutive chromatography and electrospray ionization-mass spectrometry, *Food Chem.*, **2007**, *102*: 1135-1143.

Bodor, N.; Dewar, M. J. S.; Harget, A. J. Ground States of Conjugated Molecules. XIX.' Tautomerism of Heteroaromatic Hydroxy and Amino Derivatives and Nucleotide Bases, *J. Am. Chem. Soc.*, **1970**, *92*, 2929-2936.

Boschin, G.; Scigliuolo, G. M; Resta, D.; Arnoldi, A. ACE-inhibitory activity of enzymatic protein hydrolysates from lupin and other legumes, *Food Chem.*, **2014**, *145*, 34-40.

Bressi, J. C.; Choe, J.; Hough, M. T.; Buckner, F. S.; Van Voorhis, W. C.; Verlinde, C. L.; Hol, W. G.; Gelb, M. H. Adenosine Analogues as Inhibitors of Trypanosoma brucei Phosphoglycerate Kinase: Elucidation of a Novel Binding Mode for a 2-Amino-N^6-Substituted Adenosine, *J. Med. Chem.*, **2000**, *43*, 4135-4150.

Bridson, P. K.; Markiewicz, W.; Reese, C. B. Acylation of 2',3',5'-Tri-*O*-acetylguanosine, *J. Chem. Soc., Chem. Comm.*, **1977**, 791-792.

Cairoli, P.; Pieraccini, S.; Sironi, M.; Morelli, C. F.; Speranza, G.; Manitto, P. Studies on umami taste. Synthesis of new guanosine 5'-phosphate derivatives and their synergistic effect with monosodium glutamate, *J. Agric. Food Chem.*, **2008**, *56*, 1043-1050.

Callaway, J. C. Hempseed as a nutritional resource: An overview, *Euphytica*, **2004**, *140*, 65-72.

Calleri, E.; Ceruti, S.; Cristalli, G.; Martini, C.; Temporini, C.; Parravicini, C.; Volpini, R.; Daniele, S.; Caccialanza, G.; Lecca, D., Lambertucci, C.; Trincavelli, M. L.; Marucci, G.; Wainer, I. W.; Ranghino, G.; Fantucci, P.; Abbracchio, M. P.; Massolini, G. Frontal Affinity Chromatography-Mass Spectrometry Useful for Characterization of New Ligands for GPR17 Receptor, *J. Med. Chem.*, **2010**, 53, 3489-3501.

Calleri, E.; Fracchiolla, G.; Montanari, R.; Pochetti, G.; Lavecchia, A.; Loiodice, F.; Laghezza, A.; Piemontese, L.; Massolini, G.; Temporini, C. Frontal affinity chromatography with MS detection of the ligand binding domain of PPAR gamma receptor: ligand affinity screening and stereoselective ligand-macromolecule interaction, *J. Chromatogr. A*, **2012**, 1232, 84-92.

Calleri, E.; Temporini, C.; Caccialanza, G.; Massolini, G. Target-based drug discovery: the emerging success of frontal affinity chromatography coupled to mass spectrometry, *ChemMedChem*, **2009**, *4*, 905-916.

Calleri, E.; Temporini, C.; Massolini,G. Frontal affinity chromatography in characterizing immobilized receptors, *J. Pharm. Biomed. Anal.*, **2011**, *54*, 911-925.

Casu, F.; Hartson, R. K.; Chiacchio, M. A.; Gumina, G. Synthesis of 2'-substituted inosine analogs via unusual masking of the 6-hydroxyl group, *Nucleos. Nucleot. Nucleic Acids*, **2012**, *31*, 224-235.

Chaudari, N.; Landin, A. M.; Roper, S. D. A metabotropic glutamate receptor variant functions as a taste Receptor, *Nat. Neurosci.*, **2000**, *3*, 113-119.

Chandrashekar, J.; Hoon, M. A.; Ryba, N. J. P.; Zuker, C. S. The receptors and cells for mammalian taste, *Nature*, **2006**, *444*, 288-294.

Cheftel, J. C.; Cuq, J. L.; Lorient, D. Amino acids, peptides, and proteins, In *Food chemistry*, Fennema, O. R. Ed., **1985**, New York: Marcel Dekker, pp. 246-369.

Chen, H. M.; Muramoto, K.; Yamauchi, F. Structural analysis of antioxidative peptides from soybean *β*-conglycinin, *J. Agric. Food Chem.*, **1995**, *43*, 574-578.

Chen, J. R.; Yang, S.-C.; Suetsuna, K.; Chao, J. C. J. Soybean protein-derived hydrolysate affects blood pressure in spontaneously hypertensive rats, *J. Food Biochem.*, **2004**, *28*, 61-73.

Cherubini, F. The biorefinery concept: Using biomass instead of oil for producing energy and chemicals, *Energy Conversion and Management*, **2010**, *51*, 1412-1421.

Clemente, A. Enzymatic protein hydrolysates in human nutrition, *Trends Food Sci. Tech.*, **2000**, 11, 254-262.

Córdoba, J. J.; Rojas, T. A.; González, C. G.; Barroso, J. V. Evolution of free amino acids and amines during ripening of Iberian cured ham, *J. Agric. Food Chem.*, **1994**, *42*, 2296-2301.

Cunnane, S. C.; Ganguli, S.; Menard, C.; Liede, A. C.; Hamadeh, M. J.; Chen, Z. Y.; Wolever, T. M.; Jenkins, D. J. High alpha-linolenic acid flaxseed (Linum usitatissimum): some nutritional properties in humans, *Br. J. Nutr.*, **1993**, *69*, 443-453.

Cupp-Enyard, C. Sigma's Non-specific Protease Activity Assay - Casein as a Substrate, *J. Vis. Exp.*, **2008**, *19*, 899-900.

Cushman, D. W.; Cheung, H. S. Spectrophotometric assay and properties of the angiotensin-converting enzyme of rabbit lung, *Biochem. Pharmacol.,*, **1971**, *20*, 1637-1648.

Damodaran, S. Interfaces, protein films and foams, *Adv. Food Nutr. Research*, **1990**, *34*, 1-79.

Damodaran, S. Protein-stabilized foams and emulsions, In *Food proteins and their applications*, Damodaran, S. & Paraf A. Eds., New York: Marcel Dekker, **1997**, pp. 7-110.

De Carvalho-Silva, L. B.; Bertoldo-Pacheco, M. T.; Bertoldo, R.; De Carvalho Veloso, C.; Costa Teodoro, L.; Giusti-Paiva, A.; Barboza Lollo, P. C.; Soncini, R. Anti-inflammatory activities of enzymatic (alcalase) hydrolysate of a whey protein concentrate, *African J. Biotech.*, **2012**, 11, 2993-2999.

De Rijke, E.; Ruisch, B.; Bakker, J.; Visser, J.; Leenen, J.; Haiber, S.; De Klerk, A.; Winkel, C.; König, T. LC-MS study to reduce ion suppression and to identify *N*-lactoylguanosine 5'-monophosphate in bonito: a new umami molecule?, *J. Agric. Food Chem.*, **2007**, *55*, 6417-6423.

Doyle, M. P.; Bosch, R. J.; Seites, P. G. Alkyl Nitrite-Metal Halide Deamination Reactions. 5. *In Situ* Generation of Nitrosyl Halides. Effective Product Control from Nitrosyl Chloride Diazotization of Primary Aliphatic Amines in *N,N*-Dimethylformamide, *J. Org. Chem.*, **1978**, *43*, 4120-4125.

Fernandez, Q. A.; Macarulla, M. T. Composition and functional properties of protein isolates obtained from commercial legumes grown in northern Spain. *Plant Foods for Human Nutrition*, **1997**, *51*, 331-342.

Ferrari, F.; Fumagalli, M.; Profumo, A.; Viglio, S.; Sala, A.; Dolcini, L.; *et al.* Deciphering the proteomic profile of rice (Oryza sativa) bran, A pilot study, *Electrophoresis*, **2009**, *30*, 4083-4094.

Festring, D.; Hofmann, T.; Discovery of N^2-(1-carboxyethyl)guanosine 5'-monophosphate as an umami-enhancing Maillard-modified nucleotide in yeast extracts, *J. Agric. Food Chem.*, **2010**, *58*, 10614–10622.

Festring, D.; Hofmann, T. Systematic Studies on the Chemical Structure and Umami Enhancing Activity of Maillard-Modified Guanosine 5'-Monophosphates, *J. Agric. Food Chem.*, **2011a**, *59*, 665-676.

Festring, D.; Brockhoff,A.; Meyerhof, W.; Hofmann, T. Stereoselective Synthesis of Amides Sharing the Guanosine 50-Monophosphate Scaffold and Umami Enhancement Studies Using Human Sensory and hT1R1/rT1R3 Receptor Assays, *J. Agric. Food Chem.*, **2011b**, *59*, 8875-8885.

Folin, O.; Ciocalteau, V. On tyrosine and tryptophane determinations in proteins, *J. Biol. Chem.*, **1927**, *73*, 627-650.

Francom, P.; Robins, M. J. Nucleic acid related compounds. 118. Nonaqueous diazotization of aminopurine derivatives. Convenient access to 6-halo- and 2,6-dihalopurine nucleosides and 2'-deoxynucleosides with acyl or silyl halides, *J. Org. Chem.*, **2003**, *68*, 666-669.

Frazer, G. S.; Bucci, D. M. SDS-PAGE characterization of the proteins in equine seminal plasma, *Theriogenology*, **1996**, *16*, 579-591.

Frerot, E; Escher, S. N.; to Firmenich, US Pat. 5780090 (Chem. Abstr. 2004, 141, 206089).

Frie, B.; Stocker, R.; Ames, B. N. Antioxidant defences and lipid peroxidation in human blood plasma, *Proc. Natl. Acad. Sci.*, **1988**, *37*, 569-671.

Gbogouri, G. B.; Linder, M.; Fanni, J.; Parmentier, M. Influence of hydrolysis degree on the functional properties of salmon byproducts hydrolysis, *J. Food Sci.*, **2004**, *69*, c615-c622.

Giese, J. Proteins as ingredients: types, functions, applications, *Food Technol.*, **1994**, 48, 50-60.

Girgih, A. T.; Udenigwe, C. C.; Li, H.; Adebiyi, A. P.; Aluko, R. E. Kinetics of Enzyme Inhibition and Antihypertensive Effects of Hemp Seed (Cannabis sativa L.) Protein Hydrolysates, J. Am. Oil Chem. Soc., 2011, 88, 1767-1774.

Gnanasambandam, R.; Hettiararchchy, N. S. Protein concentrates from unstabilized and stabilized rice bran, preparation and properties, *J. Food Sci.*, **1995**, *60*, 1066-1069.

Green, T. W.; Wuts, P. G. M. Protective Groups in Organic Synthesis, Wiley-Interscience, New York, **1999**, 372-381, 404-408, 415-419, 728-731.

Guang, C.; Phillips, R. D. Plant food-derived angiotensin I converting enzyme inhibitory peptides, *J. Agric. Food Chem.*, **2009**, *57*, 5113-5120.

Guille, K.; Clegg, W. Anhydrous guanine: a synchrotron study, *Acta Cryst. C*, **2006**, *C62*, o515-o517.

Gunic, E.; Amador, R.; Rong, F.; Abt J.W.; An H.; Hong Z.; Girardet J. L. Synthesis of Nucleoside Libraries on Solid Support. I. N,N-Disubstituted Diaminopurine Nucleosides, *Nucleos. Nucleot. Nucleic Acids.*, **2004**, *23*, 495-499.

Hage, D. S.; Tweed, S. S. Recent advances in chromatographic and electrophoretic methods for the study of drug-protein interactions, *J. Chromatogr. B*, **1997**, *699*, 499-525.

Halling, P. J. Protein-stabilized foams and emulsions, *Crit. Rev. Food Sci. Nutr.*, **1981**, *21*, 155-203.

Halliwell, B.; Aeschbacht, R.; Loligert, J.; Aruoma, O. I. The Characterization of Antioxidants, *Food Chem. Toxicol.*, **1995**, *33*, 601-617.

Halpern, B. P. Glutamate and the flavour of foods, *J. Nutr.*, **2000**, *130*, 910S-914S.

Hamada, J. S. Characterization and functional properties of rice bran proteins modified by commercial exoproteases and endoproteases, *J. Food Sci.*, **2000a**, *65*, 305-310.

Hamada, J. S. Ultrafiltration of partially hydrolyzed rice bran protein to recover value-added products, *J. Am. Oil Chem. Soc.*, **2000b**, *77*, 779-784.

Hamada, J. S. Use of proteases to enhance solubilization of rice bran proteins, *J. Food Biochem.*, **1999**, *23*, 307-321.

Hamada, J. S.; Spanier, A. M.; Bland, J. M.; Diack, M. Preparative separation of value-added peptides from rice bran proteins by high-performance liquid chroma-tography, *J. Chromat. A*, **1998**, *827*, 319-327.

Hermann T., Industrial production of amino acids by coryneform bacteria, *J. Biotechnol.*, **2003**, *104*, 155-172.

Huang, D. J.; Ou, B. X.; Prior, R. L. The chemistry behind antioxidant capacity assays. *J. Agric. Food Chem.*, **2005**, *53*, 1841-1856.

Huang, H.; Shu, S. C.; Shih, J. H.; Kuo, C. J.; Chiu, I. D. Antimony trichloride induces DNA damage and apoptosis in mammalian cells, *Toxicology*, **1998**, *129*, 113-123.

IEA. IEA bioenergy Task 42 on biorefineries: co-production of fuels, chemicals,power and materials from biomass. In: Minutes of the third Task meeting,Copenhagen, Denmark, 25–26 March 2007 <http://www.biorefinery.nl/ieabioenergy-task42/>; **2008**.

Ikeda, K. 1908, Japanese Patent 14805.

Ikeda, K. New Seasonings, *Chem. Senses*, **2002**, *27*, 847 (translated from J. Tokyo Chem. Soc., 1909, 30, 820).

Ikemoto, T.; Haze, A.; Hatano, H.; Kitamoto, Y.; Ishida, M.; Nara, K. Phosphorylation of Nucleosides with Phosphorus Oxychloride in Trialkyl Phosphate. *Chem. Pharm. Bull.*, **1995**, *43*, 210-215.

Imai, K.; Marumoto, R.; Kobayashi, K.; Yoshioka, Y.; Toda, J.; Honjo, M. Synthesis of compounds related to inosine 5′-phosphate and their flavor enhancing activity. IV. 2-Substituted inosine 5′-phosphate, *Chem. Pharm. Bull.*, **1971**, *19*, 576-586.

Jeon, Y. J.; Byun, H. G.; Kim, S. K. Improvement of functional properties of cod frame protein hydrolysates using ultrafiltration membranes, *Process. Biochem.*, **1999**, *35*, 471-478.

Jo, M. N.; Lee, Y. M. Analyzing the sensory characteristics and taste-sensor ions of MSG substitutes. *J. Food Sci.*, **2008**, *73*, S191-S198.

Joo, J. H.; Yi, S. D.; Lee, G. H.; Lee, K. T.; Oh, M. J. Antimicrobial Activity of Soy Protein Hydrolysate with Asp. saitoi Protease, *J. Korean Soc. Food Sci. Nutr.*, **2004**, 33, 229-235

Kadowaki, M. Production of rice protein by alkaline extraction improves its digestibility, *J. Nutr. Sci. Vitaminol.*, **2006**, *52*, 467-472.

Kamm, B.; Kamm, M. Principles of biorefineries, Appl. Microbiol. Biotechnol. 2004, 64, 137–145.

Kaneko, S.; Kumazawa, K.; Masuda, H.; Henze, A.; Hofmann, T. Molecule and sensory studies on the umami taste of Japanese green tea, *J. Agric. Food Chem.*, **2006**, *54*, 2688-2694.

Kemal, O.; Reese, C. B. Sodium borohydride reduction of adducts of primary amines with aldehydes and *p*-thiocresol. The alkylation of heterocyclic and aromatic amino-compounds, *J. Chem. Soc., Perkin Trans. 1*, **1981**, 1569-1573.

Kim, J.-H.; Lee, B.-H.; Lee, S.-H. Production of Ribonucleotides by autolysis of Hansenula anomala grown on Korean ginseng steaming effluent, *J. Biosci. Bioengineering*, **2002**, *93*, 318-321.

Kim, J. J.; Lee, M. J. Isolation and Characterization of Edestin from Cheungsam Hempseed, *J. Appl. Biol. Chem.*, **2011**, *54*, 84-88.

Kim, S. Y.; Park, P. S. W.; Rhee, K. C. Functional properties of proteolytic enzyme modified soy protein isolate, *J. Agric. Food Chem.*, **1990**, *38*, 651-657.

Kinsella, J. E. Functional properties of proteins, possible relationships between structure and function in foams, *Food Chem.*, **1981**, *7*, 273-288.

Ku, H.; Barrio, J. R. Convenient Synthesis of Arylhalides from Arylamines via Treatment of 1-Aryl-3,3-dialkyltriazenes with Trimethylsilyl Halides, *J. Org. Chem.*, **1981**, *46*, 5239-5241.

Kumagai, T.; Kawamura, H.; Fuse, T.; Watanabe, T.; Saito, Y.; Masumura, T.; Watanabe, R.; Kadowaki, M. Production of rice protein by alkaline extraction improves its digestibility, *J. Nutr. Sci. Vitaminol.*, **2006**, *52*, 467-472.

Kuninaka, A. Studies on taste of ribonucleic acid derivatives, *J. Agric. Chem. Soc. Jpn.*, **1960**, *34*, 489-493.

Kuninaka, A.; Kumagai, M.; Fujiyama, K.; Ogura, M.; Sakata, S.; Yonei, S. Flavor activity of sulfur-containing compounds related to flavor nucleotides, *Agric. Biol. Chem.*, **1980**, *44*, 1437-1439.

Kuninaka, A. Taste and flavor enhancers, In *Flavor Researchs Recent Advances*; Teranishi, R.; Flath, R. A.; Sugisawa, H., Eds.; Marcel Dekker: New York, **1981**; pp 305-353, and references cited therein.

Kunishima, N.; Shimada, Y.; Tsuji, Y.; Sato, T.; Yamamoto, M.; Kumasaka, T.; Nakanishi, S.; Jinagami, H.; Morikawa, K. Structural basis of glutamate recognition by a dimeric metabotropic glutamate receptor, *Nature*, **2000**, *407*, 971-977.

Laemmli, U. K. Cleavage of structural proteins during the assembly of the head of bacteriophage T4. *Nature*, **1970**, *227*, 680-685.

Lau A. Y.; Roux, B. The hidden energetics of ligand binding and activation in a glutamate receptor, *Nat. Struct. Mol. Biol.*, **2011**, *18*, 283-287.

Levine, M.; Ramsey, S. C.; Daruwara, R. Criteria and recommendation for Vitamin C intake, *J. Am. Med. Assoc.*, **1991**, *281*, 1415-1423.

Li, X.; Staszewski, L.; Xu, H.; Durick, K.; Zoller, M.; Adler, E. Human receptors for sweet and *umami* taste, *Proc. Natl Acad. Sci. USA*, **2002**, *99*, 4692-4696.

Li, B.; Bemish, R.; Buzon, R. A.; Chiu, C. K. F.; Colgan, S. T.; Kissel, W.; Le, T.; Leeman, K. R.; Newell, L.; Roth, J. Aqueous phosphoric acid as a mild reagent for deprotection of the *t*-butoxycarbonyl group. *Tetrahedron Lett.*, **2003**, *44*, 8113-8115.

Li, G. H.; Qu, M. R.; Wan, J. Z.; You, J. M. Antihypertensive effect of rice protein hydrolysate with in vitro angiotensin I-converting enzyme inhibitory activity in spontaneously hypertensive rats, *Asia Pac. J. Clin. Nutr.*, **2007**,16(1), 275-80.

Lin, S. Y.; Wang, C. C.; Lu, Y. L.; Wu, W. C.; Hou, W.C. Antioxidant, anti-semicarbazide-sensitive amino oxidase, and anti-hypertensive activities of gerani in isolated from Phyllanthus urinaria. *Food Chem. Toxicol.*, **2008**, *46*, 2485-2492.

Lindemann, B.; Ogiwara, Y.; Ninomiya, Y. The Discovery of Umami. *Chem. Senses*, **2002**, *27*, 843-844.

Liu, D. Z.; Wu, W. C.; Liang, H. J.; Hou, W. C. Antioxidant and semicarbazide-sensitive amine oxidase inhibitory activities of alginic acid hydroxamates, *J. Sci. Food Agric.*, **2007**, *87*, 138-146.

Lobo, V.; Patil, A.; Phatak, A.; Chandra, N. Free radicals, antioxidants and functional foods: Impact on human health, *Pharmacogn Rev.*, **2010**, *4*, 118–126.

Löliger, J. Function and importance of glutamate for savory foods, *J. Nutr.*, **2000**, *130*, 915S-920S.

Lopez Cascales J. J.; Oliveira Costa, S. D.; de Groot, B. L.; Eric Walters, D. Binding of glutamate to the umami receptor, *Biophys. Chem.*, **2010**, *152*, 139-144.

Lu, R. R.; Qian, P.; Sun, Z.; Zhou, X. H.; Chen, T. P.; He, J. F.; Zhang, H.; Wu, J. Hempseed protein derived antioxidative peptides: Purification, identification and protection from hydrogen peroxide-induced apoptosis in PC12 cells, *Food Chem.*, **2012**, *123*, 1210-1218.

Lund, P. L-Glutamine and L-Glutamate: UV-Method with Glutaminase and Glutamate Dehydrogenase, In *Methods of Enzymatic Analysis, Volume 8*, Bergmeyer, H. U. Ed., VCH, Verlagsgesellschaft, Weinheim, **1986**, pp. 357-363.

Ma, Y.; Xiong, Y. L. Antioxidant and bile acid binding activity of buckwheat protein *in vitro* digests, *J. Agric. Food Chem.*, **2009**, *57*, 4372-4380.

Manneheim, A.; Cheryan, M. Enzyme-modified proteins from corn gluten meal, Preparation and functional properties, *J. Am. Oil Chem. Soc.*, **1992**, *69*, 1163-1169.

Marambe, P. W. M. L. H. K.; Shand, P. J.; Wanasundara, J. P. D. An In-vitro Investigation of Selected Biological Activities of Hydrolysed Flaxseed (Linum usitatissimum L.) Proteins, *J. Am. Oil. Chem. Soc.*, **2008**, *85*, 1155-1164.

Marcus, B. Unleashing the power of umami, *Food Technol.*, **2009**, *63*, 23-35.

Matsuda, A.; Shinozaki, M.; Yamaguchi, T.; Homma, H.; Nomoto, R.; Miyasaka, T.; Watanabe, Y.; Abiru, T. Nucleosides and nucleotides. 103. 2-Alkynyladenosines: a novel class of selective adenosine A2 receptor agonists with potent antihypertensive effects, *J. Med. Chem.*, **1992**, *35*, 241-252.

McClements, D. J.; Decker, E. A. Eds. Proteins in food processing, In *Designing Functional Foods*, Woodhead Publishing, Cambridge, UK, **2009**.

Miller Jr., I. J. In *Handbook of Olfaction and Gustation*, Doty R. L., Ed., Marcel Dekker, New York, **1995**, pp. 521-547.

Mithen, R. Sulphur-Containing Compounds, In *Plant Secondary Metabolites*, A. Crozier, A.; Clifford, M. N.; Ashihara, H. Eds., Blackwell Publishing Ltd: Oxford, UK, **2006**, pp. 25-46.

Moaddel, R.; Lu, L.; Baynham. M.; Wainer, I. W. Immobilized receptor- and transporter-based liquid chromatographic phases for on-line pharmacological and biochemical studies: a mini-review, *J. Chromatogr. B*, **2002**, *768*, 41-53.

Molyneux, P. The use of the stable free radical diphenylpicrylhydrazyl (DPPH) for estimating antioxidant activity. *Songklanakarin J. Sci. Technol.*, **2004**, *26*, 211-219.

Morelli, C. F.; Manitto, P.; Speranza, G. Study on umami taste: the MSG taste-enhancing activity of N^2-alkyl and N^2-alkanoyl-5'-guanylic acids having a sulfoxide group inside the N^2-substituent, *Flavour Fragr. J.*, **2011**, *26*, 279-281.

Mouritsen, O. G. Umami flavour as a means of regulating food intake and improving nutrition and health, *Nutrition and Health*, **2012**, *21*, 56-75.

Mouritsen, O. G.; Khandelia H. Molecular mechanism of the allosteric enhancement of the umami taste sensation, *FEBS J.*, **2012**, *279*, 3112-3120.

Nagodawithana, T. W. *Savory Flavors*, Esteekay Associates, Inc: Milwaukee, USA, **1995**; pp 297-333.

Nagodawithana, T. W.; Nelles, L.; Trivedi, N. B.. Pasupuleti V. K.; Demain, A. Eds, State of the Art Manufacturing of Protein Hydrolysates, In *Protein hydrolysates in biotechnology*. Springer, The Netherlands, **2010**, *2*, 11-32.

Nair, V.; Fasbender, A. J. C-2 functionalized N^6-cyclosubstituted adenosines: highly selective agonists for the adenosine A$_1$ receptor. *Tetrahedron*, **1993**, *49*, 2169-2184.

Nair, V.; Ma, X.; Shu, Q.; Zhang, F.; Uchil, V.; Cherukupalli, G. R. IMPDH as a biological probe for RNA antiviral drug discovery: synthesis, enzymology, molecular docking, and antiviral activity of new ribonucleosides with surrogate bases, *Nucleos. Nucleot. Nucleic Acids*, **2007**, *26*, 651-654.

Nair, V.; Turner, G. A.; Buenger, G. B; Chamberlain, S. D. New Methodologies for the Synthesis of C-2 Functionalized Hypoxanthine Nucleosides, *J. Org. Chem.*, **1988**, *53*, 3051-3057.

Nakamura, Y.; Yamamoto, N.; Sakai, K., Okubo, A.; Yamazaki, S.; Takano, T. Purification and characterization of angiotensin I-converting enzyme inhibitors from sour milk, *J. Dairy Sci.*, **1995**, *78*, 777-783.

Nelson, G.; Chandrashekar, J.; Hoon, M. A.; Feng, L.; Zhao, G.; Ryba, N. J.; Zuker, C. S. An amino-acid taste receptor, *Nature*, **2002**, *416*, 199-202.

Nelson, G.; Hoon, M. A.; Chandrashekar, J. Zhang, Y.; Ryba, N. J. P.; Zucker, C. S. Mammalian sweet taste receptors, *Cell*, **2001**, *106*, 381-390.

Ninomiya, K. Umami, a universal taste, *Food. Rev. Internat.*, **2002**, *18*, 23-28.

Nugent, J. H .A.; Jones, W. T.; Jordan, D. J.; Mangan, J. L. Rates of proteolysis in the rumen of the soluble proteins casein, fraction I (18S) leaf protein, bovine serum albumin and bovine submaxilary mucoprotein, *British J. Nutr.*, **1983**, *50*, 357-368.

Ohno, M.; Gao, Z.-G.; Van Rompaey, P.; Tchilibon, S.; Kim, S.-K.; Harris, B. A.; Gross, A. S.; Duong, H. T.; Van Calenbergh, S.; Jacobson, K. A. Modulation of adenosine receptor affinity and intrinsic efficacy in adenine nucleosides substituted at the 2-position, *Bioorg. Med. Chem.*, **2004**, *12*, 2995-3007.

Okumura, S.; Eguchi, S.; Ogawa, W.; Suzuki, K. Peripheral neural basis for behavioral discrimination between glutamate and the four basic taste substances in mice. Methods for preparation of foods, beverages and seasoning having tomato flavor Japanese Patent Publication (kokoku), **1968**, No. 43–11731.

Oomah, B. D.; Busson, M.; Godfrey, D. V; Drover, J. C. G. Characteristics of hemp (*Cannabis sativa* L.) seed oil, *Food Chem.*, **2002**, *76*, 33-43.

Oomah, B. D.; Mazza, G. Flaxseed proteins: a review, *Food Chem.*, **1993**, *48*, 109-114.

Ottinger, H.; Hofmann, T. Identification of the taste enhancer alaypyridaine in beef broth and evaluation of its sensory impact by taste reconstitution experiments, *J. Agric. Food Chem.*, **2003**, *51*, 6791-6796.

Patel, S.; Cudney, R.; McPherson, A. Crystallographic characterization and molecular symmetry of edestin, a legumin from hemp. *J. Mol. Biol.*, **1994**, *235*: 361-363.

Pearce, K. N.; Kinsella, J. E. Emulsifying properties of proteins, evaluation of a turbidimetric technique, *J. Agric. Food Chem.*, **1978**, *26*, 716-723.

Peña-Ramos, E. A.; Xiong, Y. L.; Arteaga, G. E. Fractionation and characterization for antioxidant activity of hydrolyzed whey protein, *J. Sci. Food Agric.*, **2004**, *84*, 1908-1918.

Pettersen, E. F.; Goddard, T. D.; Huang, C. C.; Couch, G. S.; Gteenblatt, D. M.; Meng, E. C.; Ferrin, T. E. UCSF Chimera – a visualization system for exploratory research and analysis, *J. Comput. Chem.*, **2004**, *25*, 1605-1612. www.cgl.ucsf.edu/chimera

Pommer, K. New proteolytic enzymes for the production of savory ingredients. *Cereal Foods World*, **1995**, *40*, 745-748.

Pons, J.-F.; Fauchère, J.-L.; Lamaty, F.; Molla, A.; Lazaro, R. A constrained diketopiperazine as a new scaffold for the synthesis of peptidomimetics, *Eur. J. Org. Chem.*, **1998**, *5*, 853-859.

Prior, R. L.; Wu, X. L.; Schaich, K. Standardized methods for the determination of antioxidant capacity and phenolics in foods and dietary supplements, *J. Agric. Food Chem.*, **2005**, *53*, 4290-4302.

Puchades, R.; Lemieux, L.; Simard, R. E. Evolution of free amino acids during the ripening of cheddar cheese containing added lactobacilli strains, *J. Food Sci.*, **1989**, *54*, 885-887, 945.

Qian, M.; Glaser R. Demonstration of an alternative mechanism for G-to-G cross-link formation, *J. Am. Chem. Soc.*, **2005**, 127, 880-887.

Ramos, M.; Caceres, I.; Polo, C.; Alonso, L.; Juarez, M. Effect of freezing on soluble nitrogen fraction of Cabrales Cheese, *Food Chem.*, **1987**, *24*, 271-278.

274

Rassin, D. K.; Sturman, J. A.; Gaull, G E. Taurine and other amino acids in milk and other mammals, *Early Hum. Dev.*, **1978**, *2*, 1-13.

Ribeiro, B. D.; Barreto, D. W.; Coelho, M. A. Z. Enzyme-Enhanced Extraction of Phenolic Compounds and Proteins from Flaxseed Meal, *ISRN Biotechnology*, **2013**, *vol. 2013*, Article ID 521067, 6 pages.

Robins, M. J.; Uznański, B. Nucleic acid related compounds. 33. Conversions of adenosine and guanosine to 2,6-dichloro, 2-amino-6-chloro, and derived purine nucleosides, *Can. J. Chem.*, **1981**, *59*, 2601-2607.

Rock, C. L.; Jacob, R. A.; Bowen, P. E. Update o biological characteristics of the antioxidant micronutrients- Vitamin C, Vitamin E and the carotenoids, *J. Am. Diet. Assoc.*, **1996**, *96*, 693-702.

Rotzoll, N.; Dunkel, A.; Hofmann, T. Activity-guided identification of (S)-malic acid 1-O- D -glucopyranoside (morelid) and γ -aminobutyric acid as contributors to umami taste and mouth-drying oral sensation of morel mushrooms (Morchella deliciosa Fr.), *J. Agric. Food Chem.*, **2005**, *53*, 4149-4156.

Sammour, R. H. Proteins of Linseed (*Linum usitatissimum* L.), extraction and characterization by electrophoresis, *Bot. Bull. Acad. Sin.*, **1999**, *40*, 121-126.

San Gabriel, A. M.; Maekawa, T.; Uneyama, H.; Yoshie, S.; Torii, K. mGluR1 in the fundic glands of rat stomach, *FEBS Lett.*, **2007**, *581*, 1119-1123.

Sanchez-Moreno, C. Review: Methods Used to Evaluate the Free Radical Scavenging Activity in Foods and Biological Systems, *Food Sci. Tech. Int.*, **2002**, *8*, 121-137.

Sanghvi, M.; Moaddel, R.; Wainer, I.W. The Development and Characterization of Protein-Based Stationary Phases for Studying Drug-Protein and Protein-Protein Interactions, *J. Chromatogr. A*, **2011**, *1218*, 8791-8798.

Sano, C. History of glutamate production, *Am. J. Clinical Nutr.*, **2009**, *90* (Suppl.), 728S-735S.

Saunders, R. M. The properties of rice bran as a foodstuff. *Cereal Foods World*, **1990**, *35*, 632-636.

Savoie, L. Digestion and absorption of food: usefulness and limitations of in vitro models, *Can. J. Physiol. Pharmacol.*, **1994**, *72*, 407-414.

Sbarbati, A.; Merigo, F.; Benati, D.; Tizzano, M.; Bernardi, P.; Osculati, F. Laryngeal chemosensory clusters, *Chem. Senses*, **2004**, *29*, 683-92.

Schiel, J. E.; Joseph, K. S.; Hage, D. S. Biointeraction affinity chromatography: general principles and recent development, *Adv. Chromatogr.*, **2010**, *48*, 145-193.

Schlichtherle-Cerny, H.; Affolter, M. ; Cerny, C. Taste-active glycoconjugates of glutamate: new umami compounds, in Taste research: chemical and physiological aspects, *ACS Symposium Series*, **2004,** *867*, 210-222.

Schlichtherle-Cerny, H.; Amado, R. Analysis of taste-active compounds in an enzymatic hydrolysate of deamidated wheat gluten, *J. Agric. Food Chem.*, **2002**, *50*, 1515-1522.

Schriemer, D. C. Biosensor alternative: frontal affinity chromatography, *Anal. Chem.*, **2004**, *76*, 440A-448A.

Shalaby, S. M.; Zakora, M.; Otte, J. Performance of two commonly used angiotensin converting enzyme inhibition assays using FA-PGG and HHL as substrates, *J. Dairy Res.*, **2006**, *73*, 178-186.

Shi, H. L.; Noguchi, N.; Niki, N. Comparative study on dynamics of antioxidative action of α-tocopheryl hydroquinone, ubiquinol and α- tocopherol, against lipid peroxidation, *Free Radic. Biol. Med.*, **1999**, *27*, 334-346.

Shima, K.; Yamada, N.; Suzuki, E.; Harada, T. Novel brothy taste modifier isolated from beef broth, *J. Agric. Food Chem.*, **1998**, *46*, 1465-1468.

Singer, F. A. W.; Taha, F. S.; Mohamed, S. S.; Gibriel, A.; El-Nawawy, M. Preparation of mucilage/protein products from flaxseed, *Am. J. Food Technol.*, **2011**, *6*, 260-278.

Skeggs, L. T.; Jr., Kahn, J. R.; Shumway, N. P. Preparation and function of the hypertensin-converting enzyme, *J. Exp. Med.*, **1956**, *103*, 295-299.

Smith, P. K.; Krohn, R. I.; Hermanson, G. T.; Mallia, A. K.; Gartner, F. H.; Provenzano, M. D.; Fujimoto, E. K.; Goeke, N. M.; Olson, B. J.; Klenk, D. C. Measurement of Protein Using Bicinchoninic Acid. *Anal. Biochem.*, **1985**, *150*, 76-85.

Soldo, T.; Blank, I.; Hofmann T. (+)-(*S*)-Alapyridaine - a general taste enhancer ?, *Chem. Senses*, **2003**, *28*, 371-379.

Soldo, T.; Frank, O.; Ottinger, H.; Hofmann, T. Systematic studies of structure and physiological activity of alapyridaine. A novel food-borne taste enhancer, *Mol. Nutr. Food Res.*, **2004**, *48*, 270-281.

Steiner, J. E. Behavioral responses to tastes and odors in man and animals. *Proceedings of the umami international symposium,* **1993**, Society for Research on Umami Taste, Tokyo, Japan, pp.30-43.

Steiner, J. E. What the neonate can tell us about umami, In *Umami: A Basic Taste*, Kawamura, Y.; Kare, M. R. Eds., Marcel Dekker New York, NY, **1987**, pp. 97-123.

Stookey, L. L. Ferrozine-A New Spectrophotometric Reagent for Iron, *Anal. Chem.*, **1970**, *42*, 779-781.

Sugita, Y. Flavor enhancers, *Food Sci. Technol.*, **2002**, *116*, 409-445.

Szabo, M. R.; Iditoiu, C.; Chambre, D.; Lupea, A. X. Improved DPPH Determination for Antioxidant Activity Spectrophotometric Assay, *Chem. Pap.*, **2007**, *61*, 214-216.

Tachdjian, C.; Patron, A. P.; Qi, M.; Adaminski-Werner, S.; Tang, X. Q.; Qing, C.; Darmohusodo, V.; Lebl-Rinnova, M.; Priest, C. to Senomyx, PCT Int. Appl. WO 2006/084246 (Chem. Abstr. 2006, 144, 273163).

Taddei, F. *Il legame chimico*, UTET, **1976**.

Tang, C. H., Wang, X. S.; Yang, X. Q. Enzymatic hydrolisys of hemp (*Cannabis sativa L.*) protein isolate by various proteases and antioxidant properties of the resulting hydrolysates, *Food Chem.*, **2009**,*114*, 1484-1490.

Tang, C. H.; Ten, Z.; Wang, X. S.; Yang, X. Q. Physicochemical and functional properties of hemp (Cannabis sativa L.) protein isolate. *J. Agric. Food Chem.*, **2006**, *54*, 8945-8950.

Tang, C. H.; Wang, X. S.; Yang, X. Q.; Gao, W. R. Characterization, amino acid and in vitro digestibility of hemp (*Cannabis sativa L.*) proteins, *Food Chem.*, **2008**, *107*, 11-18.

Tang, S.; Hettiarachchy, N. S.; Shellhammer, T. H. Protein extraction from heat-stabilized defatted rice bran. 1. Physical processing and enzyme treatments, *J. Agric. Food Chem.*, **2002**, *5*, 7444-7448.

Tarpila, A.; Wennberg, T.; Tarpila, S. Flaxseed as functional food, *Curr. Topics Neutraceutical Res.*, **2005**, *3*, 167-188.

Tekanori, M.; Daisuke, T.; Kosuke, M.; Hisato, J. Structures of the extracellular regions of the group II/III metabotropic glutamate receptors, *Proc. Natl. Acad. Sci. USA*, **2007**, *104*, 3759-3764.

Temporini, C.; Massolini, G.; Marucci, G.; Lambertucci, C.; Buccioni, M.; Volpini, R.; Calleri, E. Development of new chromatographic tools based on A_{2A} Aadenosine A subtype receptor subtype for ligand characterization and screening by FAC-MS, *Anal. Bioanal. Chem.*, **2013**, *405*, 837-845.

Thammarat, K.; Bagnasco, L.; Benjakul, S.; Lanteri, S.; Morelli, C. F.; Speranza, G.;Cosulich, M. E. Characterisation of mucilages extracted from seven Italian cultivars of flax, *Food Chem.*, **2014**, *148*, 60-69.

Tombs, M. P.A haemoglobin-binding beta-globulin in human serum, *Nature*, **1960**,*186*, 1055-1556.

Torii, T.; Shiragami, H.; Yamashita, K.; Suzuki, Y.; Hijiya, T.; Kashiwagi, T.; Izawa, K. Practical syntheses of penciclovir and famciclovir from N^2-acetyl-7-benzylguanine, *Tetrahedron*, **2006**, *62*, 5709-5716.

Tossavainen, O.; Syvaoja, E. L.; Tuominen, J.; Heinanen, M.; Kalkkinen, N. Determination of the peptide size range of an extensively hydrolysed protein hydrolysate, *Milchwissenschaft*, **1997**, *52*, 63-67

Toyono, T.; Seta, Y.; Kataoka, S.; Kawano, S.; Shigemoto, R.; Toyoshima, K. Expression of metabotropic glutamate receptor group I in rat gustatory papillae. *Cell Tissue Res.*, **2003**, *313*, 29-35, and references cited therein.

Tuck, C. O.; Pérez, E.; Horváth, I. T.; Sheldon, R. A.; Poliakoff, M. Valorization of Biomass: Deriving More Value from Waste, *Science*, **2012**, *337*, 695-699.

Udenigwe, C. C.; Lu, Y. L.; Han, C. H.; Hou, W. C.; Aluko R. E. Flaxseed protein-derived peptide fractions: Antioxidant properties and inhibition of lipopolysaccharide-induced nitric oxide production in murine macrophages, *Food Chem.*, **2009**, *116*, 277-284.

Uttara, B.; Singh, A. V.; Zamboni, P.; Mahajan, R. T. Oxidative Stress and Neurodegenerative Diseases: A Review of Upstream and Downstream Antioxidant Therapeutic Options, *Curr. Neuropharmacol.*, **2009**, *7*, 65-74.

Van Der Borght, A.; Vandeputte, G. E.; Derycke, V.;, Brijs, K.; Daenen, G.; Delcour, J. A. Extractability and chromatographic separation of rice endosperm proteins, *J. Cereal Sci.*, **2006**, *44*, 68-74.

Villafuerte Romero, M; Raghavan, S; Ho, C. T., Eds. Enzymatic modification of wheat proteins for flavor generation via maillard reaction In *Nutrition, Functional and Sensory Properties of Foods*, New Brunswick: Rutgers The State University of New Jersey Ed., **2006**.

Wang, L. L.; Xiong, X. L. Inhibition of lipid oxidation in cooked beef patties by hydrolyzed potato protein is related to its reducing and radical scavenging ability, *J. Agric. Food Chem.*, **2005**, *53*, 9186-9192.

Wang, M.; Hettiarachchy, N. S.; Qi, M.; Burks, W.; Siebenmorgen, T. Preparation and functional properties of rice bran protein isolate. *J. Agric. Food Chem.*, **1999**, *47*, 1004-1013.

Wang, X. S.; Tang, C. H.; Chen, L.; Yang, X. Q. Characterization and antioxidant properties of hemp protein obtained with neutrase, *Food Chem.*, **2009** *47*, 428-434.

Wang, X. S.; Tang, C. H.; Yang, X. Q.; Gao, W. R. Characterization, amino acid composition and in vitro digestibility of hemp (Cannabis sativa L.) proteins. *Food Chem.*, **2008**, *107*, 11-18.

Wardman, P.; Candeias, L. P. Fenton Chemistry: An Introduction. *Radiat. Res.*, **1996**, *145*, 523-531.

Weaver, J. C.; Kroger, M. Free amino acid and rheological measurements on hydrolyzed lactose cheddar cheese during ripening, *J. Food Sci.* , **1978**, *43*, 579-583.

Wellisch, M.; Jungmeier, G.; Karbowski, A.; Patel, M. K.; Rogulska, M. Biorefinery systems – potential contributors to sustainable innovation, *Biofuels, Bioprod. Bioref.*, **2010**, *4*, 275-286.

Widder, S.; Lüntzel, C. S.; Dittner, T.; Pickenhagen, W. 3-Mercapto-2-methylpentan-1-ol, a new powerful aroma compound, *J. Agric. Food Chem.*, **2000**, *48*, 418-423, and references cited therein.

Wiechelman, K. J.; Braun, R. D.; Fitzpatrick, J. D. Investigation of the bicinchoninic acid protein assay: identification of the groups responsible for color formation. *Anal. Biochem.*, **1988**, *175*, 231-237.

Winkel, C.; de Klerk, A.; Visser, J.; de Rijke, E.; Bakker,J.; Koenig, T.; Renes, H. New Developments in Umami (Enhancing) Molecules, *Chem. Biodiv.*, **2008**, *5*, 1195-1203.

Witt, M.; Reutter, K.; Miller Jr, I. J. In *Handbook of olfaction and gestation*, Doty, R. L. Ed., Marcel Dekker, New York, **2003**, pp. 651 – 678.

Wu, J.; Aluko, R. E.; Muir, A. D. (2002). Improved method for direct high-performance liquid chromatography assay of angiotensin-converting enzyme-catalyzed reactions, *J. Chromatogr. A*, **2002**, *950*, 125-130.

Wyers, R. The fifth taste, *World Food Ingredients*, **2010**, 30-35.

Yamaguchi, S. Basic properties of umami and its effects on food flavor, *Food Rev. Int.*, **1998**, *14*(2 and 3), 139-176.

Yamaguchi, S.; Ninomiya, K. Umami and food palatibility, *J. Nutr.*, **2000**, *130*, 921S-926S.

Yamaguchi, S.; Ninomiya, K. What is umami? *Food Rev. Int.*, **1998**, *14*, 123-138.

Yamaguchi, S.; Yoshikawa, T.; Ikeda, S.; Ninomiya, T. Measurement of the relative taste intensity of some L-α-aminoacids and 5'-nuleotides, *J. Food Sci.*, **1971**, *36*, 846-849.

Yamaguchi, S. The synergistic taste effect of monosodium glutamate and disodium 5'-inosinate, *J. Food Sci.,* **1967**, *32,* 473-478.

Yamasaki, Y.; Maekawa, K. A peptide with delicious taste, *Agric. Biol. Chem.*, **1978**, *42*, 1761-1765.

Yang, H.; Li, Y.; Li, P.; Liu, Q.; Kong, B.; Huang, X.; Wu, Z. Physicochemical Changes of Antioxidant Peptides Hydrolyzed From Porcine Plasma Protein Subject to Free Hydroxyl Radical System, *Adv. J. Food Sci. Technol.*, **2013**, *5*, 14-18.

Yarmolinsky, D. A.; Zuker, C. S.; Ryba, N. J. P. Common Sense about Taste: From Mammals to Insects, *Cell*, **2009**, 234-244.

Yin, S. W.; Tang, C. H.; Cao, J. S.; Hu, E. R.; Wen, Q. B.; Yang, X. Q. Effects of limited enzymatic hydrolysis with trypsin on the functional properties of hemp (*Cannabis sativa* L.) protein isolate, *Food Chem.*, **2008**, *106*, 1004-1013.

Yoshikawa, M.; Kato, T.; Takenishi, T. Studies of phosphorylation. III. Selective phosphorylation of unprotected nucleosides. *Bull. Chem. Soc. Jpn.*, **1969**, *42*, 3505-3508.

Young, I. S.; Woodside, J.V. Antioxidants in health and disease, J. Clin. Pathol., **2001**, *54*, 176-186.

Zhang, F.; Klebansky, B.; Fine, R. M.; Xu, H.; Pronin, A.; Liu, H.; Tachdjian, C.; Li, X. Molecular mechanism for the umami taste synergism. PNAS, **2008**, *105*, 20930-20934.

Zhu, L.; Chen, J.; Tang, X.; Xiong, Y. L. Reducing, radical scavenging, and chelation properties of *in vitro* digests of alcalase-treated zein hydrolysate, *J. Agric. Food Chem.*, **2008**, *56*, 2714-2721.